



# **Giant cell formation by macrophages and lung epithelial cells: A unique method of cell-cell infection used by *B. thailandensis* involves tetraspanins**

A thesis submitted in part fulfillment of the requirements  
for the Degree of Doctor of Philosophy

by

**Muslim Idan Mohsin**

Department of Infection, Immunity & Cardiovascular  
Disease

Medical School

University of Sheffield  
October 2019

## Declaration

The work presented in this thesis is the work of the candidate, with the following exceptions:

The *B. thailandensis* E264- $\Delta$ tssK was produced by Dr. Jamie Hall (University of Sheffield) as a part of his doctoral work.

The over-expression of CD9 in the J774.2 mouse cell line was performed by Dr. Fawwaz Ali (University of Sheffield) as a part of his doctoral work.

The anti-Tspan-2 antibody and the A549 cells over-expressing Tspan-2 were produced by Dr. Ibrahim Yaseen (University of Sheffield) as a part of his doctoral work.

The A549 cells with knockouts of Tspan-15, ADAM10 and the anti-Tspan-15 antibody were produced by Dr. Mike Tomlinson, University of Birmingham.

The A549 cells with knockout of CD9 were produced by Dr. David J. Blake at Department of Biology, Fort Lewis College, Durango, Colorado.

This work was funded by the Ministry of Higher Education and Scientific Research (Iraq) as part of a scholarship program.

## Acknowledgments

I would like to express my deepest gratitude to my supervisors Prof. Peter N Monk and Dr. Mark Thomas, whose exceptional discussions and constructive criticism. They have enabled me to improve an understanding of the topic and achieve this thesis. Without your valuable support and commitment, this thesis would not have been possible. Pete, with you, I will never walk alone. Mark, you are one of the best microbiologists. I would also like to introduce my sincere appreciation and thanks to, Dr Lynda Partridge for her interesting encouragement, and theoretical and practical assistance throughout the work. She was positive all the time.

To all the wonderful friends around me, from the bottom of my heart, I appreciate your assistance. Rahaf Issa, for her support and her inducing. Shaimaa Abbas, for her pleasant conversation. Mohmmad Al-Shamrti, for his support to come to Sheffield. Sarmad Al-Sahaf, for his smile and wise talk and making me happy all the time. Chris Banyard and Aaron Butt, for their assistance in the tagged bacteria. Dr. Ahmed Al-Obaidy, Mahendra Raut and Luke Green, for their excellent advice. Ibrahim Yassin, for his assistance. Tom Champion, Atiga Elgawidi and Fawwaz Ali, for their real support at this project. Nathen Wong for the delicious cakes. Mohammed Moamin and Haider Aljanabi, for giving me wise talk. Fawzyah Albaldi, for her friendship that gives me the support for my next experiment. Ryawda Al-Hamd, for her help and her advice. Many thanks to all of my friends, including Basheer Al-Waely, Ameer Aljboori, Nawfal Aldulaimi, Dheyaa Alkhanfar, Naer Alkaabawi, Ali Al-Saraf, and Haider Amer, for their support. Especially, thanks to Dr. Shuang Ma for her encouragement.

I also much appreciate Dr Sue Clark, Julie Swales, and Kay Hopkinson (flow cytometry facility) for the technical assistance.

Special thanks to University of Kufa and Ministry of Higher Education and Scientific Research (Iraq) for their scholarship.

Finally, from my heart, big thanks to Mum, Dad, Brothers, and Sisters. I swear, my thesis would not have been finished without your encouragement.

## **List of Presentations**

- Poster: 7<sup>th</sup> European conference on tetraspanin, September 2016, Sheffield, UK.
- Poster presentation presented to the Yorkshire Immunology group, May 2017 at University of Leeds, Leeds, UK.
- Oral presentation presented to the combating infectious disease, 4 December 2017 at the University of York, UK.
- Poster: 9<sup>th</sup> International tetraspanin as targets and markers of cancer and infectious disease, April 2018 at Tucson -Arizona, USA.
- Oral presentation presented to the EMC-2018 European microbiology research, December 3-5, 2018 at Valencia, Spain.

## Summary

*Burkholderia thailandensis* is widely used as a non-pathogenic model of *Burkholderia pseudomallei*, the causative agent of melioidosis, a disease with a 90% mortality rate if untreated. One of the histopathological features of melioidosis is the presence of multinucleate giant cells (MGC). MGC formation occurs when the plasma membrane of infected cells become closely positioned with other cells, which then become attached and fuse together. Many studies have described how effector systems of *B. thailandensis* can induce the formation of MGC. It seems that these bacterial effectors can regulate this process by affecting the expression of mammalian membrane proteins, including the tetraspanins (Tspans) superfamily. Tspans are a large family of membrane proteins that bind partner proteins to form Tspan-enriched microdomains (TEM) that have many biological roles, including cell fusion, adhesion, and bacterial infection. Mammalian cells express 33 Tspans, but their specific functions during MGC formation and pathogen infection are not fully understood. Here, we have attempted to define the roles of all Tspans and some Tspan-partner proteins in *B. thailandensis* infection and/or MGC formation. We found that 5 Tspans are specifically involved in MGC formation induced by *B. thailandensis*: Tspan-2, Tspan-5, Tspan-13, CD81, and CD9. 3 Tspan-partner proteins are also specifically involved: ADAM10, CD98, and CD172 $\alpha$ .

Using antibodies, an inhibitory peptide derived from CD9 and knockouts and knockdowns of Tspans and their partners, we attempted to elucidate the roles of these molecules in MGC formation. It was observed that CD9, CD81, CD172 $\alpha$ , and ADAM10 have negative roles in MGC formation induced by *B. thailandensis* whereas Tspan-2 and Tspan-13 play positive roles and could also be required for *B. thailandensis* infection. CD98 also has a positive role in MGC formation but has no role in *B. thailandensis* infection. It was also found that the peptide derived from CD9 could reduce the total number of bacteria of *B. thailandensis*, and internalisation after 2 and 18hr.

# Contents

Declaration.....	I
Acknowledgments.....	II
List of Presentations .....	III
Summary .....	IV
List of Tables .....	XIII
List of Figures .....	XIV
List of Equations .....	XVIII
List of Abbreviations.....	XIX
Chapter 1 Introduction .....	1
1.1 Overview.....	1
1.2 Melioidosis.....	2
1.2.1 Route of infection .....	2
1.2.2 Symptoms and diagnosis .....	3
1.2.3 Global distribution of <i>B. pseudomallei</i> and melioidosis.....	3
1.2.4 Treatment and prevention .....	4
1.3 <i>B. pseudomallei</i> .....	5
1.3.1 Virulence factors of <i>B. pseudomallei</i> .....	5
1.3.1.1 Flagella and pili .....	6
1.3.1.2 Quorum sensing.....	7
1.3.1.3 Capsule.....	7
1.3.1.4 Lipopolysaccharide .....	7
1.3.1.5 Type III secretion system .....	8
1.3.1.6 Type VI secretion system.....	9
1.3.2 Mechanism of pathogenesis of <i>B. pseudomallei</i> .....	11
1.3.2.1 Bacterial attachment to the host plasma membrane .....	11
1.3.2.2 Survival of <i>B. pseudomallei</i> inside host cells.....	12
1.3.2.3 Activation of cell death by <i>B. pseudomallei</i> .....	14
1.3.2.4 Role of cell signalling molecules in <i>B. pseudomallei</i> infection and MGC formation.....	15
1.4 <i>B. thailandensis</i> as an alternative model for <i>B. pseudomallei</i> .....	16
1.5 Multinucleate giant cells.....	16

1.5.1	Types of MGC .....	17
1.5.1.1	LGC.....	17
1.5.1.2	Foreign body giant cells .....	18
1.5.1.3	Osteoclasts .....	18
1.5.1.4	MGC in cancer .....	19
1.5.2	Mechanism of macrophage fusion.....	19
1.5.3	MGC formation induced by <i>B. pseudomallei</i> .....	22
1.6	Tetraspanins overview.....	24
1.6.1	Extracellular loops of Tspans .....	25
1.6.2	Transmembrane domains of Tspans.....	26
1.6.3	Palmitoylation sites.....	26
1.6.4	Tspan enriched microdomains .....	27
1.6.5	Other membrane proteins involved in MGC formation .....	28
1.6.5.1	CD172 $\alpha$ .....	28
1.6.5.2	CD98.....	29
1.6.5.3	ADAMs.....	29
1.6.6	Functions of Tspans .....	30
1.6.6.1	Tspans in adhesion and motility .....	30
1.6.6.2	Tspans in signalling.....	30
1.6.6.3	Tspans in protein trafficking .....	31
1.6.6.4	Tspans in bacterial infections .....	32
1.6.6.5	Tspans and MGC formation .....	33
1.7	The hypothesis and aims of the study .....	36
Chapter 2	Materials and methods.....	37
2.1	Materials .....	37
2.1.1	Reagents and buffers .....	37
2.1.2	Bacterial growth media .....	39
2.1.3	Antibiotics .....	39
2.1.4	Bacterial strains.....	40
2.1.5	Plasmids.....	40
2.1.6	Primers and siRNA.....	41
2.1.6.1	Tspan primers .....	41
2.1.6.2	Other transmembrane proteins primer .....	42

2.1.6.3 Primers of some regulatory proteins .....	43
2.1.6.4 Sequence of Smart Pool Accell siRNA.....	43
2.1.7 Equipment and apparatus .....	44
2.1.8 Analysis software .....	44
2.1.9 Antibodies.....	45
2.1.9.1 Primary antibodies and isotypes .....	45
2.1.9.2 Secondary antibodies.....	46
2.1.10 Mammalian cell lines .....	46
2.2 Methods.....	48
2.2.1 Bacteriological techniques.....	48
2.2.1.1 Bacterial glycerol stocks.....	48
2.2.1.2 Estimation of viable bacteria .....	48
2.2.1.3 Preparation of competent cells.....	48
2.2.1.4 Plasmid extraction and purification.....	48
2.2.1.5 Agarose gel electrophoresis.....	49
2.2.1.6 <i>B. thailandensis</i> mutant strain production by allelic replacement .....	52
2.2.1.7 DNA sequencing .....	53
2.2.2 Tissue culture techniques.....	53
2.2.2.1 Culturing of J774.2 cells.....	53
2.2.2.2 Culturing of A549 cells .....	53
2.2.2.3 Cell freezing .....	54
2.2.2.4 Cell thawing.....	54
2.2.2.5 Viability of cells.....	54
2.2.2.6 Sulforhodamine B assay .....	54
2.2.2.7 Cytotoxicity assays–MTT .....	55
2.2.2.8 Assessment of protein level by flow cytometry .....	55
2.2.2.9 Transfection of mammalian cells.....	56
2.2.3 Peptide synthesis .....	57
2.2.4 Real-time quantitative polymerase chain reaction (RT-qPCR) .....	57
2.2.4.1 RNA extraction .....	57
2.2.4.2 RNA integrity .....	58
2.2.4.3 cDNA synthesis.....	58
2.2.4.4 Quantification of the DNA product.....	59

2.2.5 Infection assay .....	60
2.2.6 Fusion assay .....	60
2.2.7 Effect of Tspans and partner protein antibodies on bacterial infection and MGC formation in A549 cells .....	61
2.2.8 Effect of 8005 peptide derived from human CD9 on <i>B. thailandensis</i> infection and MGC formation to A549 cells .....	62
2.2.9 Flow cytometric method for measuring bacterial binding to host cells .....	62
2.2.10 Knockdown .....	62
2.2.10.1 siRNA Smart Pool Accell transfection .....	62
2.2.10.2 Effect of KD on infection and MGC formation induced by <i>B. thailandensis</i> .....	63
2.2.11 Effect of <i>B. thailandensis</i> infection on the levels of Tspans and other surface molecules. ....	63
2.2.12 Fluorescent imaging of infected mammalian cells by <i>B. thailandensis</i> .....	63
2.2.13 Statistical analyses .....	64
Chapter 3 MGC formation following <i>B. thailandensis</i> infection .....	65
3.1 Introduction .....	65
3.2 Aims .....	65
3.3 Results .....	66
3.3.1 <i>B. thailandensis</i> infection .....	66
3.3.1.1 Estimation of viable bacteria .....	66
3.3.1.2 Assessment of fluorescent proteins expression in <i>B. thailandensis</i> by flow cytometry .....	67
3.3.1.3 <i>B. thailandensis</i> infection of A549 and J774.2 cells .....	68
3.3.1.4 The effect of GFP expression in J774.2 and A549 cells on infection with <i>B. thailandensis</i> .....	69
3.3.1.5 Effect of the expression of fluorescent proteins in <i>B. thailandensis</i> CDC272 and E264 on the bacterial infection in J774.2 cells .....	70
3.3.1.6 Effect of the expression of fluorescent proteins in <i>B. thailandensis</i> CDC272 and E264 on the infection of A549 cells .....	71
3.3.2 <i>B. thailandensis</i> induces the formation of MGC formation <i>in vitro</i> in A549 and J774.2 cells .....	72
3.3.2.1 MGC formation .....	72

3.3.2.2 <i>B. thailandensis</i> <i>tssk</i> deletion mutant is incapable of inducing MGC formation.....	75
3.3.2.3 The effect of GFP expression in J774.2 and A549 cells on MGC formation induced by <i>B. thailandensis</i> .....	77
3.3.2.4 Effect of mCherry and GFP expression in <i>B. thailandensis</i> on MGC formation.....	78
3.4 Discussion .....	80
3.4.1 <i>B. thailandensis</i> infection.....	80
3.4.2 MGC formation induced by <i>B. thailandensis</i> .....	81
Chapter 4 Strategy to discriminate the role of Tspans and partner proteins involved in MGC formation and/or bacterial infection.....	83
4.1 Introduction.....	83
4.2 Aims.....	84
4.3 Results.....	85
4.3.1 Tspan genes expression at the mRNA level in A549 and J774.2 cells.....	85
4.3.2 Changes in Tspan genes expression at the mRNA level after infection of A549 and J774.2 cells.....	87
4.3.3 Tspan genes expression in A549 and J774 cells over time.....	89
4.3.4 Tspan-partner genes expression at the mRNA level in A549 and J774.2 cells .....	91
4.3.5 Tspan-partner genes expression at the mRNA level in A549 and J774.2 cells after infection by <i>B. thailandensis</i> .....	92
4.3.6 Innate immune molecules and cell signalling genes following infection with <i>B. thailandensis</i> .....	94
4.3.7 Tspan proteins expression on the cell surface of A549 cells .....	95
4.3.8 Tspan proteins expression following <i>B. thailandensis</i> infection.....	96
4.3.9 Gating strategy to detect fused and/or infected cells using flow cytometric analysis.....	97
4.3.10 Time-courses of downregulation or upregulation of selected Tspan proteins on the surface of A549 cells .....	99
4.3.11 Tspan-partner proteins expression on the surface of A549 cells ...	101
4.3.12 Tspan-partner proteins expression following <i>B. thailandensis</i> infection.....	102
4.3.13 Time-courses of Tspan-partner proteins expression following <i>B. thailandensis</i> infection on A549 cells.....	103

4.4 Discussion .....	105
4.4.1 Tspans expression change at the mRNA and protein levels following <i>B. thailandensis</i> infection.....	105
4.4.2 Tspan-partners expression change at the mRNA and protein levels following <i>B. thailandensis</i> infection.....	106
4.4.3 Innate immune molecules and cell signalling genes following infection with <i>B. thailandensis</i> in A549 and J774.2 cells .....	107
Chapter 5 Distinct roles for Tspans and Tspan-partner proteins in MGC formation during <i>B. thailandensis</i> infection .....	109
5.1 Introduction.....	109
5.2 Aims.....	109
5.3 Results.....	110
5.3.1 Role of CD9 in infection and MGC formation.....	110
5.3.1.1 The effect of anti-CD9 antibody on bacterial infection in A549 cells.....	110
5.3.1.2 The effect of anti-CD9 and anti-CD81 antibodies on MGC formation induced by <i>B. thailandensis</i> in A549 cells .....	111
5.3.1.3 Effect of CD9 over-expression on the total bacterial infection and internalised bacteria in J774.2 cells .....	112
5.3.1.4 Effect of CD9 over-expression on MGC formation induced by <i>B. thailandensis</i> .....	113
5.3.1.5 Co-localisation of <i>B. thailandensis</i> and CD9GFP .....	114
5.3.1.6 CD9-derived peptide 8005 and CD9EC2 functional studies on MGC formation and bacterial infection .....	115
5.3.2 Role of Tspan-2 and Tspan-13 in <i>B. thailandensis</i> infection and MGC formation in A549 cells.....	119
5.3.2.1 Effect of anti-CD81, anti-Tspan-2 and anti-Tspan-13 antibodies on bacterial infection of A549 cells.....	120
5.3.2.2 Effect of anti-Tspan-2 and anti-Tspan-13 antibodies on MGC formation induced by both <i>B. thailandensis</i> in A549 cells .....	121
5.3.2.3 Effect of Tspan-2 over-expression on bacterial infection.....	122
5.3.2.4 Effect of Tspan-2GFP expression on MGC formation induced by <i>B. thailandensis</i> .....	123
5.3.3 Role of Tspan-partner proteins ADAM10, CD98 and CD172 $\alpha$ in <i>B. thailandensis</i> infection and MGC formation in A549 cells.....	124
5.3.3.1 Role of ADAM10, CD98 and CD172 $\alpha$ in <i>B. thailandensis</i> infection.....	124

5.3.3.2 Roles of ADAM10, CD98 and CD172 $\alpha$ in MGC formation .....	125
5.4 Discussion .....	126
5.4.1 CD9 may be a negative regulator of MGC formation.....	126
5.4.2 CD9-derived peptides and CD9EC2 reduce <i>B. thailandensis</i> infection and may inhibit MGC formation.....	127
5.4.3 Tspan-2 and Tspan-13 are positive regulators of MGC formation and <i>B. thailandensis</i> infection.....	128
5.4.4 ADAM10, CD98 and CD172 $\alpha$ have little effect on bacterial infection but CD172 $\alpha$ may have a role in MGC formation in response to <i>B. thailandensis</i> infection .....	129
Chapter 6 Effect of manipulating the gene expression of 3 Tspans and ADAM10 on <i>B. thailandensis</i> infection and MGC formation.....	131
6.1 Introduction.....	131
6.2 Aims.....	132
6.3 Results.....	132
6.3.1 Transfection of A549 cells with Smart Pool siRNA .....	132
6.3.1.1 Delivery efficiency of Smart Pool siRNA .....	132
6.3.1.2 Expression of CD9, Tspan-13 and ADAM10 on A549 cells after treatment with siRNA KD reagents.....	134
6.3.1.3 Expression of Tspan-2 on A549 wild type cells and Tspan-2KD cells by real-time qPCR and flow cytometry .....	134
6.3.2 Effect of KD in <i>B. thailandensis</i> infection and MGC formation.....	135
6.3.2.1 Effect of CD9KD on <i>B. thailandensis</i> infection and internalisation .....	135
6.3.2.2 Effect of CD9KD reagents on MGC formation induced by <i>B. thailandensis</i> .....	136
6.3.2.3 Effect of Tspan-13KD on total <i>B. thailandensis</i> infection and internalisation .....	138
6.3.2.4 Effect of Tspan-13KD on MGC induced by <i>B. thailandensis</i> ..	139
6.3.2.5 Effect of Tspan-2KD on total <i>B. thailandensis</i> infection and MGC formation .....	140
6.3.2.6 Effect of ADAM10KD on total <i>B. thailandensis</i> infection and internalisation.....	142
6.3.2.7 Effect of ADAM10KD on MGC formation induced by <i>B. thailandensis</i> .....	143
6.3.3 CD9 expression in CD9KO A549 cells .....	144

6.3.3.1 Tspan-15 and ADAM10 expression in CD9KO A549 cells .....	145
6.3.3.2 Effect of CD9KO on total <i>B. thailandensis</i> infection and internalisation .....	145
6.3.3.3 Effect of CD9KO on MGC formation induced by <i>B. thailandensis</i> .....	146
6.3.4 ADAM10 expression in ADAM10KO and WT A549 cells .....	147
6.3.4.1 CD9 and Tspan-15 expression in ADAM10KO and WT A549 cells .....	149
6.3.4.2 Effect of ADAM10KO on total <i>B. thailandensis</i> infection and internalisation .....	149
6.3.4.3 Effect of ADAM10KO on MGC induced by <i>B. thailandensis</i> ...	150
6.3.5 Tspan-15 expression in Tspan-15KO and WT A549 cells .....	151
6.3.5.1 CD9 and ADAM10 expression on Tspan-15KO and WT A549 cells .....	152
6.3.5.2 Tspan15 expression after infection with <i>B. thailandensis</i> .....	153
6.3.5.3 Role of Tspan-15 on <i>B. thailandensis</i> infection .....	154
6.3.5.4 Role of Tspan-15 on MGC formation induced by <i>B. thailandensis</i> .....	155
6.4 Discussion .....	157
6.4.1 CD9 negatively regulates MGC formation in response to <i>B. thailandensis</i> infection .....	157
6.4.2 Tspan-2 and Tspan-13 play a role in MGC formation and <i>B. thailandensis</i> infection .....	157
6.4.3 Effect of ADAM10KD and KO on <i>B. thailandensis</i> infection and MGC formation in A549 cells.....	158
6.4.4 Tspan-15KO enhances MGC formation .....	159
Chapter 7 General discussion.....	161
7.1 Summary .....	161
7.2 Limitations .....	166
7.3 Conclusions .....	167
7.4 Future work.....	167
References .....	168
Appendix.....	193

## List of Tables

Table 1.1 Virulence factors of <i>B. pseudomallei</i> .....	6
Table 1.2 T6SS gene clusters in <i>B. pseudomallei</i> K96243 and <i>B. thailandensis</i> E264.....	9
Table 2.1 Buffers and reagent solutions. ....	37
Table 2.2 Bacterial growth media.....	39
Table 2.3 Antibiotics with working concentrations.....	39
Table 2.4 Bacterial species and their intended use.....	40
Table 2.5 Plasmids .....	40
Table 2.6 Primer sequences used to investigate Tspan genes expression. ...	41
Table 2.7 Primer sequences used to investigate Tspan-partner genes expression. ....	42
Table 2.8 Primer sequences used to investigate gene expression. ....	43
Table 2.9 Smart Pool Accell siRNA sequences. ....	43
Table 2.10 Equipment.....	44
Table 2.11 Software.....	44
Table 2.12 Primary antibodies and isotypes .....	45
Table 2.13 Secondary antibodies.....	46
Table 2.14 Mammalian cell lines.....	47
Table 2.15 Restriction digestion components. ....	50
Table 2.16 Ligation components.....	51
Table 2.17 8005 and SCR sequences. ....	57
Table 2.18 cDNA synthesis components. ....	58
Table 2.19 Thermocycler steps for cDNA generation. ....	59
Table 2.20 2x qPCR mastermix components.....	59
Table 2.21 Parameters of qPCR reaction. ....	59

## List of Figures

Figure 1.1 Distribution of melioidosis. ....	4
Figure 1.2 Type VI secretion system structure. ....	11
Figure 1.3 The mechanism of pathogenesis by <i>B. pseudomallei</i> inside the mammalian cells. ....	12
Figure 1.4 The mechanism of macrophage fusion. ....	21
Figure 1.5 The cell fusion process induced by <i>B. pseudomallei</i> . ....	24
Figure 1.6 Tspan protein structure. ....	25
Figure 1.7 Interactions of Tspans with partner proteins. ....	27
Figure 1.8 Tspans signalling at the cell membrane. ....	31
Figure 3.1 Growth curves for <i>B. thailandensis</i> strains. ....	66
Figure 3.2 Flow cytometry analysis of GFP and mCherry expression in <i>B. thailandensis</i> CDC272. ....	67
Figure 3.3 Flow cytometry analysis of GFP and mCherry expression in <i>B. thailandensis</i> E264. ....	68
Figure 3.4 <i>B. thailandensis</i> CDC272 and E264 infection in J774.2 and A549 cells at different multiplicities of infection. ....	69
Figure 3.5 Effect of GFP expression in J774.2 and A549 cells on <i>B. thailandensis</i> infection. ....	70
Figure 3.6 Effect of fluorescent proteins on <i>B. thailandensis</i> infection in J774.2 cells. ....	71
Figure 3.7 Effect of fluorescent proteins on total <i>B. thailandensis</i> infection in A549 cells. ....	72
Figure 3.8 The formation of MGC at different MOI of <i>B. thailandensis</i> CDC272 and E264. ....	73
Figure 3.9 Light micrographs of J774.2 cells infected with <i>B. thailandensis</i> E264, CDC272 and <i>E264-ΔtssK</i> . ....	74
Figure 3.10 Light micrographs of A549 cells infected with <i>B. thailandensis</i> E264, CDC272 and <i>E264-ΔtssK</i> . ....	75
Figure 3.11 MGC formation in J774.2 and A549 cells. ....	76
Figure 3.12 Effect of GFP in J774.2 cells on MGC formation induced by both <i>B. thailandensis</i> strains. ....	77

Figure 3.13 Effect of GFP in A549 cells on MGC formation induced by both <i>B. thailandensis</i> strains. ....	78
Figure 3.14 Effect of fluorescent reporter proteins on <i>B. thailandensis</i> -induced MGC formation in J774.2 cells. ....	79
Figure 3.15 Effect of fluorescent reporter proteins on <i>B. thailandensis</i> -induced MGC formation in A549 cells. ....	79
Figure 4.1 Validation of qPCR ( RNA integrity and primers specificity). ....	86
Figure 4.2 Tspan genes expression at the mRNA level in J774.2 cells. ....	87
Figure 4.3 Tspan genes expression at the mRNA level in A549 cells. ....	87
Figure 4.4 Changes in Tspan genes expression at mRNA level in response to both <i>B. thailandensis</i> fusogenic strains. ....	88
Figure 4.5 Time-courses of Tspan genes expression during <i>B. thailandensis</i> infection in J774.2 and A549 cells. ....	90
Figure 4.6 Tspan-partner genes expression at the mRNA level in J774.2 and A549 cells. ....	92
Figure 4.7 Tspan-partner genes expression changed in response to <i>B. thailandensis</i> infection. ....	93
Figure 4.8 Innate immune molecules and cell signalling genes in MGC formation and/or bacterial infection. ....	95
Figure 4.9 Tspan proteins surface expression on the cell surface of A549 cells. ....	96
Figure 4.10 Tspan-2, Tspan-13 and CD9 proteins change in response to <i>B. thailandensis</i> infection on the surface of A549 cells. ....	97
Figure 4.11 Gating strategy to detect fused or/and infected cells using flow cytometric analyses. ....	98
Figure 4.12 CD9 expression changed in response to <i>B. thailandensis</i> infection on the surface of A549 cells after gating strategy. ....	99
Figure 4.13 Time-courses of Tspan proteins expression on the surface of A549 cells in response to <i>B. thailandensis</i> infection. ....	100
Figure 4.14 Tspan-partner proteins expression on the surface of A549 cells. ....	101
Figure 4.15 Tspan-partner proteins expression in response to <i>B. thailandensis</i> infection of A549 cells. ....	102

Figure 4.16 Time-courses of Tspan-partner proteins expression on the surface of A549 cells in response to <i>B. thailandensis</i> infection.....	104
Figure 5.1 Effect of anti-CD9 antibody on total <i>B. thailandensis</i> infection....	111
Figure 5.2 Effect of anti-CD9 and CD81 antibodies on MGC formation induced by both <i>B. thailandensis</i> CDC272 and E264.....	112
Figure 5.3 Comparison of total number of bacteria and internalised bacteria at 2 and 18hr in J774.2 cells expressing GFP or CD9GFP.....	113
Figure 5.4 Effect of CD9 over-expression on MGC formation induced by both <i>B. thailandensis</i> strains.....	114
Figure 5.5 Fluorescent micrographs of CD9GFPJ774.2 cells infected by both <i>B. thailandensis</i> strains.....	115
Figure 5.6 Effect of CD9-derived peptide 8005 on <i>B. thailandensis</i> growth.	116
Figure 5.7 CD9-derived peptide 8005 reduces total <i>B. thailandensis</i> infection of A549 cells.....	117
Figure 5.8 Effect CD9-derived peptide 8005 reduces <i>B. thailandensis</i> internalisation at 2 and 18hr in A549 cells.....	118
Figure 5.9 Effect of CD9-derived peptide 8005 and GST-CD9EC2 on MGC formation induced by both <i>B. thailandensis</i> in A549 cells.....	119
Figure 5.10 Effect of anti-Tspan-2, anti-Tspan-13 and anti-CD81 antibodies on <i>B. thailandensis</i> infection.....	121
Figure 5.11 Effect of anti-Tspan-2 and anti-Tspan-13 antibodies on MGC formation induced by both <i>B. thailandensis</i> strains.....	122
Figure 5.12 Over-expression of Tspan-2 increases <i>B. thailandensis</i> CDC272 and E264 infection.....	123
Figure 5.13 Over-expression of Tspan-2 promotes MGC formation induced by both <i>B. thailandensis</i> strains.....	124
Figure 5.14 Effect of anti-ADAM10, anti-CD98 and anti-CD172 $\alpha$ antibodies on <i>B. thailandensis</i> CDC272 and E264 infection of A549 cells.....	125
Figure 5.15 Anti-ADAM10, anti-CD98 and anti-CD172 $\alpha$ antibodies reduce or enhance MGC formation induced by both <i>B. thailandensis</i> strains.....	126
Figure 6.1 Determination of <i>in vitro</i> transfection efficiency by fluorescence microscopy and flow cytometry.....	133

Figure 6.2 CD9, Tspan-13 and ADAM10KD at mRNA and protein levels in A549 cells after 48hr treatment with Smart Pool siRNA and non-targeting KD materials. ....	134
Figure 6.3 Effect of Tspan-2KD at mRNA and protein levels in A549 cells after 72hr treatment with siRNA or non-targeting materials. ....	135
Figure 6.4 Effect of CD9KD on <i>B. thailandensis</i> infection. ....	136
Figure 6.5 Effect of CD9KD on MGC formation induced by both <i>B. thailandensis</i> strains. ....	137
Figure 6.6 Effect of Tspan-13KD on <i>B. thailandensis</i> infection. ....	139
Figure 6.7 Effect of Tspan-13KD on MGC formation induced by both <i>B. thailandensis</i> strains. ....	140
Figure 6.8 Effect of Tspan-2KD on MGC formation and <i>B. thailandensis</i> infection. ....	141
Figure 6.9 Effect of ADAM10KD on <i>B. thailandensis</i> infection. ....	142
Figure 6.10 Effect of ADAM10KD on MGC formation induced by both <i>B. thailandensis</i> strains. ....	143
Figure 6.11 Measurement of CD9 expression on WT and CD9KO A549 cells by flow cytometry. ....	144
Figure 6.12 Cell surface protein expression on WT and CD9KO A549 cells. ....	145
Figure 6.13 Effect of CD9KO in A549 cells on <i>B. thailandensis</i> infection. ....	146
Figure 6.14 Effect of CD9KO on MGC formation induced by both <i>B. thailandensis</i> strains. ....	147
Figure 6.15 ADAM10 expression on WT and ADAM10KO A549 cells by flow cytometry. ....	148
Figure 6.16 Cell surface molecule expression on ADAM10KO and WT A549 cells. ....	149
Figure 6.17 Effect of ADAM10KO in A549 cells on total <i>B. thailandensis</i> infection. ....	150
Figure 6.18 Effect of ADAM10KO on MGC formation induced by both <i>B. thailandensis</i> strains. ....	151
Figure 6.19 Tspan-15 expression on WT and Tspan-15KO A549 cells by flow cytometry. ....	152

Figure 6.20 Cell surface molecules expression on WT and Tspan-15KO A549 cells.....	153
Figure 6.21 Tspan-15 protein expression after infection on the surface of A549 cells. ....	154
Figure 6.22 Effect of Tspan-15KO and anti-Tspan-15 antibody on <i>B. thailandensis</i> infection in A549 cells. ....	155
Figure 6.23 Effect of Tspan-15KO and anti-Tspan-15 antibody on MGC formation induced by both <i>B. thailandensis</i> strains.....	156

## List of Equations

Equation 2.1 Delta C <sub>t</sub> equations to analyse qPCR results .....	59
Equation 2.2 Total bacteria .....	60
Equation 2.3 Fusion index and number of nuclei per MGC.....	61

## List of Abbreviations

ADAM: A disintegrin and metalloproteinase
AHL: N-acyl-homoserine lactone
AP-1: Activator protein 1
APCs: Antigen-presenting cells
BoaA: <i>Burkholderia</i> oligomeric coiled-coil adhesin A
C3b: Complement factor 3b
Caspase-3: Cysteine-aspartic acid protease
CD: Cluster of differentiation
CFU: Colony forming units
CIS: Cytokine-inducible SRC homology 2-containing protein
C <sub>t</sub> : Threshold cycle
DAPI: 4', 6-diamidino-2-phenylindole
DC-SIGN: Dendritic cell-specific intercellular adhesion molecule-3-grabbing non-integrin
DC-STAMP: Dendritic cell-specific transmembrane protein
EC1: Small extracellular loop
EC2: Large extracellular loop
FBGC: Foreign body giant cells
FcR: The fragment crystallizable region
GAPDH: Glyceraldehyde 3-phosphate dehydrogenase
GFP: Green fluorescent protein
GPCR: G-protein coupled receptor
HisF: Histidine
ICAM-1: Intercellular adhesion molecular
IFN- $\gamma$ : Interferon gamma
IFN- $\gamma$ : Interferon gamma
IL-13: Interleukin-13
IL-4: Interleukin-4
iNOS: Nitric oxide synthase
Jnk: Jun N-terminal kinases

KD: Knockdown
KO: Knockout
LGC: Langhans' giant cells
LPS: Lipopolysaccharide
M1: Classic 1-activated macrophage
M2: Classic 2-activated macrophage
MAP: Mitogen-activated protein
MCSF: Macrophage colony stimulating factor
MGC: Multinucleate giant cells
MHC: Major histocompatibility complex
MIP: Macrophage inflammatory protein
MMP-9: Matrix metalloproteinase-9
MOI: Multiplicity of infection
NF- $\kappa$ B: Nuclear factor kappa-light-chain-enhancer of activated B cells
NOD2: Nucleotide-binding oligomerization domain-containing protein 2
OD: Optical density
OPG: Osteoprotegerin
P/S: Penicillin and streptomycin
p38: Mitogen-activated protein kinase
PI3K-Akt: Phosphatidylinositol 3-kinase
PM: Plasma membrane
PMN: Polymorphonuclear cell
ProHB-EGF: Pro-heparin-binding growth factor
PS: Phosphatidylserine
PTP-PEST/PTPN12: Cytoplasmic protein tyrosine phosphatase
RANKL: Receptor activator of NF- $\kappa$ B ligand
RPE: RNA precipitating elution buffer
RpL13 $\alpha$ : Ribosomal protein L13 $\alpha$
RpoS: RNA polymerase sigma factor
RW1: RNA washing buffer
SOCS3: Suppressor of cytokine signalling 3
STAT: Signal transducer and activator of transcription

T3SS: Type III secretion system
T3SS-3: Type III secretion system cluster 3
T6SS: Type VI secretion system
T6SS-5: Type VI secretion system cluster-5
TAA: Trimeric autotransporter adhesion proteins
TEM: Tetraspanin-enriched microdomains
Th1: Type 1 T helper lymphocytes
Th2: Type 2 T helper lymphocytes
TLR: Toll-like receptors
TNF: Tumor-necrosis factor
Tspan: Tetraspanin
UPEC: Uropathogenic <i>Escherichia coli</i>
WT: Wild type

# Chapter 1 Introduction

## 1.1 Overview

Lower respiratory tract pathogens result in a wide range of human diseases such as melioidosis, tuberculosis and pneumonia (Marrie, 1994, Brett and Woods, 2000). Melioidosis is a chronic endemic disease, which is distributed through the tropical zone, and is caused by *B. pseudomallei*, an opportunistic pathogen in the human lower respiratory tract and on the skin. Annually, there are many recorded cases in southeast Asia, specifically Thailand, Malaysia and Vietnam, and it has also been recorded in northern Australia (Brett and Woods, 2000).

*B. pseudomallei* and *B. thailandensis* (see **sections 1.3** and **1.4**) are related Gram-negative bacteria (Yu *et al.*, 2006, Atkins *et al.*, 2002). Stagnant water and moist soil are considered the main reservoirs for both of these pathogens (Wiersinga *et al.*, 2008). Both provoke a similar immune response, and have a similar mechanism of immune response (Yu *et al.*, 2006, Haraga *et al.*, 2008). Laboratory researchers use *B. thailandensis* in animal models because it has little effect on humans compared to *B. pseudomallei* (West *et al.*, 2012). The ability of *B. pseudomallei* to bind and invade epithelial cells in the human lung is an important part of the process of colonization. Bacterial surface proteins, called trimeric autotransporter adhesions (TAA), may achieve the binding. These outer membrane proteins have a cooperative role in bacterial pathogenesis and adhesion at the host cell surface (Edwards *et al.*, 2010). Pili, lipopolysaccharide (LPS) and flagella can help bacteria attach to the cell surface as well (DeShazer *et al.*, 1997, Essex-Lopresti *et al.*, 2005, Burtnick *et al.*, 2002, DeShazer *et al.*, 1999).

*B. pseudomallei* can also invade mammalian cells and stimulate them to form a complex structure known as a multinucleate giant cell (MGC) (Wiersinga *et al.*, 2006, Kespichayawattana *et al.*, 2000, Harley *et al.*, 1998). There is insufficient understanding of how MGC formation is induced in monocyte/macrophages and other cells. A good understanding of the mechanisms of formation would be helpful in determining the role of MGC in

chronic disease to avoid *B. pseudomallei* infection. Tetraspanins (Tspans) are a large family of mammalian cell surface proteins known to be involved in MGC formation induced by *B. thailandensis* (Elgawidi, 2016). An important feature of Tspan molecules is their ability to form multiplexes of membrane proteins called Tspan-enriched microdomains (TEM) (Maecker *et al.*, 1997). Tspan molecules can bind together or with partner proteins, such as immunoglobulin superfamily members and CD46, to make TEM. There are many functions facilitated by TEM, including cell fusion, signalling and the adhesive attaching of leukocytes to endothelial and epithelial cells (Maecker *et al.*, 1997). Pathogens can also attach to TEM on the plasma membrane (Green *et al.*, 2011).

## 1.2 Melioidosis

Melioidosis has been an emerging infection over the past two decades, more frequently recognized in endemic areas (southeast Asia and northern Australia) (Currie, 2003). However, melioidosis is now being seen in many additional countries since people travel more and the microorganism may spread through new environmental conditions, although, as yet, there is no evidence to fully substantiate this (Dance, 1991, Dance, 2000). *B. pseudomallei* is also possibly spread by contaminated soil and water imported from an endemic area (Kaestli *et al.*, 2007). After exposure to *B. pseudomallei*, the range of incubation times of melioidosis is between 1 and 10 days, although much longer periods (up to 62 years) are possible before the occurrence of clinical symptoms (Ngauy *et al.*, 2005). Twenty percent of all community-acquired septicaemias and 40% of sepsis-related mortality in northern Thailand is from melioidosis. There is no vaccination to prevent this disease, and the causative agent of the disease is highly resistant to antibiotics (Häußler *et al.*, 1999).

### 1.2.1 Route of infection

The causative agent of melioidosis can infect host cells at different sites (Brett and Woods, 2000). The most common route is inhalation of aerosolised bacteria (Zueter *et al.*, 2016). Also, burn or wound infection may commonly occur (Limmathurotsakul *et al.*, 2016). Furthermore, infection can also occur

by drinking contaminated water (Limmathurotsakul *et al.*, 2016). Dendritic cells can facilitate the dissemination of pathogens in these different sites of infection (Williams *et al.*, 2014).

### 1.2.2 Symptoms and diagnosis

Melioidosis is a very serious disease that can present itself with different symptoms such as skin lesions, pneumonia and septicaemia (Gibney *et al.*, 2008, Reissig *et al.*, 2012). Infection by *B. pseudomallei* can be classified into asymptomatic, localised, chronic and systemic septicaemia. Symptomatic infections normally occur via the respiratory tract, and can result in high mortality. The patients usually suffer with headache, myalgia, and high fevers, followed by rigors and chest pain. The bacterium also has the ability to persist for more than one decade asymptotically. In a case in Texas, the bacterium was dormant for more than 60 years until a cut in the man's thumb became ulcerated (Ngauy *et al.*, 2005). Septicaemia infection is much more serious than other categories; the case mortality rate is about 90%. However, the mortality rates have decreased in recent years because of newer more effective antibiotics such as the third-generation cephalosporin, ceftazidime.

There are many diagnoses that confuse melioidosis with chronic pneumonia and tuberculosis (Wiersinga *et al.*, 2006). The current clinical diagnosis of the melioidosis agent is culture on Ashdown's agar (Limmathurotsakul *et al.*, 2010). Also, *B. pseudomallei* can be diagnosed using the latex agglutination assay (Ekpo *et al.*, 2007). Another technique that is sometimes used is an immunofluorescence assay (IFA) to diagnose melioidosis disease by using a fluorescently labelled antibody specific to the bacterium (Puah, 2014).

### 1.2.3 Global distribution of *B. pseudomallei* and melioidosis

The first observation of melioidosis was in Myanmar in 1912 (Whitmore and Krishnaswami, 1912, Whitmore, 1913). Recently, many countries and regions have reported that melioidosis is endemic, such as southeast Asia, northern Australia, Brazil, India, southern China, Bangladesh (Jilani *et al.*, 2016) and Malawi (Currie *et al.*, 2008, Katangwe *et al.*, 2013). **Fig 1.1** shows the global distribution of melioidosis.

Lack of awareness is one of the factors that make diagnosis difficult and gives an opportunity for the global distribution of *B. pseudomallei* and an increasing number of melioidosis cases (Schweizer *et al.*, 2014). Another factor is the absence of coherent strategies to detect *B. pseudomallei* in the soil (Potisap *et al.*, 2018). However, human activities and their impact on the environment could increase the suitability of areas for *B. pseudomallei* colonisation (Shams *et al.*, 2007). For instance, farming and waste disposal can be classified as ‘anthrosol’, which is related with human activities, including partial removal, filling and cutting, waste disposal and irrigated agriculture (Limmathurotsakul *et al.*, 2016).

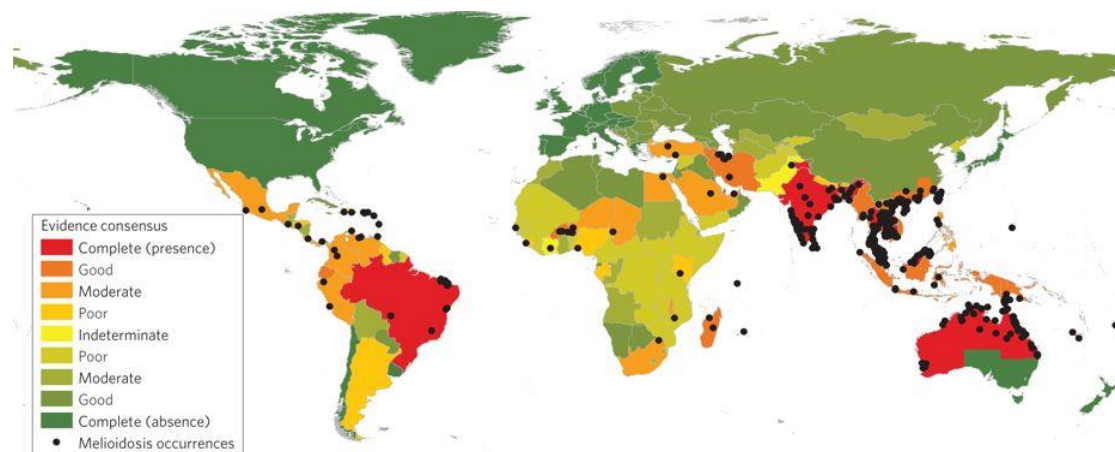


**Figure 1.1 Distribution of melioidosis.**

The different colour means countries according to epidemic area that present the causative agent of melioidosis. Black dots indicate a recorded case of melioidosis. Reproduced with permission (Limmathurotsakul *et al.*, 2016).

### 1.2.4 Treatment and prevention

Ceftazidime is the most effective treatment of melioidosis. It can reduce mortality by 50% compared to other antibiotic treatments. However, the rates of mortality are still high (Wiersinga *et al.*, 2012). Treatment with ceftazidime is usually followed by a regime of co-trimoxazole to destroy *B. pseudomallei* (Limmathurotsakul and Peacock, 2011, Dance, 2014).

Several vaccines have been tested in animal models (Phuong *et al.*, 2008). Some of them have attempted to use live bacteria attenuated by the mutation of genes (Phuong *et al.*, 2008) and virulence factors (Stevens and Galyov, 2004). A whole killed *B. pseudomallei* has been tested as an inactivated vaccine (Gilmore *et al.*, 2007, Barnes and Ketheesan, 2007). In addition, other

researchers have used *B. pseudomallei* proteins including type III and type VI secretion system proteins as antigens (Druar *et al.*, 2008, Burtnick *et al.*, 2008). To date, no vaccine has offered complete protection from infection (Silva and Dow, 2013, Fertitta *et al.*, 2018). However, it was reported recently that an attenuated vaccine of *B. pseudomallei* PBK001 could activate the immune response and offer full protection against aerosol infection by *B. pseudomallei* (Khakhum *et al.*, 2019).

### 1.3 *B. pseudomallei*

*B. pseudomallei* is a Gram-negative, motile, lactose non-fermenting, oxidase positive, non-spore forming aerobic bacillus (Hemarajata *et al.*, 2016). Ashdown's medium is a selective medium used to identify *Burkholderia* species (Ashdown, 1979).

#### 1.3.1 Virulence factors of *B. pseudomallei*

*B. pseudomallei* has many virulence factors, including pili, flagella, capsule, bacterial lipopolysaccharide (LPS) and the type III and type VI secretion systems (T3SS and T6SS) (Estrada-De Los Santos *et al.*, 2016, Adler, 2011, Galyov *et al.*, 2010), as shown in **Table 1.1**.

**Table 1.1 Virulence factors of *B. pseudomallei*.**

Virulence factors	Role	References
Capsular polysaccharide	Adhesion to host cells; defense against complement	(Reckseidler-Zenteno <i>et al.</i> , 2005)
Flagella	Movement	(DeShazer <i>et al.</i> , 1997)
Fimbriae and pili	Adhesion to host cells	(Essex-Lopresti <i>et al.</i> , 2005)
Quorum sensing	Stationary phase gene regulation, including secreted enzymes and oxidative stress protein	(Lumjiaktase <i>et al.</i> , 2006, Song <i>et al.</i> , 2005)
LPS	Resistance to complement and defenses against native immune response.	(DeShazer <i>et al.</i> , 1999, Burtnick <i>et al.</i> , 2002)
Type I, II, III, V and VI secretion systems	To invade and escape from host cells; Secretion of effector proteins for example BopA, BopE phospholipase C, protease, and lipase required for interaction with host cells.	(Stevens and Galyov, 2004, Stevens <i>et al.</i> , 2002, Burtnick <i>et al.</i> , 2008)

### 1.3.1.1 Flagella and pili

The flagellum plays a role in the invasion of human lung epithelial cells (Chua *et al.*, 2003). Wikraiphat and co-workers have shown that the flagellum can protect bacteria from human polymorphonuclear cells (PMNs) and macrophages (Wikraiphat *et al.*, 2009). Chua and co-workers have shown that the flagellum has a role in the pathogenesis of *B. pseudomallei*. However, an *in vitro* study that used A549 cells showed that there were no significant differences between wild type and flagella mutant strains of *B. pseudomallei* (Chua *et al.*, 2003). A second important virulence factor is the type IV pilus, which has two subclasses (IVA and IVB). A putative pilus protein of IVA is used as an adhesive factor to attach to epithelial cells. Some studies showed

that the percentage of adhesion to epithelial cells is reduced in pili mutant strains (Essex-Lopresti *et al.*, 2005).

#### 1.3.1.2 Quorum sensing

*Burkholderia*. spp can produce N-acyl-homoserine lactone (AHL or N-AHL) signal molecules, which are involved in cell to cell communication (Chan *et al.*, 2015). Many species of bacteria use quorum sensing to coordinate gene expression according to the density of their local populations (Keller and Surette, 2006). The signal is controlled by gene regulators, which can change gene expression, switching between flagella and pili genes during biofilm production (Antunes *et al.*, 2010, LaSarre and Federle, 2013). The *luxR* gene family is responsible for the synthesis of AHLs (Subramoni and Venturi, 2009). There are some data showing that AHL synthase has negative effects on the formation of MGC (Horton *et al.*, 2013). The absence of all three AHL synthases in *B. pseudomallei* strongly promotes MGC formation in RAW264 mouse macrophages. However, when murine models were infected with the AHL null mutant, there was no effect on virulence in mice (Horton *et al.*, 2013).

#### 1.3.1.3 Capsule

The capsule has a key role in bacterial attachment and infection (Wiersinga *et al.*, 2006). Perry and co-workers have observed that the bacterial capsule is composed of 3-2-O-acetyl-6-deoxy- $\beta$ -D-manno-heptopyranose-1 (Perry *et al.*, 1995). The capsule also is important to prevent the binding between bacteria and components of innate immunity such as complement C3b, an opsonin that promotes phagocytosis (Reckseidler-Zenteno *et al.*, 2005). Deletion of genes encoding capsule components has been shown to affect bacterial infection in a mouse model (Atkins *et al.*, 2002). Wikraiphat and co-workers have shown that mutation of capsule components reduces the ability for internalisation and replication inside macrophages (Wikraiphat *et al.*, 2009).

#### 1.3.1.4 Lipopolysaccharide

LPS is the major component of the outer membrane of Gram negative bacteria (Whitfield and Trent, 2014). It is considered the key marker for recognition by the innate immune system (Yoon *et al.*, 2009, Brennan *et al.*,

2013). LPS consists of 3 components, which are lipid A, O-antigen and core-oligosaccharide (Nikaido, 2003). The LPS of *B. pseudomallei* is a type II O-antigen, and is required for pathogenesis in guinea pigs, mice and infant diabetic rats (Wikraiphath *et al.*, 2009, Brett *et al.*, 1998). In addition, LPS of *B. pseudomallei* is also not capable of stimulating inducible nitric oxide synthase, which is a part of host defence (Utaisincharoen *et al.*, 2003).

#### 1.3.1.5 Type III secretion system

Most Gram-negative pathogens secrete proteins important for virulence. The type III secretion system (T3SS) is one of the secretion systems that are important for the invasion of host cells (Coburn *et al.*, 2007). The T3SS is composed of more than 20 proteins (Morales *et al.*, 2008). These include proteins that assemble the T3SS secretion machine, and two or three additional proteins known as translocator proteins that insert into the membrane of the target eukaryotic cell and are responsible for delivering effector proteins into target eukaryotic cells. The translocator proteins are responsible for delivering effector proteins into target eukaryotic cells. Although of course the other components of the T3SS are required for this, otherwise the effectors would not be secreted (Marlovits and Stebbins, 2010).

Three T3SSs are encoded in the genome of *B. pseudomallei* (T3SS-1 and -3) (Vander Broek and Stevens, 2017). T3SS-1 and -2 are not well defined (Vander Broek and Stevens, 2017). T3SS-3 is also known as the *Burkholderia* secretion apparatus (Bsa) (Pumirat *et al.*, 2010). This system is similar to the T3SS of *Salmonella enterica* with regard to virulence characteristics and structure (Stevens *et al.*, 2002). The deletion of the translocator gene of the Bsa could reduce virulence in a mouse infection model (Stevens *et al.*, 2004). The effect of T3SS-3 on the HeLa cell line has also been investigated (Stevens *et al.*, 2002). Stevens *et al.* have found that the inactivation of *bopE* (effector protein of T3SS-3) could reduce bacterial invasion, but not reduce bacterial replication in a mouse macrophage-like cell line (Stevens *et al.*, 2002). However, knockout of *bsaZ* (effector protein of T3SS-3) leads to the reduction of the number of intracellular bacteria (Stevens *et al.*, 2002). Interestingly, a device called 'photothermal nanoblade' has been used to deliver a *B. thailandensis* mutant lacking a functioning T3SS-3 and wild type

(WT) directly to the cytosol of HEK293 cells (French *et al.*, 2011). It was noticed that MGC were formed normally with the WT but not with the mutant strain using the regular mode of infection, however, there were no differences between MGC formation induced by WT and mutant bacteria that were delivered by photothermal nanoblade. This may suggest that this secretion system could play a role in the initial infection of bacteria, perhaps in the escape from endosomes (French *et al.*, 2011). Their results also suggest that the *B. thailandensis* might transfer between cells to others through membrane protrusion formation into neighbouring cells resulting in the formation of vacuoles.

### 1.3.1.6 Type VI secretion system

T6SS is a specific macromolecular machine that is able to deliver proteins into host cells. The genes of T6SS have been identified in roughly a quarter of all Gram-negative bacterial genomes (Bingle *et al.*, 2008). The genome of *B. pseudomallei* is predicted to encode six T6SSs known as T6SS-1 to T6SS-6, as shown in **Table 1.2** (Shalom *et al.*, 2007).

**Table 1.2 T6SS gene clusters in *B. pseudomallei* K96243 and *B. thailandensis* E264.**

<i>B. thailandensis</i> E264	<i>B. pseudomallei</i> K96243	T6SS gene cluster <sup>a</sup>
BTH_I294-BTH_I2968	BPSL3097-BPSL3111	1
BTH_II0119-BTH_II0140	BPSS0095-BPSS0116	2
Absent	BPSS0167-BPSS0185	3
BTH_II1885-BTH_II1902	BPSS0515-BPSS0532	4
BTH_II0873-BTH_II0854	BPSS1493-BPSS1511)	5
BTH_II0249-BTH_II0265	BPSS2093-BPSS2109	6

<sup>a</sup> According to the nomenclature of Shalom *et al.*, 2007

Interestingly, only T6SS-5 has a known role in bacterial pathogenesis (Shalom *et al.*, 2007). T6SS-5 has a major role for MGC formation (Schwarz *et al.*, 2010). Shalom and colleagues have used *in vivo* expression technology (IVET) to identify upregulated genes within bacteria during infection (Shalom *et al.*, 2007). They showed that the gene expression of T6SS-5 components increased during macrophage infection (Shalom *et al.*, 2007). Furthermore, the deletion of the T6SS-5 subunit gene *vgrG-5* (*tssl-5*) in *B. pseudomallei* confirmed the role of T6SS-5 in bacterial pathogenesis in a hamster model of infection (Lennings *et al.*, 2019, West *et al.*, 2008).

French *et al.* performed the nanoblade experiment using double mutants of T3SS-3 and T6SS-5 of *B. thailandensis* (French *et al.*, 2011). It was demonstrated that the mutant strain was incapable of inducing MGC formation when delivered directly to the cytosol of a host cell line (French *et al.*, 2011). This suggests that MGC formation is mediated specifically by T6SS-5. This could support the argument that demonstrates the role of MGC formation in facilitating intercellular spreading, as explained in **section 1.3.1.5**.

The precise mechanism by which T6SS-5 can facilitate MGC formation by *B. pseudomallei* and *B. thailandensis* is unclear. Two studies have demonstrated a vital role for the C-terminal domain (CTD) of VgrG-5 (Tssl-5) in MGC formation (Toesca *et al.*, 2014, Schwarz *et al.*, 2014). VgrG (Tssl) proteins are components of the T6SS that are secreted along with (TssD) Hcp and PAAR and their presence in culture supernatants is considered a 'hallmark' of a functional T6SS as shown in (**Fig 1.2**). Some VgrG subunits contain a C-terminal extension that serves as an effector protein (Coulthurst, 2019). VgrG-5 also appears to have a C-terminal extension. The deletion of the CTD of VgrG-5 (Tssl-5) in *B. pseudomallei* and *B. thailandensis* can abolish their ability to induce the formation of MGC (Toesca *et al.*, 2014, Schwarz *et al.*, 2014). In addition, Toesca and colleagues have demonstrated that the deletion of the CTD of VgrG-5 has no effect on the secretion of TssD-5 (Toesca *et al.*, 2014). Although the CTD of VgrG-5 is important for MGC formation, it is still unclear if any other factors are needed.

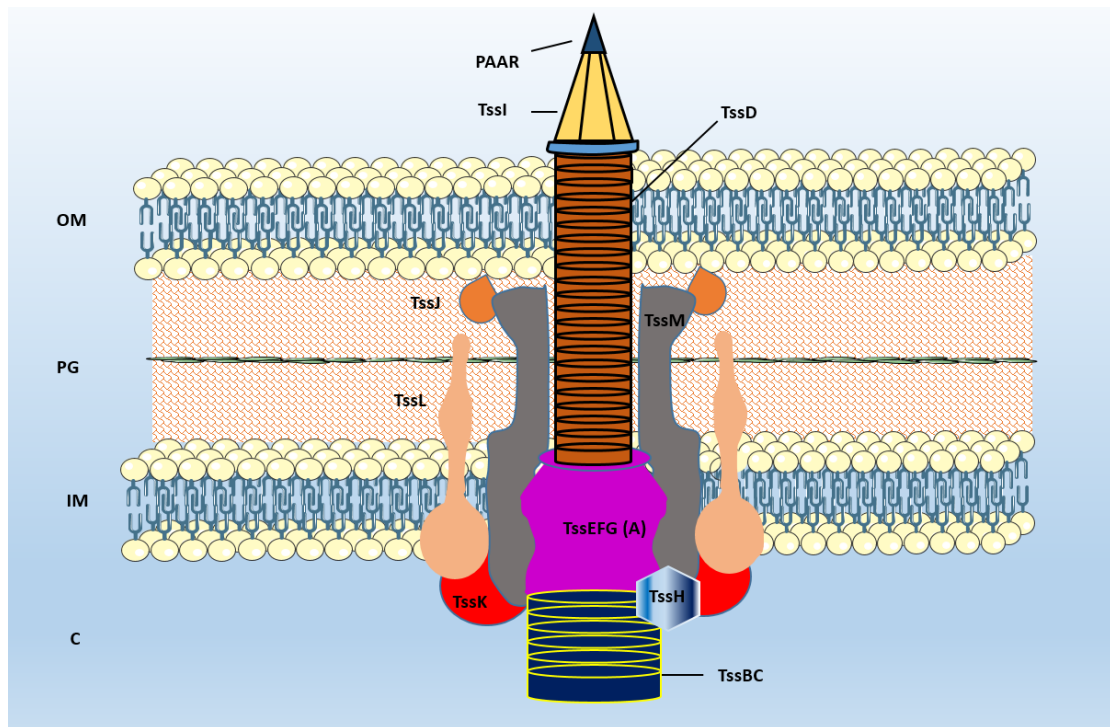


**Figure 1.2 Type VI secretion system structure.**

The T6SS is a protein secretion machine containing 14 different subunits (TssA-TssM and the PAAR protein) that injects effector proteins into target cells (either other bacteria or eukaryotic cells). It is required for pathogenicity in some bacteria. The T6SS-5 is used by *B. pseudomallei* and *B. thailandensis* to induce MGC formation. C: Cytoplasm, PG: peptidoglycan, IM: inner membrane and OM: outer membrane.

### 1.3.2 Mechanism of pathogenesis of *B. pseudomallei*

#### 1.3.2.1 Bacterial attachment to the host plasma membrane

*B. pseudomallei* can adhere to the host cell surface (Brown *et al.*, 2002). There are some proteins on the host cell surface that play a role in bacterial adhesion and signalling, such as Toll-like receptor (TLR), which is activated by *B. pseudomallei* LPS and flagella, which tend to activate types of innate immune cells such as neutrophils, macrophages and natural killer cells. Proinflammatory cytokines are released, as shown in **Fig 1.3** (Lazar Adler *et al.*, 2009).

Gori *et al.* suggest that the asialoganglioside aGM1–aGM2 receptor complex is one of the receptors to bind *B. pseudomallei* (Gori *et al.*, 1999). Furthermore, there is study that shows *P. aeruginosa* attachment to host cells through this complex, via type IV pili (Comolli *et al.*, 1999).

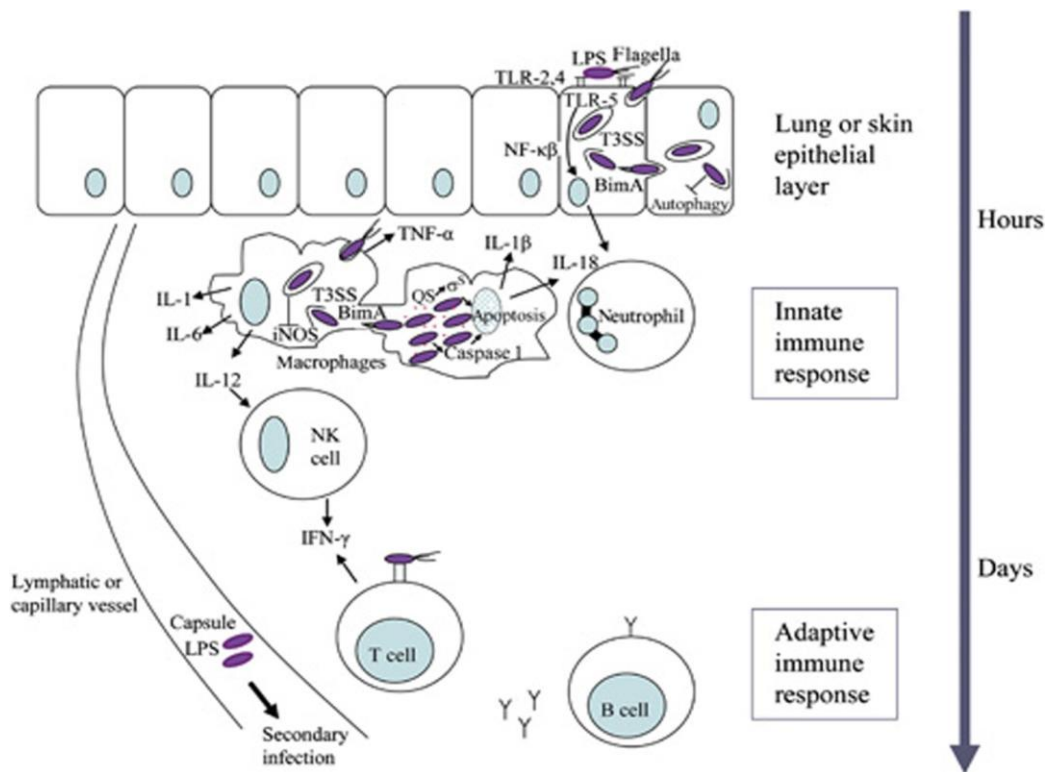


**Figure 1.3 The mechanism of pathogenesis by *B. pseudomallei* inside the mammalian cells.**

It is likely that *B. pseudomallei* initiates attachment to host cells using specific virulence factors such as capsule or pili. Invasion of the epithelial cells uses T3SS3 effector subunit proteins. TLR2 and TLR4 are activated by LPS of *B. pseudomallei*, activating innate immune cells including neutrophils, natural killer cells (NK) and macrophages. These activated cells produce pro-inflammatory cytokines that cause host tissue damage in acute cases of melioidosis. *B. pseudomallei* can replicate inside macrophages. The number of bacteria produced is determined by regulatory factors, for example, RpoS and QS. Bacteria can also escape via activation of apoptosis (**section 1.3.2.3**). Lymphatic vessels can facilitate the spreading of *B. pseudomallei* possibly carried within macrophages. *B. pseudomallei* infection can induce the host adaptive immunity by inducing IFN- $\gamma$  production, recruiting T cells and causing antibody production by B cells. With permission from Lazar Adler *et al.*, 2009.

### 1.3.2.2 Survival of *B. pseudomallei* inside host cells

*B. pseudomallei* can escape from the membrane-bound phagosome into the cytoplasm in infected macrophages or other mammalian cells (Kespichayawattana *et al.*, 2000). *B. pseudomallei* is able to propel itself within infected host cells using actin polymerisation, resulting in distinctive 'comet tails' (Kespichayawattana *et al.*, 2000). The mechanism of actin polymerisation, which can be induced by *B. pseudomallei* to achieve intracellular motility, is different from mechanisms of actin motility used by other intracellular pathogens (Breitbach *et al.*, 2003). *BimA* is a trimeric autotransporter protein and each subunit contains three WASP homology 2 (WH2) motifs, two of them are required for actin polymerisation activity

(Benanti *et al.*, 2015, Sitthidet *et al.*, 2011). *B. pseudomallei* can use *bimA* protein for inducing actin polymerisation. *B. pseudomallei bimA* mutants are unable to form actin tails *in vitro* (Stevens *et al.*, 2005).

There is evidence that this pathogen can invade macrophages without activating a key enzyme in the antimicrobial activity of the macrophages, known as inducible nitric oxide synthase (iNOS). *B. pseudomallei* could be surviving and replicating inside the phagocytic cells, due to lack of induction of iNOS expression (Utaisincharoen *et al.*, 2006). The reason for repression of iNOS might be the overexpression of Suppressor of Cytokine Signalling 3 (SOCS3) and Cytokine-Inducible SRC Homology 2-containing protein (CIS) inside the macrophage (Baral and Utaisincharoen, 2012). These proteins are negative regulators of cytokine production (Ekchariyawat *et al.*, 2005). The activation of these negative regulators is not well defined (Ekchariyawat *et al.*, 2007). Furthermore, Burtnick and co-workers have shown that T3SS-1 and T3SS-2 have no role in bacterial escaping from phagosome in RAW264.7 cells but have observed that T3SS-3 is involved in delayed phagosomal escape in RAW 264.7 cells (Burtnick *et al.*, 2011). However, Adler has found that the T3SS-1 ATPase mutant shows reduced intracellular replication in RAW 264.7 macrophage-like cells, suggesting that the T3SS-1 plays a role in the intracellular replication of *B. pseudomallei* (Adler, 2011).

In addition, *B. pseudomallei* can invade the A549 lung epithelial cell line and activate nuclear factor kappa-light-chain-enhancer of activated B cells (NF- $\kappa$ B), leading to the generation of IL-8 (Hengge-Aronis, 2002). Interestingly, *B. pseudomallei* invasion does not require NF- $\kappa$ B activation or IL-8 production (Hengge-Aronis, 2002). *B. pseudomallei* adhesion to the surface membrane of the epithelial cells causes signalling (Adler, 2011). The mitogen-activated protein (MAP) kinases are essential to many signalling pathways in the host cells (Utaisincharoen *et al.*, 2001). It has been reported that signalling proteins may be involved in many immune responses in the host against the bacterial invasion (Krachler *et al.*, 2011). There are specific inhibitors which can inhibit MAP kinase so that the activation of cells is significantly decreased and cytokine production from infected cells is also reduced (Utaisincharoen *et al.*, 2001). There are some findings which implicate MAP kinases in bacterial

internalisation. When a MAP kinase inhibitor is added to epithelial cells, *Listeria monocytogenes* invasion can be inhibited (Nickerson and Curtiss, 1997, Frederiksen and Leisner, 2015). However, this inhibitor has no effect on *S. enterica* serova *typhimurium* (*S. typhimurium*) invasion (Utaisincharoen *et al.*, 2006). One of the most important MAP kinase proteins is p38, which has a vital role in immune responses against a bacterial infections (Zhang *et al.*, 2007). To illustrate this, p38 MAP kinases can be activated in *S. typhimurium*-infected epithelial cell lines, so that it leads not only to NF- $\kappa$ B activation but also induces activator protein 1 (AP-1), which has a role in a number of cellular processes (Mynott *et al.*, 2002). Cytokine (such as IL-8) expression is switched off by inhibition of p38 MAP kinase with epithelial cells infected by *S. typhimurium* (Mynott *et al.*, 2002).

#### 1.3.2.3 Activation of cell death by *B. pseudomallei*

Pathogen clearance induces cell death in innate phagocytes (Haase *et al.*, 2003). There are different types of cell death in phagocytes including apoptosis, pyroptosis, necroptosis and necrosis (Fink and Cookson, 2005). There are two pathways that can trigger apoptosis: extrinsic or intrinsic (Wali *et al.*, 2013), involving death receptors and mitochondrial damage, respectively. The induction of apoptosis in infected cells depends on proteolytic enzymes caspase-7 and caspase-3, while pyroptosis depends on caspase-1 and caspase-11 (Lamkanfi and Dixit, 2010). Neutrophil apoptosis can be induced by intracellular bacteria and the oxidative burst (González-Cortés *et al.*, 2009). *B. pseudomallei* can delay the spontaneous apoptosis of human neutrophils via LPS and proinflammatory cytokines (Chanchamroen *et al.*, 2009).

In contrast, pyroptosis is another form of lytic cell death which can be activated by caspase-1 or caspase-11 (Mathur *et al.*, 2018). Human macrophages and mouse macrophages infected by *B. pseudomallei* can die due to caspase-1-dependent pyroptosis (Chanchamroen *et al.*, 2009, Miao *et al.*, 2010). However, a small number of cells also succumb by necrosis (Chanchamroen *et al.*, 2009). The knockout of caspase-1 in mice increases susceptibility to *B. pseudomallei* infection (Ceballos-Olvera *et al.*, 2011).

However, pyroptosis does not occur during the death of neutrophils (Chanchamroen *et al.*, 2009).

#### 1.3.2.4 Role of cell signalling molecules in *B. pseudomallei* infection and MGC formation

##### 1.3.2.4.1 p38

p38 plays a vital role in skeletal muscle biology, myoblast differentiation and myofibrillogenesis (Gardner *et al.*, 2015). Recently, a study has reported that p38, ERK, and mitogen-activated protein kinases play a role during *B. pseudomallei* infections (D'elia *et al.*, 2017). However, during infection, no modulation of the anti-or pro-inflammatory cytokines was shown (D'elia *et al.*, 2017). p38 activation could be controlled by M-CSF and can induce the receptor activator of NF- $\kappa$ B ligand (RANKL) that enhances cell fusion in osteoclast (Baek *et al.*, 2015). It was suggested that p38 could regulate NFATc1 expression and activity that regulates DC-STAMP expression. NFATc1 plays a positive role in osteoclast (Song *et al.*, 2009).

##### 1.3.2.4.2 p53

p53 is a transcription factor that controls programmed cell death (Crighton *et al.*, 2007). p53 is known also to prevent tumorigenesis induced through the apoptosis process (Deng and Wu, 2000). p53 plays a role in many cell functions including tissue homeostasis, metabolism, aging and stem cell state (Jackson *et al.*, 2012). It has been shown that the role of p53 in HPV infection (Levine, 2009). It can regulate many immune molecules via NF- $\kappa$ B and STAT pathways, such as IL-6 and inducible nitric oxide synthase (iNOS), which are important during bacterial infection (Levine, 2009). Recently, a study has reported that p53 regulates MGC formation in cancer cell lines (Fu *et al.*, 2013). Mirzayans and co-workers have observed that the deletion of p53 led to the induction of MGC formation (Mirzayans *et al.*, 2018). Gauster *et al.* have also demonstrated the positive involvement of p53 in the production of syncytia (Gauster *et al.*, 2018). The deletion of p53 induced autophagy, which could ensure survival in times of moderate nutrient depletion and/or oxidative stress (Humpton and Vousden, 2016).

## 1.4 *B. thailandensis* as an alternative model for *B. pseudomallei*

*B. thailandensis* is a saprophytic bacterium and is a non-pathogenic species for humans, although having a similar mechanism to *B. pseudomallei* in respect of immune response and cell attachment (Chen *et al.*, 2006, Yu *et al.*, 2006, Brett *et al.*, 1997, Wongprompitak *et al.*, 2009).

Both species have the same ability to invade and replicate inside macrophages or monocytes and A549 human lung epithelial cells (a carcinoma cell line) (Kespichayawattana *et al.*, 2004, Charoensap *et al.*, 2009). *B. pseudomallei* is more efficient than *B. thailandensis* in invasion, adherence and inducing cellular damage in A549 cells (Kespichayawattana *et al.*, 2004, Charoensap *et al.*, 2009). There is another difference between these two species, which is that *B. thailandensis* can assimilate L-arabinose, but *B. pseudomallei* cannot (Thibault *et al.*, 2004).

Although *B. thailandensis* is non-pathogenic to humans, severe infections can be caused by an inhalation challenge on mice with *B. thailandensis*, which possibly depends on virulence factors shared with *B. pseudomallei* (Yu *et al.*, 2006). In spite of *B. pseudomallei* being more virulent than *B. thailandensis*, doses of more than 10000 colony forming unit (CFU) of *B. thailandensis* killed mice (West *et al.*, 2008). Because *B. thailandensis* is less virulent but causes similar immune response to *B. pseudomallei*, *B. thailandensis* has been used as an alternative infection model (West *et al.*, 2012).

## 1.5 Multinucleate giant cells

MGCs are fused cells that are formed in some pathological states (Möst *et al.*, 1997, Milde *et al.*, 2015). These include melioidosis, tuberculosis, and the presence of foreign bodies (Möst *et al.*, 1997). The mechanisms of formation and pathological roles of MGC are not fully understood yet.

*In vitro* studies showed that monocytes can be induced to form MGC by using different conditioned media or by mixtures of cytokines (Möst *et al.*, 1990, Postlethwaite *et al.*, 1982). Some studies used lectins alone or in combination with IFN- $\gamma$ , others used phorbol myristate acetate (PMA) to induce cell fusion (Takashima *et al.*, 1993, Hassan *et al.*, 1989). Moreover, cytokines can play a role in monocyte fusion to inhibit or enhance MGC formation (Möst *et al.*,

1990). Fais *et al.* have shown that Interleukin-4 (IL-4) has the ability to inhibit MGC formation (Fais *et al.*, 1994).

### 1.5.1 Types of MGC

MGC can be classified depending on morphology into several types of cells: Langhan's giant cells (LGC), which occur during granulomatous inflammation and depend on epithelioid macrophages; the number of nuclei in this type of MGC is usually less than 20 (Okamoto *et al.*, 2003). Foreign-body giant cells (FBGC) occur in chronic disease and during responses to foreign bodies such as prostheses (Anderson, 2000); they can occur in epithelioid macrophages as well but the number of nuclei is typically more than 20 (Anderson, 2000).

#### 1.5.1.1 LGC

LGC have been identified in granulomatous diseases, for example, tuberculosis (TB), a serious lung disease caused by *Mycobacterium tuberculosis* (Sandor *et al.*, 2003). LGC have also been observed in sarcoidosis, a granulomatous disorder of unknown causes (Anderson, 2000). *M. tuberculosis* can induce LGC by stimulating cytokine and chemokine production (Saunders and Britton, 2007). LGC are formed by macrophages, lymphocytes and dendritic cells aggregated together in a granuloma (Saunders and Britton, 2007). The main features of LGC are the number of nuclei (around 20 nuclei per cell), in a circular or horseshoe-shape within giant cells (Okamoto *et al.*, 2003a). The mycobacterial envelope induces the macrophages to produce proinflammatory cytokines that are important in cellular aggregation and cell-cell fusion (Gasser and Möst, 1999). For example, interferon- $\gamma$  (IFN- $\gamma$ ) is induced by monocytes and macrophages to form LGC (Gasser and Möst, 1999). Toll-like Receptor 2, metalloproteinase domain-containing protein 9 (ADAM9) and integrin  $\beta$ 1-mediated pathways are also important during bacterial stimulation of LGC formation (Puissegur *et al.*, 2007). *M. tuberculosis* can penetrate into cells and tissues and can remain for decades before activation to form LGC (Parrish *et al.*, 1998). Parrish *et al.* also reported that DC-STAMP was increased during LGC formation and that the DC-STAMPKD reduced LGC formation (Parrish *et al.*, 1998).

### 1.5.1.2 Foreign body giant cells

Medical devices implanted in tissues cause the formation of FBGC, which are observed at the tissue-material interface *in vivo*, and are thought to remain there for the lifetime of the device. FBGCs have been involved in biodegradation of such medical devices (Anderson, 2000). The number of nuclei in FBGC is typically more than 20, and the shape of these giant cells are irregular and have a variety of shapes. FBGC formation is dependent on the surface area and the nature of the biomaterial used in the devices (Anderson, 2000).

McNally and colleagues used human IL4 to induce FBGC formation (McNally and Anderson, 2005). It was observed that IL4 could induce macrophages and monocytes to form very large FBGC. It has also been reported that Type 2 T helper lymphocytes (Th2) have a role in inducing cell fusion at the tissue-material interface in macrophages, due to the secretion of a high level of IL4 and IL13 (DeFife *et al.*, 1997). McNally and colleagues have demonstrated that during the adhesion process, the  $\beta 1$  and  $\beta 2$  integrin receptor families have a positive role in FBGC formation induced by IL4 (McNally and Anderson, 2002). Other integrins have been implicated in FBGC formation such as  $\alpha M\beta 2$ ,  $\alpha X\beta 2$ ,  $\alpha 5\beta 1 > \alpha V\beta 1 > \alpha 3\beta 1$ , and  $\alpha 2\beta 1$  (McNally *et al.*, 2007). In addition, several studies have reported that matrix metalloproteinase MMP-9 and DC-STAMP have a role in FBGC formation (MacLauchlan *et al.*, 2009, Yagi *et al.*, 2005).

### 1.5.1.3 Osteoclasts

Osteoclasts play important roles in the physiological bone remodelling process, bone development and regeneration (Hernández-Gil *et al.*, 2006, Charles and Aliprantis, 2014). The lack of osteoclasts leads to bone disorders such as osteoporosis (Segovia-Silvestre *et al.*, 2009, Jones *et al.*, 2011) whereas the increased activity of osteoclasts leads to disorders such as osteoporosis (Boyle *et al.*, 2003, Segovia-Silvestre *et al.*, 2009). The number of nuclei in this type of MGC is around 5-10. The osteoclast is formed from tissue-specific macrophages and myeloid precursor cells at or near the bone surface (Vignery, 2005). Osteoclasts can be induced by cytokines such as receptor activator of NF- $\kappa$ B ligand (RANKL) and macrophage colony-

stimulating factor (MCSF) (Aubin and Bonnelye, 2000). Osteoblasts produce osteoprotegerin (OPG) which can interact with RANKL, and RANKL also can interact with its RANKL receptor (Teitelbaum *et al.*, 2006). Simonet and colleagues have shown that OPG can reduce osteoclast formation in *vitro* and block bone resorption in *vivo* (Simonet *et al.*, 1997). Osteoclast-stimulating agents such as TNF- $\alpha$  can enhance RANKL production (Teitelbaum, 2005). Many cell surface molecules are involved in the formation of these giant cells (Yagi *et al.*, 2005). However, the pathway of how these osteoclasts form is still unclear. For example, DC-STAMP is implicated in osteoclast formation (Chiu and Ritchlin, 2016). Yagi and co-workers have used knock-out of DC-STAMP to investigate mice osteoclast formation and found that osteoclast formation was completely abrogated, leading to osteoporosis (Yagi *et al.*, 2005). Tspan-29 (CD9) has a positive involvement in osteoclast formation stimulated by RANKL in the RAW264.7 macrophage cell line (Ishii *et al.*, 2006). They also noticed that the CD9KD reduced osteoclast formation. In addition, it was noticed that CD9 distributed into lipid raft microdomains in RANKL-treated cells but not in untreated cells (Ishii *et al.*, 2006). This would suggest that the distribution of CD9 in microdomains plays a role during osteoclastogenesis (Ishii *et al.*, 2006).

#### 1.5.1.4 MGC in cancer

Cell-cell fusion may occur between somatic and tumour cells, leading to cancer (Wang *et al.*, 2012). There are several types of fusogenic cancers such as melanoma, in which malignant melanocytes can fuse with macrophages (Rachkovsky *et al.*, 1998). In breast cancer, cancerous cells can fuse with endothelial cells, and tumour cells can fuse each other (Mortensen *et al.*, 2004). Tumour cells also can fuse with somatic cells like monocytes, enhancing metastasis, epigenetic regulation and chromosomal aberration (Duelli and Lazebnik, 2003).

#### 1.5.2 Mechanism of macrophage fusion

Cytokines IL-4 and RANKL can induce the formation of different types of MGC, such as osteoclasts, FBGC and LGC (Jeganathan *et al.*, 2014). However, the specific mechanism of the MGC formation process is not well defined. Several studies have demonstrated that many surface molecules and

proteins play roles in macrophage fusion such as CD44, CD47, CD98, P2X<sub>7</sub>CD9, CD81, CD63, DC-STAMP, ADAMs and integrins (Shuster *et al.*, 2000, Yagi *et al.*, 2005, Chakraborty *et al.*, 2001, Takeda *et al.*, 2003). A study has reported that the cytoplasmic protein tyrosine phosphatase PTP-PEST (also known as PTPN12) plays a negative role *in vivo* and *in vitro* in macrophage fusion (Martinez *et al.*, 2009). Rhee and co-workers have demonstrated that the lack of PTP-PEST leads to hyperphosphorylation of the protein tyrosine kinase Pyk2, and then in response to cytokines, the ability of macrophages to migrate is increased whereas cell-cell adhesion and the rearrangement of the cytoskeleton was suppressed (Rhee *et al.*, 2013). Another pathway was demonstrated by Martinez and others who showed that transmembrane protein signalling adaptor protein DAP12 is crucial for cytokine-stimulated macrophage fusion (Martinez *et al.*, 2009). The depletion of DAP12 reduced MGC formation both *in vivo* and *in vitro* (Martinez *et al.*, 2009). The over-expression of DAP12 could also induce MGC formation by regulation of surface protein expression such as DC-STAMP, MMP9 and cadherin (Martinez *et al.*, 2009, Brown, 2011). Actin cytoskeleton rearrangement is important in MGC formation and it has been reported that it acts as the driving force for MGC formation by establishing membrane protrusions (Shilagardi *et al.*, 2013). These membrane protrusions are required to control the fusion process promoted by fusogenic proteins (Shilagardi *et al.*, 2013).

Moreover, it has been proposed that the mechanism of MGC formation is similar to phagocytosis (Vignery, 2005). Briefly, macrophages adhere to, and internalise, each other, then aggregated macrophages coated by two cell membranes. These two membranes are recycled, and host cells become integrated (Vignery, 2005).

This mechanism of macrophage fusion was also supported by other researchers. McNally *et al.* have shown that endoplasmic reticulum (ER) promoted cell fusion, with some markers of ER such as calregulin and calnexin co-localized at interfaces of cell fusion on cell surfaces during FBGC formation induced by IL4 (McNally and Anderson, 2005, McNally *et al.*, 1996). They also proposed that the FBGC formation could be reduced by inhibition of

ER components or by blockade of mannose receptor expression, a known regulator of FBGC formation (McNally and Anderson, 2005, McNally *et al.*, 1996).

As shown in **Fig 1.4**, the different stages of osteoclast formation in RAW264.7 EGFP cells stimulated by RANKL have been demonstrated using confocal microscopy (Takito *et al.*, 2012, Takito *et al.*, 2015). Two macrophages attached together show a delay before cell fusion occurs, which is required for a temporary actin superstructure formation, a zipper-like structure, at the contact site. This structure disappeared during the initial stage of cell fusion. A gap was formed between the parallel plasma membranes, and then membranes were fused, due to the podosome belts of distinct osteoclasts. Podosome is actin-rich structures found on the outer surface of the cell membrane of host cells (Takito *et al.*, 2012).

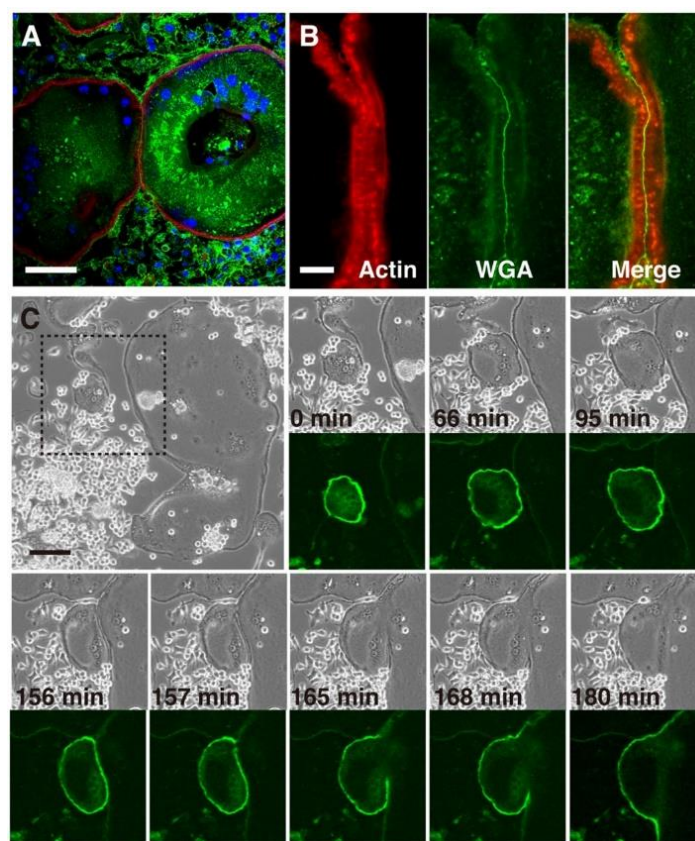


**Figure 1.4 The mechanism of macrophage fusion.**

A: Confocal microscopy images of RAW 264 mouse macrophages forming osteoclasts, the cells were stained with actin (red), plasma membrane (green) and nuclei stained DAPI (blue). Scale bar: 50µm. B: The site of connection between cell:cell in A. Scale bar 10µm. C: Confocal microscopy images at different time points show mouse macrophages, cell transfected with EGFP-actin. The grey images are phase contrast. With permission from (Takito *et al.*, 2012).

### 1.5.3 MGC formation induced by *B. pseudomallei*

The induction of MGC formation in host cells could enhance the ability of *B. pseudomallei* to survive and replicate inside host cells (Benanti *et al.*, 2015, Stevens *et al.*, 2005, French *et al.*, 2011, Kespichayawattana *et al.*, 2000). MGC are observed in some tissues of melioidosis cases including the lung, spleen and kidney (Wong *et al.*, 1995). *B. pseudomallei* also induces phagocytic and non-phagocytic cells to form MGC in tissue models (Franco *et al.*, 2018). *B. pseudomallei*, *B. mallei* and *B. thailandensis* employ the T6SS-5 to induce cell membrane fusion between the cell in which they are present and an adjacent host cell. This process leads to MGC formation and facilitates bacterial access to other uninfected cells (Chen *et al.*, 2011, Schwarz *et al.*, 2014, Toesca *et al.*, 2014, Whiteley *et al.*, 2017).

It has been shown that peripheral membrane protrusions form in both phagocytic and non-phagocytic cells after infection by *B. pseudomallei*, which are closely related to the protrusions that created in infected cells by *L. monocytogenes* and *Shigella flexneri* (Stevens and Galyov, 2004, de Chastellier and Berche, 1994, Kespichayawattana *et al.*, 2000). *B. pseudomallei* can escape from endosomes and can replicate in the cytoplasm of the cell to induce cell fusion (Ray *et al.*, 2009, Kespichayawattana *et al.*, 2004).

Another bacterial factor involved in MGC formation is (T6SS-5), as discussed above (Schell *et al.*, 2007, Shalom *et al.*, 2007). Shalom and co-workers showed that T6SS-5 expression was increased at the mRNA level following infection (Shalom *et al.*, 2007). Burtnick and colleagues have also shown the role of TssI-5 in MGC formation (Burtnick *et al.*, 2011).

In terms of the molecular mechanisms of MGC formation, Boddey *et al.* found that *B. pseudomallei* infection significantly increased the expression of NFATc1 nuclear factor of activated T-cells cytoplasmic 1, calcitonin receptor (CTR), tartrate-resistant acid phosphatase (TRAP), cathepsin K (CTSK). This data suggested that *B. pseudomallei* is able to induce many host cells factors involved in membrane fusion processes (Boddey *et al.*, 2007). However, these osteoclast markers did not change after *B. thailandensis* infection.

Boddey *et al* also showed that the expression of *lfpA* mRNA (lactonase family protein A) in *B. pseudomallei* is massively increased during infection of the RAW264.7 cell line compared to bacteria growing in the absence of RAW264.7 cells. Interestingly, the lack of *lfpA* dramatically decreased the expression of these host genes compared to the wild type *B. pseudomallei* (Boddey *et al.*, 2007).

Furthermore, bacterial infection can induce epigenetic changes such as histone modification, and chromatin regulation that have effects on small signalling molecules either increase or decrease host defence (Bierne *et al.*, 2012). Pegoraro *et al* investigated 43 epigenetic regulation compounds on MGC formation induced by *B. pseudomallei*. These epigenetic regulation compounds are Histone Deacetylase (HDAC) inhibitors. Interestingly, one of them called M-344 has a negative effect on MGC formation induced by *B. pseudomallei* (Pegoraro *et al.*, 2014).

Interestingly, Whiteley *et al* demonstrated that cholesterol depletion and proteins exposed on the host cell surface affected MGC formation induced by *B. thailandensis*. The ratio of MGC formation and the number of nuclei per MGC were reduced when infected cells were treated with trypsin compared with not treated. Furthermore, the modulation of cholesterol on the surface of host cells by methyl- $\beta$ -cyclodextrin treatment or exogenous addition of cholesterol reduced the ability of *B. thailandensis* to induce MGC formation. Methyl- $\beta$ -cyclodextrin (M $\beta$ CD) is an oligosaccharide with a hydrophobic cavity and a low ability to cross membranes. These findings suggested that the organization of the lipid bilayer in the cell membrane is involved in MGC formation (Whiteley *et al.*, 2017).

In addition, MGC formation induced by *B. pseudomallei* could be controlled by several host cell surface proteins including E-cadherin (CD324), fusion regulatory protein (CD98), E-selectin (CD62E), integrin-associated protein (CD47), and CD172 $\alpha$  (Suparak *et al.*, 2011). Anti-CD98, CD47, CD62E and CD324 antibodies completely blocked MGC formation induced by *B. Pseudomallei* in U937 human monocytic cells while anti-ICAM-1 (CD54) and LFA-1 antibodies only partly blocked the cell fusion (Suparak *et al.*, 2011).

The mechanism of fusion induced by *B. pseudomallei* and *B. thailandensis* is shown in **Fig 1.5**.

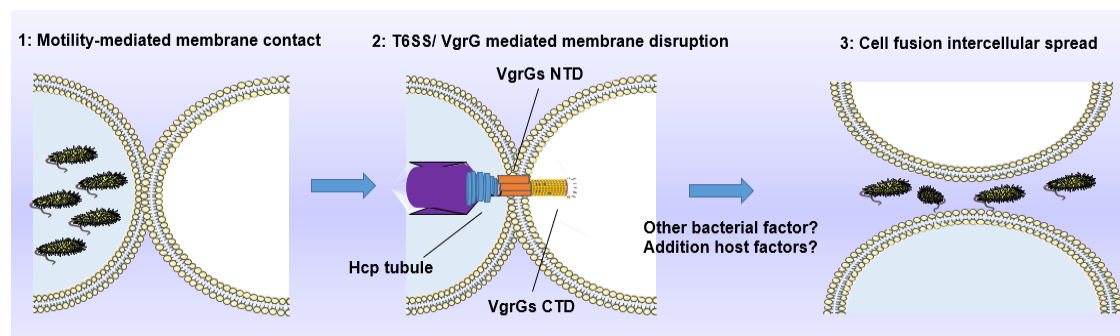


**Figure 1.5 The cell fusion process induced by *B. pseudomallei*.**

Host cells can be stimulated to form MGC by *B. pseudomallei* which can travel between cell and replicate inside the host cells. Bacteria can form actin mediated and deliver several proteins inside the host cells such as T3SS and T6SS, in regards its requirements to survive and spread. T3SS-3 proteins are involved in invasion and replication, rarely in cell fusion. T6SS-5 plays a major role in MGC formation by creating a hemi fusion zone that facilitates the membrane fusion process. Adapted from Toesca *et al.*, 2014.

## 1.6 Tetraspanins overview

Tspan molecules are a superfamily of membrane proteins with distinctive properties. Tspan molecules are expressed in different organisms ranging from invertebrates, including sponges, to the higher vertebrates, including mammals (Garcia-España *et al.*, 2008). 37 Tspans have found in insects (*Drosophila sp.*), 23 Tspans in sea anemones (*Nematostella sp.*) and 17 Tspans in plant (*Arabidopsis sp.*) (Todres *et al.*, 2000, Garcia-España *et al.*, 2008, Huang *et al.*, 2005). Their diversity of expression and specific roles in several biological processes have encouraged scientists to focus and shed light on the structure and function of Tspans since their discovery more than two decades ago (Oren *et al.*, 1990).

Recently, our group has demonstrated the role of Tspan molecules in MGC formation induced by *B. thailandensis*. It has been observed that CD9, CD63 and CD81 play a role in mouse macrophage cell fusion induced by *B. thailandensis* (Elgawidi, 2016). CD9 and CD81 are known to be involved in the MGC formation (Elgawidi, 2016). 33 human Tspan molecules have been identified (Todres *et al.*, 2000, DeSalle *et al.*, 2010, Charrin *et al.*, 2014). These proteins can also be expressed on cell organelles, for instance, the endosome and lysosome (Hemler, 2005, Hemler, 2003, Garcia-España *et al.*, 2006, Lakkaraju and Rodriguez-Boulán, 2008). Some Tspan molecules, for

example, CD9 are universally expressed, while others are only expressed in certain cells (Leung *et al.*, 2011).

Tspans are distinguished from other proteins by several motifs in the large extracellular loop (Seigneuret *et al.*, 2001). **Fig 1.6** shows simple Tspan structure (Seigneuret *et al.*, 2001). There are two extracellular loops: a small and large extracellular loop (EC1 and EC2), containing 20–28 and 76–131 amino acids, respectively (Seigneuret *et al.*, 2001). The intracellular termini consist of a short N terminal and a typically longer C-terminal cytoplasmic domain (Boucheix and Rubinstein, 2001). The EC2 can be divided into two regions: the variable and the constant region. The constant region of EC2 loop has 3 helices (A, B and E).

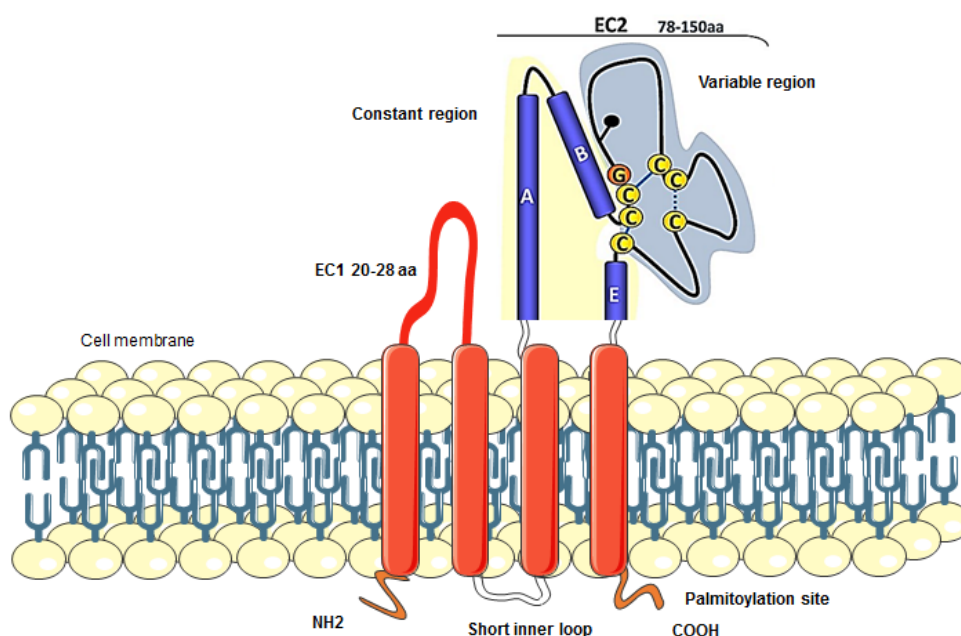


**Figure 1.6 Tspan protein structure.**

Tspan proteins are made of 4 transmembrane domains (TM), two extra-loops (large and small), and two intracellular domains (N-terminus NH<sub>2</sub>) and (C-terminus COOH). Adapted from Hemler, 2005.

### 1.6.1 Extracellular loops of Tspans

The EC2 is a variable domain that has a highly conserved Cys-Cys-Gly motif. The stability of Tspan structure is dependent on the formation of disulphide bridges by these Cys residues and others elsewhere in the EC2 (Parthasarathy *et al.*, 2009, Hemler, 2001). EC2 is considered an essential part of the protein for binding or association with partner proteins. For

example, Kazarov and co-workers have shown that CD151 can associate with  $\alpha 3\beta 1$  and  $\alpha 6\beta 1$ , which plays a role in cell migration (Kazarov *et al.*, 2002). Deletion of Gln-Arg-Asp 194–196 residues in the EC2 of CD151 leads to the blocking of cell migration. In another example, studies have shown that the deletion of Ser-Phe-Gln 173-175 residues from EC2 of CD9 in oocytes of the mouse leads to the blocking of sperm-egg fusion (Ha, 2004, Ellerman *et al.*, 2003). Furthermore, soluble recombinant EC2 domains of Tspans have also been used to interfere with interactions with other proteins (Takeda *et al.*, 2003, Parthasarathy *et al.*, 2009, Yáñez-Mó *et al.*, 2001).

Masciopinto and co-workers have revealed the function of the EC1 region (Masciopinto *et al.*, 2001). The deletion of EC1 of CD81 leads to a failure in the CD81 trafficking in the Golgi, and then decreased expression of CD81 on the cell surface (Masciopinto *et al.*, 2001).

### 1.6.2 Transmembrane domains of Tspans

All Tspan molecules have 4 helices in the transmembrane domain (Hemler, 2005). These helices are important for the facilitation of the Tspans interaction with their partner proteins in Tspan enriched microdomains (TEM) (Kashef *et al.*, 2013). It has been demonstrated that the deletion of CD151EC2 did not inhibit co-localisation with other Tspans, including CD9, CD63 and CD8, suggesting that there is intramembrane interaction (Berditchevski, 2001).

### 1.6.3 Palmitoylation sites

The hydrophobicity of Tspan proteins is enhanced by palmitoylation (Hemler, 2005). The intracellular side of all Tspan proteins have palmitic acid covalently linked to Cys residues during post-translational modification (Hemler, 2005). Many Tspan molecules have six conserved Cys that act as palmitoylation sites (Berditchevski, 2001, Kraus, 1991, Yang *et al.*, 2002, Zhou *et al.*, 2004, Seehafer *et al.*, 1988). This modification is important to stabilise the Tspan structure (Yang *et al.*, 2002). It has been demonstrated that palmitoylation can also contribute to the Tspan-Tspan interactions in the TEM and important in the rigidity of the protein (Charrin *et al.*, 2002, Yang *et al.*, 2004). Yang and colleagues have also shown that the deletion of palmitoylation sites from CD151 led to the reduction of the interaction between CD151, CD9 and

CD63, but not with  $\alpha 3\beta 1$  integrin (Yang *et al.*, 2002). In another example, Charrin and co-workers demonstrated that the mutation of palmitoylation sites in CD9 reduced the association between CD9 and CD81 (Charrin *et al.*, 2002).

#### 1.6.4 Tspan enriched microdomains

One of the main features of Tspan molecules is their capacity for interaction with other Tspan molecules and with other transmembrane proteins such as integrins, thereby acting as molecular coordinators to modulate the functional clustering of proteins in TEMs (Levy and Shoham, 2005, Charrin *et al.*, 2002, Hemler, 2008). It has been shown that Tspans can bind with other proteins such as immunoglobulin superfamily members to form TEMs (Maecker *et al.*, 1997, Seigneuret *et al.*, 2001). Furthermore, Suzuki *et al.* have shown that Tspans can bind with other proteins in lipid rafts such as CD14 and TLR4 proteins (Suzuki *et al.*, 2009), as described in **Fig 1.7**.

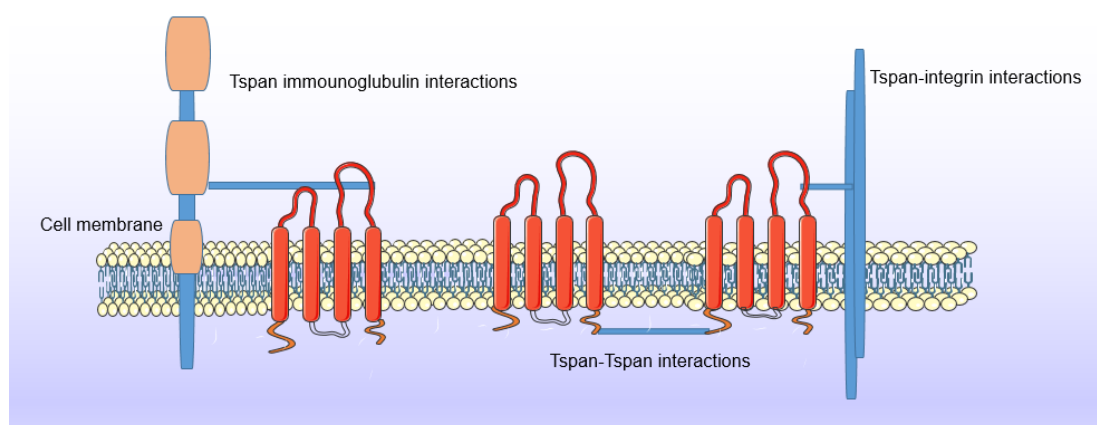


**Figure 1.7 Interactions of Tspans with partner proteins.**

It simply shows the Tspan-Tspan and Tspan-partner interaction with different regions of Tspan. The red colour shows Tspans, partner immunoglobulin (orange) and integrin (pale blue) family members. Tspan-partner interactions (blue interactions). Adapted from Levy and Shoham, 2005.

In addition, Hemler and Stipp have shown that many Tspans can bind with partners (Hemler, 2008, Stipp, 2010). It has been shown that Tspans can also co-localise with other Tspan molecules (Nydegger *et al.*, 2006, Andreu and Yáñez-Mó, 2014). However, Zuidsherwoude and colleagues have used stimulated emission depletion microscopy, to show that CD37, CD81, CD82 and CD53 are localised in separate clusters (Zuidsherwoude *et al.*, 2015).

Tspan-partner protein interactions can be categorized into different groups depending on the strength of interaction (Yauch and Hemler, 2000, Kovalenko *et al.*, 2007). Primary interactions are a direct interaction which is stable in strong detergents such as TritonX-100 (Kovalenko *et al.*, 2007). Secondary interactions are indirect interactions, which lose stability in strong detergent (Charrin *et al.*, 2002, Hemler, 2005).

Tertiary interactions are likely to be indirect interactions which display stability only in some weak detergents such [3-[(3-cholamidopropyl) dimethylammonio]-1-propanesulfonate] (CHAPS) (Tarrant *et al.*, 2003). van Spriël and Figdor have shown that Tspans can modulate the function of pathogen recognition receptors (PRRs) and signalling of specific PRRs by their recruitment into TEMs, hence leading to immune activation or tolerance (van Spriël and Figdor, 2010).

### 1.6.5 Other membrane proteins involved in MGC formation

#### 1.6.5.1 CD172 $\alpha$

Signal regulator protein  $\alpha$  (SIRP $\alpha$  or CD172 $\alpha$ ) plays a role in cell fusion (Galson and Roodman, 2011, Suparak *et al.*, 2011). It is also known as macrophage fusion receptor (MFR) (Vignery, 2008). CD172 $\alpha$  is a membrane glycoprotein that contains immunoglobulin superfamily domains (Gautam and Acharya, 2014). CD172 $\alpha$  interacts with CD47 and CD44, other transmembrane glycoproteins (Saginario *et al.*, 1998). Many studies have reported that these two membrane proteins have a role in the macrophage fusion process (Saginario *et al.*, 1998, Suparak *et al.*, 2011). The interaction between CD47 and CD172 $\alpha$  is due to the variable IgV loop of an immunoglobulin domain that plays a role in the stabilisation of the plasma membrane (Beare *et al.*, 2008).

In addition, a role for CD172 $\alpha$  has been demonstrated in osteoclast formation due to its interaction with CD47 (Koskinen *et al.*, 2013). It has also been reported that the deletion of CD47 could inhibit CD172 $\alpha$  signalling, blocking osteoclast formation (Koskinen *et al.*, 2013).

#### 1.6.5.2 CD98

CD98 is a type 2 transmembrane protein, having a large glycosylated extracellular domain a short transmembrane domain and a cytoplasmic tail (Campbell and Ginsberg, 2004). CD98 is also called a fusion regulatory protein-1 that plays a role in humoral immunity and cancer progression, as reviewed by (Cantor and Ginsberg, 2012). Anti-CD98 antibody can enhance MGC formation *in vitro* without any other trigger (Okamoto *et al.*, 2003b, Ohgimoto *et al.*, 1995). The role of CD98 could be related to its interaction with other proteins (Higuchi *et al.*, 1998, Ohgimoto *et al.*, 1995). It has been shown that TEM on the surface of eggs includes ADAM3, integrins, CD9 and CD81, which are positive regulators of sperm-egg fusion (Takahashi *et al.*, 2001).

#### 1.6.5.3 ADAMs

The disintegrin and metalloprotease domain (ADAM) membrane protein family have a role in ectodomain shedding, myoblast fusion, bacterial infection and inflammation (Huovila *et al.*, 1996, Gonzales *et al.*, 2004, Von *et al.*, 2016). Several distinct protein domains are contained in ADAMs proteins. The prodomain, a domain with a similar sequence to snake venom metalloproteases; the transmembrane domain with a Cys-rich region which promotes membrane fusion and a disintegrin like domain (Huovila *et al.*, 1996). It has been reported that the fertilin- $\alpha$  fusion peptide from the transmembrane Cys-rich domain could induce myoblast fusion (Huovila *et al.*, 1996). Furthermore, it has been reported that ADAM9 and ADAM11 also have a potential role in fusion in monkey and mouse cell fusion induced by RANKL and anti-CD98 antibody (Namba *et al.*, 2001).

ADAM10 is expressed in many cell types and several tissues and is considered as a key regulator of cellular processes including shedding extracellular domains of transmembrane proteins, lymphocyte development reviewed in (Chaimowitz *et al.*, 2012). Many studies have been reported that ADAM10 has a role in bacterial infection and MGC formation. For example, a role for ADAM10 in *Staphylococcus aureus* and *P. aeruginosa* infection has been demonstrated (Von *et al.*, 2016, Reboud *et al.*, 2017). It was observed that ADAM10 has a role in the control of the cytosolic  $\text{Ca}^{2+}$  concentration in

host cells, which is important to activate ExlA from *P. aeruginosa* on host cell-cell junctions (Reboud *et al.*, 2017). ExlA (Exolysin) is a pore-forming toxin in this bacterial species (Boukerb *et al.*, 2015).

Due to the liberation of the ectodomain from ADAM10 by the  $\gamma$ -secretase complex, the Notch Intracellular Domain (NICD) was released by this enzyme complex (Groot *et al.*, 2014). Interestingly, due to ADAM10 interactions with other partners, several different human diseases and pathological processes are associated with ADAM10 dysregulation (Seals and Courtneidge, 2003, Haining *et al.*, 2012, Ichiro *et al.*, 2011, Von *et al.*, 2016). For example, ADAM10 interacts with SAP97 and the clathrin adaptor molecule AP2, and these interactions are thought to regulate plasma membrane transport and internalisation (Elena *et al.*, 2007).

## 1.6.6 Functions of Tspans

### 1.6.6.1 Tspans in adhesion and motility

The role of many Tspans in cell-cell adhesion has been reported. For example, Yáñez-Mó *et al.* have demonstrated that Tspan molecules are engaged in the adhesion between neighbouring skin cells (Yáñez-Mó *et al.*, 2001). Peter *et al.*, and Dominguez-Bello and co-workers have demonstrated a role for Tspans in embryonic implantation (Peter, 2009), (Dominguez-Bello *et al.*, 2010). Barreiro and colleagues have also observed the role of Tspans in adhesion and extravasation of leukocytes (Barreiro *et al.*, 2005). In addition, the role of Tspans in membrane adhesion has been reported in a case with syncytia formation (Gordón-Alonso *et al.*, 2006), and the same role in myotubes formation (Hemler, 2003). Tspan interactions with other proteins such as integrins could promote the control of cell motility and cell migration. These complex processes involve extracellular proteins, signalling molecules, the components of cytoskeletal and adhesion receptors (Boucheix and Rubinstein, 2001).

### 1.6.6.2 Tspans in signalling

Some studies have shown that TEMs play a role in intracellular signalling pathways. Delaguillaumie *et al.* demonstrated that Tspan-28 (CD82) links the Rho-GTPase with the cytoskeleton (Delaguillaumie *et al.*, 2002). Furthermore,

integrin partner Tspans including CD9, CD81, CD151 can interact with phosphatidylinositol 4-kinase and protein kinase C (Hemler, 2005). Immunoprecipitation tests showed direct associations between CD9, CD53, CD81, CD82 and CD151 with phosphatidylinositol 4-kinase protein (P-I4K) (Zhang *et al.*, 2001). As shown in **Fig 1.8**, the role of Tspan molecules in cell processes requires interactions mediated by Tspan intra-cytoplasmic regions with the PDZ domains of as yet unknown intracellular proteins. For example, the intra-cytoplasmic regions of Tspans contribute to the activation of P-I4K to produce phosphatidylinositol-4, 5-bisphosphate (PtdIns (4, 5) P<sub>2</sub>), which is important to activate the SHCSRC-homology-2 domain-containing transforming protein (Hemler, 2005).

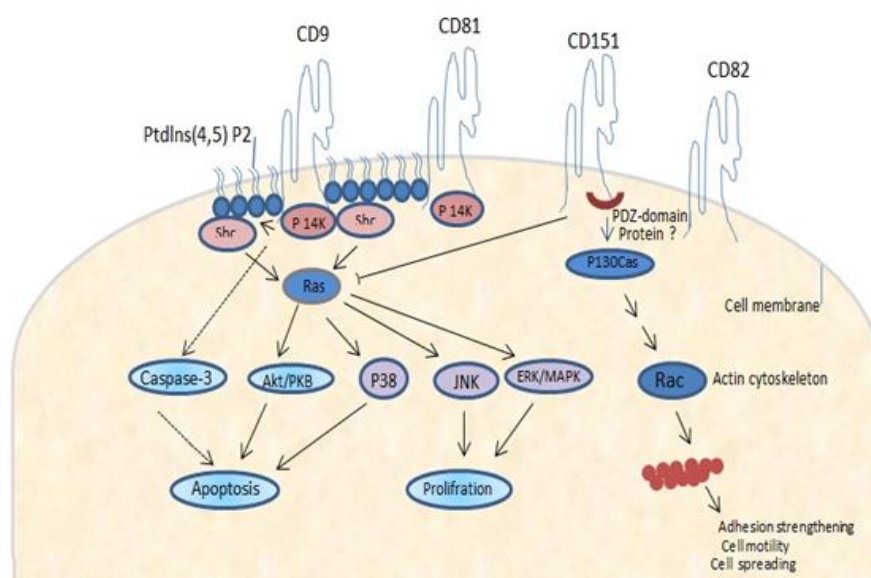


**Figure 1.8 Tspans signalling at the cell membrane.**

It is likely to show the CD9, CD81, CD151 and CD82 are involved with different cell signalling pathway such as JNK, MAPK and Akt/PKB pathway. These pathways have a major role in cell processes such as cell fusion, apoptosis, cell motility and proliferation. Adapted from Hemler, 2005.

#### 1.6.6.3 Tspans in protein trafficking

CD81 deletion in mice reduces the expression of CD19 at the B cell surface by 50%, and the CD19 glycosylation is also abnormal (Tsipi *et al.*, 2003). Furthermore, it has also been shown that a defect in ER to Golgi complex trafficking causes the entire loss of CD19 on the surface of cells deficient in CD81 (Zelm *et al.*, 2010). EWI-2 could also be controlled by CD81 (Stipp *et al.*, 2003). Moreover, uroplakins UPIa and UPIb interact with their partner

proteins and are involved in biosynthetic maturation to form complexes. The trafficking of UPII and UPIII in ER to cell membrane can be regulated by this interaction (Tu *et al.*, 2002). Furthermore, the interaction of CD63 with H<sup>+</sup>/K<sup>+</sup>-ATPase promotes trafficking to the plasma membrane (Juan *et al.*, 2005, Amy *et al.*, 2003).

In addition, the TspanC8 subfamily of Tspans (Tspan 5, Tspan-10, Tspan-14, Tspan-15, Tspan-17 and Tspan-33) have been shown to be involved in ADAM10 trafficking (Prox *et al.*, 2012, Emmanuel *et al.*, 2012, Haining *et al.*, 2012). ADAM10 expression is reduced by more than 50% from the surface of A549 cells following knock out of Tspan-15 (Haining *et al.*, 2012).

#### 1.6.6.4 Tspans in bacterial infections

##### 1.6.6.4.1 *Corynebacterium diphtheriae*

*C. diphtheriae* causes diphtheria and produces a cellular protein synthesis inhibitor called diphtheria toxin (DT) (Pappenheimer, 1977). Iwamoto and co-workers have shown that CD9 can indirectly interact with DT (Iwamoto *et al.*, 1994). CD9 can associate with pro-heparin-binding EGF-like growth factor (proHB-EGF), which is the direct receptor of DT (Mitamura *et al.*, 1992).

##### 1.6.6.4.2 Uropathogenic *Escherichia coli* (UPEC)

Tspan-20 and 21 are implicated in *E. coli* infection and adhesion (Wu *et al.*, 1996). Tspan-20 and 21 in the urinary tract epithelium can bind with fimbriated UPEC *E. coli* (Wu *et al.*, 1996), via FimH, a Type I fimbriae (Zhou *et al.*, 2001, Bo *et al.*, 2006). It has been demonstrated that CD63 is important in the internalisation of UPEC into vesicles within bladder epithelium cells (Bishop *et al.*, 2007).

##### 1.6.6.4.3 *Listeria monocytogenes*

*L. monocytogenes* is the causative agent of listeriosis (Gray and Killinger, 1966). There have been studies indicating that Tspan molecules have a cooperative role in the attachment of *L. monocytogenes* to the surface of cells (Tham *et al.*, 2010). *L. monocytogenes* needs CD81 for entry into epithelial cells (Tham *et al.*, 2010). It was also observed that CD9, CD63 and CD81 were recruited to bacterial uptake sites on host cells (Pizarro-Cerdá *et al.*, 2010). CD81 knockdown (KD) was found to inhibit bacterial uptake and could

block the type II phosphatidylinositol-4-kinase activation that is important in bacterium uptake (Pizarro-Cerdá *et al.*, 2010).

#### 1.6.6.4.4 *Chlamydia trachomatis*

*C. trachomatis* is an intracellular bacterium, the causative agent of sexually transmitted infections and trachoma (Peeling and Brunham, 1996). CD63 plays a role in *Chlamydia* infection (Beatty, 2006). It was found that CD63 can mobilise from multi-vesicular bodies and then be recruited into inclusion bodies of *Chlamydia* (Beatty, 2006). CD63KD or anti-CD63 antibody treatment affects this trafficking, leading to inhibition of *C. trachomatis* growth in host cells (Beatty, 2006, Beatty and Immunity, 2008).

#### 1.6.6.4.5 Role of Tspans in other bacterial species

Green *et al.* have shown that CD9, CD63 and CD151 are facilitators of adhesion of *S. pneumoniae*, *E. coli*, *Neisseria meningitidis*, *Neisseria lactamica* and *S. aureus* on the host cells (Green *et al.*, 2011). In published studies, members of my laboratory group have shown that CD9 and CD81 have positive effects on invasion and localization of *S. typhimurium* NCTC12023 (Hassuna *et al.*, 2017). Our lab showed that recombinant soluble EC2 of CD9, CD81 and CD63 had no effects on *B. thailandensis* infection, while the CD9KO in a mouse cell line reduced *B. thailandensis* uptake in the early stages of infection (Elgawidi, 2016). Ultimately, these studies have shown that bacterial colonisation and invasion of host cells can require the microdomain of Tspan molecules. However, these cooperative roles of Tspan molecules in bacterial infection needs further investigations to understand the specific roles of these proteins.

#### 1.6.6.5 Tspans and MGC formation

Tspan molecules have a role in some types of cell fusion including MGC, myoblast fusion, virus syncytium and sperm-egg fusion. Part of this project will be focused on the involvement of Tspan molecules in the formation of MGC in response to infection.

##### 1.6.6.5.1 CD9

The involvement of CD9 in MGC formation has been widely studied. CD9 in mice has a positive role in fertility, demonstrated using CD9KO (Kaji *et al.*,

2000, Le Naour *et al.*, 2000). Interestingly, the CD9KO seems to have a positive effect on the fusion of myoblasts (Charrin *et al.*, 2013). CD9 antibody also have been found to have a positive effect on human monocyte fusion, causing an increased number of nuclei in MGC (Charrin *et al.*, 2013).

CD9 is associated with many membrane proteins linked to fusion, such as CD47, CD44, and CD36 scavenger receptor, MMP-9, EWI-2 and DC-STAMP (Longhurst *et al.*, 1999, Dirk-Steffen *et al.*, 2004, Yashiro-Ohtani *et al.*, 2000, Huang *et al.*, 2011, Herr *et al.*, 2013, Stipp and Kolesnikova, 2001). Garner and *et al* have also found that CD9KD in human kidney cell lines reduced 80% of E-cadherin protein that has a role in cell fusion (Garner *et al.*, 2016). In contrast, Mirkina and colleagues have found that the CD63KD caused the up-regulation of E-cadherin, and the down-regulation of  $\beta$ -catenin, which has a role in cell fusion (Mirkina *et al.*, 2014). CD9 interaction with other fusion molecules makes it difficult to identify the specific role of CD9 in MGC formation. In addition, Takeda and co-workers have shown that the expression of CD9 is down-regulated when the monocytes are cultured under fusogenic conditions, but that CD63 is up-regulated in MGC formation under the same condition (Takeda *et al.*, 2003).

In addition, in previous publications by our group have revealed that soluble recombinant EC2 domains can inhibit giant cell formation from human monocytes or macrophages (Parthasarathy *et al.*, 2009, Hulme *et al.*, 2014). Furthermore, recombinant EC2 of CD9 inhibits MGC formation (Takeda *et al.*, 2003). In previous publications, members of my laboratory have demonstrated that constant regions from the large extracellular loop of CD9 can affect the formation of MGC. Recombinant CD9 chimeric EC2 protein and point mutants have been used to map the specific regions of the CD9EC2 which have the negative effect on MGC formation (Parthasarathy *et al.*, 2009, Hulme *et al.*, 2014). Interestingly, our research team have observed that CD9KO enhances MGC formation in a mouse macrophages cell line infected with *B. thailandensis* (Elgawidi, 2016). It was speculated that the deletion of CD9 might affect the expression level of other Tspans and Tspan-partner proteins.

#### 1.6.6.5.2 CD81

CD81 is also involved in MGC formation (Parthasarathy *et al.*, 2009, Hulme *et al.*, 2014). CD81 is also associated with partner proteins such as CD36 (Yount *et al.*, 2013) and EWI-2 (Mónica *et al.*, 2006). CD81 is also involved in MGC formation and may have a similar role to CD9 in fertility (Eric *et al.*, 2006). Wang and Pfenninger demonstrated that CD81 can associate with MFR, when bound with CD47 and could generate TEMs (Wang and Pfenninger, 2006). EWI-2 is also associated with many Tspan molecules such as CD9, CD81, CD82 and CD151 (Xin *et al.*, 2003, Charrin *et al.*, 2013).

#### 1.6.6.5.3 CD151

Many studies have reported that CD151 is involved in cell fusion. For example, Ziyat and co-workers noted that sperm-egg fusion could be reduced by using anti-CD151 antibody (Ziyat *et al.*, 2006). In addition, CD151 is involved in cell regulation processes (Hong *et al.*, 2006). For example, overexpression of CD151 can increase MMP-9 production and enhance cell motility (Hong *et al.*, 2006). CD151 can also control  $\beta$ 1 integrin trafficking, demonstrated using deletion of CD151 in mouse embryonic fibroblasts that resulted in increased cellular migration due to integrin cycling arrest (Li *et al.*, 2007).

#### 1.6.6.5.4 Other Tspans involved in MGC formation

Tspan-2 can interact with CD9, CD81 (Hemler, 2008, Nobuo *et al.*, 2002, Yaseen *et al.*, 2017). Tspan-2 has a high sequence identity to CD9 and CD81 (Nobuo *et al.*, 2002). Tspan-5 and Tspan-13 are implicated in many cell functions, for example in cell fusion and metastasis of breast cancer (Iwai *et al.*, 2007, Arencibia *et al.*, 2009, Sala-Valdés *et al.*, 2012). It has been shown that Tspan-13 plays a negative role in osteoclast formation, but that Tspan-5 has a positive role in osteoclast formation induced by RANKL (Iwai *et al.*, 2007). Tspan-15 can regulate TspanC8 and ADAM10 expression (Haining *et al.*, 2012). Interestingly, it has been shown that ADAM10 expression was reduced around 50% in Tspan-15KO A549 cells when compared with WT A549 cells (Jouannet *et al.*, 2016, Haining *et al.*, 2012).

## 1.7 The hypothesis and aims of the study

Previous studies suggest that Tspans are involved in MGC formation and may have indirect roles in MGC formation by affecting partner proteins that form TEM. *B. thailandensis* can induce MGC formation and is an alternative model of the causative agent of melioidosis, *B. pseudomallei*. We hypothesise that Tspans and Tspan-partner molecules are involved in MGC formation induced by *B. thailandensis*. Secondly, we hypothesise that the disruption of TEM by Tspan-related reagents could inhibit the adhesion or invasion of host cells by *B. thailandensis* and/or the formation of MGC, and thus prevent infection and fusion.

Overall aim: to investigate the roles of all human and mouse Tspans in infection by *B. thailandensis* and the resulting MGC formation in macrophages and lung epithelial cells.

Specific aims:

- To systemically investigate changes in Tspan and Tspan-partner genes expression in response to *B. thailandensis* infection, using real-time qPCR.
- To validate changes in gene expression at the protein level.
- To validate roles of selected Tspan molecules and partner proteins in MGC formation or/and bacterial infection, using KOs and KDs of Tspans and Tspan-partners in human lung epithelial cells.
- To investigate the effects of a Tspan-derived peptide on *B. thailandensis* infection.

## Chapter 2 Materials and methods

### 2.1 Materials

#### 2.1.1 Reagents and buffers

The reagents and buffer solutions were prepared according to the manufacturers' instructions and other resources (Roskams and Mellick, 2002, Lausted *et al.*, 2004, Wilson and Corlett, 2005). Sterile distilled water (dH<sub>2</sub>O) was used throughout the project unless otherwise stated. Bacteria culture media, buffers, glassware, tips and reagents were sterilised by autoclaving at 121°C for 20min. Stock solutions were autoclave-sterilised, and antibiotics were filtered using 0.2µm filter units. The following tables summarise the reagents, buffer solutions and other materials used in this project. Buffers and reagents used in this study are listed in **Table 2.1**.

**Table 2.1 Buffers and reagent solutions.**

Buffer/reagent	Preparation
TAE 50X (1l)	57.1ml glacial acetic acid, 242.2g Tris base, and 100ml 0.5M EDTA pH8
DNA loading dye 6X (100ml)	10mg bromophenol blue and 60g glycerol, 12ml 0.5M EDTA pH 8
RF1	100mM KCl, 61.1mM MnCl <sub>2</sub> , 30mM CH <sub>3</sub> CO <sub>2</sub> K, 10mM CaCl <sub>2</sub> , 15% (w/v) glycerol were dissolved in distilled water/the pH was 5.8 with 0.2M acetic acid. The components were filter sterilised through a 0.22µm membrane, and stored at 4°C.
RF2	Solution A: -0.5 M MOPS (4-morpholinepopenesulfonic acid) Solution B: 10mM KCl, 75mM CaCl <sub>2</sub> , 15% (w/v) glycerol, RF2 solution was prepared fresh (0.2ml of Solution A to 9.8ml of solution B)
0.4% (SRB) Sulforhodamine B	400mg SRB sodium salt (Sigma), 100ml 1% acetic acid
10mM (1X) PBS,	0.26g KH <sub>2</sub> PO <sub>4</sub> , 2.17g Na <sub>2</sub> HPO <sub>4</sub> -7H <sub>2</sub> O, 8.71g NaCl, 800ml

pH 7.4	dH <sub>2</sub> O
Flow cytometry and immunofluorescence microscopy blocking buffer (B/B/N)	0.1% sodium azide, 0.1% BSA in HBSS with Mg <sup>2+</sup> and Ca <sup>2+</sup> ions.
Cell lysis buffer (mammalian)	1% TritonX-100 in PBS
Freezing mixture (bacterial cells)	20% glycerol in LB medium
Freezing mixture (mammalian cells)	15% dimethyl sulphoxide (DMSO), 85% foetal calf serum (FCS)
HBSS (Hanks balanced salt solution) with divalent Mg and Ca elements	5.4mM KCl, 0.3mM Na <sub>2</sub> HPO <sub>4</sub> , 0.4mM KH <sub>2</sub> HPO <sub>4</sub> , 4.2mM NaHCO <sub>3</sub> , 1.3mM CaCl <sub>2</sub> , 0.5mM MgCl <sub>2</sub> , 0.6mM MgSO <sub>4</sub> , 137mM NaCl, 5.6mM D-glucose, 0.02% (w/v) phenol red (optional) with H <sub>2</sub> O to 1l, pH 7.4 (purchased from Lonza)
Giemsa solution (Sigma) 0.6% w/v	10% of Giemsa solution in 1x PBS
Acid/ethanol	5% acetic acid (v/v), 5% dH <sub>2</sub> O, 90% ethanol (v/v)
Trypsin/EDTA solution 10X	Prepared in sterile HBSS (see above): 0.25% (w/v) trypsin, 0.2% (w/v) EDTA (Sigma)
10x phosphate-buffered saline	80g NaCl, 2g KCl, 11.5g Na <sub>2</sub> HPO <sub>4</sub> , 2g KH <sub>2</sub> PO <sub>4</sub> dissolved in 1l H <sub>2</sub> O
Paraformaldehyde solution 4%	4g paraformaldehyde was added to 50ml of dH <sub>2</sub> O and 1ml 1M NaOH. The mixture was placed in a glass beaker, then the beaker was placed in a water bath for 1hr at 60°C, then 10ml of 10x PBS with pH 7.4 was added. Finally, the volume was made up to 100ml using dH <sub>2</sub> O. The prepared solution was cooled and filtered and was kept at 4°C.

## 2.1.2 Bacterial growth media

**Table 2.2 Bacterial growth media.**

Medium	Preparation
LB (Lysogeny Broth) (1l)	10g tryptone, 5g yeast extract, 10g NaCl. LB agar prepared with the same recipe with an additional 15g agar to make up to 1l medium
SOC (Super optimal broth) (1l)	20g tryptone, 5g yeast extract, 0.5g NaCl, 0.186g KCl, 0.952g MgCl <sub>2</sub> in dH <sub>2</sub> O
M9 Minimal Agar	0.5g glucose and 1.5g agar were dissolved in 90ml H <sub>2</sub> O, autoclaved then 10ml M9 salts, 0.1ml 1M MgSO <sub>4</sub> ·7H <sub>2</sub> O, 0.1ml 0.1M CaCl <sub>2</sub> (sterile) were added
Iso-Sensitest Broth (IST)	It was prepared by dissolving 21.4g IST powder in 1l dH <sub>2</sub> O. Agar was added to 1.5% (w/v)
Brain-Heart Infusion Broth (BHI)	37g of BHI powder in 1l ddH <sub>2</sub> O

## 2.1.3 Antibiotics

**Table 2.3 Antibiotics with working concentrations.**

Antibiotic	Concentration (µg/ml)
Amikacin	500
Kanamycin	500
Chloramphenicol	34-50
Neomycin (G418)	250-1000
Ampicillin	50-100
Penicillin/Streptomycin	10 units/100
Tetracycline	12.5
Hygromycin	250-500
Gentamicin	25-50

## 2.1.4 Bacterial strains

**Table 2.4 Bacterial species and their intended use.**

Bacterium	Description/Source
<i>E. coli</i> SM10 $\lambda$ pir	Dr Mark Thomas at the University of Sheffield, UK, Department of Infection and immunity and Cardiovascular Disease
<i>E. coli</i> S17 $\lambda$	
<i>E. coli</i> JM83	
<i>E. coli</i> DH5 $\alpha$	Life technologies
<i>B. thailandensis</i> E264	Soil isolates obtained from a rice field in central Thailand (Brett <i>et al.</i> 1998)
<i>B. thailandensis</i> E264- $\Delta$ tssK	E264 with a markerless in-frame deletion of 1,194bp of the central portion of <i>tssk</i> (BTH_I10857) (Hall, 2016)
<i>B. thailandensis</i> CDC272	This strain is a clinical isolate and was obtained from the patient (Glass <i>et al.</i> 2006)

## 2.1.5 Plasmids

**Table 2.5 Plasmids**

Plasmid	Description
pCMV6-AV-Tspan-2GFP	Human Tspan-2GFP expression construct, OriGene
MG226288 (CD9GFP)	Mouse CD9GFP expression construct, OriGene
pEGFP-N2	Mammalian GFP expression construct, Clontech
pBBR1MCS	Bacterial broad host range cloning vector, (Cm <sup>R</sup> )
pSHAFT-GFP	Containing GFP cloned between HindIII and PstI, (Amp <sup>R</sup> )
ptetmcCherry_pre-2	Containing mcCherry cloned between HindIII and xhoI, (Cm <sup>R</sup> )
pEX18Tp- <i>pheS</i> - <i>tssk</i>	pEX18Tp- <i>pheS</i> containing <i>tssk</i> cloned between Acc65I and BamHI (Tnp <sup>R</sup> )
pBBR1MCS-mcCherry	pBBR1MCS containing mcCherry cloned between HindIII and XhoI, (Cm <sup>R</sup> )
pBBR1MCS-GFP	pBBR1MCS containing GFP cloned between HindIII and PstI, (Cm <sup>R</sup> )

## 2.1.6 Primers and siRNA

NCBI Blast ([www.ncbi.nlm.nih.gov/tools/primer-blast](http://www.ncbi.nlm.nih.gov/tools/primer-blast)) was used to design all the primers. The parameters, which were used to all primers design, are exon-exon junction targeting, length of PCR product between 50 to 150bp and GC ratio at least 50% from all primers. All of the primers were purchased from Thermofisher. The primers were dissolved in TE buffer at 100 $\mu$ M and stored at -20°C.

### 2.1.6.1 Tspan primers

**Table 2.6 Primer sequences used to investigate Tspan genes expression.**

Tspan	Human primers	Mouse Primers
Tspan-1	F CGACCAAAAAGTAGAGGGTTGC R ACAATCATGGCAGCCAGCTC	F TGAAGCAGGTGATGGCATAGA R GCACTGCATGGTGTGTCTAT
Tspan-2	F 5'AAGGGGGTAGCTATCCGACA R 5' TGGACCTGTTCCGAGCTTTC	F CCATCATCTTCGGCGGCATC R TACAGCCCCACATAGAAATACTCT
Tspan-3	F CCTCATCTTCTGGTTTGTATCATC R GGGTTGGTCCATTGTAGGTCT	F TGGACTTGCCACGTTTGTCT R TGCGATCAACCTCGTTCTCC
Tspan-4	F GTGGCTGTGGAGAGCTTGG R GCCACAGGAAAGAGACCAGG	F GGACTGAAGACTGCTGGTGG R CACCCAGCCAGAAGAGCAG
Tspan-5	F GTGGGCATGGAATGAAAAAGGAG R CCAATGCACCCTGCAATCC	F GTCCTGCGTACTGCAGAGTT R GGACACCTTTTTTCATTCCACGC
Tspan-6	F TTTGCAAAGGCAAGCAAGGC R ATAACGCCAGTGATCTGCGA	F TGCCGCCATTGTTGGATTTG R CACCGCAACAATGCAACGTA
Tspan-7	F TCGTCTTCTGGATCACTGGG R CCGATGAGCACATAGGGAGC	F CTTTCGTCTTCTGGATCACTGG R GCTTTCCCAGACTCCAACG
Tspan-8	F GCCCCAGGAGCTATGACAAG R AGAGATTTCTGTATCCACGGACA	F AGGAAAAGAATCTGCAGGCAC R GCGTAGGCTCTGACGGATTT
Tspan-9	F TTGTTTGTGTCAGCAGCCAAGG R ACAGCCACAGAGCCAGAATATC	F TGAGAGGATCCAGCTCAGGT R CACAGCCACAGAGCCAGAAT
Tspan-10	F GAAGCAAAGACGAGCATCCG R GGGCTAGTCTGTGCATGGAG	F CAGAGAAGCCAAGGGACACC R GCAGTGTCTGAGACAGCAAG
Tspan-11	F CATGTGAGCAGGCCAGAA R CCCCAGCCAGAAGAAGAAG	F ACAGCGCGTACATCTTGTCT R GCCATACAGCCTCCCTCTAC
Tspan-12	F CCTGCTCTACGCCCTCAATC R ACTGCTTCTCTACCCTCGT	F TGCTGCAAGGACTCCTCCTA R CGTCGCTAACTCCCAGAGTG
Tspan-13	F GACACCTGTCTGGCTAGCTG R GGCCAATGCCACCAACAAAT	F GGTTTGTGGTGGCATTGGT R CCAAACACCCAGGATCTCTGTAA
Tspan-14	F CAAGGTCAGCTGCTGGTACA R GACAACCTCCAGCCAACCAGA	F GGAGCTGCTGAACTTGCTCT R AAGGAGGACCCGGGCG
Tspan-15	F GAGCGCCAGGATGCC R CCAATCAGCCAGAACACGGT	F GTTCAGGGTGGGGTATGTCG R GCCACAGCACTTGAACCTTCTC
Tspan-16	F GAAATGACAACGGGCCACAC R AACAGCCCTTCTGGTGGATG	not accessible in database
Tspan-17	F CTCAAAGTGGTGGAGGGGGAG R ATGCCAAAGATCTGGAGGAGG	F GTTAGGGACCCAGCGATGTC R TCACCGCCTTGATGTCACCTC
Tspan-18	F ACATCTCAACGCTGGCTCTC R GCCCCGCCAGAAATATGAA	F GCATCATCAGCAGGTCACCA R CCATGGTTCTTACCTGGGC
Tspan-19	F ACGCAGCATTTACGGGACTG RGTCCAAGAACCAAGAAAGCTCC	not accessible in database
Tspan-20	F TCCCGAAGATGGCCAAAGAC R GCAATGCCGCAACAACCAAT	F CTGGAGTCCCCTGGATGTTT R CGATGCCACACATACCAACAAT

Tspan-21	F CTGTTACCAAGGGCTGCTTC R GGATGGCAAACCCAAACCAC	F TACACGTGGGGCATATCGTG R CAACATCACAGGGAGGGTCC
Tspan-22	F GGCTCTTCGAGGTGACCATT R GGCTCTCGCTCTCAGATTCC	F CGTCTGGCTCTTTGAGGTGA R GTCCTCCGGGTTAGACACAC
Tspan-23	F GCCAAAAGGCTGGTGGATGA R TTGCTCTGGATCCGGTCAGC	F CAGTGGGTGAGCAACCGTTA R TGCTCTGGATCCGGTCAACT
CD151	F TGCGCCTGTACTTCATCCTG R GCTGCTGGTAGTAGGCGTAG	F GAGTGATCGCTCCTACCGTG R CCACCAGATCAACCACGCTT
CD53	F TTTTACACAAATAGCCCCGGA R ATTCTTGCCCTTTTCCAGGCA	F GTGGCTGAGGGTCTGAATGA R ACTGCAGTTGTGTCTGGATGA
CD37	F TTCGTGTCTTTGTGGGCTT R AAAATACAGGCCCAGGAGGC	F GGAAGTCCATCAGAAGCCCC R GACATCTTCGCCTGAGGGTC
CD82	F GGCTGCTGAAGCAGGAGAT R CAGCACTTCACCTGAGCCTG	F GGAGGCCTAAGGTGTGTCCA R AGAGAAGCAATTCTGTGGCA
CD81	F ACTGGGTTGGACGACACTTG R CTCCAGCCAGCTGGGAAC	F TCCTGTTTGCCTGTGAGGTG R ACATCCTTGGCGATCTGGTC
CD9	F AGGTCCC GCCAGTCCC R CCGGCAAGCCAGAAGATGAA	F CATCGCCGTGGTGTATGATCT R AGTCTTCAGGGCCGTTGTTC
CD63	F AGCCCTTGGAATTGCTTTTGT R AGACCCCTACATCACCTCGT	F TAGGAGTGTAAGGCCGGTCCG R CTGTTGGGCCTTTCTCCCG
Tspan-31	F GAAGACGGTCCCAATACCC R GCTCACCAGCATGTAGACCA	F CTGTAGTGCAGGTGTGCAAAA R AGGAACCTCTCCCACACAT
Tspan-32	F TCTGAGTCTGCCCTATCCACAG R CCCGCAGAGAAGGCCATT	F TTCCTAGTCTTGCTGCTGGG R GCCCAATAGCGCAGTGTTC
Tspan-33	F AGCCCGCTGGTAAAATACCT R AGGGCTGCTTCTGCATGCTT	F TGCTCTTCTGGGTAATCTCCA R CTGCTGCTGCTTATTAGC
GAPDH (human) RpL13a (Mouse)	F TGCACCACCAACTGCTTAGC R GGCATGGACTGTGGTCATGAG	F CCTGGAGGAGAAGAGGAAAAGAGA R TTGAGGACCTCTGTGTATTTGTCA

### 2.1.6.2 Other transmembrane proteins primer

**Table 2.7 Primer sequences used to investigate Tspan-partner genes expression.**

Name	Human Primers	Mouse Primers
CD44	F TGGCACCCGCTATGTGCGAG R GTAGCAGGGATTCTGTCTG	F CACCTTGGCCACCACTCCTAAT R CCCTTCTGTACATGGGAGTC
CD47	F AACCTCCTTCGTCATTGCCA R CATTGGTATACACGCCGCAA	F GAAAAACCGCACGGCCTTC R ACCTCCTTTCTCCTCCTCGT
CD98 (Slc3a2)	FTCATCATCCGGCCTTCATCG R: GAGCAGCAGCACGCAGA	F CCGCGTGTGATCCATCTCTA R TCATGGTGCCTGAGTCGC
CD49 $\alpha$	F GCCGCGCGGAAAAGATGAAT R CACAATTTGGCCCTGCTTGTA	F CGGACGCTGCGAAAAGATGA R CCGCAAGATTTGGCATTGCT
CD29	F GGTGCTCCTCGGGCAAATTA R GAGCCAATCTGGTCACCTCG	F TGCGGCTGCTAATGCTAGTT R CCAGTAGCCAGTTGCCTTGT
CD172 $\alpha$	F ATGAGCCCGAGAAGAATGCC R TGTGATATCATTGTGTCTGTGT	F CATCTTCCACACGGTTGCAC R CTGGGTTATTTCCCTGGCGT
CD206	F CGATCCGACCCTTCCTTGAC R TGTCTCCGCTTCATGCCATT	F GGCTGATTACGAGCAGTGGA R CATCACTCCAGGTGAACCCC
CD36	FGGTCCTACATCTCCGAAAGCA R ACAAGCTCTGGTTCTTATTACA	F TCCCAGAATTCTCAGCTGCTC R CACATTTGAGAAGGCAGCAAC
DC STAMP	F CCTACAGCCCTTGGGAAGTG R CCTGCGTCAGGTTTCTCTCA	F GTGTGCTTTGTGCTTGTGGA R CTCCCTGTGTCTAAGTTCCGC
EWIF	F TCCTGTCGTTGGCTCTTTGC R CAAAGTTTTGCTCGTGGGG	F CTCCTGTCGCTGGCTGTC R AGCTCCAGTCAAGTTCTGTC
EWI2	F TACATGCATGCCCTGGACAC R TGGGGAGTAAGGGATCACCG	F CCTGTTGGTGGGTACAGGAG R TGCAAGAACTGGGGTGCTAC

### 2.1.6.3 Primers of some regulatory proteins

**Table 2.8 Primer sequences used to investigate gene expression.**

Name	Human Primers	Mouse Primers
Caspase-1	F GCCCACCCTGAAAGAGTGA R TTCACCTTCTGCCACAGAC	F AAGAAACATGCGCACACAGC R CCTCAGGATCTTGTGAGCCA
Caspase-3	F CTCTGGTTTTTCGGTGGGTGT R CGCTTCCATGTATGATCTTTGGTT	F GGGGAGCTTGGAACGCTAAG R GAGTCCACTGACTTGCTCCC
P53	F TTCACCAAAGGTGCTGGAGTT R ACCCATCGACCATCAAGAGC	F GCCCATGCTACAGAGGAGTC R TCTAGGCTGGAGGCTGGAG
P38	F ATTTGTCAGGACAAGGGCTC R TCCAAACGGCTCAAAGGAGT	FAATTGGTCAGGACAAGGGCT R GAGTGGGTAAGCTGAGACGG
SOSC 3	F ACCTTTCTTATCCGCGACAG R TGCACCAGCTTGAGTACACAG	F TAGACTTCACGGCTGCCAAC R CGGGGAGCTAGTCCCGAA
iNOS	F TCCCGAAGTTCTCAAGGCAC R TTCTTCACTGTGGGGCTTGC	F CCCAGCTATGCGCGAGG R TTGTATTGTTGGGCTGGCTGG
$\beta$ -actin	F CCTTTGCCGATCCGCCG R GATATCATCATCCATGGTGAGCTGG	F CACTGTGCGAGTCGCGTCC R TCATCCATGGCGAACTGGTG

### 2.1.6.4 Sequence of Smart Pool Accell siRNA

**Table 2.9 Smart Pool Accell siRNA sequences.**

siRNA	Sequence
Tspan-13 siRNA, Dharmacon	UGAGUAAUCAGGAAGUAUA, CUGUUAAGCUCCAUUUGCC, GCCAUGUGCUCCAUCAUA, UCUGUUACUUGUAUUUUAUU
CD9 siRNA, Dharmacon	GUUGUAACUUCUCUUGAAG, CCAUGAAGAUUGGUGGGAU, GCAUGAUCUUCAGUAUGAU, CGUUGAACUGCUGUGGUUU
ADAM10 siRNA, Dharmacon	CAGUCAUGUUAAGCGAUU, GCAACGAUUUUAGAGGUUA, CCACUAAAGAUGAGUAAUU, GUGAUGAAUUUAAAGUAGA
Tspan-2 siRNA, Dharmacon	ON-TARGETplus SMARTpool siRNA: AUACGAAACUCACGAGAUG, CCUCAUAACUUACGUUUAC, CAUUGGAAUUGUCGGUAUU, CAAGAAUUGCAUCGAUGAA
Non-targeting siRNA, Dharmacon	ON-TARGETplus Non-Targeting Pool: UGGUUUACAUGUCGACUAA, UGGUUUACAUGUUGUGUGA, UGGUUUACAUGUUUUCUGA, UGGUUUACAUGUUUCCUA

## 2.1.7 Equipment and apparatus

**Table 2.10 Equipment**

Equipment and apparatus	Manufacturer
Electroporator	Bio-Rad (Gene pluser <sup>RII</sup> )
Bench centrifuge	Sigma (SciQuip)
Microscopes	light Olympus (CK40-SLP)
	Nikon (MAZUREK)
	Nikon A1+ Confocal imaging system
FACS Attune	Applied Biosystems Inc. (BD)
FACS LSR <sup>II</sup>	Applied Biosystems Inc (BD)
Spectrophotometer	Bio-Rad (S2000 UV/VIS) Diode-array
NanoDrop lite	Thermo Scientific (6VDC-18W)
Sensitive balance	Swiss Quality (Precisa 125A)
Thermocycler	G-STORM
Incubators	BIOHIT LTE laboratory thermal equipment LTD
Class I Microbiological Safety Cabinet	WALKER
Class II Microbiological safety Cabinet	BioMAT <sup>2</sup>
LT-4000 Microplate Reader	Labtech
7900HT Fast real-Time PCR	Applied Biosystems AbiPrism sequence

## 2.1.8 Analysis software

**Table 2.11 Software**

Programme	Comment
FlowJo	Analysis of flow cytometry results Source: <a href="http://www.flowjo.com">http://www.flowjo.com</a>
GraphPad Prism v6	Statistical and graphical analysis Source: <a href="http://www.graphpad.com/scientific-software/prism/">http://www.graphpad.com/scientific-software/prism/</a>
Image J	Calculation of number of nuclei per giant cell; image manipulation Source: <a href="http://imagej.nih.gov/ij/">http://imagej.nih.gov/ij/</a>
SnapGene Viewer	Plasmid gene map viewer Source: <a href="http://www.snapgene.com/products/snapgene_viewer/">http://www.snapgene.com/products/snapgene_viewer/</a>
Cell Quest Pro Flow cytometry software	Data acquisition and analysis
Excel Microsoft	Analysis of qPCR data

## 2.1.9 Antibodies

The primary and secondary antibodies and isotype controls used for immunofluorescent studies, fusion and infection assays are summarised in the following tables.

### 2.1.9.1 Primary antibodies and isotypes

**Table 2.12 Primary antibodies and isotypes.**

Antibody	Target	Specificity	Conc.µg/ml	Isotype	Cat.no. or Source
Mouse anti-human CD9 (602.29)	CD9	Human	10	Mouse IgG1	Prof. Andrews, University of Sheffield, UK
Mouse anti-CD151 (14A2)	CD151	Human	10	Mouse IgG1	Prof. Leonie Ashman University of Newcastle, Australia
Mouse anti-CD81	CD81	Human	10	Mouse IgG1	AbD serotec, 241202
Mouse anti-Tspan-11 (CF9)	Tspan-11	Human	10	Mouse IgG1	In house, CF9 (Jiraviriyakul, 2010)
Mouse anti-Tspan-15	Tspan-15	Human	10	Mouse IgG1	Dr. Mike Tomlinson, University of Birmingham
Rabbit anti-human Tspan-13	Tspan-13	Human	10	Rabbit IgG1	Genetex DK2291, GTX52155
Mouse anti-human Tspan-2 pAb	Tspan-2	Human	20	Mouse IgM	Dr. Ibrahim Yassin, University of Sheffield, UK
Mouse anti-human ADAM10	ADAM10	Human	1	Mouse IgG1	Abcam, 352702
Goat anti-mouse ADAM10	ADAM10	Mouse	5	Goat IgG	Abcam, 1475583
Mouse anti-human CD172α	CD172α	Human	5	Mouse IgG2a	Abcam, AED11629

### 2.1.9.2 Secondary antibodies

**Table 2.13 Secondary antibodies**

Antibody	Target	Specificity	Conc.	Source
anti-mouse IgG	Mouse IgG	FITC	1:300	Sigma
anti-rabbit IgG	rabbit IgG	FITC	1:300	Sigma
anti-Goat IgG	Goat IgG	FITC	1:300	Sigma

### 2.1.10 Mammalian cell lines

Two cell lines were used, A549 human lung epithelial cells and J774.2 mouse macrophage/monocyte cells. Both cells are commonly used as models to study the interaction of the bacterium with a host cell. A549 cells were obtained from the European Collection of Authenticated Cell Cultures (ECACC) and other cell lines from laboratories, as indicated in **Table 2.14**. All of them were grown under same conditions at 37°C with 5% CO<sub>2</sub>, and the media (from Gibco) were supplemented with 10% FCS with penicillin/streptomycin (P/S) (10 units/100µg/ml).

**Table 2.14 Mammalian cell lines.**

Cell line	Growth medium	Source	Comment
Human lung adenocarcinoma A549 (ECACC)	High glucose (4.5g/l) DMEM	ECACC	Used for fusion, infection transfection and functional studies
Human lung adenocarcinoma A549 transfected with TSPAN-2GFP overexpression	High glucose (4.5g/l) DMEM with G418 antibiotics	Dr.Yassin, University of Sheffield, made in house (Yaseen, 2017)	Used for fusion, infection and functional studies
Human lung adenocarcinoma A549 transfected GFP overexpression	High glucose (4.5g/l) DMEM with G418 antibiotics	Dr.Yassin, University of Sheffield, made in house (Yaseen, 2017)	Used for fusion, infection and functional studies as a control
Human lung adenocarcinoma A549 KO ADAM10 and Tspan-15	High glucose (4.5g/l) DMEM	Dr Mike Tomlinson, University of Birmingham	Used for infection and fusion studies
Human lung adenocarcinoma A549 KO CD9	High glucose (4.5g/l) DMEM	Dr David Blake, Department of Biology at Fort Lewis College	Used for infection and fusion studies
Mouse BALB/c monocyte/macrophage cell line J774.2	High glucose (4.5g/l) DMEM	ECACC, BALB/c	Used for fusion, infection, transfection and functional studies
Mouse BALB/c monocyte/macrophage cell line J774.2-GFP-CD9 overexpression	High glucose (4.5g/l) DMEM with G418 antibiotics	Dr Fawwaz Ali, University of Sheffield, made in house (Ali, 2016)	Used for fusion, infection, and functional studies
Mouse BALB/c monocyte/macrophage cell line J774.2-GFP	High glucose (4.5g/l) DMEM with G418 antibiotics	Dr Fawwaz Ali, Univ of Sheffield, made in house (Ali, 2016)	Used for fusion, infection, and functional studies as a control

## 2.2 Methods

### 2.2.1 Bacteriological techniques

#### 2.2.1.1 Bacterial glycerol stocks

Bacteria were incubated overnight in LB broth at 37°C in a shaking incubator. 850µl bacterial culture was added to 150µl of sterile glycerol in a cryovial tube. The final concentration of bacteria was about 85%. The mixture was transferred into labelled cryovial tubes, and then the bacterial cells were mixed gently with glycerol and made aliquots. Finally, tubes were stored at -80°C.

#### 2.2.1.2 Estimation of viable bacteria

The relationship between numbers of living bacteria and optical density (OD<sub>600</sub>) was evaluated using viable count and optical density at different time points (0, 2, 4, 6, 8 and 24hr). The number of bacteria were determined according to colony-forming units (CFU) and OD<sub>600</sub> at different time points (0, 2, 4, 6 and 8 hr). The number of bacterial cells were approximately 1x10<sup>8</sup> per ml at OD<sub>600</sub> 0.4. All the following assays in this study were used at OD<sub>600</sub> 0.4 to determine multiplicity of infection (MOI).

#### 2.2.1.3 Preparation of competent cells

Hanrahan's method was used to prepare *E. coli* to take genetic materials (Sambrook and Russell, 2006). Briefly, *E. coli* strains were grown for 24hr and a single colony was inoculated in 50ml of appropriate media at 37°C in shaking incubator. Typically, bacteria were grown to reach an OD<sub>600</sub> 0.4-0.5 and then placed on ice for 20min. The culture was centrifuged at 4000xg for 10min. The pellet was gently resuspended in 16ml of RF1 and then placed on ice for 30min. The cell suspension was centrifuged again at 4000xg for 10min and discarded the supernatant. The pellet was gently resuspended with 4ml of RF2 solution. The bacteria were placed on ice for 20min and were kept as 200-400µl aliquots in microcentrifuge tubes. Competent cells were stored indefinitely at -80°C, and could be used immediately.

#### 2.2.1.4 Plasmid extraction and purification

A miniprep kit from QIAGEN (QIAGEN Plasmid Mini Kit) was used, and the protocol was followed as the manufacturer's instructions. Briefly, 10ml LB

medium containing antibiotics was inoculated by a single colony of bacteria and was grown in shaking incubator for 18hr at 37°C. Bacteria culture was centrifuged at 4000xg for 10min at 4°C. The supernatant was discarded, and the pellet was re-suspended with 250µl of a resuspension buffer (P1), and there were no cells clump in a cell pellet. Lysis buffer (P2) was added and mixed thoroughly by inverting the sealed tube 4-6 times. After 3-5min, the mixture should be viscous and slightly clear. The neutralization buffer (N3) buffer 350µl was added and gently inverted 4-6 times. The mixture was centrifuged at 13,000xg for 10min at 4°C and the supernatant containing the plasmid. 800µl of supernatant was taken and put in spin column tube, and then spent down 1min 13000xg. 500µl of binding buffer was added and centrifuged at 13,000xg for 1min at 4°C. Then, 750µl of a wash buffer (PE) buffer was added to wash the DNA. Finally, the DNA was dissolved using 50µl Tris:EDTA (TE) buffer in the collection tube. The yield was quantified using a NanoDrop lite (Thermo) UV spectrophotometer at 260nm.

#### 2.2.1.5 Agarose gel electrophoresis

This method was used for the separation of DNA molecules based on their size. 0.8-1.5g/ml of agarose (Fisher Scientific) was dissolved in tris base, acetic acid and EDTA (TAE) buffer by boiling in a microwave. The volume of the gel was between 100ml and 200ml according to a number of samples. The agarose solution was left in room temperature to allow to cool around 55°C, and then the GelRed stain was added 5µl per each 100µl of agarose gel to stain the DNA fragments in agarose gel. A suitable comb was placed into a gel cast before pouring. The comb was removed after 30min to set, and the gel was transferred to an electrophoresis tank and the position of wells at the cathode end. TAE buffer was covered a gel cast. Typically, 1µl of 6X DNA gel loading dye (Thermo) and 5µl of samples were mixed before loading in the gel. DNA ladder was loaded with a suitable volume recommended by the manufacturer. Depending on the gel size, the gel was electrophoresed at 80-120V for 45-60min. To visualise the DNA pieces, the UV transilluminator was used an EDAS 290 imaging system (Kodak).

#### 2.2.1.5.1 Gene cloning strategy

Gene cloning was used to insert DNA fragments encoding (mCherry and GFP proteins) in an appropriate vector for *B. thailandensis*, pBBR1MCS. The p<sub>tet</sub>mCherry<sub>prey-2</sub> and pSHAFT-GFP vectors were used to take the mCherry and GFP fragments, respectively. These fragments were taken and inserted in broad host vector (pBBR1MCS), as shown in **Appendix Fig 1**.

#### 2.2.1.5.2 Restriction digestion

DNA restriction digestion was carried out according to manufacturer's (Promega) instructions in a volume of 30µl. DNA segments were purified by either GeneJET PCR purification to remove all contaminating enzymes and other molecules, or after separation on agarose gels and using the QIAquick Gel Extraction Kit Prior. The restriction digestion components were used as following:

**Table 2.15 Restriction digestion components.**

Materials	Sample
Vector DNA	1µg
Restriction enzyme	1µl
An appropriate buffer 10x	6µl
10x BSA	3µl
Nuclease-free water	To reach 30µl

#### 2.2.1.5.3 Gel extraction

QIAquick Gel Extraction Kit was used to extract appropriate fragments of DNA, according to the manufacturer's instructions. After DNA electrophoresis, the samples were illuminated using UV. Depending on size, DNA fragments were taken from the agarose using a sterile scalpel and transferred into a microcentrifuge tube for weighing. 3 volumes of buffer QG was added for each 1 volume of gel, and then samples were dissolved in a 60°C using a heater with vortexing. After dissolving the gel slice, the solution was added to a spin column and centrifuged at 13000xg for 1min. 750µl of buffer PE was added to the column to wash and then was centrifuged at max speed for 1min to remove all debris. The fragment of DNA was eluted using 30µl of water into a clean microcentrifuge tube.

#### 2.2.1.5.4 Ligation

After restriction enzyme digestion, the vectors and fragments were quantified using a NanoDrop 2000 (Thermo) UV spectrophotometer at 260nm. For ligation of DNA fragments, T4 DNA ligase enzyme (purchased from Promega) was used as manufacturer's instructions. The ratio was used around 3 insert DNA to 1 vector DNA with a total volume of ligation mixture of 30 $\mu$ l. Two negative controls were used to assess the ligation efficiency: a vector control with no ligase enzyme, and a ligation control with no insert DNA. Finally, these components were incubated overnight at 16°C. The ligation components were used as following:

**Table 2.16 Ligation components**

Materials	Sample	no ligase	No-insert DNA
Vector DNA	(25ng)	(25ng)	(25ng)
Insert DNA	(75ng)	(75ng)	-
Ligase buffer	1 $\mu$ l	1 $\mu$ l	1 $\mu$ l
DNA ligase	1 $\mu$ l	-	1 $\mu$ l
Nuclease-free water	To reach 30 $\mu$ l	30 $\mu$ l	30 $\mu$ l

#### 2.2.1.5.5 2 Bacterial transformation

*E. coli* SM10 ( $\lambda$ pir) and S17 $\lambda$  competent bacteria were used to transform the genetic materials into a heat-shock protocol. These bacteria were thawed on ice, and 1-2 $\mu$ l of a solution, containing more than 200-300 DNA, was mixed gently with 25 $\mu$ l of competent cells. The mixture was chilled on ice for 20-30min, and then the bacteria were shocked by placing the tube into a 42°C water bath for 80sec. The microcentrifuge tube was placed back on the ice for 2-5min. 750 $\mu$ l of LB medium was added to the mixture and left in a shaking incubator at 37°C for 2hr. 50 $\mu$ l of the mixture was plated on LB agar which has selective antibiotic marker chloramphenicol.

#### 2.2.1.5.6 Conjugation

The plasmid DNA was introduced to *B. thailandensis* using bacterial conjugation. This was accomplished using SM10 ( $\lambda$ pir) and S17 $\lambda$  competent cells with the self-transmissible plasmid RP4 integrated into the chromosome. 10ml overnight cultures of SM10 (donor) and *B. thailandensis* (recipient) were

prepared. 1ml from each bacterium into microcentrifuge tubes were taken from overnight cultures and centrifuged at 13000xg for 5min. The pelleted cells were washed by resuspension in 1ml of 0.85% (w/v) normal saline. The cells were centrifuged again at 13000xg for 5min, and the supernatant was discarded, and then the pellet was re-suspended in 100µl of 0.85% (w/v) saline.

50µl of donor and recipient cells were added to a new microcentrifuge tube and mixed gently. 25mm circular nitrocellulose filter membranes with a pore size of 0.45µm were placed on LB agar plates with sterile forceps. The cell mixture was then dropped onto the nitrocellulose membranes. The plates with the inoculated nitrocellulose filters were then incubated at 37°C for 18hr before the cells were recovered. The nitrocellulose filters were transferred into 25ml universal tubes with 4ml of 0.85% saline on the following day. The suspension was plated in medium with a selective antibiotic for recipient cells. This method was used for the transfer of GFP and mCherry plasmids.

#### 2.2.1.6 *B. thailandensis* mutant strain production by allelic replacement

Jamie Hall at the University of Sheffield, UK, Department of Infection and immunity and Cardiovascular Disease, generated *B. thailandensis* E264- $\Delta$ *tssK* strain (Hall, 2016) according to Barrett's method (Barrett *et al.*, 2008). The suicide pEX18Tp-pheS plasmid was applied to insert the guide of *tssk*. The first recombination used a trimethoprim resistance gene as a selective marker for plasmid delivery into the chromosome. The second recombination was detected by growth on plates, which contain p-chlorophenylalanine (cPhe). In the presence of cPhe, this plasmid caused cell death in *B.thailandensis*.

After insertion of the deleted gene of *tssk* into pEX18Tp-pheS, the plasmid was transformed into an *E. coli* SM10 $\lambda$ pir strain and then transferred into *B. thailandensis* E264 by conjugation as mentioned in **section 2.2.1.5.5**. As above, the first recombination was detected using the selection on plates containing trimethoprim. Then every single colony was streaked on the agar with 0.1% (w/v) cPhe to select cross recombination which confirmed the loss of plasmid from mutant and the wild type bacteria. Genomic DNA was

prepared from every single colony to confirm the deletion of the allele using colony PCR with primers flanking the original cloned region.

#### 2.2.1.7 DNA sequencing

Samples of plasmids were purified by the miniprep technique. Plasmid DNA concentration was around 100ng/µl and forward and reverse primers. An applied Biosystems' 3730 DNA analyser and Big Dye 3.1 sequencing kits were used in the DNA sequencing service at Genomics Core Facility, the University of Sheffield, UK. All data was analysed by SnapGene viewer program.

### 2.2.2 Tissue culture techniques

All experimental work in tissue culture was carried out in Class I and Class II laminar flow hoods (BioMAT).

#### 2.2.2.1 Culturing of J774.2 cells

The cells were cultured in DMEM with 10% FBS. When the cells were confluent, the medium was discarded, and the cells washed in 5ml HBSS. The adherent cells were harvested using 25mm a cell scraper with 5ml HBSS, then all harvested cell suspensions were placed in 5ml fresh medium. The cells were centrifuged at 200xg for 5min, and then the media was discarded, and the pellet mixed with 5ml fresh medium. Finally, the cells were split 1:14ml fresh medium.

#### 2.2.2.2 Culturing of A549 cells

The incubation conditions were at 37°C in 5% CO<sub>2</sub>. The harvesting of A549 cells was carried out using trypsinisation. After discarding the medium, the cells were washed with 5ml HBSS to remove all traces of serum. Then 3ml 1x Trypsin/EDTA (Lonza) was added and incubated for 6-8min. 7ml of DMEM medium containing serum was added and re-suspended by gentle aspiration. The pellet was centrifuged at 200xg for 5min. 5ml media was added to the pellet and re-suspended with complete media. Then cells were counted using a haemocytometer, and an appropriate number of cells were used for seeding for the next experiments. The cells were split 1ml:14ml fresh medium.

#### 2.2.2.3 Cell freezing

The confluent cells which reached 85-90% density were harvested and counted using a haemocytometer. The harvested cells were centrifuged at 200xg for 5min, then the supernatant was removed and the pellet was re-suspended with freezing medium (as mentioned in 2.3) at  $1-2 \times 10^6$  cells/ml. 1ml of cells was transferred to each cryovial tube, and then the vials were transferred to freezing plug-in liquid nitrogen for 2-3hr. Finally, the vials were stored in liquid nitrogen. All vials are labelled with the date of freezing and name of cells.

#### 2.2.2.4 Cell thawing

The cryovial was taken from a liquid nitrogen dewar and was shaken under warm water until the contents became semisolid. To avoid contamination, the outside of the cryovial was dried off and wiped with a 70% ethanol solution before opening. The cells were transferred quickly to a universal tube with 9ml fresh medium, and were centrifuged at 200xg for 5min. The supernatant was removed, and the pellet was re-suspended with 10ml complete medium, and then placed in a new flask.

#### 2.2.2.5 Viability of cells

After harvesting, the cell suspension was transferred to a haemocytometer counting chamber. Viability of cells was measured by adding 0.5ml of 0.2% trypan blue and 0.5ml of cell suspension to a tube. These were gently mixed after standing for 5min, and then loaded into the haemocytometer. Dead cells were stained with the blue dye, whereas live cells did not stain with trypan blue.

#### 2.2.2.6 Sulforhodamine B assay

A549 and J774.2 cells were used to investigate the effects of CD9 peptide 8005 and control on cell numbers in tissue culture 96-well plates. The colourimetric sulforhodamine B dye method was carried out according to (Vanicha and Kanyawim, 2006). Overnight incubation of 96 well plates with  $1 \times 10^4$  cells per well in 100ul at 37°C in 5% CO<sub>2</sub>. The plates were washed 3 times in 1x PBS and fixed with 50µl of trichloroacetic acid (TCA) at 4°C for 1hr. The plates were washed thoroughly using water and kept inverted on

tissue paper to dry. 100µl 0.4% SRB dye was added to each well for 45min with shaking at room temperature. The plates were washed with dH<sub>2</sub>O and then added 1% acetic acid and air-dried. Then 50µl of 10mM unbuffered Tris was added per well for the solubilisation of SRB dye, and incubated at room temperature with gentle shaking for 5min. A LT-4000 microplate reader at 570nm was used to measure absorbance.

#### 2.2.2.7 Cytotoxicity assays–MTT

Cells were seeded of  $1 \times 10^5$  cell/ml in a flat bottomed 96-well tissue culture plate in 100µl complete media (DMEM + 10% FBS) per well and incubated at 37°C, 5% CO<sub>2</sub> for 24hr to allow the cells to attach to the wells. The media was gently aspirated with a multi-channel pipette and washed 2x with 100µl HBSS. The bacteria were prepared at different MOI (1, 3, 5, 10 and 100) in DMEM +1% FBS. The cells were infected by adding 100µl from each MOI to 8 replicate wells. There were also 2 controls: no treatment positive cell death (with 1% TritonX-100), and only media without cells. After incubation for 2hr at 37°C in 5% CO<sub>2</sub>, the bacteria were removed using a multichannel pipette and washed 2x with HBSS. The media was replaced with DMEM +1% FBS with 500µg/ml kanamycin and amikacin to kill all outside bacterial and incubated for 16hr at 37°C in 5% CO<sub>2</sub>. The cells were washed 2x with HBSS. MTT (Sigma M5655) was prepared at 0.5mg/ml in medium without FBS, and 100µl added to each well. After 3hr of incubation at 37°C in 5% CO<sub>2</sub> in the dark, the media was gently aspirated and washed again with HBSS one time. Finally, 100µl DMSO was added to each well and left at room temperature for 1hr to solubilise in the dark. A LT-4000 microplate reader was used to measure absorbance at 540nm.

#### 2.2.2.8 Assessment of protein level by flow cytometry

Tspans and partner protein expression in J774.2 macrophages and A549 cells were measured using flow cytometry. WT J774.2 and A549 cells were harvested and kept on ice at all times at 4°C to avoid antigen capping. The cells were centrifuged at 200xg for 5min, and then the pellet was taken and re-suspended with BBN to approximately  $0.5 \times 10^6$ /ml. Cells were washed 2x with cold BBN by centrifugation. Cell pellets were incubated with 30µl of primary antibody (with a suitable concentration of antibody around 1-10µg/ml

in BBN) on ice for 45min. Cells were then washed 3 times with BBN and centrifugation at 500xg for 5min. Then, labelled secondary antibody was diluted 1:250 and 30µl added to the cell pellet and incubated on ice in the dark for 45min, and then washed 3 times as well. A LSRII flow cytometer used at the Medical School Flow Cytometry Facility, University of Sheffield. For analysis by flow cytometry, cells were gently resuspended with 0.3ml BBN and stored on ice until sampled. The data was manipulated using FlowJo software.

#### 2.2.2.9 Transfection of mammalian cells

Transfection of mammalian cells was performed by chemical and physical techniques.

##### 2.2.2.9.1 Transfection system using Gene Pulser II

J774.2 cells were seeded in a tissue culture plate to reach 90% confluency. Cells were harvested as mentioned in **section 2.2.2.1**.  $1 \times 10^7$  cells were re-suspended with 1ml of serum free-DMEM. 10µg of plasmid was mixed with cells in a tube and transferred to a chilled electroporation cuvette (Bio-Rad, 0.2cm gap width), then left on ice for 15min. The cells were pulsed in an electroporator at 250V/975µF for 4sec. The cells were placed on ice for 30min, re-suspended in DMEM+5% FCS, and then incubated overnight. After 18hr, the medium was replaced by fresh DMEM+10% FCS with a suitable concentration of selective antibiotic G418.

##### 2.2.2.9.2 Transfection system using Turbofect

Turbofect transfection (Thermo Scientific) was performed according to the manufacturer's instructions. Briefly,  $4 \times 10^5$  A549 cells/well were seeded in a tissue culture six-well plate. Cells were incubated overnight, and the confluency was around 70-85% confluent prior to transfection. 5µg of plasmid was added in 500µl of free media. 6µl of Turbofect transfection reagent was added to the mixture with vortexing and left at room temperature for 20min. After that, 500µl of the diluted DNA mixture was added to each well in a drop-drop gently, and then was incubated 24hr post-transfection. The media was removed from the plate and replaced with media containing selective marker, G418.

### 2.2.3 Peptide synthesis

8005 and control (SCR) peptides were provided by Dr Rahaf Issa at Department of Infection and Immunity and Cardiovascular Disease, the University of Sheffield, UK. The 8005 peptide is part of the CD9EC2. It was synthesised using solid-phase peptide synthesis with Fmoc chemistry by GenScript UK (**Table 2.17**). SCR peptide is randomly synthesized from the 8005 amino acid sequence. DMSO was used to dissolve the lyophilised stock at 2mM and stored at -20°C.

**Table 2.17 8005 and SCR sequences.**

Peptide	Comments	Peptide sequence
8005		SHKDEVIKEVQEFYKDTYNKLKTK DEPQRETLKAIHYALN
8005 SCR	Scrambled control	THDAEKKNPINDLKKEVLERVKQK TYESTHFADLYQIEYK

### 2.2.4 Real-time quantitative polymerase chain reaction (RT-qPCR)

The mRNA levels of Tspans in infected and uninfected cells were measured using qPCR.

#### 2.2.4.1 RNA extraction

QIAGEN RNeasy Mini Kits were used to extract mRNA from J774.2 and A549 cells before and after infection by *B. thailandensis*. J774.2 and A549 cells were grown overnight at  $8 \times 10^5$  cells in tissue culture 6 well plates. *B. thailandensis* CDC272 or E264 and E264- $\Delta$ tssK strains were grown in overnight culture. The cells were infected with *B. thailandensis* CDC272, E264 and E264- $\Delta$ tssK at MOI 3 for J774.2 and at MOI 5 for A549 cells. The medium was discarded after 2hr of infection and the cells were washed 2x with HBSS. Then medium containing 500µg/ml kanamycin and amikacin was added to kill all extracellular bacteria. After 16hr, the infected cells were scraped from the plates and centrifuged at 200xg for 5min. Cells were re-suspended in 350µl of lysis buffer, and then 350µl of 70% ethanol was added and mixed gently. The solution was transferred to RNA kit tubes and centrifuged at 9000xg for 15sec, then 700µl of RNA washing buffer (RW1) was added to remove carbohydrates, proteins and fatty acids and centrifuged at 9000xg for 15sec, after that 500µl of RNA precipitating elution buffer (RPE) was added, and then centrifuged for 15sec at 9000xg to remove traces of salts. 500µl of RPE was

added and centrifuged at 9000xg for 2min. Finally, 50µl of RNA-free water was added and centrifuged at 9000xg for 1min to get the RNA sample. The total concentration of RNA was measured using the NanoDrop lite spectrophotometer.

#### 2.2.4.2 RNA integrity

The RNA samples were treated by DNase I to remove genomic DNA contamination. The TURBO DNase kit was used according to the manufacturer's instructions. Briefly, 0.1 volume of 10xTURBO DNase buffer and 1µl TURBO DNase were added to RNA samples and kept in an incubator at 37°C for 30min. Then, 0.1x volume DNase inactivation reagent was added to all samples and the tubes were incubated at room temperature for 5min. The RNA samples were centrifuged at 10,000xg for 90sec, and then supernatants were collected in other tubes. Finally, the samples were stored at -80°C.

#### 2.2.4.3 cDNA synthesis

A High-Capacity cDNA Reverse Transcription Kit was used to make complementary DNA (cDNA) for the qPCR assay. All RNA samples (infected and uninfected) were standardized to a concentration of 75ng/µl. cDNA materials were prepared for each reaction as shown in **Table 2.18**. All samples were loaded into the thermal cycler machine. The settings of the thermal cycler machine are shown in **Table 2.19** and the cDNA samples were directly used for qPCR. There are two negative controls: no-RT (no reverse transcriptase), and no RNA (no sample, only master mix).

**Table 2.18 cDNA synthesis components.**

Materials	Volume (µl) Sample	Volume (µl) no-RT	Volume (µl) no RNA
10X RT buffer	2.0	2.0	2.0
10X RT random primer	2.0	2.0	2.0
25X dNTP mix (100mM)	0.8	0.8	0.8
Reverse transcriptase	1.0	0	1.0
Nuclease-free H <sub>2</sub> O	4.2	5.2	14.2
RNA samples	10	10	0
Total volume	20	20	20

**Table 2.19 Thermocycler steps for cDNA generation.**

Thermocycler steps	Step 1	Step 2	Step 3	Step 4
Temperature	25°C	37°C-45°C	85°C	4°C
Time	10min	120min	5min	Hold

**2.2.4.4 Quantification of the DNA product**

The SYBR green method was used to quantify PCR product. The reactions were prepared (**Table 2.20**) using 2x qPCR SYBR Green Master Mix (Primer Design Precision) according to the manufacturer's instructions. All samples were loaded into a 384 well plate and centrifuged at 200xg for 2min. Then the qPCR plate was placed into the 7900HT AbiPrism sequence detection system and run according to the following cycles (**Table 2.21**). In addition, the melting point of the primers was added to machine setting to detect primer specificity.

**Table 2.20 2x qPCR mastermix components.**

Materials	Volume (µl)
2x master mix with SYBR green (with ROX)	5
Forward primer	0.5
Reverse primer	0.5
Nuclease-free H <sub>2</sub> O	3
cDNA	1
A total volume	10

**Table 2.21 Parameters of qPCR reaction.**

qPCR reaction	x1 cycle	x40 cycles	
Reaction step	Enzyme activation	Denaturation	Data collection
Cycle length	10min	15sec	1min
Temperature	95°C	95°C	60°C

**Equation 2.1 Delta C<sub>t</sub> equations to analyse qPCR results**

The threshold cycle (C<sub>t</sub>) value were calculated as below:

$\Delta C_t$  value (Control) ( $\Delta C_t C$ ) = Average control C<sub>t</sub> value (test gene) - Average experimental C<sub>t</sub> value (housekeeping gene)

$\Delta C_t$  value experimental ( $\Delta C_t E$ ) = Average experimental C<sub>t</sub> value (test gene) - Average experimental C<sub>t</sub> value (housekeeping gene)

Delta Delta C<sub>t</sub> value ( $\Delta \Delta C_t$ ) =  $\Delta C_t E - \Delta C_t C$

The fold change ( $\Delta \Delta C_q$ ) =  $2^{-\Delta \Delta C_t}$

Percentage of KD was calculated as follows:

% KD =  $(1 - \Delta \Delta C_q) \times 100$

### 2.2.5 Infection assay

The modified kanamycin-protection assay was used to measure bacterial infection, internalised bacteria and intracellular survival. Overnight cultures of bacteria were centrifuged, washed and re-suspended in DMEM to prepare MOI 0.5, 1 and 3 for J774.2 cells, and MOI 3, 5 and 10 for A549 cells. They were incubated with the bacteria at 37°C in 5% CO<sub>2</sub> for 2hr and then washed 2x with HBSS to remove extracellular bacteria that have not adhered to the mammalian cells. One group of wells was washed 3x with HBSS and added 0.1% (v/v) TritonX-100 (lysis solution) for 15min. Serial dilutions of the lysates were plated onto LB agar and incubated at 37°C for 48hr. Colonies of bacteria were counted and the number of bacteria was calculated using the CFU equation as below. Furthermore, to measure internalised bacteria, cells were washed 2x with HBSS and incubated in DMEM containing 500µg/ml kanamycin and amikacin for 10min, and again washed 2x with HBSS. Then, the cells were lysed with 0.2% (v/v) TritonX-100 for 15min. The serial dilution and bacterial counting were followed as above.

#### Equation 2.2 Total bacteria

CFU/ml = (no. of colonies x dilution factor) / volume of culture plate

The total number of bacteria and internalised bacteria were routinely measured at 2hr post-infection. However, intracellular survival bacteria were routinely measured at 16hr post-infection.

### 2.2.6 Fusion assay

This assay was performed using the infection assay, as mentioned in **section 2.2.5**. The fusion index and the number of nuclei per MGC were measured at 2, 4, 10 and 16 hr post-infection. J774.2 cells were infected with *B. thailandensis* CDC272, E264 and E264- $\Delta$ tssK strains at MOI 0.5, 1, and 3. A549 cells were infected at MOI 3, 5 and 10. After 2hr of infection, the cells were washed 2x with HBSS. The infected cells were incubated for 16hr using kanamycin with amikacin at 500µg/ml to kill all extracellular bacteria. Then, the cells were washed with HBSS and fixed by absolute ethanol at room temperature for 30min. After that, cells were washed 2x with HBSS and stained with 20% Giemsa solution at room temperature for 30min. Finally, the

cells were washed with dH<sub>2</sub>O and allowed to dry. Images were captured with a Nikon light microscope using the 40x objective with at least 10 images per each well. The fusion index was calculated relative to normal host cells per field of view, as demonstrated in **Equation 2.3**.

#### **Equation 2.4 Fusion index and number of nuclei per MGC**

$$\text{Fusion index} = \frac{\text{number of nuclei in MGC}}{\text{total number of nuclei counted}} \times 100\%$$

$$\text{Nuclei per MGC} = \frac{\text{number of nuclei in MGC}}{\text{number of MGC}}$$

#### **2.2.7 Effect of Tspans and partner protein antibodies on bacterial infection and MGC formation in A549 cells**

1x10<sup>5</sup> A549 cells were seeded in tissue culture 96-well plates (100µl medium per well) overnight to reach 70% confluency. Cells were washed with warm HBSS and treated for 1hr with antibodies diluted with BBN (**Table 2.12**). 10µg/ml concentration of antibodies was used. Then cells were washed with HBSS and infected with *B. thailandensis* CDC272 and E264 at MOI 5. As described in **section 2.2.5**, the infected cells were incubated for 2hr and then washed 2x with HBSS. To determine the total number of bacteria, each well was washed 3x with HBSS and added 0.1% TritonX-100 for 15 min. Serial dilutions of the cell lysate were performed in HBSS and plated on LB agar at 48hr, and then the equation of CFU was used to measure bacteria. To determine only internalised bacteria, the wells were incubated with medium containing kanamycin and amikacin at 500µg/ml for 15min, to kill extracellular bacteria. The cells were washed with HBSS, 0.2% (v/v) TritonX-100 added for 15min, then CFU was quantified as above. To measure the fusion index and the number of nuclei per MGC after 2hr of infection, the cells were washed and incubated for a further 16hr with medium containing kanamycin and amikacin at 500µg/ml to prevent continued bacterial growth. The protocol described in **section 2.2.6** was then followed.

### 2.2.8 Effect of 8005 peptide derived from human CD9 on *B. thailandensis* infection and MGC formation to A549 cells

This modified method was performed to investigate the effect of peptides derived from human CD9 on bacterial infection and MGC formation. Briefly,  $1 \times 10^5$  A549 cells were seeded in 96-well tissue culture plates (100 $\mu$ l medium/well) overnight to reach 70% confluency. Cells were washed with warm HBSS and treated with 8005 and SCR for 1hr. The cells were washed with warm HBSS and infected with *B. thailandensis* CDC272 and E264 at MOI 5:1 bacteria. Then, the protocol mentioned in **section 2.2.5** and **section 2.2.6** was carried out for bacterial infection and fusion index.

### 2.2.9 Flow cytometric method for measuring bacterial binding to host cells

Binding was measured using flow cytometry (Valdivia, 1998, Pils *et al.*, 2006). Bacteria were labelled with two plasmids expressing GFP and mCherry. In brief, A549 cells were seeded  $1 \times 10^5$ /ml in 6 well tissue culture plate overnight at 37c in 5% CO<sub>2</sub> and bacteria were inoculated overnight culture. Cells were washed and infected with *B. thailandensis* CDC272, E264 and E264- $\Delta$ tssK labelled with mCherry and GFP at MOI 10, 25 and 50 for 2hr on the following day. The infected cells were washed 3 times with HBSS and gently scraped using a scraper, and then were washed and centrifuged at 200xg for 5min to remove unbound bacteria. Finally, they were fixed with 2% PFA and analysed by flow cytometry machine.

### 2.2.10 Knockdown

#### 2.2.10.1 siRNA Smart Pool Accell transfection

Smart Pool Accell was purchased from Dharmacon company, and the transfection method was performed according to the manufacturers' instructions. Briefly, cells were grown overnight with Accell medium plus 2.5% FBS to reach 70-90% confluency in 6 well tissue culture plate. 7.5 $\mu$ l of 100nM siRNA was mixed with 700 $\mu$ l Accell medium plus serum 2.5% FBS. The mixture was added in a dropwise fashion to each well of a 6 well plate. The cells were incubated at 37°C in 5% CO<sub>2</sub> for 72hr. Cell dissociation solution was used to harvest the cells and RNA extracted for measurement of the

gene KD efficiency after 72hr using qPCR. After 72hr, protein level changes were measured using flow cytometry which was described in **section 2.2.7**.

#### 2.2.10.2 Effect of KD on infection and MGC formation induced by *B. thailandensis*

This method was carried out to investigate the roles of Tspans and ADAM10 in bacterial infection and MGC formation induced by *B. thailandensis*. Typically, cells were grown overnight in Accell media with 2.5% of FBS (Sigma), as mentioned in **section 2.2.6.1**. After 72hr, the cells were harvested and seeded in tissue culture 96 well plates flat bottom. The cells were infected with bacteria. The protocol was followed as mentioned in **section 2.2.5** for infection assay to calculate the total number of bacteria and internalised bacteria, and as mentioned in **section 2.2.6** for measuring fusion index and a number of nuclei per MGC.

#### 2.2.11 Effect of *B. thailandensis* infection on the levels of Tspans and other surface molecules.

The levels of cell surface membrane protein levels were measured for uninfected and infected A549 cells by flow cytometry. Cells were seeded in 6 well tissue culture plates at  $2 \times 10^5$ /well for overnight. Cells were infected for 2hr with *B. thailandensis* CDC272, E264 and E264- $\Delta$ tssK. Bacteria were removed and cells were washed 2x with HBSS. The cells were incubated with medium containing 500 $\mu$ g/ml of kanamycin/amikacin antibiotics. For 2, 8 and 16hr of infection, the cells were harvested and prepared for flow cytometry (**section 2.2.7**) using appropriate concentrations of the primary antibodies, matching isotype controls and FITC-labelled secondary antibodies as shown in **Table 2.12** and **Table 2.13**.

#### 2.2.12 Fluorescent imaging of infected mammalian cells by *B. thailandensis*

On day 1, J774.2CD9GFP cells were grown at  $1.5 \times 10^5$  cells/ml on 6mm glass coverslips in 24 well tissue culture plates. In addition, *B. thailandensis* CDC272 and E264, labelled with mCherry protein, were grown in overnight culture. On day 2, the CD9GFP cells were infected at MOI 3 and incubated at 37°C in 5% CO<sub>2</sub> for 2hr. The infected cells were washed 2x with HBSS and

incubated with media containing 500µg/ml kanamycin and amikacin to kill all extracellular bacteria. Then they were incubated for 2hr. Finally, they were fixed in 2% paraformaldehyde for 10min, followed by washing 2x with HBSS. Coverslips were mounted using Vectashield (with DAPI) that was sealed onto slides, in darkness. The images are single optical sections and performed under identical conditions using immunofluorescence microscopy.

### 2.2.13 Statistical analyses

Statistical analyses were performed using GraphPad Prism.8. Significance was determined using an unpaired t-test, two-way or one-way ANOVA using Bonferroni post hoc analysis for multiple comparisons. Data are presented as mean  $\pm$ SEM unless otherwise stated. Flow cytometry results were normalized related to uninfected cells unless otherwise stated.

## Chapter 3 MGC formation following *B. thailandensis* infection

### 3.1 Introduction

*B. thailandensis* is a non-pathogenic bacterium and is widely used as a model of *B. pseudomallei*, the causative agent of melioidosis. In tissues infected with *B. pseudomallei*, one of the histopathological features is the presence of distinctive MGC formation, potentially a protective structure for the bacteria. However, the molecular mechanisms of this pathogenic process have not been elucidated. The two main features of *B. pseudomallei* infections are long periods of latency, due to the ability to survive intracellularly, and MGC formation. *B. pseudomallei* can infect a range of cell types, is able to avoid killing by macrophages and is also able to promote cell fusion and induce MGC formation by bacterial effectors (Wong *et al.*, 1995). Previous studies have shown that T6SS-5 of *B. pseudomallei* and *B. thailandensis* have a major role in MGC formation (Toesca *et al.*, 2014, Schwarz *et al.*, 2014, French *et al.*, 2011). Interestingly, *B. thailandensis* was able to induce MGC formation in a strain-dependent manner. In particular, *B. thailandensis* CDC272 was most effective at causing MGC formation in J774.1 cells. In contrast, *B. thailandensis* E264 was poor at causing MGC formation in J774.1 cells (Wand *et al.*, 2011). This chapter will describe how *B. thailandensis* CDC272 and E264 can induce MGC formation in J774.2 mouse macrophages and A549 human lung epithelial cells. This chapter will also demonstrate the transformation of fluorescent protein expression vectors into two *B. thailandensis* strains. These were generated as such strains could facilitate the quantification and characterization of infected mammalian cells. In addition, mammalian cells were transfected with CD9GFP to facilitate the tracking of this protein during infection and MGC formation.

### 3.2 Aims

In this chapter, tools for subsequent experiments were generated and tested. Firstly, the growth characteristics of two strains of *B. thailandensis* (CDC272 and E264) were characterized using different counting methods. Secondly, two cells lines, A549 human lung epithelial and J774.2 mouse macrophage,

were investigated for infection and induction of MGC formation by the two strains of *B. thailandensis* and a non-fusogenic mutant strain (*B. thailandensis* E264- $\Delta$ tssK). Thirdly, fluorescent *B. thailandensis* strains were produced and characterised to determine if MGC formation and bacterial infection are the same as the wild-type strains. Finally, fluorescently labelled A549 and J774.2 cells were investigated to determine if they have similar properties to the wild type cell lines.

### 3.3 Results

#### 3.3.1 *B. thailandensis* infection

##### 3.3.1.1 Estimation of viable bacteria

Two methods of quantifying the number of bacteria in growth cultures were compared to determine the most accurate and convenient method for the preparation of MOI for the subsequent experiments: optical density (OD<sub>600</sub>) or colony forming unit (CFU). As described in **section 2.2.1.2**, bacterial strains were grown in LB medium at 37°C, then numbers were estimated by measuring both the OD<sub>600</sub> and CFU of the culture at 0, 2, 4, 6 and 8hr after inoculation. As **Fig 3.1** shows, bacterial growth gradually increased over the given time. Also, the number of bacteria, calculated by the CFU method, was about  $1 \times 10^8$  cells per ml when the OD<sub>600</sub> was approximately 0.4. This value of OD<sub>600</sub> was used in all following experiments.

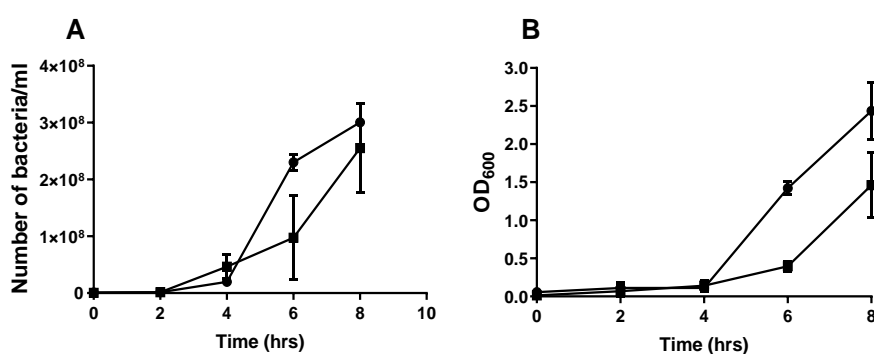


**Figure 3.1 Growth curves for *B. thailandensis* strains.**

Both strains of bacteria were cultured and incubated in Luria-Bertani broth and were incubated in a shaking incubator at 37°C. CFU and OD<sub>600</sub> methods were used to measure the numbers of bacteria at different time points. **A:** growth curves of *B. thailandensis* CDC272 and E264 strains using OD<sub>600</sub>. **B:** growth curves of *B. thailandensis* CDC272 and E264 strains using CFU. The results are the means ( $\pm$  SEM) of 2 independent experiments each performed in 2 technical replicates.

### 3.3.1.2 Assessment of fluorescent proteins expression in *B. thailandensis* by flow cytometry

In this work, plasmids encoding mCherry and GFP were used to tag *B. thailandensis* E264 and CDC272, as described in **section 2.2.1.5**. *B. thailandensis* expressing mCherry was used to detect any co-localisation between *B. thailandensis* and CD9 during infection. *B. thailandensis* expressing GFP were used to detect binding to host cells using flow cytometry. Flow cytometry showed that more than 95% of bacteria have mCherry and GFP expression (**Fig 3.2** and **Fig 3.3**). According to this result, we decided mCherry or GFP-tagged bacteria could be used for bacterial binding and microscopic studies.

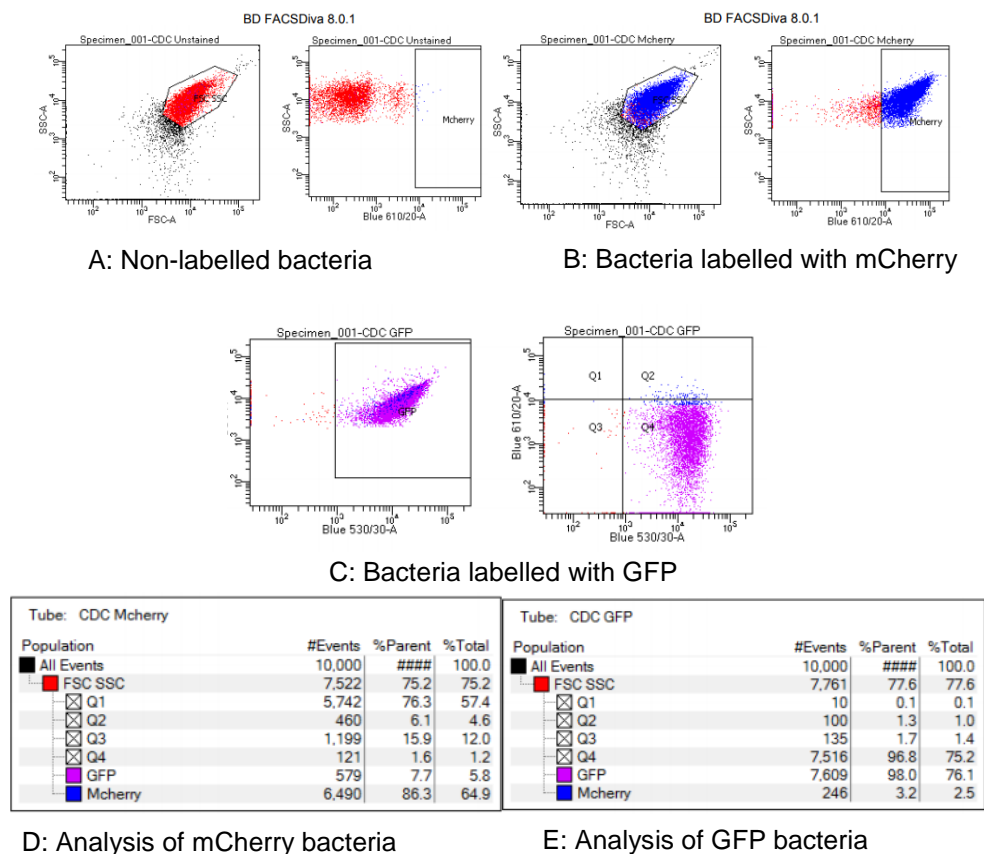


**Figure 3.2 Flow cytometry analysis of GFP and mCherry expression in *B. thailandensis* CDC272.**

*B. thailandensis* CDC272 were transformed with mCherry or GFP as described in **section 2.2.1.5**. Fluorescent bacteria were detected using BL-1 A530-30 and red 610-20A channels of an LSR-II flow cytometer. Untagged bacteria were used as a negative control. **A:** Negative control *B. thailandensis* CDC272, showing the gating strategy. **B:** *B. thailandensis* CDC272 tagged with GFP. **C:** *B. thailandensis* CDC272 tagged with mCherry. **D:** Percentage of positive *B. thailandensis* CDC272 tagged with mCherry compared with untagged bacteria. **E:** Percentage of positive *B. thailandensis* CDC272 tagged with GFP compared with untagged strain. The results are representative of 2 independent experiments each performed in 2 technical replicates.

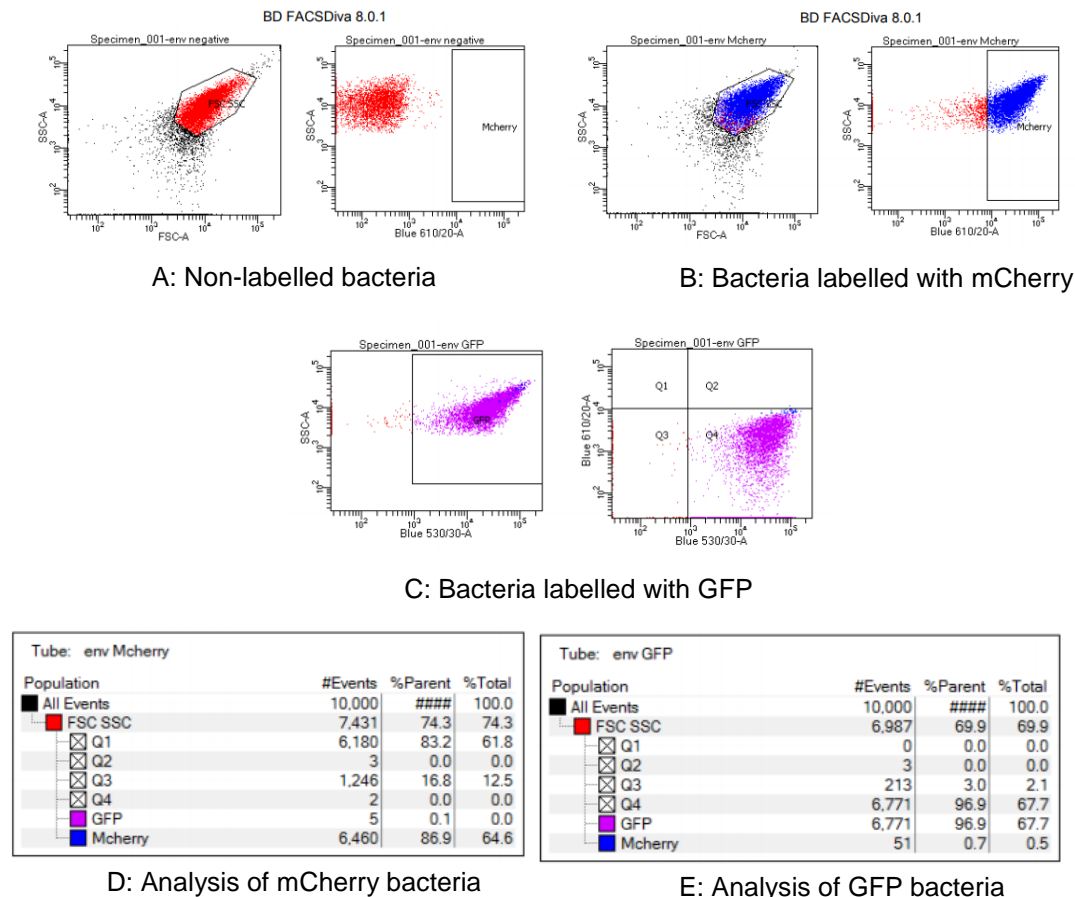


**Figure 3.3 Flow cytometry analysis of GFP and mCherry expression in *B. thailandensis* E264.**

*B. thailandensis* E264 were transformed with mCherry or GFP as described in section 2.2.1.5. Fluorescent bacteria were detected using BL-1 A530-30 and red 610-20A channels of an LSR-II flow cytometer. Untagged bacteria were used as a negative control. **A:** Negative control *B. thailandensis* CDC272, showing the gating strategy. **B:** *B. thailandensis* CDC272 tagged with GFP. **C:** *B. thailandensis* CDC272 tagged with mCherry. **D:** Percentage of positive *B. thailandensis* CDC272 tagged with mCherry compared with untagged strain. **E:** Percentage of positive *B. thailandensis* CDC272 tagged with GFP compared with untagged bacteria. The results are representative of 2 independent experiments each performed in 2 technical replicates.

### 3.3.1.3 *B. thailandensis* infection of A549 and J774.2 cells

This section was to determine the number of bacteria that can attach to, and be internalised into, two cell lines, J774.2 and A549. These cell lines were infected with *B. thailandensis* CDC272 and E264 for 2hr to measure the total number of bacteria and to determine which MOI is the best in the subsequent investigations. The CFU equation was used to count the total number of bacteria (i.e. adherent and internalised) as described in section 2.2.5. The MOI used were 0.5, 1, 3 and 5 bacteria/cell. The data showed that CFU per host cells was increased when using a higher MOI (**Fig 3.4**). For the J774.2 cells, MOI 3 was the best ratio of infection compared with other MOIs,

because the results were statistically significantly different between MOI 3 and other MOIs. However, the best MOI for A549 cells was 5 because the data was statistically significantly different between MOI 5 and other MOIs.

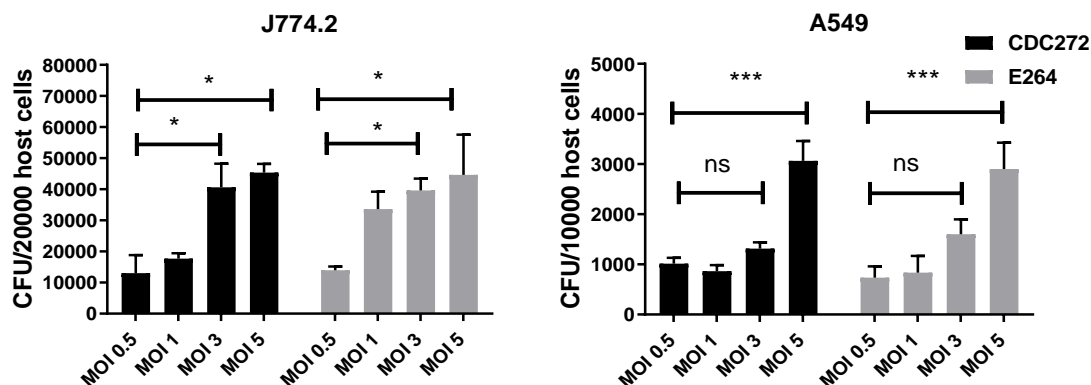


**Figure 3.4 B. thailandensis CDC272 and E264 infection in J774.2 and A549 cells at different multiplicities of infection.**

Cells were infected at MOI 0.5, 1, 3 and 5 for J774.2 cells and A549 human lung cells as described in **section 2.2.5**. The total number of bacteria (adhered and internalised bacteria) was counted after 2hr of infection using CFU for counting. The black bars are *B. thailandensis* CDC272 infecting cell lines after 2hr, and the grey bars are *B. thailandensis* E264 infecting cell lines after 2hr. The significance of the differences between treatments was tested by two-way ANOVA, where \*  $p < 0.05$ ; \*\*\*  $p < 0.001$  significant; ns=non-significant. The results are the means ( $\pm$  SEM) of 3 independent experiments each performed in 4 technical replicates.

### 3.3.1.4 The effect of GFP expression in J774.2 and A549 cells on infection with *B. thailandensis*

The first study investigated the effect of GFP, which was transfected into both cell lines J774.2 and A549, on *B. thailandensis* infection. Briefly, bacteria released from lysed J774.2 and A549 cells 2hr post-infection were enumerated on agar plates. The results demonstrated that in regards to the total number of bacteria per host cell, there were no significant differences between WTA549 and J774.2 cells compared to GFP A549 and J774.2 cells (**Fig 3.5**). It seems that GFP has no effect on the number of bacteria per host cell for these two cell lines.

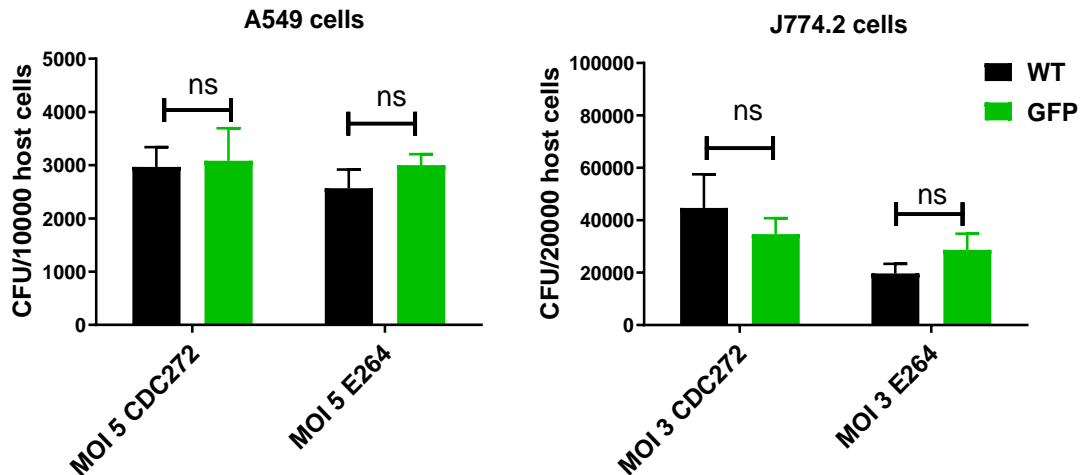


**Figure 3.5 Effect of GFP expression in J774.2 and A549 cells on *B. thailandensis* infection.**

WT and GFP tagged A549, and J774.2 cells were infected with *B. thailandensis* CDC272 or E264 at MOI 5 for 2hr. The graph shows the effect of GFP on the total number of bacteria (adhered and internalized bacteria) in both cell lines and both bacteria strains per 20000 for J774.2 cells and 10000 for A549 cells. The significance of the differences between treatments was tested by two-way ANOVA, ns=non-significant. The results are the means ( $\pm$  SEM) of 3 biological experiment performed in 3 technical replicates.

### 3.3.1.5 Effect of the expression of fluorescent proteins in *B. thailandensis* CDC272 and E264 on the bacterial infection in J774.2 cells

In this section, we investigated the effect of two fluorescent proteins, mCherry and GFP, on the ability of bacteria to infect mammalian cells. The infection assay was performed as described in **section 2.2.5**. In brief, J774.2 cells were seeded in a 96 well plate. After 2hr of infection with WT and *B. thailandensis* containing the GFP and mCherry, the wells were washed 3x with HBSS and lysed by the addition of 100 $\mu$ l of 1% TritonX-100 for 15min. The lysis mixture was serially diluted before 10 $\mu$ l of each dilution was pipetted onto LB agar plates. After 48hr of incubation at 37 $^{\circ}$ C, colonies were counted and used to calculate bacteria per well. The results demonstrated that the presence of fluorescent proteins have no affect on the efficiency of infection of J774.2 cells with both strains of *B. thailandensis*, as shown in **Fig 3.6**.

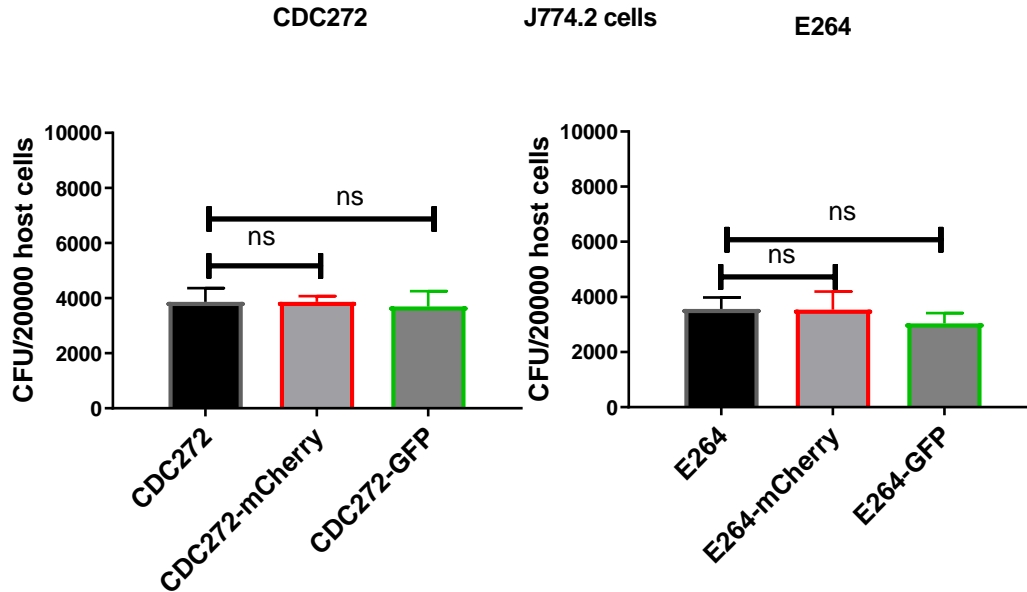


**Figure 3.6 Effect of fluorescent proteins on *B. thailandensis* infection in J774.2 cells.**

Cells were infected by tagged and untagged bacteria at MOI3 for J774.2 cells, as described in **section 2.2.5**. The total number of bacteria (adhered and internalized bacteria) was counted after 2hr of infection using CFU for counting. Black bars show the total WT bacteria in J774.2; grey bars show the total tagged bacteria with GFP and mCherry in J774.2 at MOI 3 per 20000 cells. The effects of different treatments were tested by two-way ANOVA, where ns=non-significant. The results are the means ( $\pm$  SEM) of 3 independent experiments each performed in 3 technical replicates.

### 3.3.1.6 Effect of the expression of fluorescent proteins in *B. thailandensis* CDC272 and E264 on the infection of A549 cells

These experiments were performed to ensure that there is no effect of fluorescent proteins expressed in *B. thailandensis* in A549 cells infection. The infection assay was performed as described in **section 2.2.5**. The A549 cells were seeded in a 96-well plate and infected with *B. thailandensis* CDC272 or E264 and *B. thailandensis* containing GFP and mCherry for 2hr. Measurement of the bacterial infection was assessed as CFU. As demonstrated in **Fig 3.7**, the presence of fluorescent proteins does not effect the efficiency of infection of A549 cells with either strain of *B. thailandensis*.

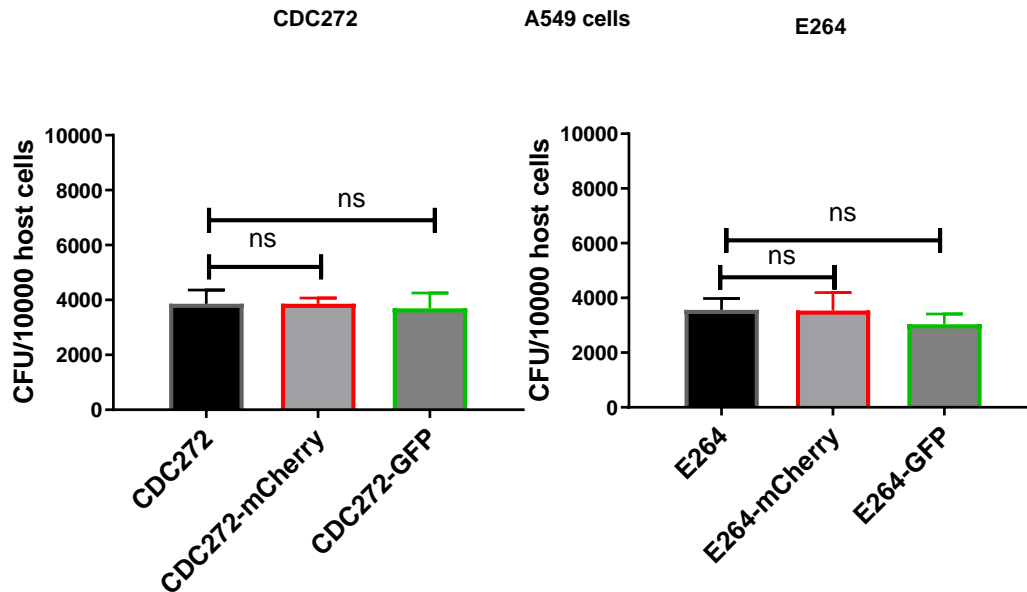


**Figure 3.7 Effect of fluorescent proteins on total *B. thailandensis* infection in A549 cells.**

Cells were infected by tagged and untagged bacteria at MOI5 for A549 cells, as described in **section 2.2.5**. The total number of bacteria (adhered and internalised bacteria) was counted after 2hr of infection using CFU counting. Black bars show the total untagged bacteria in per 10000 A549; grey bars show the total bacteria tagged with GFP and mCherry in A549 at MOI 5 per 10000 cells. The significance of the difference between treatments was tested by two-way ANOVA, ns=non-significant. The results are the means ( $\pm$  SEM) of 3 independent experiments each performed in 4 technical replicates.

### 3.3.2 *B. thailandensis* induces the formation of MGC formation *in vitro* in A549 and J774.2 cells

#### 3.3.2.1 MGC formation

Previous studies in our group have described MGC formation in J774.2 cells after infection by *B. thailandensis* (Elgawidi, 2016). Here, we show that *B. thailandensis* has the ability to induce human lung epithelial A549 cells to form MGC (**Figs 3.8 and 3.11**). This is consistent with findings in the literature (Micheva-Viteva *et al.*, 2017). In addition, we used a *B. thailandensis* E264- $\Delta$ tssK mutant strain as a negative control for MGC formation. This strain does not induce MGC formation (Hall, 2016, Whiteley *et al.*, 2017). Briefly, J774.2 and A549 cells were infected at MOI 0.5, 1 and 3 and 5 with *B. thailandensis* CDC272, E264 and E264- $\Delta$ tssK for 2hr and added medium containing amikacin and kanamycin to kill extracellular bacteria. MGC formation was assessed at 18hr post-infection. Cells were stained with Giemsa, and the fusion index was calculated relative to normal host cells per field of view. MGCs were defined as cells containing 3 or more nuclei. Our results

demonstrated that the fusion index for both J774.2 and A549 cells were increased only by CDC272 and WT E264 strains but not the mutant (**Fig 3.8**).

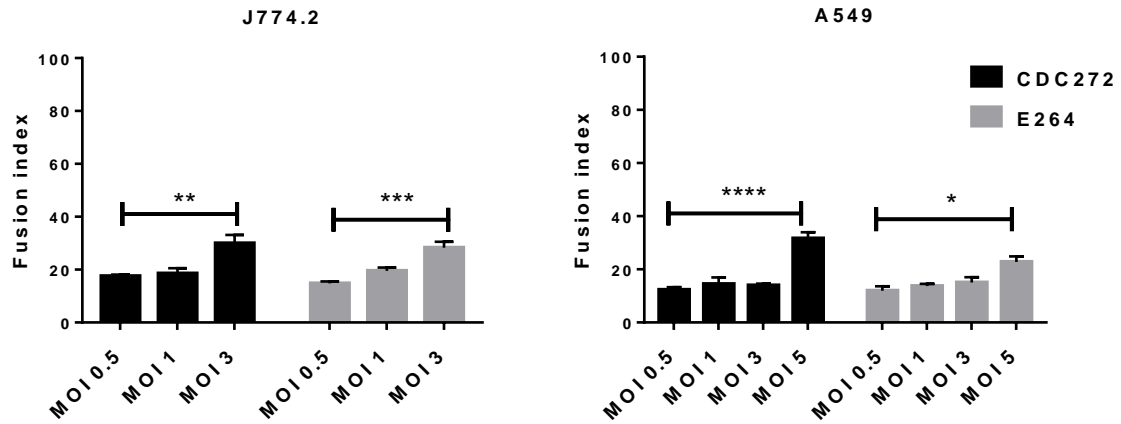


**Figure 3.8 The formation of MGC at different MOI of *B. thailandensis* CDC272 and E264.**

Cells were infected at MOI 0.5, 1, 3 and 5 for J774.2 cells and A549 human lung cells as described in **section 2.2.5**. The fusion index was measured as described in **section 2.2.6**. Black bars show the fusion index induced by CDC272; grey bars show the fusion index induced by E264. The significance of the difference between treatments was tested by two-way ANOVA, where \*  $p < 0.05$ ; \*\*  $p < 0.01$ ; \*\*\*  $p < 0.001$ ; \*\*\*\*  $p < 0.0001$  significant; ns=non-significant. The results are the means ( $\pm$  SEM) of 3 independent experiments each performed in 4 technical replicates.

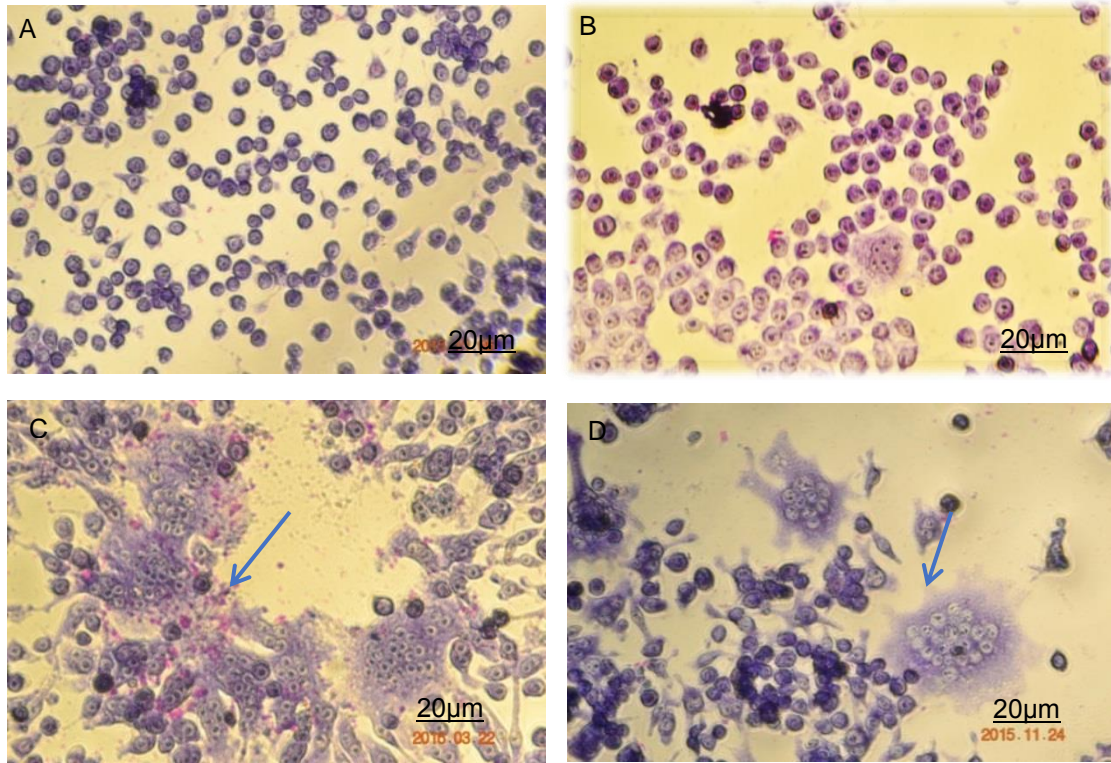


**Figure 3.9 Light micrographs of J774.2 cells infected with *B. thailandensis* E264, CDC272 and E264- $\Delta$ tssK.**

J774.2 cells were cultured in 96 well plates overnight and then infected with two fusogenic strains *B. thailandensis* CDC272, E264 and non-fusogenic mutant *B. thailandensis* E264- $\Delta$ tssK at MOI 3. Cells were fixed and stained at 18hr post-infection. **A:** Uninfected. **B:** *B. thailandensis*,  $\Delta$ tssK-E264. **C:** WT *B. thailandensis* E264. **D:** *B. thailandensis* CDC272. Images are representative of 3 independent experiments each performed in 8 technical replicates. Images were taken using a Nikon light microscope 40x objective.

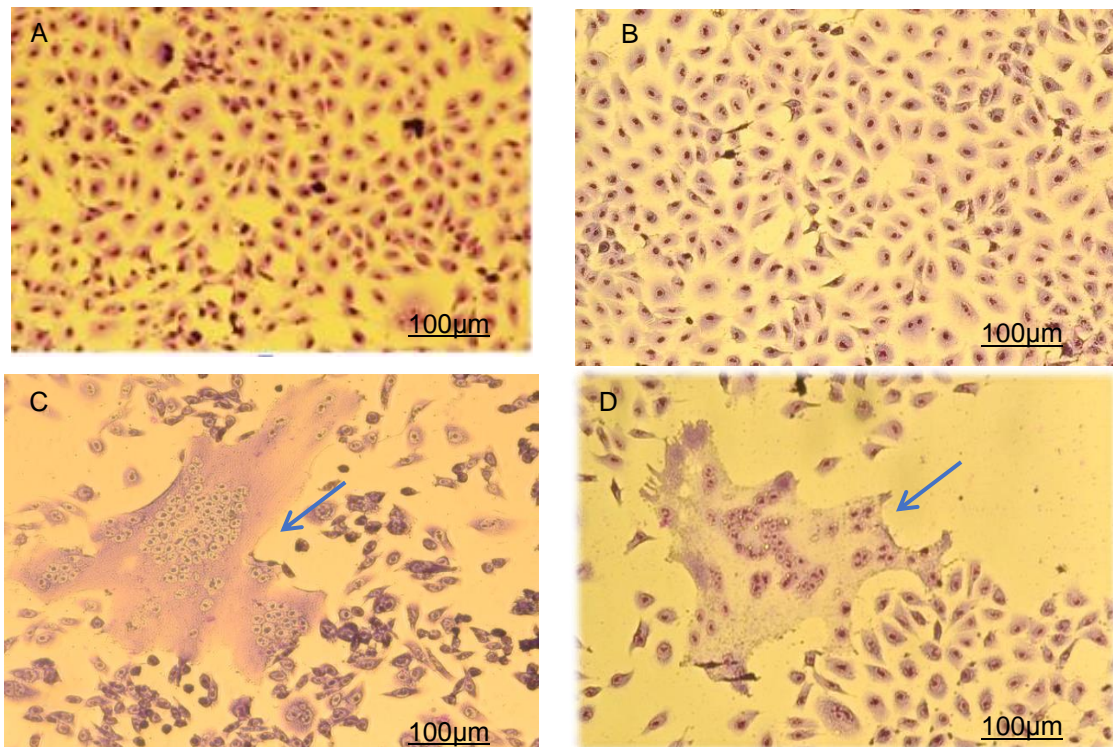


**Figure 3.10 Light micrographs of A549 cells infected with *B. thailandensis* E264, CDC272 and E264- $\Delta$ tssK.**

A549 cells were cultured in 96 well plates overnight and then infected with two fusogenic strains *B. thailandensis* CDC272, E264 and non-fusogenic mutant *B. thailandensis* E264- $\Delta$ tssK at MOI 5. Cells were fixed and stained at 18hr post infection. **A:** uninfected. **B:** *B. thailandensis*, E264- $\Delta$ tssK. **C:** WT *B. thailandensis* E264. **D:** WT *B. thailandensis* CDC272. Images are representative of 3 independent experiments each performed in 8 technical replicates. Images were taken using a Nikon light microscope 40x objective.

### 3.3.2.2 *B. thailandensis* tssk deletion mutant is incapable of inducing MGC formation

It is known that *B. thailandensis* has several type VI secretion systems, but only one (T6SS-5) is required for inducing MGC formation (Toesca *et al.*, 2014, Schwarz *et al.*, 2014, Whiteley *et al.*, 2017). Here we intend to use *tssK* mutant to differentiate between mechanisms involved in infection and fusion. To do this, four wells of a 96 well plate were infected at MOI 5 for A549 cells, MOI 3 for J774.2 cells with both E264- $\Delta$ tssK and WT strains. 2hr post-infection, the DMEM medium was replaced with medium containing kanamycin and amikacin to kill extracellular bacteria. At different time points after the initial infection, wells were washed 2x with HBSS before fixing with 100% ethanol for 30min. The ethanol was removed and the wells were allowed to dry before immersing in 20% of Giemsa for 30min. The stain was removed before the cells were destained with tap water until the cytoplasm

and nuclei of J774.2 and A549 cells could be distinguished. The 10x objective of a Nikon (MAZUREK) inverted microscope was used to capture five random fields of view per well. Nuclei within cells containing three or more nuclei were counted, as well as the number of nuclei in the field of view. The fusion index in J774.2 and A549 cells infected with E264- $\Delta$ tssK was less than 3%, much lower than cells infected with two strains of WT *B. thailandensis*, which induced the cells to form MGC with a fusion index of more than 30%. *B. thailandensis* E264- $\Delta$ tssK can infect cells normally but can only weakly induce fusion (**Fig 3.11**). As expected from the published literature, T6SS-5 is required for MGC formation (Toesca *et al.*, 2014, Schwarz *et al.*, 2014, Hall, 2016, Whiteley *et al.*, 2017). This is consistent with our findings where there was a significant difference in the fusion index between WT and E264- $\Delta$ tssK strains, as shown in **Fig 3.11**.

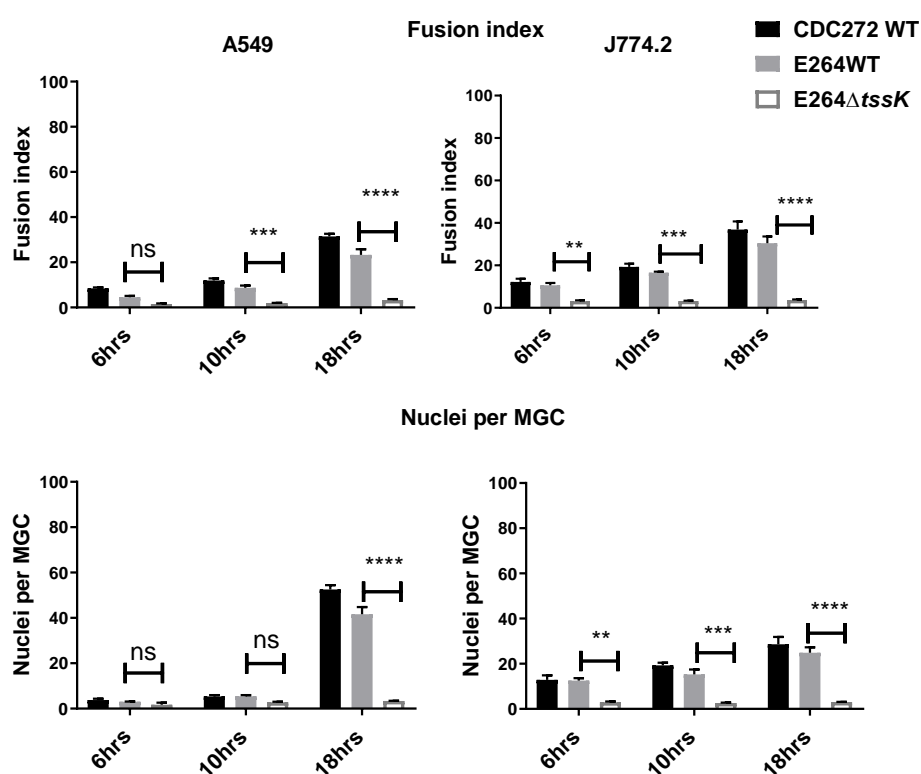


**Figure 3.11 MGC formation in J774.2 and A549 cells.**

Cells were cultured in 96 well plates overnight and then infected with fusogenic and non-fusogenic mutant (E264- $\Delta$ tssK) of *B. thailandensis* at MOI 3 and 5 as described in **section 2.2.6**. Cells were fixed and stained at 6, 10 and 18hr infection. **Upper panel:** The bars show the fusion index for J774.2 and A549 cells induced bacteria. **Lower panel:** The bars show the number of nuclei per MGC for J774.2 and A549 cells induced by WT and mutant E264- $\Delta$ tssK bacteria at MOI 3 for J774.2 cells and at MOI 5 for A549 cells. The significance was tested by two-way ANOVA, where \*  $p < 0.05$ ; \*\*  $p < 0.01$ ; \*\*\*  $p < 0.001$ ; \*\*\*\*  $p < 0.0001$  significant; ns=non-significant. The results are the means ( $\pm$  SEM) of 3 independent experiments each performed in 8 technical replicates.

### 3.3.2.3 The effect of GFP expression in J774.2 and A549 cells on MGC formation induced by *B. thailandensis*

We performed infection and fusion assay to investigate the effect of GFP on MGC formation. As mentioned in **section 2.2.2.9**, the J774.2 and A549 cells were labelled with GFP using transfection assay. The percentage of transfection was about 80% of cells (data are shown in **Appendix Figs 2 and 3**). The transfected and WT J774.2 and A549 cells were infected by *B. thailandensis* using fusion assay, as mentioned in **section 2.2.6**. In brief, after infection for 18hr, all wells were washed 2x with HBSS before fixing with 100% ethanol for 30min. The ethanol was removed and the wells were allowed to dry before immersing in 20% of Giemsa for 30min. The stain was removed before the cells were destained with tap water until the cytoplasm and nuclei of J774.2 and A549 cells could be distinguished. A Nikon (MAZUREK) inverted microscope was used to capture five random fields of view per well. Nuclei within cells containing three or more nuclei were counted, as well as the number of nuclei in the field of view. The results demonstrated that there were no significant difference between tagged J774.2 and A549 cells and their WT counterparts regarding MGC formation (**Figs 3.12 and 3.13**).

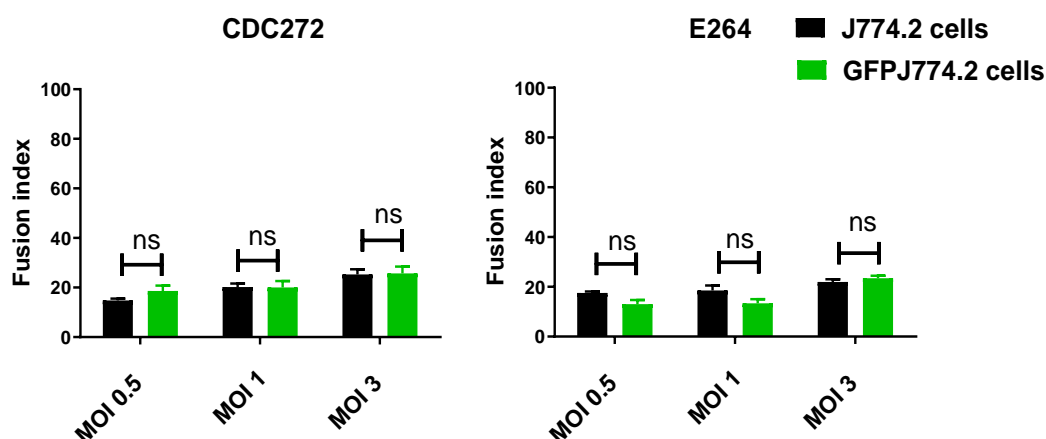


**Figure 3.12 Effect of GFP in J774.2 cells on MGC formation induced by both *B. thailandensis* strains.**

Cells were cultured in 96 well plates overnight and then infected with two fusogenic strains *B. thailandensis* CDC272 and E264 at MOI 0.5, 1 and 3 as described in **section 2.2.6**. Cells were fixed and stained at 18hr post-infection. Black bars show the fusion index for WT J774.2 cells; green bars show the fusion index for GFPJ774.2 cells at MOI 0.5, 1 and 3, respectively. The significance of the difference between treatments was tested by two-way ANOVA; ns=non-significant. The results are the means ( $\pm$  SEM) of 3 independent experiments each performed in 4 technical replicates.

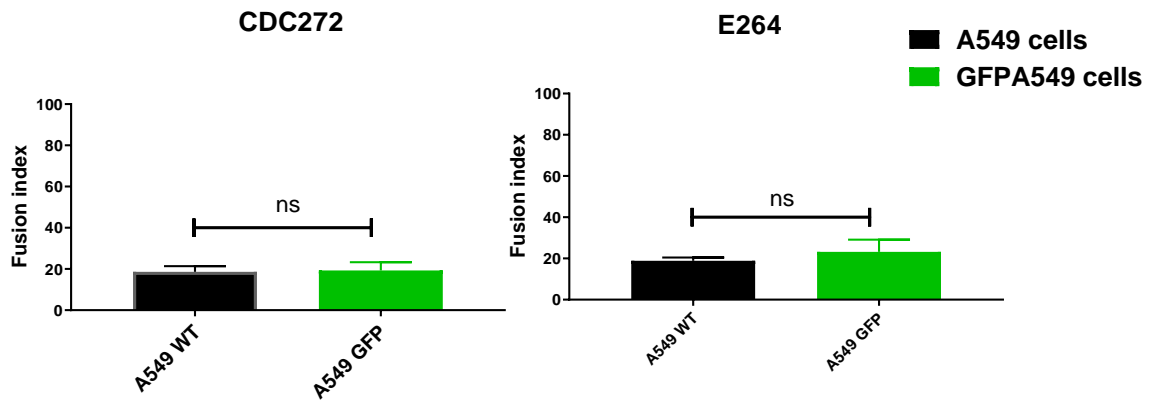


**Figure 3.13 Effect of GFP in A549 cells on MGC formation induced by both *B. thailandensis* strains.**

Cells were cultured in 96 well plates overnight and then infected with *B. thailandensis* CDC272 and E264 at MOI 3 as described in **section 2.2.6**. Cells were fixed and stained at 18hr post-infection. Black bars show the fusion index for WT A549 cells; green bars show the fusion index for GFP A549 cells at MOI 5. The significance of the difference between treatments was tested unpaired t-test, ns=non-significant. The results are the means ( $\pm$  SEM) of 3 independent experiments each performed in 4 technical replicates.

#### 3.3.2.4 Effect of mCherry and GFP expression in *B. thailandensis* on MGC formation

To investigate whether mCherry and GFP have an effect on *B. thailandensis*-induced MGC formation in either A549 or J774.2 cells, bacteria were labelled with these fluorescent proteins as mentioned in **section 2.2.1.5.6**. The fusion assay was performed to quantify the percentage of fusion caused by either WT *B. thailandensis* or *B. thailandensis* carrying the mCherry and GFP fluorescent markers. The results demonstrated that there were no significant differences between labelled bacteria and non-labelled bacteria in regards to the fusion index (**Fig 3.14** and **Fig 3.15**).

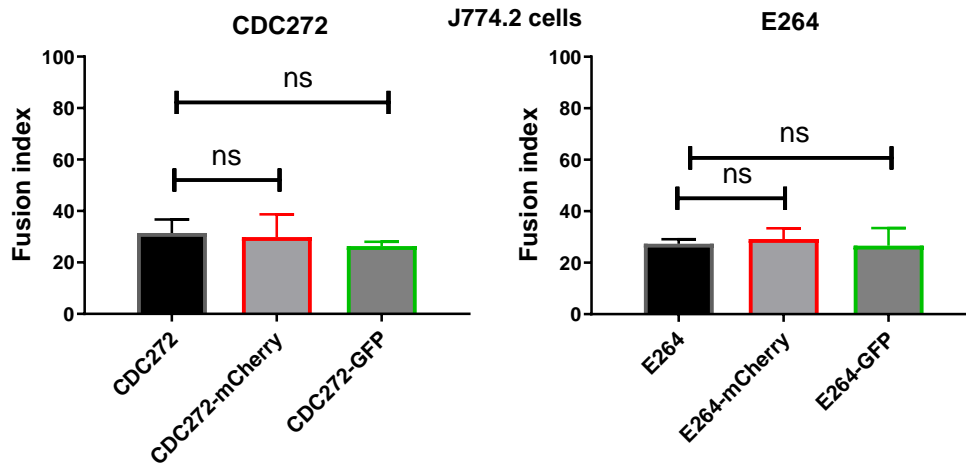


**Figure 3.14 Effect of fluorescent reporter proteins on *B. thailandensis*-induced MGC formation in J774.2 cells.**

Cells were seeded in 96 well plates overnight. The cells were infected by tagged and untagged *B. thailandensis*, GFP and mCherry at MOI 3. Cells were fixed and stained at 18hr post-infection. Black bars show the fusion index for WT J774.2 cells infected with untagged bacteria; grey bars show the fusion index for J774.2 cells infected with tagged bacteria at MOI 3. The significance of the difference between treatments was tested by two-way ANOVA, where ns=non-significant. The results are the means ( $\pm$  SEM) of 3 independent experiments each performed in 4 technical replicates.

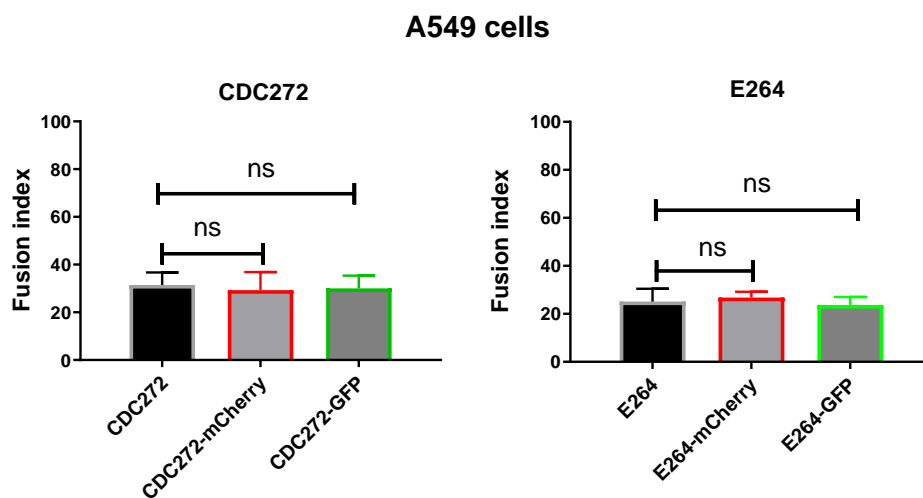


**Figure 3.15 Effect of fluorescent reporter proteins on *B. thailandensis*-induced MGC formation in A549 cells.**

Cells were seeded in 96 well plates overnight. The cells were infected by tagged and untagged *B. thailandensis*, GFP and mCherry at MOI 5. Cells were fixed and stained at 18hr post-infection. Black bars show the fusion index for WT A549 cells infected with untagged bacteria; grey bars show the fusion index for A549 cells infected with tagged bacteria at MOI 5. The significance of the difference between treatments was tested by two-way ANOVA, where ns=non-significant. The results are the means ( $\pm$  SEM) of 3 independent experiments each performed in 4 technical replicates.

## 3.4 Discussion

### 3.4.1 *B. thailandensis* infection

Many studies have demonstrated that *B. pseudomallei* and *B. thailandensis* can replicate and survive inside RAW 264.7 and A549 cells following infection (Utaiincharoen *et al.*, 2001, Kespichayawattana *et al.*, 2004, Lamothe and Valvano, 2008). A previous study found that *B. pseudomallei* and *B. thailandensis* can infect mouse macrophage cell lines (J774.2 and RAW 264) and human monocytes cell lines (THP1 and U937) (Benanti *et al.*, 2015, Stevens *et al.*, 2005, French *et al.*, 2011, Kespichayawattana *et al.*, 2000). In our lab, a study demonstrated that there was also no difference in the ability of clinical and environmental *B. thailandensis* strains to adhere to, and internalise into, mammalian cells (Elgawidi, 2016). Human lung epithelial A549 and mouse macrophage J774.2 cells were infected with *B. thailandensis* E264 and CDC272 to measure the total bacterial infection and/or internalisation to mammalian cells after 2hr exposure of infection.

The first aim of this study was to determine which MOI will be used in the next investigations. In **section 3.3.1.2**, our results showed that the infection efficiency of J774.2 cells at MOI 3 was significantly higher than MOI 0.5. It seems that MOI 3 was the appropriate ratio of infection for J774.2 cells. These results with J774.2 were similar to the previous study that used MOI 2 to infected RAW 264 (Utaiincharoen *et al.*, 2006). Stevens and co-workers used MOI 1 for *B. pseudomallei* infection and MOI 10 for *B. thailandensis* to study the replication of bacteria inside J774.2 macrophages (Stevens *et al.*, 2002). We also found that the A549 cells can be infected by *B. thailandensis* CDC272 and E264 at MOI 1, 3 and 5. However, the optimum MOI was 5 with both strains for A549 cells, as described in **Fig 3.5**. The total bacterial infection at MOI 5 was significantly larger than at MOI 1. We also compared this with another researcher's findings. For example, Haraga and colleagues have noticed that MOI 10 was the best ratio of infection for Hela cells (Haraga *et al.*, 2008).

The second aim was to know if there was any effect of fluorescent protein tags in the mammalian cells on the bacterial infection. The findings showed

there no significant differences between GFP and WT J774.2 cells after 2hr infection. The results also showed non-significant differences between A549 GFP and WT A549 cells (**Fig 3.5** and **Fig 3.6**). There are no publications about the effect of GFP tags in mammalian cells on bacterial infection.

The third aim was to determine whether there was any effect of two different fluorescent protein tags in the infection efficiency of *B. thailandensis*. Our data demonstrated that there were no differences with J774.2 or A549 cells infected with tagged or untagged *B. thailandensis* (**Fig 3.6** and **Fig 3.7**). These results were similar to a previous study that used RAW 264.7 macrophage cells, as they found that GFP had no effect on the total bacterial infection (Burtnick *et al.*, 2011, Burtnick *et al.*, 2010). Moreover, our findings were also similar to those obtained when GFP was used to tag *Pseudomonas syringae* (Wang *et al.*, 2007). In addition, it has been observed that there is no effect of GFP tag on *S. typhimurium* infection and internalisation (Ma *et al.*, 2011).

#### 3.4.2 MGC formation induced by *B. thailandensis*

Here, I have characterised *B. thailandensis* induction of MGC formation. This section will discuss 3 aims. The first aim was to detect which MOI will be used in the next MGC formation investigations. Both host cell types were infected at different MOIs, as described in **section 2.2.6**. The experiment was optimised for the fusion index during different periods.

In **section 3.3.2.1**, we observed that the best MOI to induce the cells to form MGC is 3 in J774.2 and 5 in A549 cells. These results were similar to previous studies which found that the optimum MOI to infect RAW264.7 and J774.2 mouse cell lines was 3 (Elgawidi, 2016, Hall, 2016). However, Whiteley *et al.* used MOI 33 in RAW264.7 to induce the cells to form MGC to reach ~40% fusion index (Whiteley *et al.*, 2017). We found that the fusion index with A549 cells infected with *B. thailandensis* CDC272 at MOI 5 ~32%; however, Micheva-Viteva *et al.* used *B. thailandensis* CDC272 at MOI 50 to infect A549 cells (Micheva-Viteva *et al.*, 2017). They found that the MGC fusion index was ~10% after 24hr of infection. The reasons for this difference are unclear.

In **section 3.3.2.2**, we tested if a *tssK* mutant could induce the cells to form MGC. Our results showed that  $\Delta tssK$  could not cause fusion in two types of cells, A549 and J774.2, at different time points. This supports data from a previous study at University of Sheffield, which showed that E264- $\Delta tssK$  cannot induce RAW cells to form MGC (Hall, 2016). This is also in support of results that show that T6SS-5 is required in MGC formation induced by *B. thailandensis* E264- $\Delta tssK$  and  $\Delta tssI-5$  (Schwarz *et al.*, 2014, Toesca *et al.*, 2014, Whiteley *et al.*, 2017) .

The results shown in this chapter indicate that the J774.2 cells fused within 6hr of infection and A549 cells fused within 10hr of infection. Whiteley *et al.* showed that RAW264.7 macrophages could also fuse to form MGC after 6hr of infection (Whiteley *et al.*, 2017). These results were in agreement with our study that reported that the start point of fusion is 6hr post-infection. However, these were not in agreement with our finding with A549 cells, which can fuse 10hr post-infection. It might be because these cells are human lung epithelial cells, which are not professional phagocytes like macrophages.

The second aim was to know if the fluorescent protein tags in mammalian cells have any effect on MGC formation. There are no published studies about the effect of GFP tag protein on MGC formation. These investigations were necessary to confirm that the fusion index did not change because of the protein tag. Our results in **Fig 3.12** and **Fig 3.13** suggested that there was no effect of GFP expression in A549 and J774.2 cells. The third aim was to know if there was any effect of fluorescent protein tags in the bacteria on MGC formation. In **section 3.3.2.4**, our results demonstrated clearly that there was no effect of bacterially-expressed GFP and mCherry proteins on MGC formation. There are no publications about the effect of GFP and mCherry proteins on MGC formation.

## Chapter 4 Strategy to discriminate the role of Tspans and partner proteins involved in MGC formation and/or bacterial infection

### 4.1 Introduction

It was demonstrated in **chapter 3** that A549 and J774.2 cells can be induced to form MGC by *B. thailandensis*. In fact MGC formation is involved in pathogenesis and important in melioidosis. For example, MGCs have been found in the tissues of patients with melioidosis (Wong *et al.*, 1995). *B. pseudomallei* can survive intracellularly, and also induce phagocytic and non-phagocytic cells to form MGC in tissue models (Franco *et al.*, 2018). MGC formation is also a means of *B. pseudomallei* spreading from cell to cell (Kespichayawattana *et al.*, 2000). Using actin-associated plasma membrane protrusions, the bacteria co-localise and spread directly from cell to cell (Kespichayawattana *et al.*, 2000). However, the mechanism of MGC formation is not fully understood. It is likely that host cell factors are involved.

Previous studies showed that cell fusion and bacterial infection could be regulated by host membrane proteins. Helming and Gordon have observed that CD36 might contribute to cell fusion of macrophages stimulated by the cytokines IL-4 and GM-CSF. Anti-CD36 antibody can also inhibit macrophage fusion (Helming and Gordon, 2009). It was also observed that CD47 integrin-associated protein could participate in cell fusion, Hobolt *et al.* have used monoclonal antibody against CD47, which strongly inhibited cell fusion in a murine osteoclast culture system (Hobolt-Pedersen *et al.*, 2014). CD98 protein can also regulate cell fusion (Yoshiki and Boyd, 2004). DC-STAMP plays an essential role in cell fusion (Yagi *et al.*, 2005). Suparak *et al.* observed MGC formation induced by *B. pseudomallei* and found that it could be significantly inhibited when antibodies against CD47 and CD98 were used on U937 macrophages, whereas antibodies against CD44 and CD14 (LPS receptor) had no effect on MGC formation in U937 macrophages (Suparak *et al.*, 2011). Borisova *et al.* found that integrin  $\beta 3$  mRNA was raised after *Staphylococcus* infection (Borisova *et al.*, 2013).

Tspan molecules have been implicated in regulating cell:cell fusion and virus:cell fusion. Previous studies have indicated roles for Tspan molecules in mononuclear phagocyte fusion, including osteoclast formation and the formation of MGC associated with chronic inflammation (Iwai *et al.*, 2007). It has been observed that antibodies against CD9 and CD81 can enhance the fusion of peripheral blood monocytes stimulated by Con A, and the deletion of CD9 and CD81 can also enhance MGC formation *in vivo* and *in vitro* (Takeda *et al.*, 2003). Recently, a previous PhD student from University of Sheffield has shown roles for Tspan molecules in cell fusion in mouse macrophages induced by *B. thailandensis* (Elgawidi, 2016). Here the role of Tspan molecules in bacterial infection and/or MGC formation induced by *B. thailandensis* was investigated.

## 4.2 Aims

This work aims to investigate the role of Tspan molecules in MGC formation during *B. thailandensis* infection using mouse macrophage J774.2 cells and human lung epithelial A549 cells, as they are commonly used as models to study the interaction of the bacterium with host cells. We used a *B. thailandensis* T6SS mutant strain ( $\Delta tssK$ , which can infect cells without stimulating MGC formation) to distinguish between Tspans involved in infection from those with a role in MGC formation and *B. thailandensis* infection

The first aim was to investigate if Tspans and Tspan-partner genes expression are changed in response to *B. thailandensis* infection, using real-time qPCR. Three criteria were used to discriminate a role for Tspans and Tspan-partner proteins in MGC formation and/or infection. Firstly, the levels of Tspans and partner proteins mRNA should show consistent changes in both host cell types (A549, J774.2) regarding MGC formation and/or bacterial infection. Secondly, the levels of Tspans mRNA should show consistent changes with two fusogenic bacterial strains (E264, CDC272) regarding MGC formation and/or bacterial infection. Thirdly, there should be no change with the non-fusogenic E264- $\Delta tssK$  mutant for a gene involved only in MGC formation. The second aim was to use flow cytometry to validate the data on gene expression by measuring cell surface protein levels.

## 4.3 Results

### 4.3.1 Tspan genes expression at the mRNA level in A549 and J774.2 cells

This study was to investigate the gene expression of Tspans at the mRNA level in the J774.2 and the A549 cells. According to the criteria for primer design for real-time qPCR, we designed 33 human Tspan primers and 31 mouse Tspan primers (there are two mouse Tspan genes that do not appear in the NCBI database, Tspan-16 and Tspan-19). The study used the qPCR assay, as described in **section 2.2.4**. The expression of mRNA is determined by the accumulation of a fluorescent signal, using SYBR green fluorescent dye. The number of PCR cycles required for the fluorescent signal to cross the threshold is the cycle threshold ( $C_t$ ). The  $C_t$  value was used to calculate the relative amount of RNA. The relative expression of Tspans mRNA is calculated against a suitable housekeeping gene, ribosomal protein 13 $\alpha$  (RpL13 $\alpha$ ) for mouse J774.2 cells and glyceraldehyde 3-phosphate dehydrogenase (GAPDH) for human A549 cells.

As described in **section 2.2.4**, RNA was extracted and treated with DNaseI to avoid genomic DNA contamination. As shown in **Fig 4.1A**, there was no genomic DNA after treatment with DNaseI. cDNA was prepared using a thermocycler machine. cDNA samples and all reverse and forward primers for Tspans (human and mouse) were prepared and tested in a real-time PCR machine. The primer specificity was checked using melting curves as an extra step in a real-time machine, as shown in **Appendix Fig 4**, and this was confirmed by running a selection of random wells on an agarose gel after amplification in real-time PCR machine (**Fig 4.1B**). In a representative experiment, it can be clearly seen that all the mouse and human Tspan genes are expressed in J774.2 and A549 cells, respectively (**Fig 4.1C**). We used two negative controls: 1) RNA samples without reverse transcriptase enzyme (NRT), and 2) reverse transcriptase enzyme without RNA sample (NRNA) (**shown in Appendix Table 1**). The qPCR data showed that all 31 murine Tspan genes are expressed by J774.2 as shown in **Fig 4.2**, while the qPCR

results showed that all 33 human Tspan genes are expressed by A549 cells as shown in **Fig 4.3**.

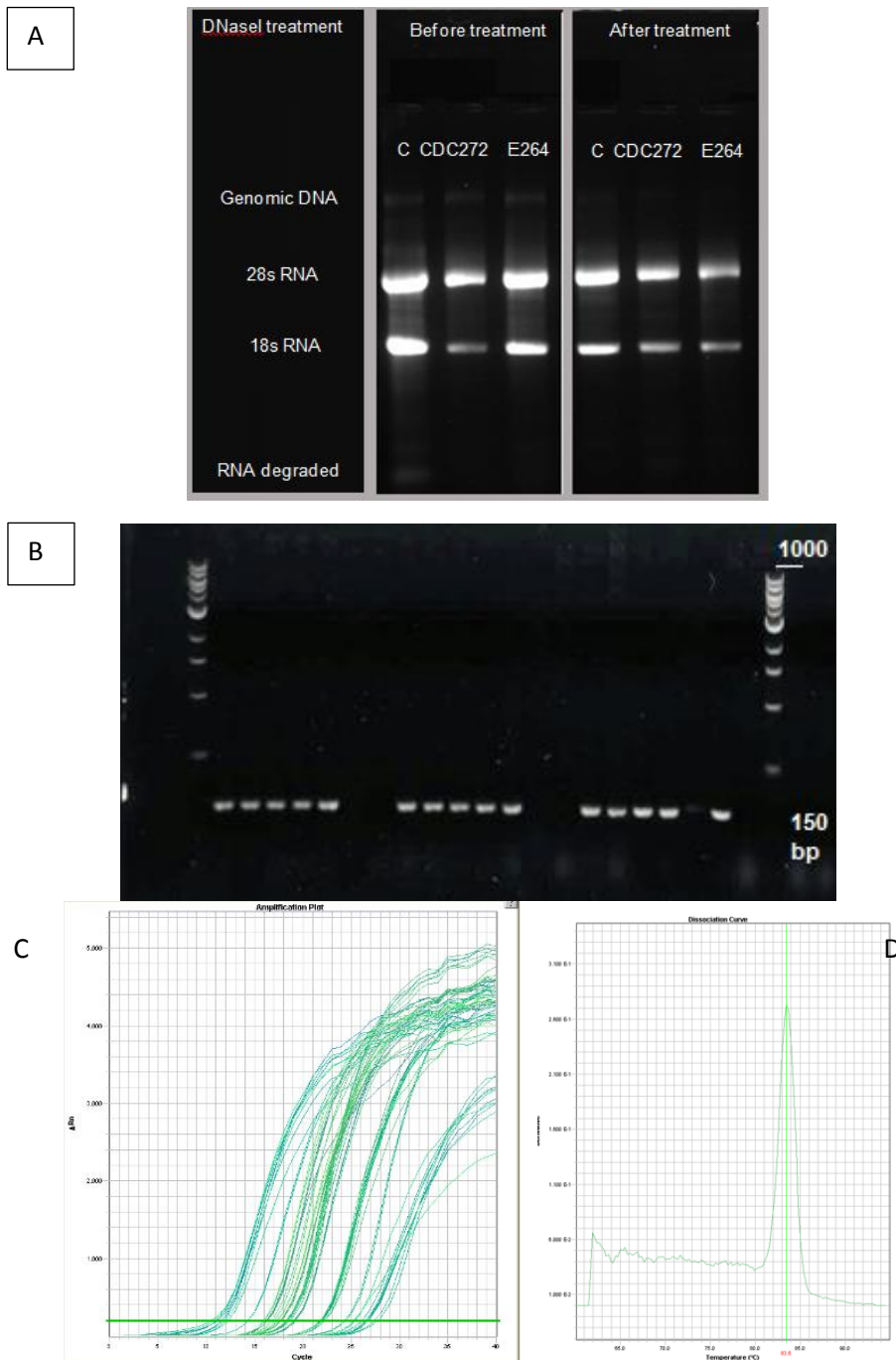


**Figure 4.1 Validation of qPCR ( RNA integrity and primers specificity).**

**A:** Gel electrophoresis of RNA. The 18S and 28S rRNA bands are clearly visible in the intact RNA samples. NI: non-infected cells, E264: Infected J774.2 cells with environmental strain and CDC272: Infected J774.2 cells with clinical strain. **B:** Gel electrophoresis of a selection of random wells after amplification in real-time PCR machine. Bands showing ~150bp PCR products of CD9 and Tspan-2. **C:** qPCR output of a typical experiment, showing the increase of SYBR Green fluorescence with qPCR cycle number. The point at which the curve intersects the threshold (horizontal green line) is the  $C_t$  value; failure to reach the threshold indicates non-expression of that gene. **D:** The plot shows how PCR product fluorescence changes with temperature. A single peak on the melting curve analysis indicates a single PCR product. These optimisations are representative data for all qPCR experiments.

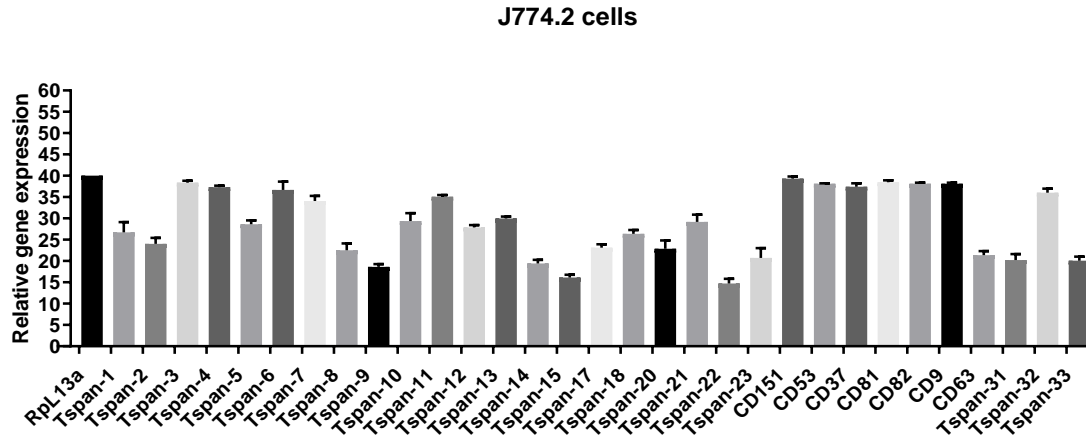


**Figure 4.2 Tspan genes expression at the mRNA level in J774.2 cells.**

All data have been calculated with a suitable housekeeping gene (Rpl13 $\alpha$ ), and the relative  $\Delta C_t$  levels of Tspans are presented in the Y-axis. The results are the means ( $\pm$  SEM) of 3 independent experiments each performed in 2 technical replicates.

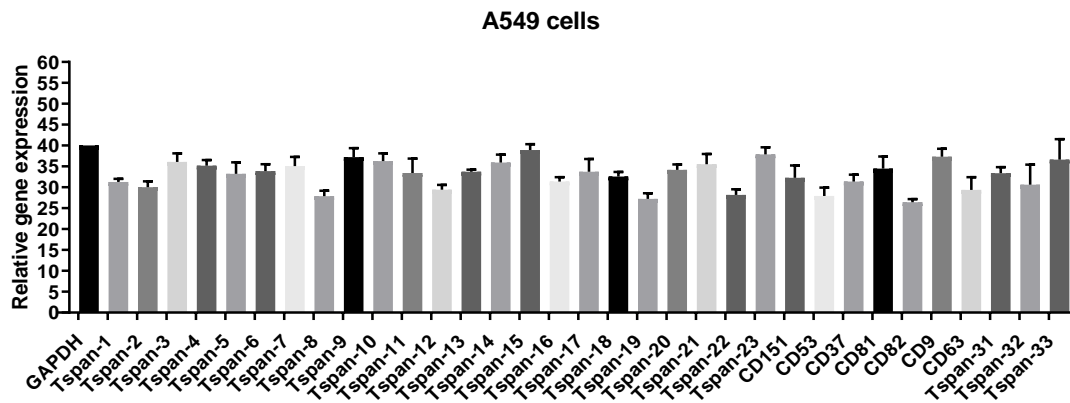


**Figure 4.3 Tspan genes expression at the mRNA level in A549 cells.**

All data have been calculated with a suitable housekeeping gene (GAPDH), and the relative  $\Delta C_t$  levels of Tspans are presented in the Y-axis. The results are the means ( $\pm$  SEM) of 3 independent experiments each performed in 2 technical replicates.

### 4.3.2 Changes in Tspan genes expression at the mRNA level after infection of A549 and J774.2 cells

To analyse which gene expression levels are changed during *B. thailandensis* infection, qPCR was used. Tspan genes expression changes were analysed in both cell lines in response to infection by *B. thailandensis* mutant and wild type. The fold change was calculated using the equation  $2^{(-\Delta\Delta C_t)}$ . In brief, RNA was extracted and treated with DNaseI to avoid genomic DNA contamination. cDNA was prepared using a reverse transcriptase kit. The primer specificity was checked using melting curves as an extra step in a real-time PCR machine (**Fig 4.1D**). Amplification was performed on cDNA samples

using reverse and forward primers for Tspans (human and mouse) using a real-time PCR machine. All 33 Tspans of A549 cells and 31 Tspans of J774.2 cells had detectable mRNA levels in uninfected cells but the mRNA levels of 10 Tspans were found to change 18hr post-infection, as shown in **Appendix Fig 5**. However, only 5 Tspans met the criteria for specific involvement in fusion rather than infection (namely, changes in both host cell types, both bacterial strains but no change with *B. thailandensis* E264- $\Delta$ tssK mutant strain) and so these were selected as candidates for further study as described in **Fig 4.4**.

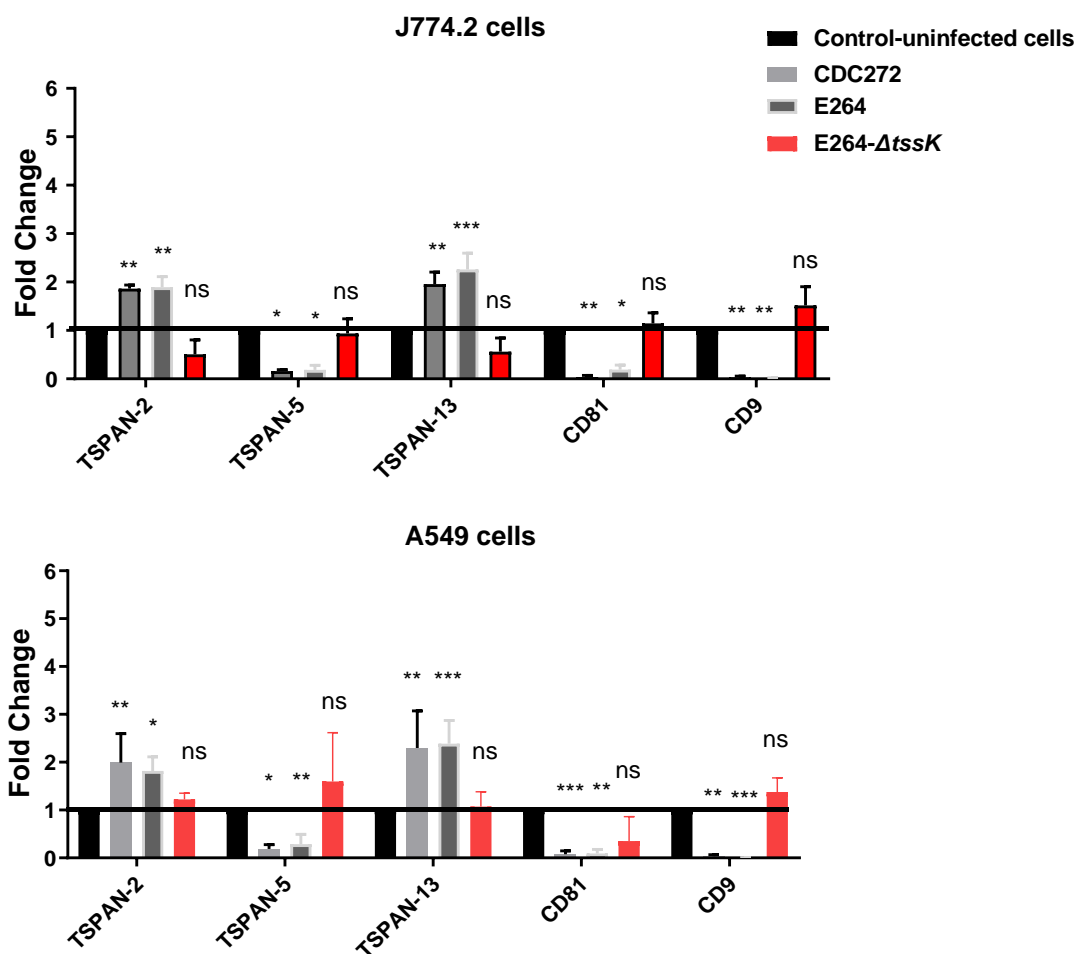


**Figure 4.4 Changes in Tspan genes expression at mRNA level in response to both *B. thailandensis* fusogenic strains.**

Tspan genes expression were measured by qPCR after 18hr infection with *B. thailandensis* CDC272 or E264 and non-fusogenic mutant (E264- $\Delta$ tssK). Expression of Tspans was calculated using the  $2^{-\Delta\Delta C_t}$  method relative to the results to the housekeeping genes RpL13 $\alpha$  and GAPDH. 5 Tspans showed consistent changes in both host cell types and no change with non-fusogenic mutant (E264- $\Delta$ tssK). The significance of differences were tested by one-way ANOVA, where \*  $p < 0.05$ ; \*\*  $p < 0.01$ ; \*\*\*  $p < 0.001$  significant (vs. control-uninfected cells). The results are the means ( $\pm$  SEM) of 3 independent experiments each performed in 2 technical replicates.

### 4.3.3 Tspan genes expression in A549 and J774 cells over time

To further analyse the 5 differentially expressed genes associated with MGC formation, we performed an expression analysis over 5 time points during bacterial infection. To do this, QIAGEN RNeasy Mini Kits were used to extract mRNA from J774.2 and A549 cells before and after infection by *B. thailandensis*. TURBO DNase kit was used according to the manufacturer's instructions to remove the genomic DNA. A High-Capacity cDNA Reverse Transcription Kit was used to make complementary DNA (cDNA) for all samples over 5-time points. The SYBR green method was used to quantify the DNA product formed, as demonstrated in **section 2.2.4**. In order to normalise the qPCR data, the  $\Delta C_t$  was used to analyse the data. Also, the fold change was calculated using equation  $2^{-\Delta\Delta C_t}$  for all genes.

The expression of genes was normalised to the GAPDH and RpL13 $\alpha$  levels in all samples at 0, 2, 4, 10, and 18hr. The melting curve analysis (at 65-95°C) was performed at the end of each experiment to determine the primers' specificity. As shown in **Fig 4.4**, Tspan-2, Tspan-13, Tspan-5, CD81 and CD9 mRNA levels appeared to correlate closely with the onset of fusion in both cell types. Significant induction of Tspan-2 and Tspan-13 mRNA was observed between 6 and 18hr ( $p \leq 0.001$ ) in both cell lines, while CD9 and CD81 mRNA was reduced at 18hr ( $p \leq 0.01$ ). The results also show that Tspan-5 mRNA was increased at 6hr ( $p \leq 0.001$ ) but reduced at 18hr ( $p \leq 0.01$ ) in both cell lines. It is apparent that Tspan-2 and Tspan-13 gene expression increased relative to uninfected controls during early time points after infection (highest at 6hr), and CD9 and CD81 gene expression reduced during infection, as shown in **Fig 4.5**.

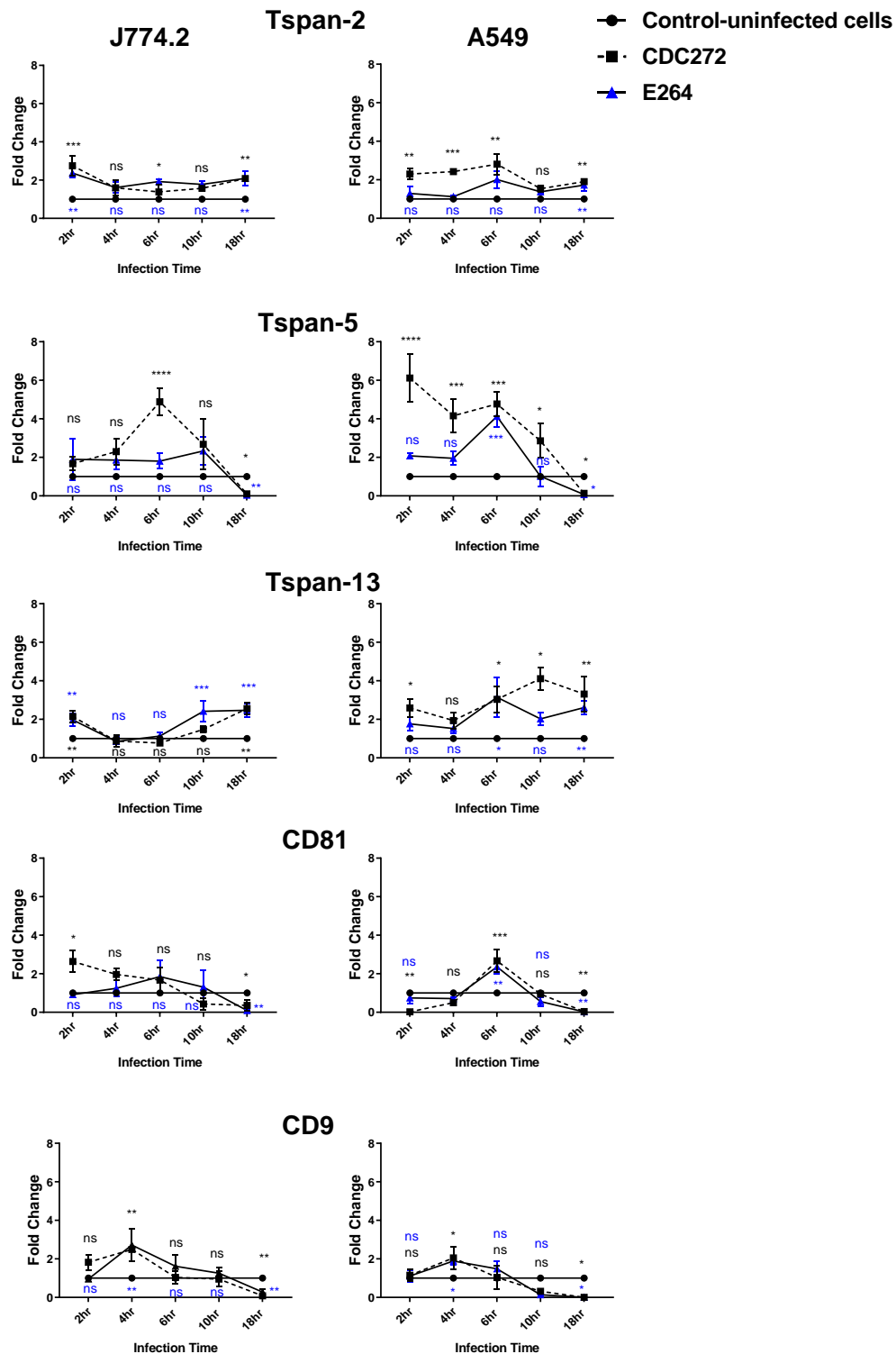


**Figure 4.5 Time-courses of Tspan genes expression during *B. thailandensis* infection in J774.2 and A549 cells.**

Samples of infected and uninfected cells were taken at 0, 2, 4, 6, 10 and 18hr from the initial infection. Gene transcripts were determined by qPCR. The significance of differences were tested by one-way ANOVA, where \*  $p < 0.05$ ; \*\*  $p < 0.01$ ; \*\*\*  $p < 0.001$  significant; ns=non-significant using one-way ANOVA (vs. control-uninfected cells). Blue colour indicates cells infected by E264, and black colour indicates cells infected by CDC272. The results are the means ( $\pm$  SEM) of 3 independent experiments each performed in 2 technical replicates.

#### 4.3.4 Tspan-partner genes expression at the mRNA level in A549 and J774.2 cells

The main feature of Tspan molecules is their interaction capability with other transmembrane molecules such as integrins, ADAM10, CD47, CD98, CD206 and DC-STAMP, thereby acting as molecular coordinators to modulate the functional clustering of proteins in TEM (Levy and Shoham, 2005). This study used the qPCR method to measure the mRNA level of Tspan-partner genes. To do this, RNA was extracted and treated with DNaseI to avoid genomic DNA contamination. cDNA was prepared using a thermocycler machine. cDNA samples and all reverse and forward primers for Tspan-partners (human and mouse) were prepared and tested in a real-time PCR machine. The primer specificity was checked using melting curves as an extra step in a real-time machine. GAPDH was used as a housekeeping gene for Tspan genes expression in human A549 cells and RpL13 $\alpha$  for mouse J774.2 cells.  $\beta$ -actin has been reported as a suitable housekeeping gene for both human as well as mouse (Patil *et al.*, 2015, Eissa *et al.*, 2016, Palacz-Wrobel *et al.*, 2017). GAPDH and RpL13 $\alpha$  were tested by qPCR and were consistent with  $\beta$ -actin (data not shown). Therefore, we decided to use only  $\beta$ -actin instead of using two different housekeeping genes to calculate the relative expression of Tspan-partners mRNA for both mouse J774.2 and human A549 cells. It was observed that all of the selected Tspan-partner genes were highly expressed by both cells types. The relative gene expression of CD98, integrins, ADAM10 and CD172 $\alpha$  genes were more highly expressed than other Tspan-partner genes, as shown in **Fig 4.6**.

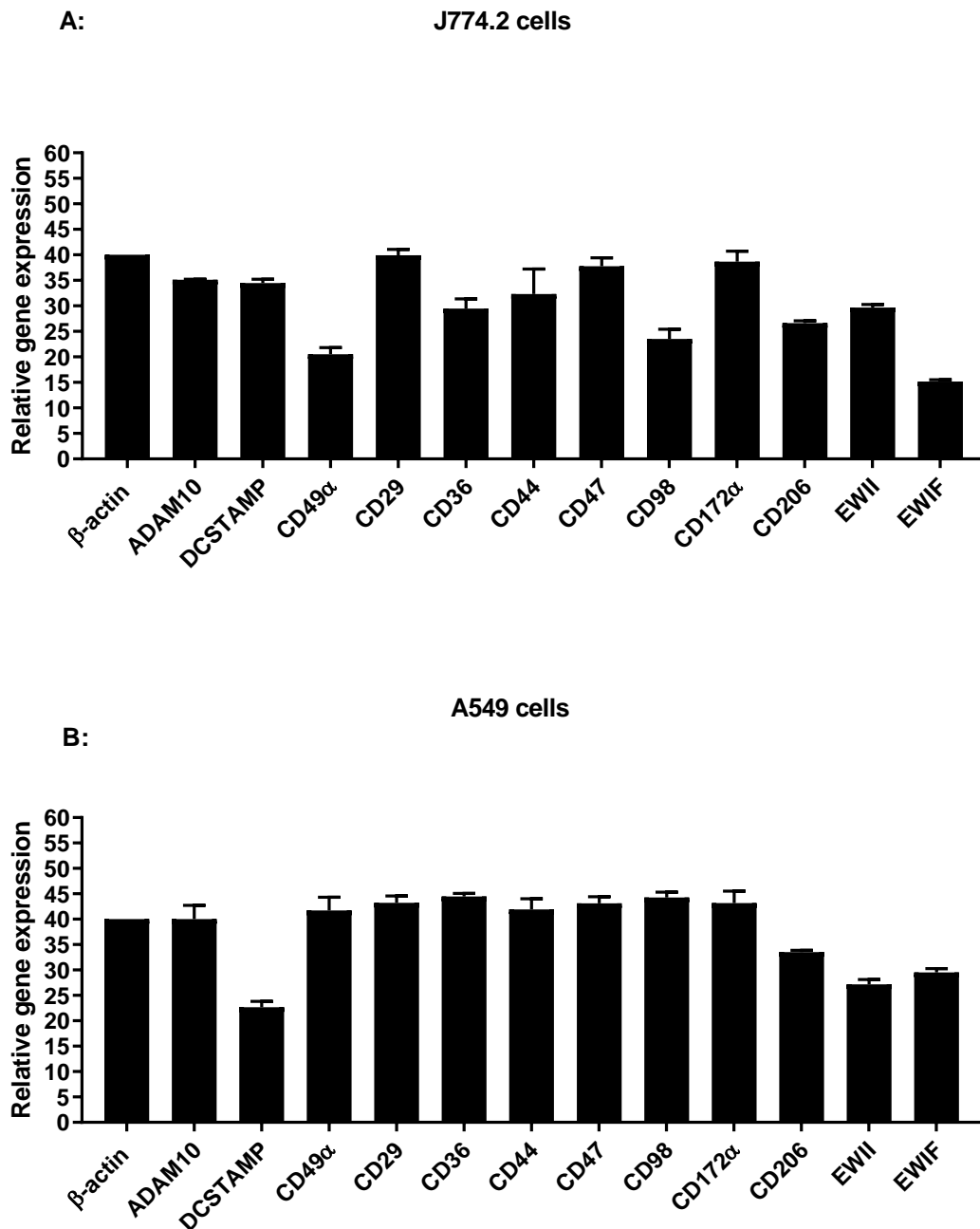


**Figure 4.6 Tspan-partner genes expression at the mRNA level in J774.2 and A549 cells.**

All data have been calculated relative to a suitable housekeeping gene ( $\beta$ -actin). Bars show the mRNA level of Tspan-partner proteins by J774.2 (A) and A549 (B) cells. The results are the means ( $\pm$  SEM) of 3 independent experiments each performed in the 2 technical replicates.

#### 4.3.5 Tspan-partner genes expression at the mRNA level in A549 and J774.2 cells after infection by *B. thailandensis*

This study used the qPCR method to measure the changes of Tspan-partner genes in response to bacterial infection. In order to normalise the qPCR data,

the  $\Delta C_t$  was used to analyse the data. Also, the fold change was calculated using equation  $2^{-\Delta\Delta C_t}$  for all genes. As shown in **Fig 4.7** and **Appendix Fig 6**, 12 Tspan-partner genes had detectable mRNA levels in uninfected cells and 5 Tspan-partner genes were found to change 18hr post-infection. However, only 3 Tspan-partner genes showed consistent changes in expression in both host cell types and both bacterial strains but not with non-fusogenic mutant (E264- $\Delta tssK$ ). These were selected as candidates for further study.

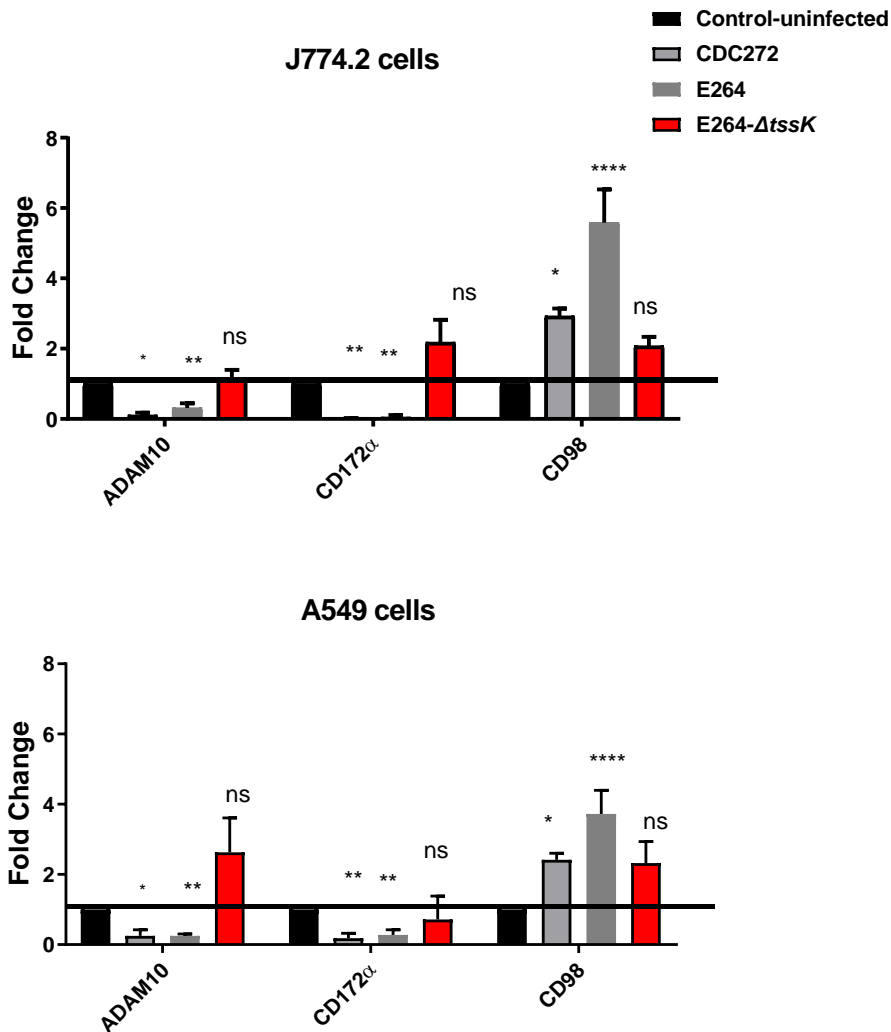


**Figure 4.7 Tspan-partner genes expression changed in response to *B. thailandensis* infection.**

Tspan-partner genes expression were measured by qPCR after 18hr infection with *B. thailandensis* CDC272 or E264 and non-fusogenic mutant (E264- $\Delta tssK$ ). Expression of Tspan-partner proteins was calculated using the  $2^{-\Delta\Delta C_t}$  method relative to the results to the housekeeping gene  $\beta$ -actin. Five Tspan-partner proteins were found to change 18hr post-infection. 3 Tspan-partner proteins showed consistent changes in both host cell types and no change with non-fusogenic mutant (E264- $\Delta tssK$ ). The significance of differences was tested by one-way ANOVA, where \*  $p < 0.05$ ; \*\*  $p < 0.01$ ; \*\*\*  $p < 0.001$ ; \*\*\*\*  $p < 0.0001$  significant (vs. control-uninfected cells). The results are the means ( $\pm$  SEM) of 3 independent experiments performed each in 2 technical replicates.

#### 4.3.6 Innate immune molecules and cell signalling genes following infection with *B. thailandensis*

This experiment was performed to investigate if innate immune or cell signalling molecules are involved in MGC formation and/or bacterial infection. It is known that several innate immune molecules have a role in bacterial infection in many cell types. In particular, signalling molecules SOCS3 and iNOS are involved in *B. pseudomallei* infection (Ekchariyawat *et al.*, 2005). It is also known that this bacterium induces expression of suppressor of cytokine signalling 3 (SOCS3) which inhibits concomitant iNOS activation (Ekchariyawat *et al.*, 2005). The gene expression of these molecules was measured in response to *B. thailandensis* infection in both cell types using qPCR. Data shows gene expression of signalling molecules and 3 innate immune molecules were changed in both host cell types and were also changed with non-fusogenic mutant (E264- $\Delta$ tssK). It seems that they may have a regulatory role in bacterial infection, but not in MGC formation. SOCS3 was upregulated more than 10 fold after 18hr infection, while iNOS was switched off during bacterial infection. 3 factors that have a role in apoptosis were also tested: caspase-1 and p53 were up-regulated after infection, while caspase-3 was not different 18hr post-infection. One main signalling protein p38 was also tested. However, it was not changed with fusogenic or non-fusogenic bacteria, as shown in **Fig 4.8**.

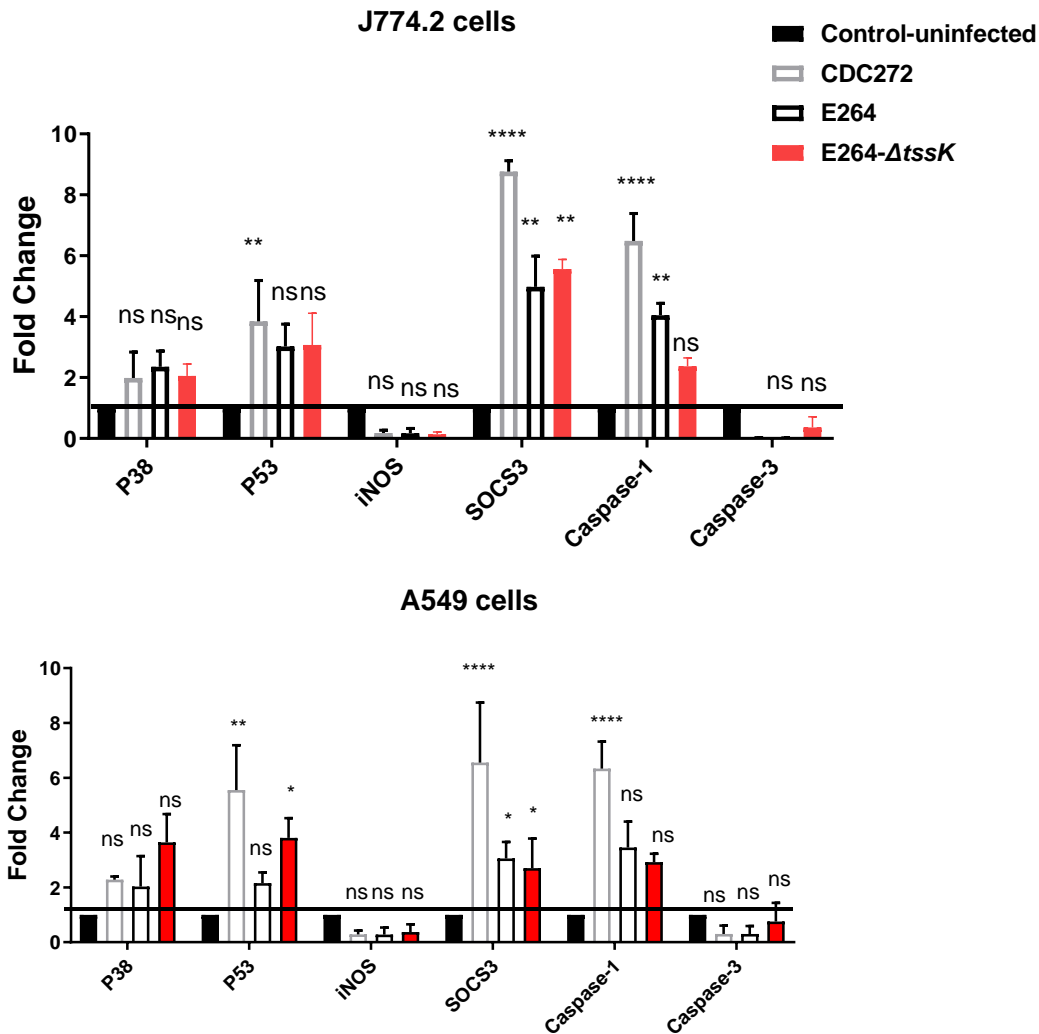


**Figure 4.8 Innate immune molecules and cell signalling genes in MGC formation and/or bacterial infection.**

p38, p53, iNOS, SOCS3, caspase-3, and caspase-1 expression was measured by qPCR after 18hr infection with *B. thailandensis* CDC272 or E264 and non-fusogenic mutant (E264-ΔtssK). Expression of these markers in uninfected and infected J774.2 and A549 cells was calculated using the  $2^{-\Delta\Delta C_t}$  method following the estimation of the house-keeping gene  $\beta$ -actin. p53, SOCS3 and caspase-1 showed changes in both host cell types and showed changes with non-fusogenic mutant (E264-ΔtssK). The significance of differences was tested by one-way ANOVA, where \*  $p < 0.05$ ; \*\*  $p < 0.01$ ; \*\*\*  $p < 0.001$ ; \*\*\*\*  $p < 0.0001$  significant; ns=non-significant (vs. control-uninfected cells). The results are the means ( $\pm$  SEM) of 3 independent experiments each performed in 2 technical replicates.

#### 4.3.7 Tspan proteins expression on the cell surface of A549 cells

Currently, monoclonal or polyclonal antibodies to human Tspan molecules are not available for all proteins. Only the level of Tspan-2, Tspan-11, Tspan-13, Tspan-15, CD151, CD9, CD63 and CD81 proteins were tested on human lung cell lines A549 by flow cytometry. To do this, we used FACS analysis of the binding of these antibodies to live A549 cells. Cells were harvested using a non-enzymatic cell dissociation solution and stained, as described in **section**

**2.2.3.2.1.** A FITC-labelled secondary antibody was used at the manufacturer's recommended concentration 1:250. The data are shown as median fluorescence intensity (MFI). The negative controls here were cells treated with the binding buffer BBN or irrelevant antibody with the same isotype. This study was not used to screen the level of Tspan proteins expression on the J774.2 cells because this has already been done in a previous study (Elgawidi, 2016) in some cases or the anti-mouse antibodies are not available. The data showed that CD9, CD81, Tspan-2, Tspan-13, Tspan-15 and CD151 are expressed on the surface of A549 cells (**Fig 4.9**).

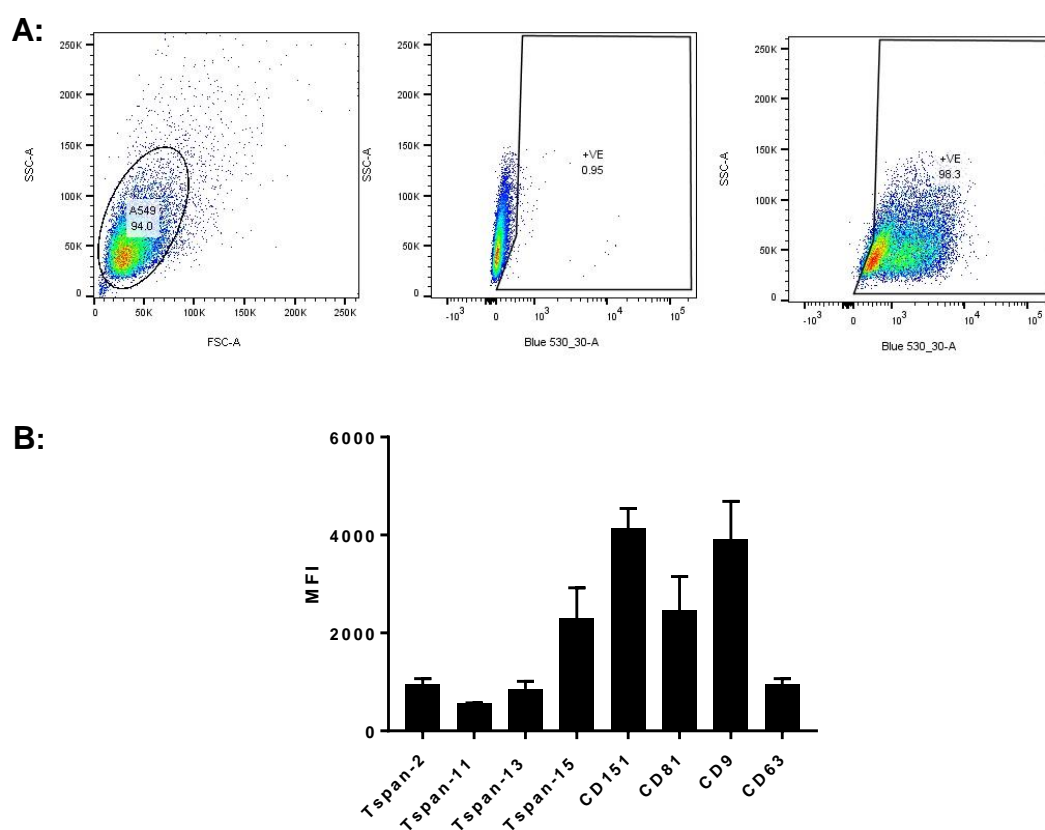


**Figure 4.9 Tspan proteins surface expression on the cell surface of A549 cells.**

The analysis was performed by flow cytometry on A549 cells. **A:** Dot plot showing the gated population (encircled) of A549 selected for analysis according to their side scatter (SSC) and forward (FCS) characteristics. **B:** The means of median fluorescence intensities relative to their isotypes. The results were the mean ( $\pm$  SEM) of 4 independent experiments each performed in 2 technical replicates.

#### 4.3.8 Tspan proteins expression following *B. thailandensis* infection

This experiment was performed to investigate if the selected Tspan proteins changed in response to 18hr of bacterial infection. The levels of Tspan-2,

Tspan-13, CD9 and CD81 proteins on the cell surface were investigated at 18hr post-infection using flow cytometry. Interestingly, the results show an elevation in the levels of Tspan-2 and Tspan-13 during infection by *B. thailandensis* CDC272 and WT E264 compared with their levels during infection by mutant *B. thailandensis* E264- $\Delta$ tssK. However, the results show that the levels of CD9 and CD81 did not change during infection by *B. thailandensis* CDC272 or WT E264 and E264- $\Delta$ tssK, as shown in **Fig 4.10**. These data indicate that whilst Tspan-2 and Tspan-13 may have a role in MGC formation, they could also be involved in the bacterial infection.

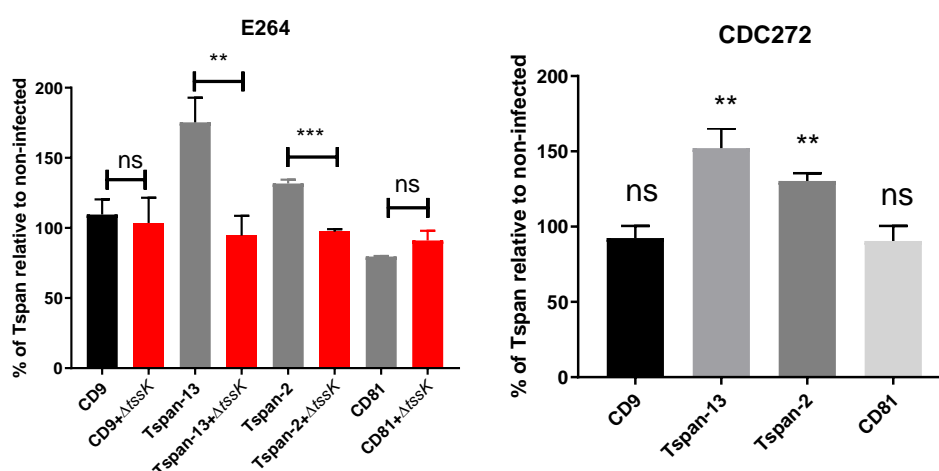


**Figure 4.10 Tspan-2, Tspan-13 and CD9 proteins change in response to *B. thailandensis* infection on the surface of A549 cells.**

A549 cells were infected with fusogenic *B. thailandensis* CDC272 and WT E264 or non-fusogenic mutant (E264- $\Delta$ tssK). A549 cells left uninfected were used as controls. After 18hr of infection, the cells were stained with primary anti-Tspan antibodies and labelled secondary antibodies and then analysed by flow cytometry. Expression of Tspan proteins after infection were normalized to the levels on uninfected cells (100%). The significance of differences was tested by one-way ANOVA, where \*\* p<0.01; \*\*\* p<0.001 significant; ns=non-significant. The results are the means ( $\pm$  SEM) of 3 independent experiments each performed in 2 technical replicates.

#### 4.3.9 Gating strategy to detect fused and/or infected cells using flow cytometric analysis.

To determine if CD9 expression changed only on infected and/or fusing cells, we devised a strategy to measure levels only on these cells. It was expected that the fused or infected cells would be larger and located in lower right quadrant (Q3) of an SSC/FSC, as shown in **Fig 4.11**. The percentage of A549 infected cells by *B. thailandensis* CDC272 was about 13.1%, while the percentage was 11.3% for A549 cells infected with *B. thailandensis* E264.

Furthermore, the percentage of A549 cells infected with E264- $\Delta$ tssK is about 8%. However, it is possible that some MGC would be too large to flow through the cytometer nozzles and these would be excluded from this analysis. The data showed that there is a significant reduction of CD9 on A549 cells after 18hr E264 infection but not CDC272 (Fig 4.12). Other Tspans did not show any changes in expression when analysed with the same strategy (data not shown).

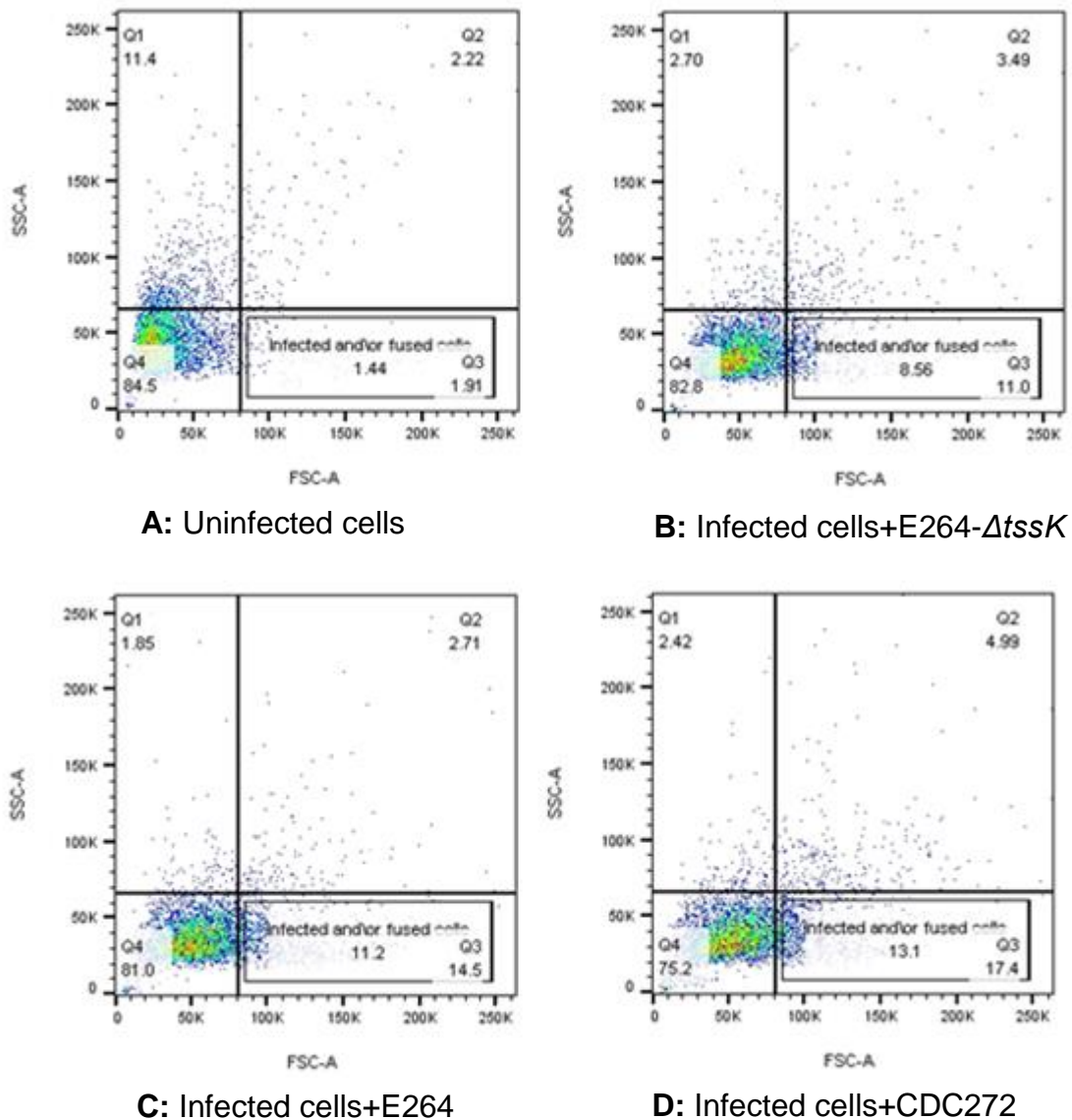


**Figure 4.11 Gating strategy to detect fused or/and infected cells using flow cytometric analyses.**

The dot plots show A549 cells gated according to forward scatter (FSC), and side scatter, the Q3 gates show fused cells infected by *B. thailandensis*. The graphs represented for the means ( $\pm$  SEM) of 3 independent experiments each performed in 2 technical replicates.

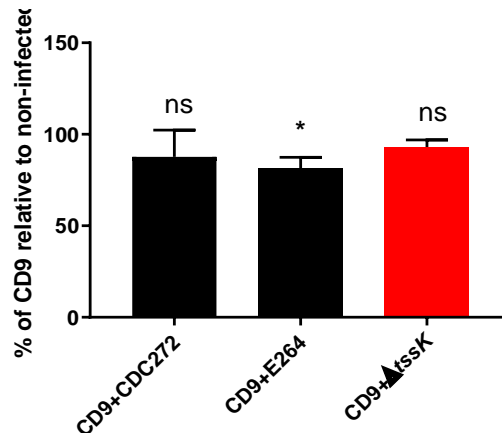


**Figure 4.12 CD9 expression changed in response to *B. thailandensis* infection on the surface of A549 cells after gating strategy.**

A549 cells were infected with either fusogenic *B. thailandensis* CDC272 or E264 and non-fusogenic mutant (E264- $\Delta$ tssK) for 2hr. A549 cells left uninfected were used as controls. After 16hr of kanamycin and amikacin treatment, cells were stained with primary anti-CD9 antibody and secondary antibody and then analysed by flow cytometry. Percentages of MFI of gated larger A549 cells from Q3 after infection were normalized to uninfected cells. The significance of differences was measured by unpaired t-test, where \*  $p < 0.05$  significant; ns=non-significant. The results are the means ( $\pm$  SEM) of 3 independent experiments each performed in 2 technical replicates.

#### 4.3.10 Time-courses of downregulation or upregulation of selected Tspan proteins on the surface of A549 cells

The levels of CD9, CD81, Tspan-2 and Tspan-13 proteins on the cell surface during the infection were also investigated at different time courses to try and correlate Tspan proteins expression with the onset of fusion. The quantification was performed using flow cytometry, as described in **section 2.2.3.5**. Briefly, both infected and uninfected cells were harvested and washed with BBN. Appropriate primary antibodies were incubated with cells for 45min. A FITC-labelled secondary antibody was used at the recommended concentration. The negative controls here were cells treated with the binding buffer BBN or irrelevant antibody with the same isotype. The MFI was normalized to uninfected cell expression levels for all samples. The results show that Tspan-13 and Tspan-2 expression during bacterial infection did not change at 2 and 8hr after infection, but showed a significant increase after 18hr infection, compared with uninfected cells. Expression of CD9 and CD81 significantly increase after 8hr infection and then reduced at the later time points. Tspan-13 and Tspan-2 expression were correlated with mRNA levels at the same time points. CD9 and CD81 showed differences between mRNA and protein levels, as shown in **Fig 4.13**.

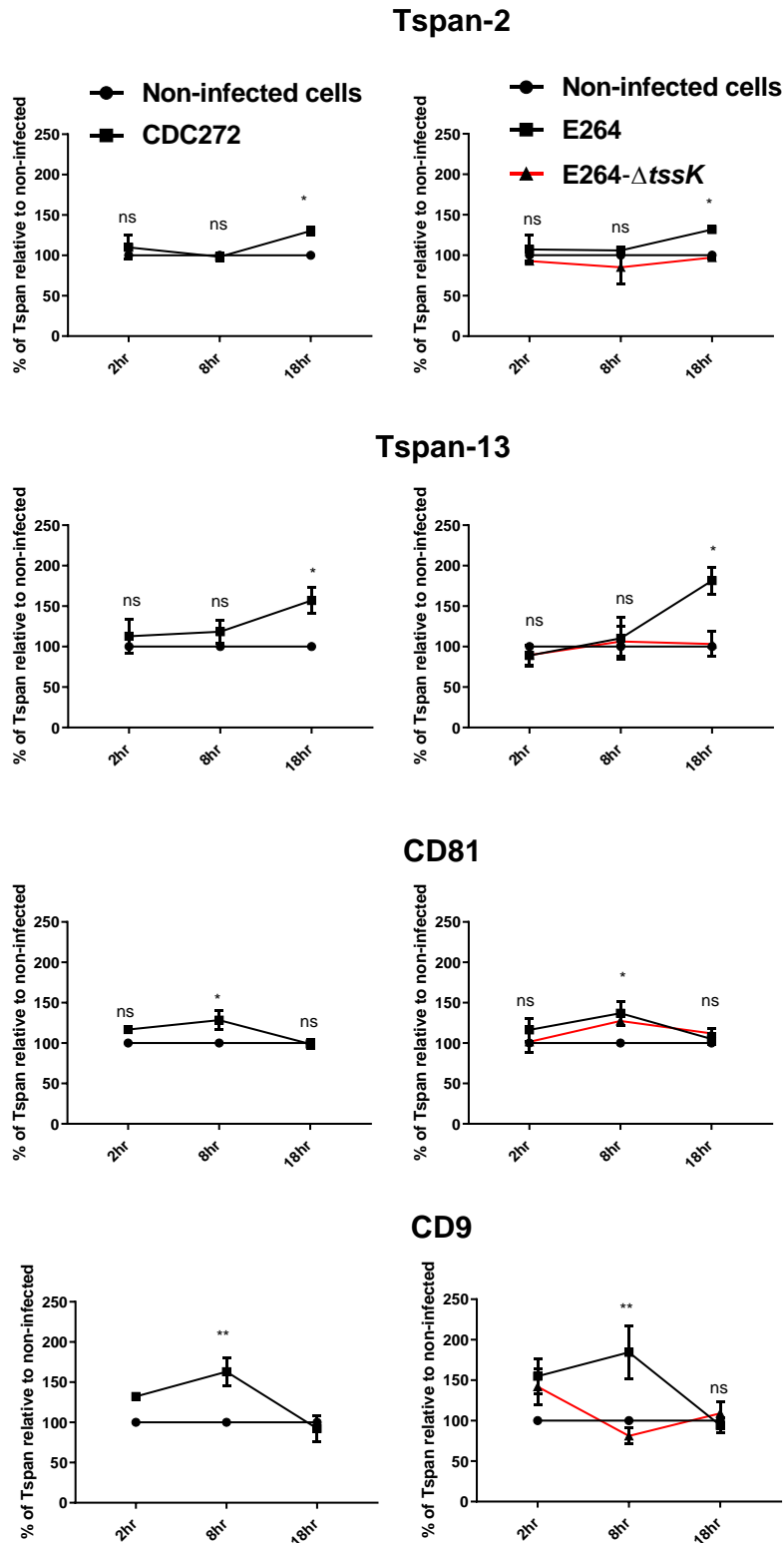


**Figure 4.13 Time-courses of Tspan proteins expression on the surface of A549 cells in response to *B. thailandensis* infection.**

A549 cells were infected with either fusogenic *B. thailandensis* CDC272 or E264 and non-fusogenic mutant (E264- $\Delta tssK$ ). A549 cells left uninfected were used as controls. Samples were taken at 2, 8 and 18hr after the initial infection. Cells were stained with primary antibodies and analysed by flow cytometry at each time course of infection. The significance of differences was tested by one-way ANOVA, where \*  $p < 0.05$ ; \*\*  $p < 0.01$  significant; ns=non-significant (vs control uninfected cells). The results are the means ( $\pm$  SEM) of 3 independent experiments each performed in 2 technical replicates.

#### 4.3.11 Tspan-partner proteins expression on the surface of A549 cells

Only ADAM10, CD98 and CD172 $\alpha$  were measured on the surface of A549 cells by flow cytometry as described in **section 2.2.3.2.1**. To do this, we used FACS analysis of the binding of these antibodies to live A549 cells. Cells were harvested using a non-enzymatic cell dissociation solution and stained, as described in **section 2.2.3.2.1**. A FITC-labelled secondary antibody was used at the manufacturer's recommended concentration 1:250. The negative controls here were cells treated with the binding buffer BBN or irrelevant antibody with the same isotype control. The data showed that ADAM10, CD98 and CD172 $\alpha$  were expressed on the surface of A549 cells, with high levels of ADAM10 and CD98 but low levels of CD172 $\alpha$  (**Fig 4.14**).

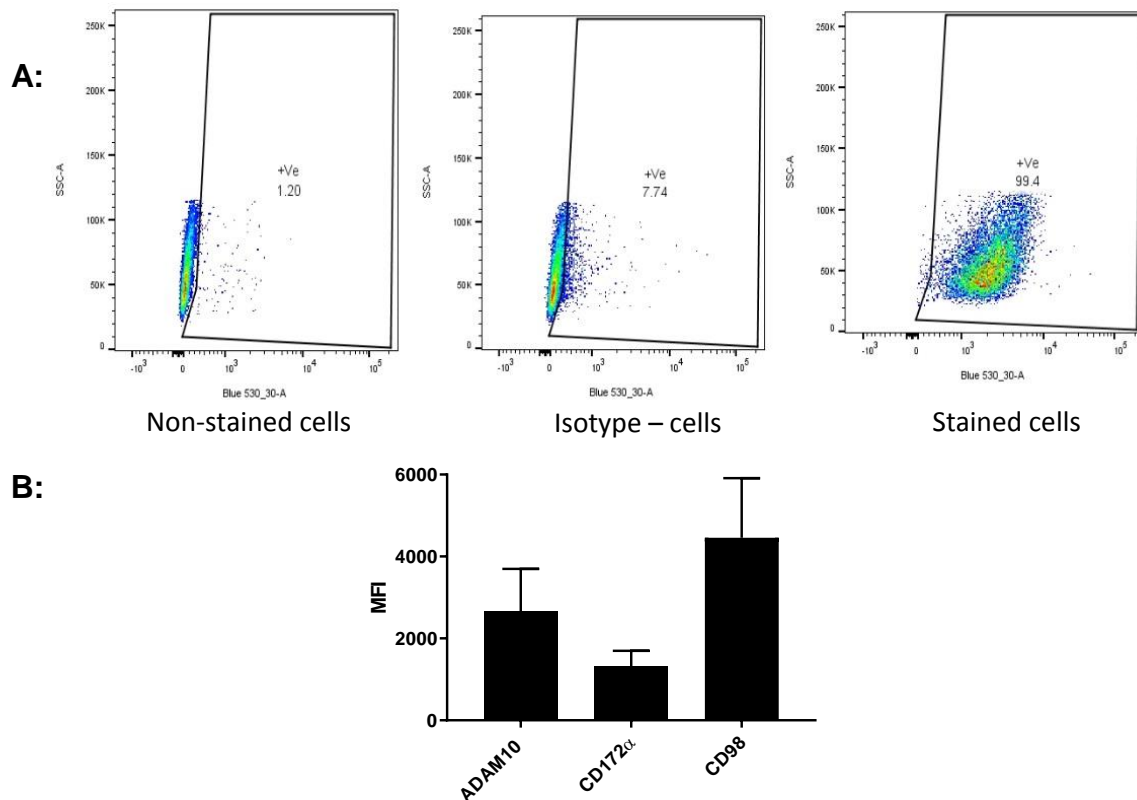


**Figure 4.14 Tspan-partner proteins expression on the surface of A549 cells.**

The analysis was performed by flow cytometry on A549 cells. Primary anti-ADAM10, CD98 and CD172 $\alpha$  antibodies in BBN were used with non-specific mouse IgG1a as isotype control. Secondary antibodies were an anti-mouse IgG-FITC antibody for anti-ADAM10, while anti-CD172 $\alpha$  was a conjugated antibody **A:** Dot plot showing the gated population (encircled) of A549 selected for analysis according to their side scatter (SSC) and forward (FCS) characteristics. **B:** The means of median fluorescence intensities relative to their isotypes. The results are the means ( $\pm$  SEM) of 3 independent experiments each performed in 2 technical replicates.

#### 4.3.12 Tspan-partner proteins expression following *B. thailandensis* infection

The expression of Tspan-partner proteins was investigated to determine if a change occurs in response to infection with the WT strain, but remains unchanged with the mutant strain. Briefly, both infected and uninfected cells were harvested and washed with BBN. Appropriate primary antibodies were incubated with cells for 45min. A FITC-labelled secondary antibody was used at the recommended concentration. The negative controls here were cells treated with the binding buffer BBN or irrelevant antibody with the same isotype. Interestingly, the results show that there is no change in the level of ADAM10, and CD98 did not change in response to both WT and E264- $\Delta$ tssK infection. However, CD172 $\alpha$  was observed to significantly decrease after infection by *B. thailandensis* CDC272 and E264 compared with the level of CD172 $\alpha$  during infection by *B. thailandensis* E264- $\Delta$ tssK, as described in **Fig 4.15**.

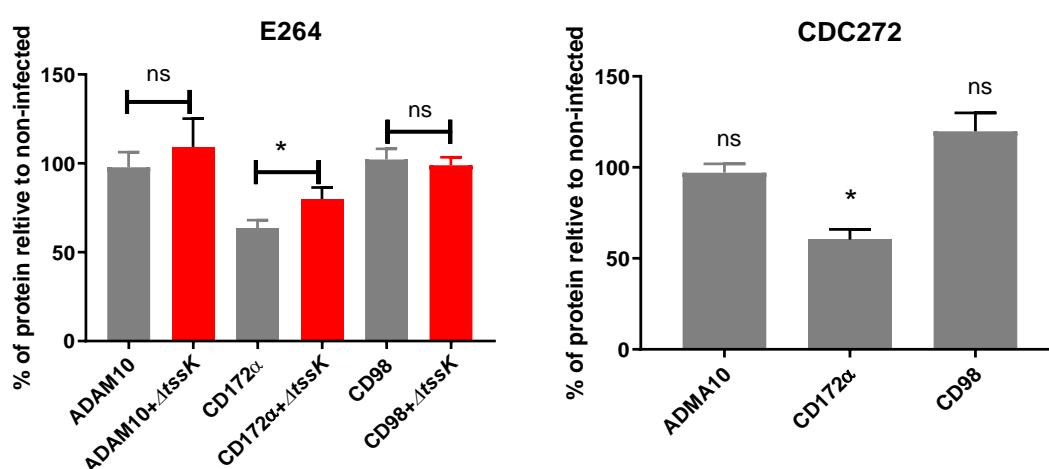


**Figure 4.15 Tspan-partner proteins expression in response to *B. thailandensis* infection of A549 cells.**

A549 cells were infected with either fusogenic *B. thailandensis* CDC272 and WT E264 or non-fusogenic E264  $\Delta$ tssK. A549 cells left uninfected were used as controls. After the 16hr of kanamycin and amikacin treatment, cells were stained with primary antibodies and analysed by flow cytometry. Expression of Tspan-partner proteins after infection was normalized to the expression on uninfected cells. The significance of differences to  $\Delta$ tssK was measured by t-test, where \* p<0.05 significant. The results are the means ( $\pm$  SEM) of 3 independent experiments each performed in 2 technical replicates.

#### 4.3.13 Time-courses of Tspan-partner proteins expression following *B. thailandensis* infection on A549 cells

The levels of Tspan-partner proteins were measured over time during bacterial infection. These molecules might have a role in the MGC formation as negative or positive regulators. ADAM10 expression during bacterial infection was increased significantly after 8hr and then reduced compared with uninfected cells, while CD98 was only increased significantly during 8hr infection compared with infected cells by E264- $\Delta tssK$  (**Fig 4.16**). However, CD172 $\alpha$  did not change after 2hr and 8hr infection but was significantly decreased after 18hr infection compared with uninfected cells and infected cells by E264- $\Delta tssK$ . It seems that there is no correlation between mRNA and protein expression for either ADAM10 and CD98. It is also apparent that CD172 $\alpha$  was decreased in response to bacterial infection and that there are no differences between the two types of fusogenic bacterial strains.

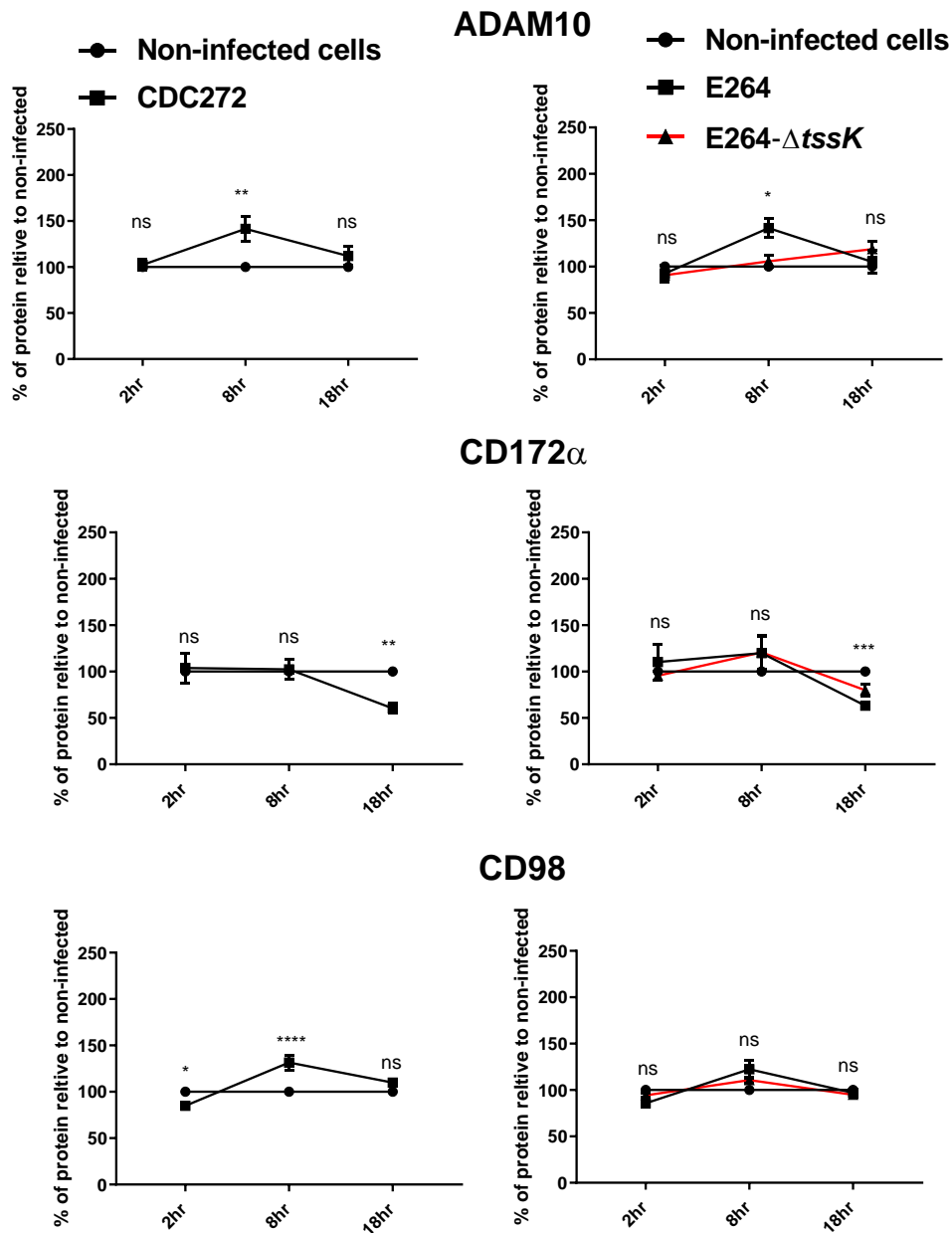


**Figure 4.16 Time-courses of Tspan-partner proteins expression on the surface of A549 cells in response to *B. thailandensis* infection.**

A549 cells were infected with either fusogenic *B. thailandensis* CDC272 or E264 and non-fusogenic mutant (E264- $\Delta tssK$ ). A549 cells left uninfected were used as controls. Samples were taken at 2, 8 and 18hr from the initial infection. Cells were stained with primary antibodies and analysed by flow cytometry at each time point. The significance of differences was tested by one-way ANOVA, where \*  $p < 0.05$ ; \*\*  $p < 0.01$ ; \*\*\*  $p < 0.001$ ; \*\*\*\*  $p < 0.0001$  significant; ns=non-significant. The results are the means ( $\pm$  SEM) of 3 independent experiments each performed in 2 technical replicates.

## 4.4 Discussion

This chapter focused on Tspans expression at the mRNA and the protein levels in J774.2 and A549 cells. In addition, some innate immunity and cell signalling genes were also examined. The hypothesis behind this work was conceived following previous reports that Tspans and Tspan-associated proteins have a role in MGC formation and/or *B. thailandensis* infection of these two cell lines.

### 4.4.1 Tspans expression change at the mRNA and protein levels following *B. thailandensis* infection

The main aim was to detect which Tspan molecules are changed during *B. thailandensis* infection and/or MGC formation. Here, all 33 human and 31 mouse Tspans had detectable at mRNA in uninfected A549 and J774.2 cells; 10 Tspans were found to change post-infection but only 5 Tspans showed consistent changes in both host cell types and no change with E264- $\Delta$ tssK (Tspan-2, Tspan-5, Tspan-13, CD81 and CD9) (**Fig 4.4**). The mRNA levels of Tspan-2 and Tspan-13 increased but mRNA levels of Tspan-5, CD81 and CD9 decreased. It would be predicted that there might be an essential role for these proteins primarily in MGC formation rather than a bacterial infection. To our knowledge, there is no other study that has systematically measured Tspan genes expression during bacterially-induced MGC formation.

In **sections 4.3.3** and **4.3.10**, these 5 Tspans were selected for further study using 2-18hr time courses. All of these appeared to correlate quite closely with the onset of fusion in both cell types. Expression of Tspan-2, Tspan-5 and Tspan-13 at the mRNA level in the earlier stages of infection increased rapidly, perhaps indicating that the cells increased gene expression to improve their ability to engulf bacteria. However, Tspan-5 decreased in the later stages of infection. It seems that Tspan-5 has a different role during bacterial infection, while Tspan-2 and Tspan-13 might promote bacterial infection and might also induce MGC formation. Flow cytometry confirmed changes at the protein level for only 2 Tspans (Tspan-2 and Tspan-13). CD9 and CD81 mRNA were reduced during the later stages of the fusogenic bacterial infection but reductions were not seen at the protein level (**Figs 4.5**

**and 4.13**). That does not mean that CD9 and CD81 have no role in MGC formation because larger fusing cells with reduced protein levels may not be detectable by flow cytometry as MGC could be too large to flow through the cytometer nozzles. There are only a limited number of publications on Tspan functions in MGC formation. For example, Iwai *et al.* have tested CD9 at the mRNA level in RAW264 cells and found that CD9 expression increases during osteoclastogenesis (Iwai *et al.*, 2007). These results were different from our finding that expression of CD9 in both J774.2 and A549 cells was decreased during MGC formation. In addition, we attempted to analyse the results on the principles of flow cytometric analysis, which are the larger cells would be in the same location in plotting (**Fig 4.11**). It was observed that only CD9 in infected cells was reduced compared with uninfected cells (**Fig 4.12**). Our finding here was supported by Takeda *et al.* who found that CD9 has a negative role in MGC (Takeda *et al.*, 2003).

Iwai *et al.* also observed that the expression of Tspan-13 decreased and Tspan-5 increased during osteoclastogenesis (Iwai *et al.*, 2007). Our findings suggest that Tspan-13 and Tspan-5 may have different roles in *Burkholderia*-induced MGC formation. Zhou *et al.* also found that Tspan-5 was upregulated in RAW264 cells during osteoclastogenesis (Zhou *et al.*, 2014). This result also did not correlate with ours in regards to Tspan-5. It seems that Tspan-5 and Tspan-13 play different roles during fusion, depending on the types of inducers.

#### 4.4.2 Tspan-partners expression change at the mRNA and protein levels following *B. thailandensis* infection

There are studies that report that Tspan-partner proteins, including CD98, CD44, CD47 and DC-STAMP, are important in macrophage fusion (Ozge *et al.*, 2009, Yagi *et al.*, 2005, Martinez *et al.*, 2009, Weiguo *et al.*, 2006). Here, we investigated 12 Tspan-partners after 18hr of infection with *B. thailandensis*. The expression of 5 Tspan-partners at the mRNA level was found to change post-infection, but only 3 showed consistent changes in both host cell types and no change with E264- $\Delta$ tssK (ADAM10, CD172 $\alpha$  and CD98) (**Fig 4.7**). We observed that ADAM10 and CD172 $\alpha$  decreased at the

mRNA level, whereas CD98 significantly increased. Interestingly, flow cytometry confirmed changes at the protein level at 18hr only for CD172 $\alpha$  (**Fig 4.15**). That does not mean there is no role for ADAM10 and CD98 in MGC formation induced by *B. thailandensis* because a large MGC cannot flow through the cytometer nozzles and some expression changes at the later stages of fusion may have been missed.

These findings were not in agreement with Gautam and Acharya who found that CD172 $\alpha$  and CD47 gene expression were increased in cells stimulated by Hsp70-peptide complex to form MGC (Gautam and Acharya, 2014). However, Verrier *et al.* observed that ADAM10, 17 and 15 decreased during osteoclastogenesis (Verrier *et al.*, 2004). This finding is in agreement with our data that shows ADAM10 decreases during MGC formation. We found that CD98 gene expression at 18hr increased in response to bacterial infection, but CD98 protein expression significantly increased only at 8hr infection (**Fig 4.16**). This finding is supported by Suparak *et al.* who showed that CD98 increased after *B. pseudomallei* infection (Suparak *et al.*, 2011). Paola *et al.* have shown that CD98 has a role in MGC formation by activating integrin in a human placental trophoblast cell line (BeWo) (Paola *et al.*, 2007). Yoshiki and Boyd have also demonstrated the positive role of CD98 in MGC formation (Yoshiki and Boyd, 2004). It seems that CD98 may also have a role in MGC formation and/or bacterial infection.

#### 4.4.3 Innate immune molecules and cell signalling genes following infection with *B. thailandensis* in A549 and J774.2 cells

It is known that some innate immune molecules and cell signalling genes have a role in bacterial infection with many cell types. It is also known that this bacterium induces expression of SOCS3, which inhibits concomitant iNOS activation (Ekchariyawat *et al.*, 2005).

Changes in gene expression of p53, caspase-1 and SOCS3 genes were detected in response to *B. thailandensis* infection in both cell types. However, they were also changed after infection with the non-fusogenic mutant (E264- $\Delta$ tssK), suggesting that these are primarily involved in infection rather than fusion (**Fig 4.8**). These data were partly supported by Ekchariyawat *et al* who

observed that *B. pseudomallei* can increase expression of SOCS3 (Ekchariyawat *et al.*, 2005). A study has also shown that three factors (p53, caspase-1 and caspase-3) were involved in apoptosis and pyroptosis (Crighton *et al.*, 2007). Kang *et al.* have found that caspase-1 was up-regulated in response to infection with both *B. pseudomallei* (Kang *et al.*, 2016). Polyak *et al.* demonstrated that p53 could induce apoptosis via the generation of reactive oxygen species that damage mitochondria (Polyak *et al.*, 1997). It could be suggested that infected cells were ready to undergo apoptosis after 18hr bacterial infection.

## Chapter 5 Distinct roles for Tspans and Tspan-partner proteins in MGC formation during *B. thailandensis* infection

### 5.1 Introduction

It has been widely shown that *B. thailandensis* and *B. pseudomallei* can induce MGC formation by bacterial effectors (Toesca *et al.*, 2014, Schwarz *et al.*, 2014). It is possible that the bacteria can regulate this process by affecting the expression of host cell membrane molecules, including Tspan members. It has been found that anti-CD9 antibody and recombinant soluble forms of the extracellular domain (EC2) of CD9 have a negative effect on bacterial adhesion to epithelial cells, including adhesion of *E. coli*, *S. aureus* and *N. meningitides* (Green *et al.*, 2011). Furthermore, Hassuna has shown that CD9 is implicated in *S. typhimurium* infection of monocyte-derived macrophages at different stages (Hassuna, 2010). Furthermore, our research team have observed that using antibodies against mouse CD9, CD81 and CD63 enhances MGC formation in J774.2 and RAW264 mouse macrophages cell lines infected with *B. thailandensis* (Elgawidi, 2016).

In this chapter, we investigated the roles of the Tspans and partner proteins identified in **chapter 4**, using antibodies, recombinant proteins and a peptide derived from CD9EC2. This may give clues about the mechanism of infection and MGC formation.

### 5.2 Aims

To investigate the effects on bacterial infection and MGC formation of A549 cells of:

- 1) anti-human antibodies against CD9, CD81, Tspan-2, Tspan-13, ADAM10, CD98 and CD172 $\alpha$ ;
- 2) over-expressed proteins, recombinant GST-CD9EC2 and CD9EC2-derived peptide.

The possible co-localization of *B. thailandensis* with CD9GFP in the mouse cell line, J774.2 was also investigated.

## 5.3 Results

### 5.3.1 Role of CD9 in infection and MGC formation

#### 5.3.1.1 The effect of anti-CD9 antibody on bacterial infection in A549 cells

This experiment was to investigate if there is any role for CD9 in *B. thailandensis* infection, in particular, the total bacterial infection and internalisation in A549 cells after 2hr infection. The infection assay was performed as described in **section 2.2.5**. In brief, A549 cells were seeded in 96 well plates and some treated for 1hr with the anti-CD9 antibody. Both treated and untreated cells were infected with *B. thailandensis* CDC272 and E264. To count the total bacterial infection, the wells were washed 3x with HBSS and lysed by the addition of 100µl of 1% TritonX-100 for 15min. To count only internalised bacteria, the cells were cultured with DMEM containing antibiotics, washed, and lysed using TritonX-100. The lysis mixture was serially diluted before 10µl of each dilution was pipetted onto LB agar plates. After 48hr of incubation at 37°C, colonies were counted and used to calculate CFU per well. Data showed that anti-CD9 antibody has no effect on the total bacterial infection associated with cells or internalisation when compared with the effect of isotype antibody control on both *B. thailandensis* strains (**Fig 5.1**). It might be that CD9 has no role in *B. thailandensis* infection.

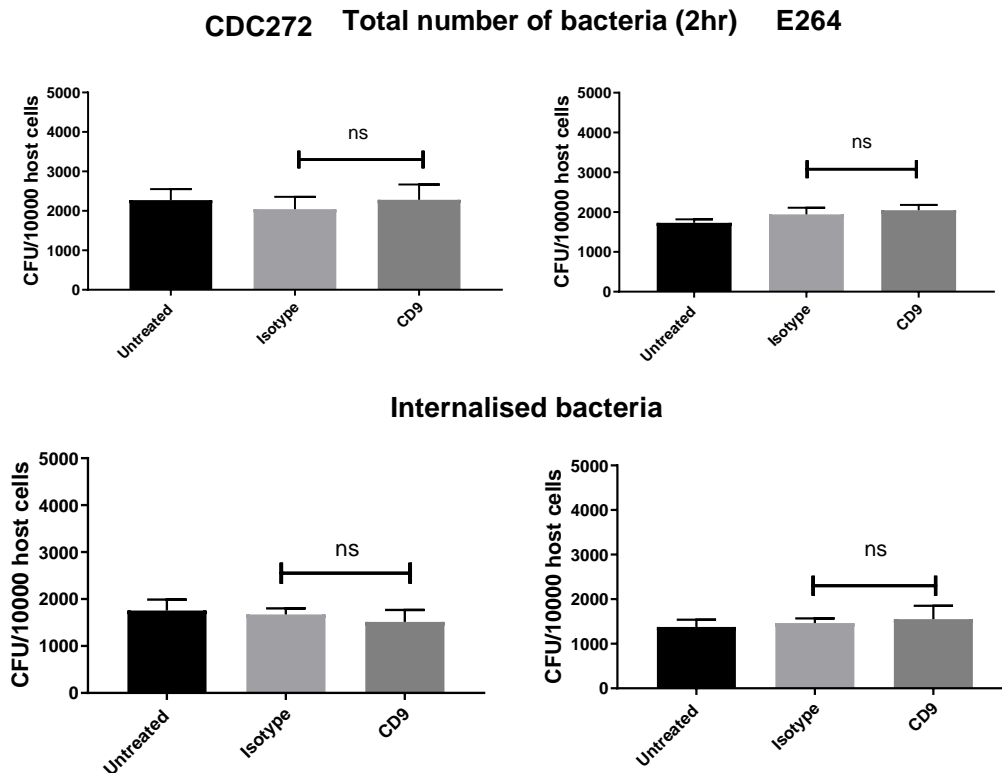


**Figure 5.1 Effect of anti-CD9 antibody on total *B. thailandensis* infection.**

A549 cells were pre-treated with isotype control (JC1) and anti-CD9 antibody before infection, as described in **section 2.2.7**. Bars total number of bacteria and/or internalised bacteria per 10000 cells for A549 cells infected by two bacterial strains, CDC272 and E264. The effects of anti-CD9 treatments were tested against the isotype control by unpaired t-test, where ns=non-significant. The results were the mean for 3 independent experiments each performed in 4 technical replicates.

### 5.3.1.2 The effect of anti-CD9 and anti-CD81 antibodies on MGC formation induced by *B. thailandensis* in A549 cells

This experiment was performed using anti-human antibodies against CD9 and CD81, as described in **section 2.2.8**. To do this, A549 cells were seeded in 96 well plates and treated for 1hr with anti-CD9 and anti-CD81 antibodies. Then the cells were infected with *B. thailandensis* CDC272 and E264 for 2hr and then changed the medium to DMEM containing antibiotics for 16hr. The fusion index was quantified relative to unfused cells per field of view. MGCs were defined as cells containing 3 or more nuclei. Data shows that anti-CD9 and anti-CD81 antibodies enhanced MGC formation when compared with the effect of isotype control in both bacteria strains, and increased the nuclei per MGC, as shown in **Fig 5.2**. Effect of anti-CD81 antibody on bacterial infection was tested, as shown in **section 5.3.2.1**. It might be that CD9 and CD81 may have a negative role in MGC formation induced by *B. thailandensis*.

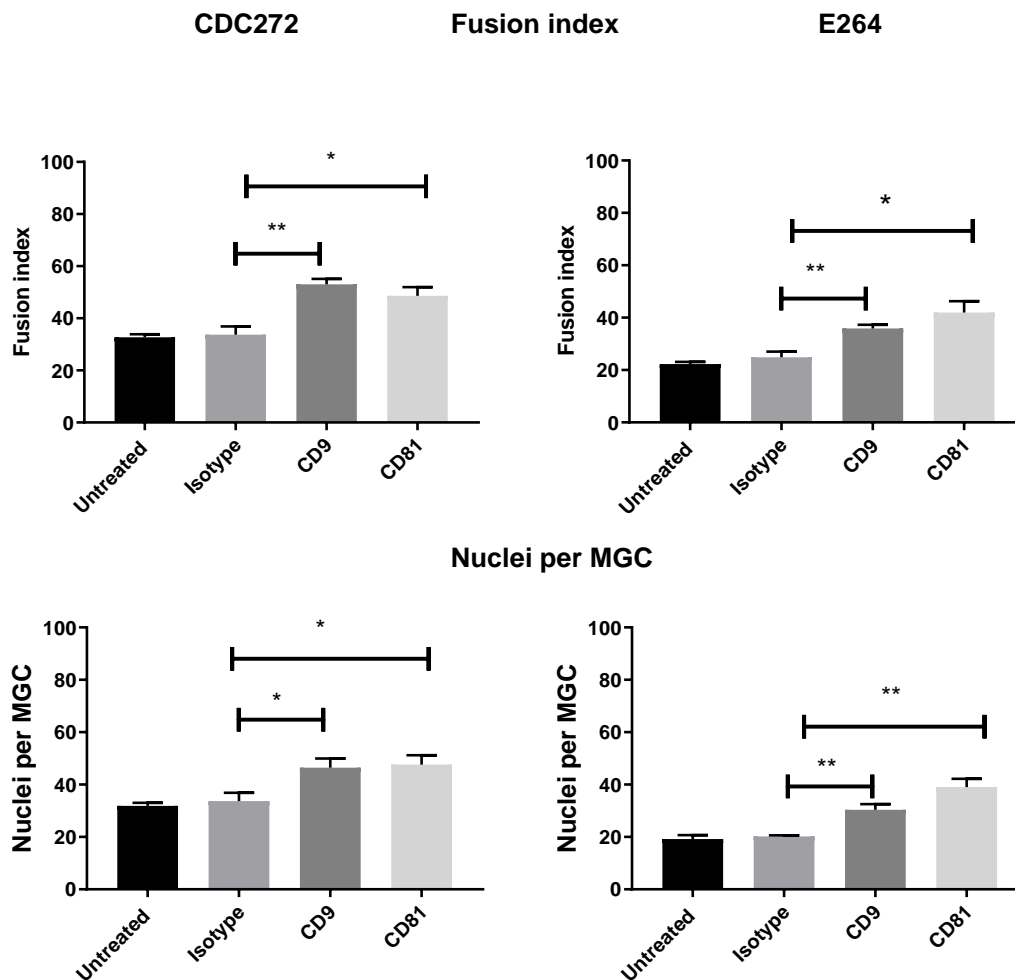


**Figure 5.2 Effect of anti-CD9 and CD81 antibodies on MGC formation induced by both *B. thailandensis* CDC272 and E264.**

A549 cells were pre-treated with isotype control and anti-CD9 and CD81 antibodies before *B. thailandensis* infection, as described in **section 2.2.7**. Bars show the fusion index and nuclei per MGC for A549 cells infected with both strains of *B. thailandensis*. The effects of different treatments were tested by unpaired t-test, where \*  $p < 0.05$ ; \*\*  $p < 0.01$  significant. The results were the mean for 3 independent experiments each performed in 4 technical replicates.

### 5.3.1.3 Effect of CD9 over-expression on the total bacterial infection and internalised bacteria in J774.2 cells

This study aimed to compare the total bacterial infection at 2hr and internalised bacteria at 18hr in WT J774.2 and cells over expressing GFP (GFPJ774.2) or mouse CD9GFP (CD9GFPJ774.2). Transfected and non-transfected J774.2 cells were seeded in 96 well plates and infected with either CDC272 or E264 strains for 2 and 18hr. The results show that there are no

differences between WT J774.2, GFPJ774.2 and CD9GFPJ774.2 cell lines for the total bacterial infection at 2hr or internalised bacteria at 18hr (**Fig 5.3**).

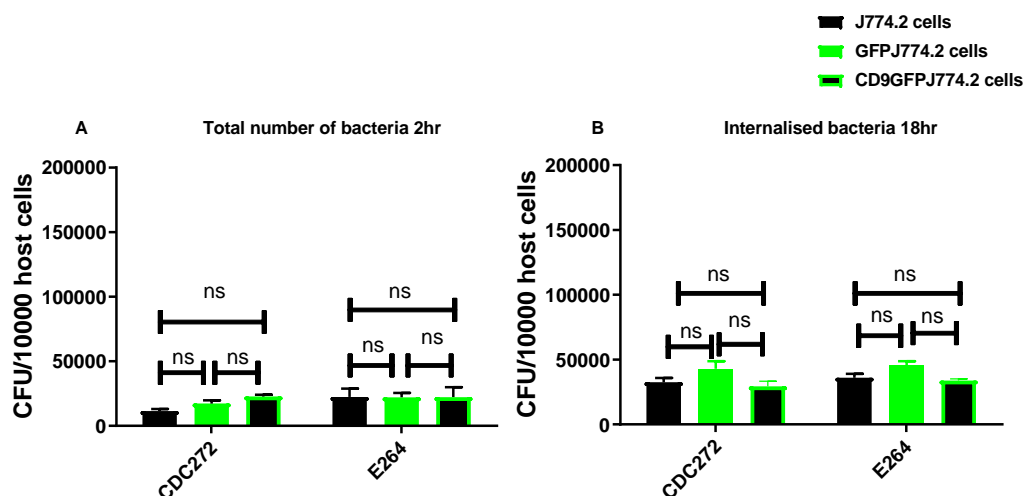


**Figure 5.3 Comparison of total number of bacteria and internalised bacteria at 2 and 18hr in J774.2 cells expressing GFP or CD9GFP.**

WT, GFP and CD9GFPJ774.2 cells were washed two times before infection, as described in **section 2.2.7**. **A:** Bars show total number of bacteria after 2hr per 10000 cells for J774.2 cells infected by both *B. thailandensis* strains, CDC272 and E264. **B:** Bars show internalised bacteria after 18hr per 10000 cells for J774.2 cells infected by two *B. thailandensis* strains, CDC272 and E264. The effects of different treatments were tested by unpaired t-test, where ns=non-significant. The results are the means ( $\pm$  SEM) of 3 independent experiments each performed in 4 technical replicates.

#### 5.3.1.4 Effect of CD9 over-expression on MGC formation induced by *B. thailandensis*

*B. thailandensis* CDC272 and E264 have the ability to cause similar levels of MGC formation in GFP, CD9GFP and WT J774.2 cells following infection when compared with uninfected cells, as shown in **section 3.3.2.1**. The GFP, CD9GFP and WT J774.2 cells were infected at MOI 0.5, 1 and 3 for 2hr, and then the medium was changed to DMEM containing amikacin and kanamycin for 16hr. The cells were fixed and stained to count the fusion index. Interestingly, the fusion index in CD9GFPJ774.2 cells infected at these MOI values was significantly lower than the fusion index of GFPJ774.2 cells for both bacterial strains (**Fig 5.4**). This may be evidence to support the previous findings that CD9 has a negative effect on MGC formation.

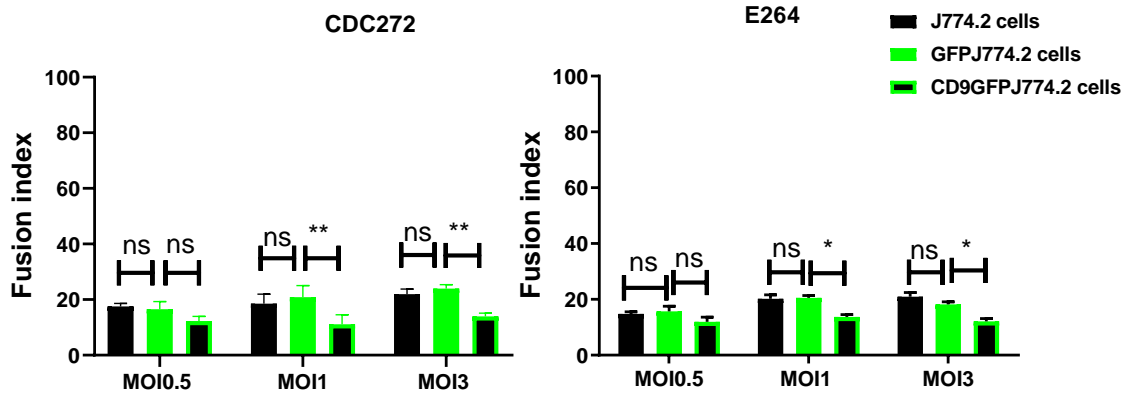


**Figure 5.4 Effect of CD9 over-expression on MGC formation induced by both *B. thailandensis* strains.**

GFP, CD9GFP and WT J774.2 cells were infected as described in **section 2.2.8**. Bars show fusion index in J774.2 cells infected by two *B. thailandensis* strains, CDC272 and E264. Black bars show the fusion index for WT J774.2; black bars with green border show the fusion index for GFPJ774.2; green bars show the fusion index for CD9GFPJ774.2 at MOI 0.5, 1 and 3. The effects of different treatments were tested by two-way ANOVA, where \*  $p < 0.05$ ; \*\*  $p < 0.01$  significant; ns=non-significant. The results are means ( $\pm$  SEM) of 3 independent experiments each performed in 8 technical replicates.

#### 5.3.1.5 Co-localisation of *B. thailandensis* and CD9GFP

The above data showed that the over-expression of CD9GFP has a negative effect on MGC induction by *B. thailandensis*. This work was to investigate if CD9 may have co-localisation with attached or internalised *B. thailandensis* CDC272 or E264 using fluorescence microscopy. In this study, bacteria were transfected with plasmids encoding mCherry fluorescent proteins as described in **section 2.2.3**. The CD9GFPJ774.2 cells were infected by bacteria for 2hr. Then the cells were treated with DMEM containing antibiotics for 3hr, and cells were fixed with PFA 2%. Coverslips were mounted using Vectashield (with DAPI) and sealed onto slides, in darkness. The finding shows that there is only a slight co-localization of CD9 with the CDC272 strain while finding shows that there is no co-localisation between CD9 and the E264 strain, as shown in **Fig 5.5**.

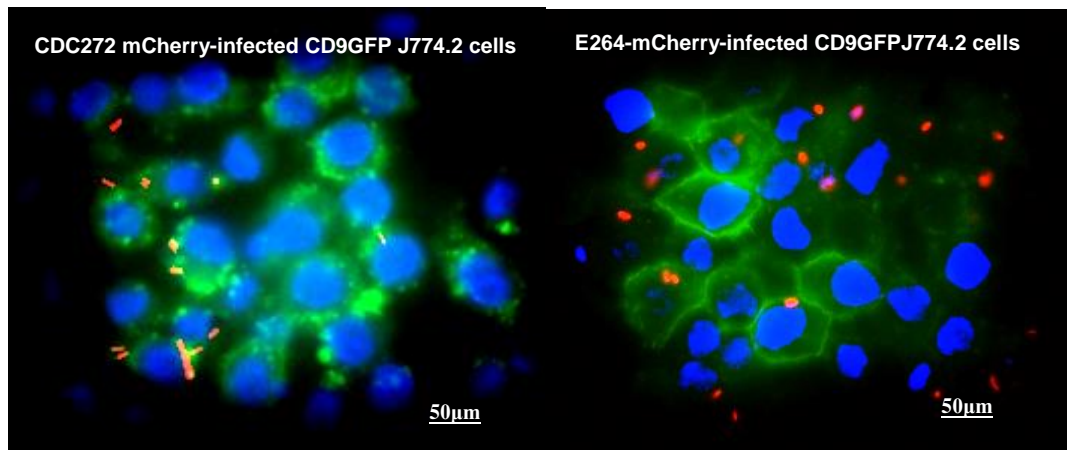


**Figure 5.5 Fluorescent micrographs of CD9GFPJ774.2 cells infected by both *B. thailandensis* strains.**

CD9GFPJ774.2 cells were infected for 2hr, washed by HBSS 2x and incubated with media containing 500µg/ml kanamycin and amikacin to kill all extracellular bacteria. Then, infected cells were incubated for 2hr, washed 2x and fixed for 10min, then stained. The blue colour indicates nuclei were stained with DAPI, the green colour indicates CD9GFP, and the red colour means bacteria labelled with mCherry. The images are representative of several fields of view from a single experiment.

#### 5.3.1.6 CD9-derived peptide 8005 and CD9EC2 functional studies on MGC formation and bacterial infection

The EC2 is variable in length and amino acid sequence among Tspans. This region is thought to be important for Tspan-partner interactions, and consequently, it facilitates Tspan functions (Takeda *et al.*, 2003, Parthasarathy *et al.*, 2009, Yáñez-Mó *et al.*, 2001). Recombinant protein corresponding to EC2 of Tspans is an alternative tool to mAbs that are used in determining Tspans functions. This protein is expressed in *E. coli* as fusion protein with glutathione S-transferase (GST). This GST fusion protein is soluble and stable, so it can be purified using non-denaturing procedures (Smith and Johnson, 1988). Previous work in the laboratory has shown that a peptide (8005; 40 amino acids) directly derived from the sequence of the EC2 of CD9 has potent anti-adhesive effects against *S. aureus* (unpublished data, Rahaf Issa) and *P. aeruginosa* in epithelial cell lines (Alrahimi, 2017). In addition these peptides have no adverse effects on bacterial metabolism (unpublished data, Rahaf Issa) and may be an important new class of antibacterial agents.

#### 5.3.1.6.1 CD9-derived peptide 8005 effects on *B. thailandensis* growth

The effects of 8005 peptides on the growth of *B. thailandensis* in LB broth is shown in **Fig 5.6**. 500nM peptide 8005 and SCR peptide were added to LB media, and then the bacteria were inoculated. Data showed that there is no effect of 8005 or SCR growth at any time point.

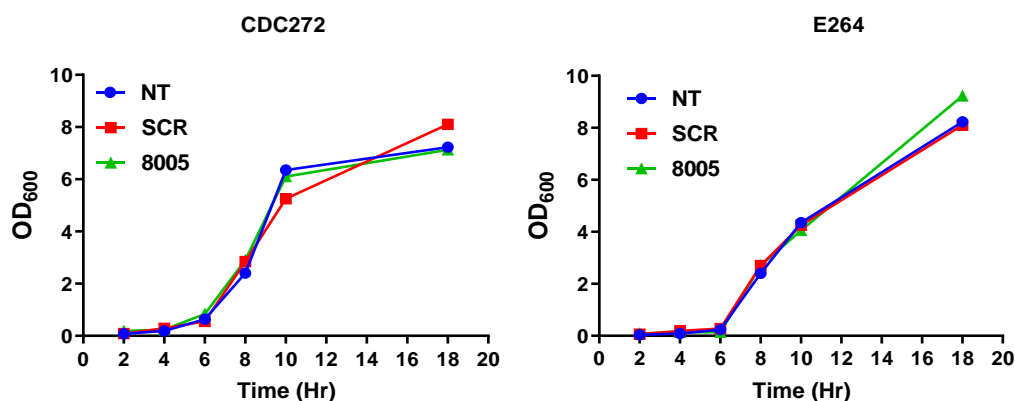


**Figure 5.6 Effect of CD9-derived peptide 8005 on *B. thailandensis* growth.**

*B. thailandensis* was cultured in LB media with normal saline, control (SCR) or 8005 peptides. Both strains of bacteria were incubated in a shaking incubator, and OD<sub>600</sub> was measured at different time points. Data are means ( $\pm$  SEM) of 2 independent experiments each performed in 2 technical replicates.

#### 5.3.1.6.2 CD9-derived peptide 8005 effects on infection of A549 cells with *B. thailandensis*

The effects of 8005 peptides on the total bacterial infection and internalised *B. thailandensis* of A549 cells are shown in **Fig 5.7** and **Fig 5.8**. The infection assay was performed and the cells were treated with 8005 and SCR peptide for 1hr. The cells were washed and infected with *B. thailandensis* for 2 and 18hr. To count the total number of bacteria after 2hr, the wells were washed 3x with HBSS and lysed by the addition 1% TritonX-100 for 15min. To count internalisation after 2hr and bacterial replication after 18hr, the cells were cultured with DMEM containing antibiotics, washed, and lysed after 2 and 18hr using TritonX-100. The lysis mixture was serially diluted and plated onto LB agar plates. After 48hr of incubation at 37°C, colonies were counted and used to calculate CFU per well. Pre-treatment of cells with 8005 and SCR peptides at a concentration of 25, 50, 100 and 200nM significantly reduced *B. thailandensis* infection, in terms of the number of infected cells at 2hr compared to untreated and control peptide treatment. The results also showed that there is a reduction in the number of intracellular bacteria after 2

or 18hr with 8005 peptide compared with SCR and untreated A549 cells, although the effect was most marked for E264 (Fig 5.8).

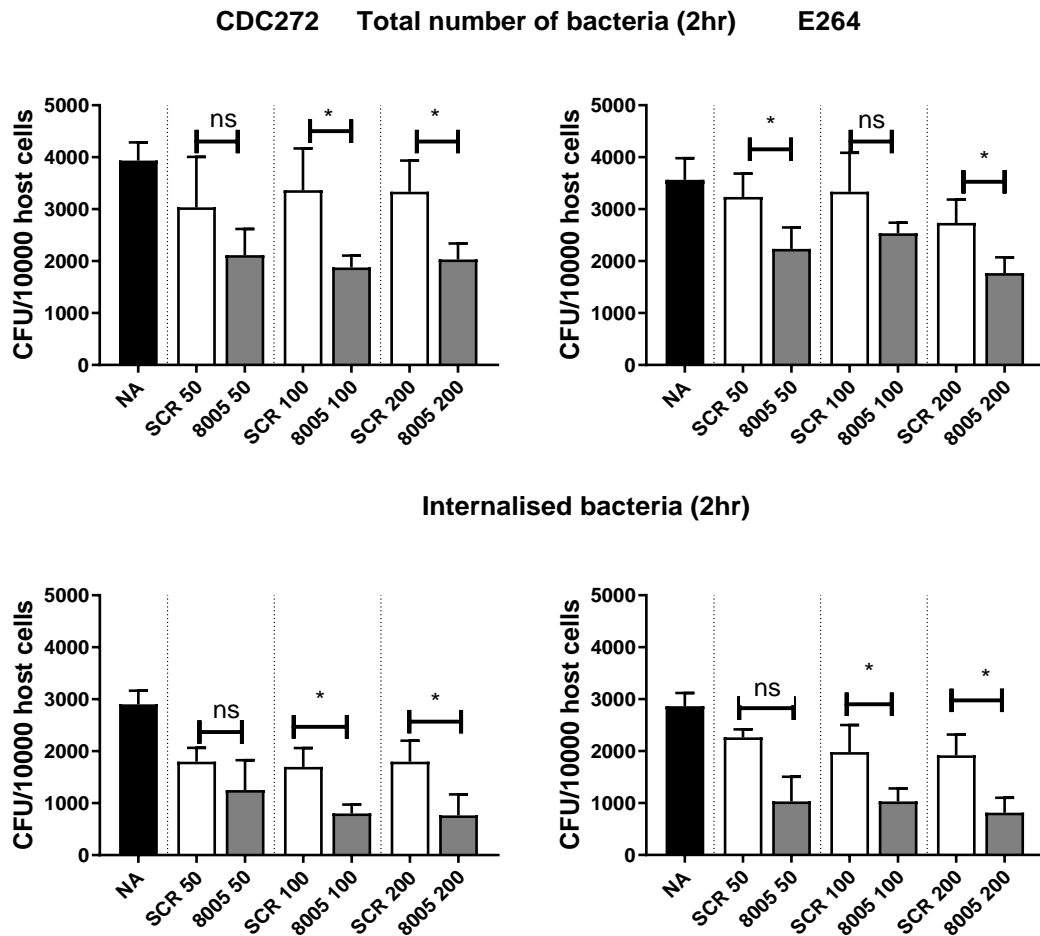


**Figure 5.7 CD9-derived peptide 8005 reduces total *B. thailandensis* infection of A549 cells.**

Cells were treated with different concentrations of CD9 peptide 8005 or SCR control for 60min, and then infected with bacteria for 2hr. They were then washed 2x and lysed with TritonX-100 and bacteria quantified by CFU to count the bacterial infection (bacteria per 10000 A549 cells). The treated cells were infected for 2hr, they were then washed 2x and treated with amikacin and kanamycin for 1hr, and then infected cells were lysed with TritonX-100 to quantify the internalised bacteria effects of different treatments. The effects of different treatments were tested by unpaired t-test where \*  $p < 0.05$  significant; ns=non-significant. The results are the means ( $\pm$  SEM) of 3 independent experiments each performed in 4 technical replicates.

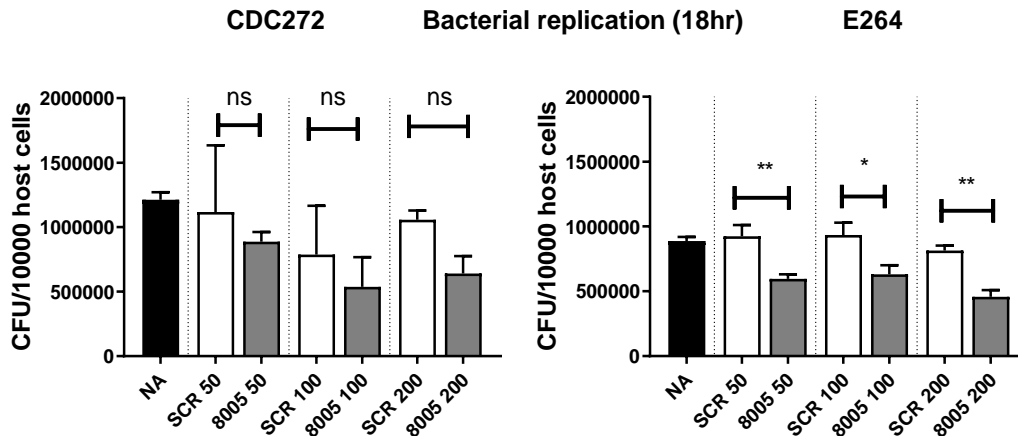


**Figure 5.8 Effect CD9-derived peptide 8005 reduces *B. thailandensis* internalisation at 2 and 18hr in A549 cells.**

Cells were treated with different concentrations of CD9 peptide 8005 or SCR control for 60min, then infected with bacteria for 2hr. They were then washed 2x, treated with amikacin and kanamycin, and incubated for a further 16hr to count internalised bacteria. The total bacterial infection was at MOI 5 per 10000 A549 cells. The effects of different treatments were tested by unpaired t-test where \*  $p < 0.05$ ; \*\*  $p < 0.01$  significant; ns=non-significant. The results are the means ( $\pm$  SEM) of 3 independent experiments each performed in 3 technical replicates.

#### 5.3.1.6.3 Effect of CD9-derived peptide 8005 on MGC formation induced by both *B. thailandensis* strains

The effects of 8005 peptides on MGC induced by *B. thailandensis* was investigated. To do this, the fusion assay was conducted. The cells were treated with 8005 peptides and SCR after and before infection to determine if the effects of peptide related primarily to bacterial infection or fusion. After treatment with peptide for 1hr, cells were infected for 2hr and then incubated for 18hr with DMEM containing amikacin and kanamycin. The fusion index was quantified as described in 2.2.6. Pre-treatment of A549 cells with 8005 at concentrations of 25, 50, 100 and 200nM significantly reduced MGC formation induced by *B. thailandensis* infection. Data also showed that GST-CD9EC2 treated cells showed no reduction in MGC formation (Fig 5.9A). However, there was no reduction in MGC formation when the cells were infected for 2hr and then treated with 8005 or SCR (Fig 5.9B). This suggests that 8005 has a direct effect on the bacterial infection but only an indirect effect on MGC formation.

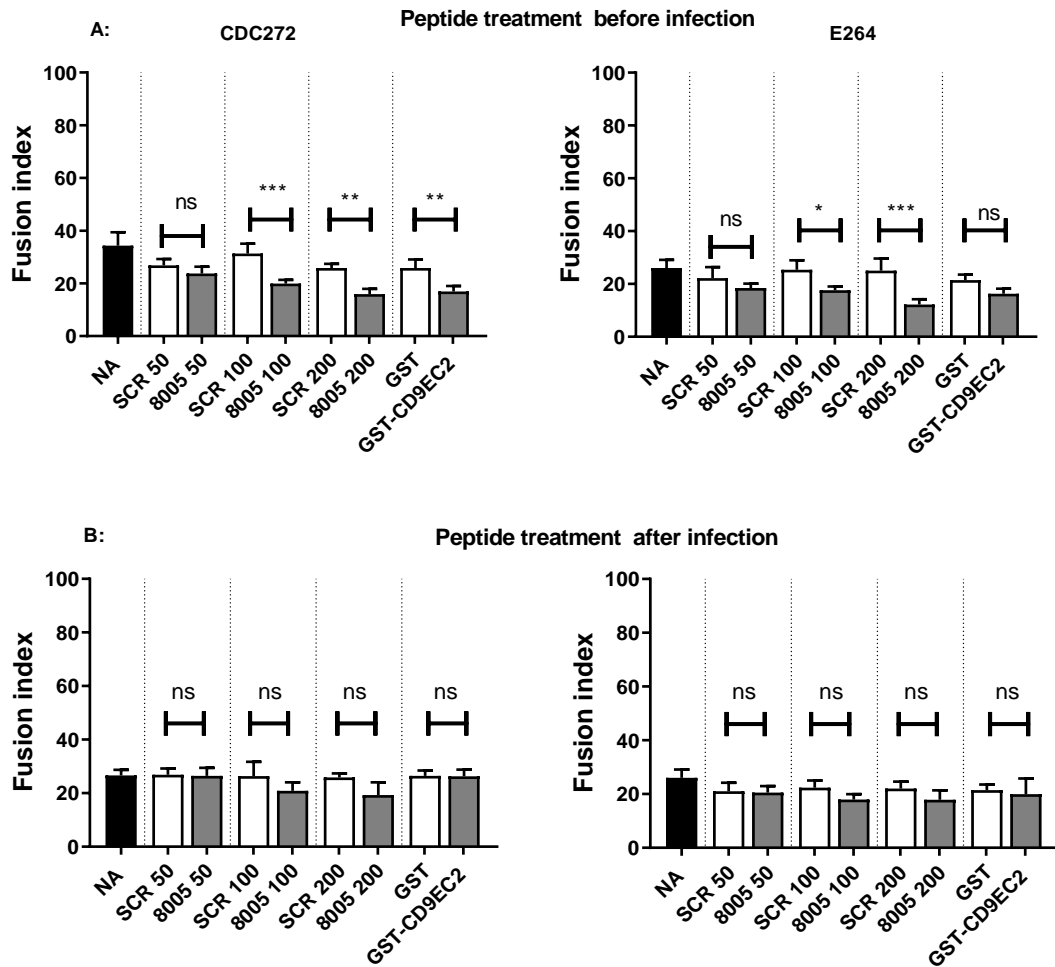


**Figure 5.9 Effect of CD9-derived peptide 8005 and GST-CD9EC2 on MGC formation induced by both *B. thailandensis* in A549 cells.**

A: Cells were pre-treated with different concentrations of peptide 8005, GST-CD9EC2 or control scrambled peptide for 60min, and then infected with bacteria for 2hr. B: Cells were infected for 2hr and then pre-treated with peptide 8005 or control scrambled peptide for 60min. The effects of different treatments were tested by unpaired t-test where \*  $p < 0.05$  \*\*  $p < 0.01$  \*\*\*  $p < 0.001$  significant. The results are the means ( $\pm$  SEM) of 4 independent experiments each preformed in 3 technical replicates.

### 5.3.2 Role of Tspan-2 and Tspan-13 in *B. thailandensis* infection and MGC formation in A549 cells

The anti-Tspan-2 antibody and cells over-expressing Tspan-2 were provided by Ibrahim Yasseen, and all experiments to investigate the role of Tspan-2 on A549 cell infected by *B. thailandensis* CDC272 were performed by me with a previous PhD student from University of Sheffield, Yaseen (Yaseen, 2017).

### 5.3.2.1 Effect of anti-CD81, anti-Tspan-2 and anti-Tspan-13 antibodies on bacterial infection of A549 cells

The present study was conducted to investigate the possible roles of CD81, Tspan-13 and Tspan-2 in the bacterial infection and MGC formation in A549 cells. For infection, A549 cells were seeded in 96 well plates and some treated for 1hr with anti-CD81, anti-Tspan-2 and anti-Tspan-13 antibodies, or the relevant isotype controls. The treated and untreated cells were infected for 2hr with *B. thailandensis* CDC272 and E264. To count the total bacterial infection, the cells were washed 3x with HBSS and lysed by the addition of 100µl of 1% TritonX-100 for 15min. To count only internalised bacteria, the cells were cultured with DMEM containing antibiotics for 1hr, washed, and lysed using TritonX-100. The lysis mixture was serially diluted and plated onto LB agar plates for CFU counting. The results show that antibodies against Tspan-2 and Tspan-13 could significantly reduce *B. thailandensis* infection and internalisation compared with isotype control, while anti-CD81 antibody reduces internalisation compared with isotype control but not the total bacterial infection, as shown **Fig 5.10**. It seems that both Tspans play a role in total bacterial infection and internalisation.

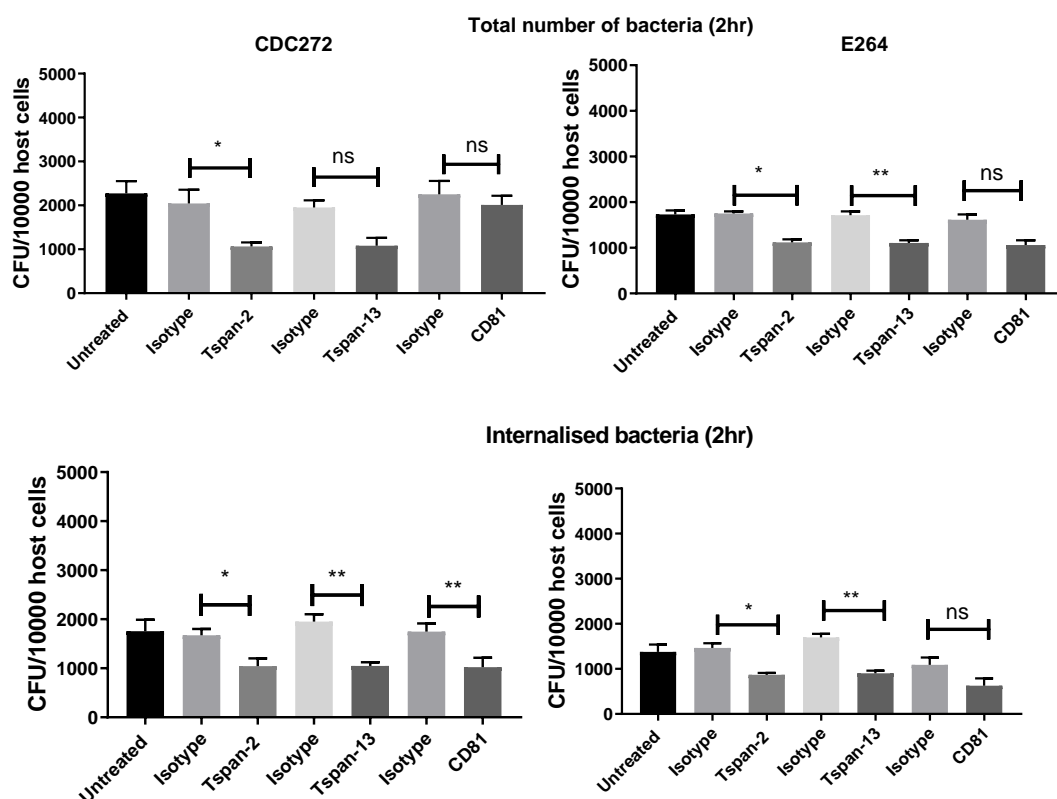


**Figure 5.10 Effect of anti-Tspan-2, anti-Tspan-13 and anti-CD81 antibodies on *B. thailandensis* infection.**

A549 cells were pre-treated with isotype control (JC1, IgM), anti-CD81, anti-Tspan-2 and anti-Tspan-13 antibodies before infection as described in **section 2.2.7**. Bars show total bacterial infection per 10000 cells for A549 cells infected by two bacterial strains. The effects of different treatments were tested one-way ANOVA, where \*  $p < 0.05$ ; \*\*  $p < 0.01$  significant; ns=non-significant. The results are the means ( $\pm$  SEM) of 3 independent experiments each performed in 4 technical replicates.

### 5.3.2.2 Effect of anti-Tspan-2 and anti-Tspan-13 antibodies on MGC formation induced by both *B. thailandensis* in A549 cells

This experiment was performed to investigate the effect of anti-Tspan antibodies (anti-Tspan-2 and anti-Tspan-13) on MGC formation induced by *B. thailandensis* in A549 cells. Both treated and untreated cells were infected for 2hr with both strains of WT bacteria and then cultured with media containing antibiotics for 16hr. The fusion index was quantified relative to uninfected cells per field of view. MGCs were defined as cells containing 3 or more nuclei. Data showed that antibodies against Tspan-2 and Tspan-13 significantly reduced the fusion index. Anti-Tspan-2 antibody-treated cells have a fusion index reduced by more than 40% compared with isotype control, and anti-

Tspan-13 antibody showed more than 50% reduction compared with isotype control, as shown in **Fig 5.11**.

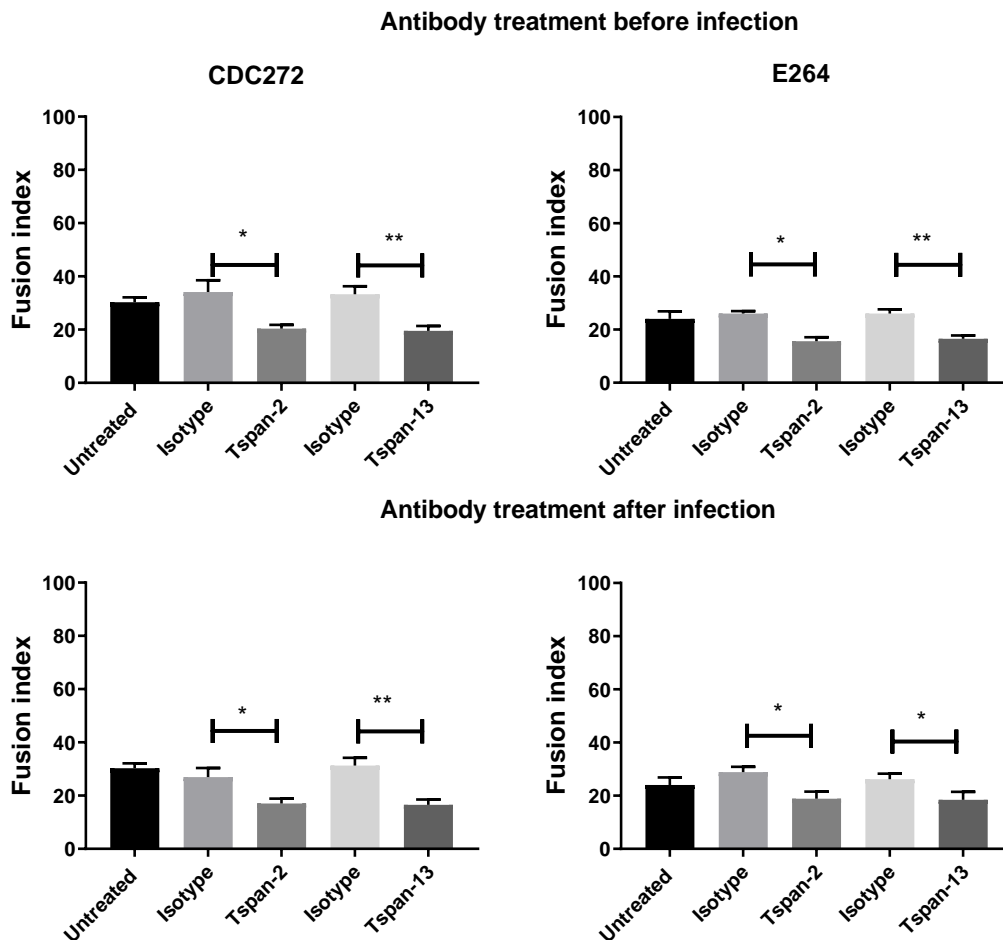


**Figure 5.11 Effect of anti-Tspan-2 and anti-Tspan-13 antibodies on MGC formation induced by both *B. thailandensis* strains.**

A549 cells were treated with isotype or anti-Tspan-2 and anti-Tspan-13 antibodies after *B. thailandensis* infection for 2hr, as described in **section 2.2.7**. Bars show the fusion index for A549 cells infected by two types of strains. The effects of different treatments were tested by t-test, where \*  $p < 0.05$ ; \*\*  $p < 0.01$  significant. The results are the means ( $\pm$  SEM) of 3 independent experiments each performed in 4 technical replicates.

### 5.3.2.3 Effect of Tspan-2 over-expression on bacterial infection

This study aimed to compare total number of bacteria and internalised bacteria after 18hr in GFP, Tspan-2GFP and WT A549 cells. Our results have demonstrated that over-expression of Tspan-2GFP in A549 cells slightly increases the total number of bacteria by E264 but not CDC272 at 2hr compared with GFP A549 infected cells. However, there was no difference in internalised bacteria at 18hr, as shown in **Fig 5.12**.

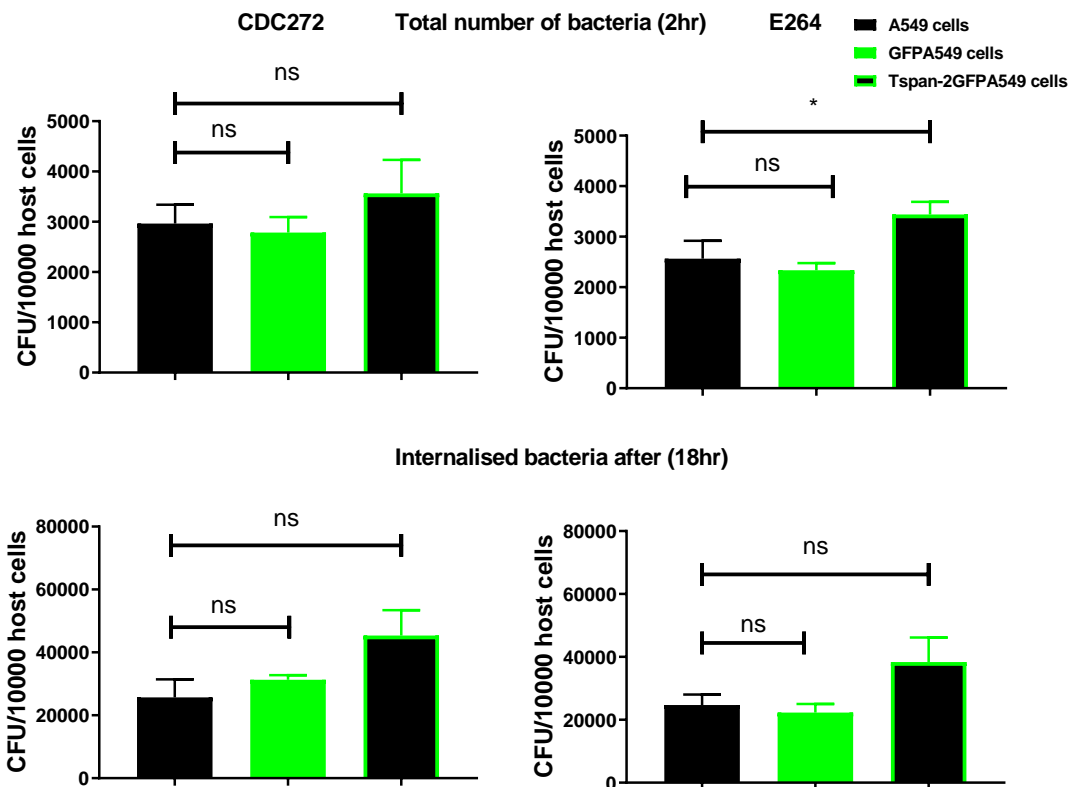


**Figure 5.12 Over-expression of Tspan-2 increases *B. thailandensis* CDC272 and E264 infection.**

GFP, Tspan-2GFP and WT A549 cells were infected as described in **section 2.2.8**. Bars show total number of bacteria after 2hr and internalised bacteria post 18hr of *B. thailandensis* strains, CDC272 and E264. Black bars show A549 infected with bacteria; black bars with green borders show Tspan-2GFP A549 cells infected with bacteria; green bars show GFP A549 cells infected with bacteria at MOI 5. The effects of different treatments were tested by one-way ANOVA, where \*  $p < 0.05$  significant; ns=non-significant. The results are the means ( $\pm$  SEM) of 3 independent experiments each performed in 3 technical replicates.

#### 5.3.2.4 Effect of Tspan-2GFP expression on MGC formation induced by *B. thailandensis*

The aim of this experiment was to determine if over-expression of Tspan 2-GFP in A549 cells affects MGC formation induced by *B. thailandensis*. The GFP, Tspan-2GFP and WT A549 cells were infected by both *B. thailandensis* CDC272 and E264. Interestingly, the fusion index in Tspan-2GFP A549 cells was significantly increased compared with GFP A549 cells for both *B. thailandensis* strains (**Fig 5.13**).

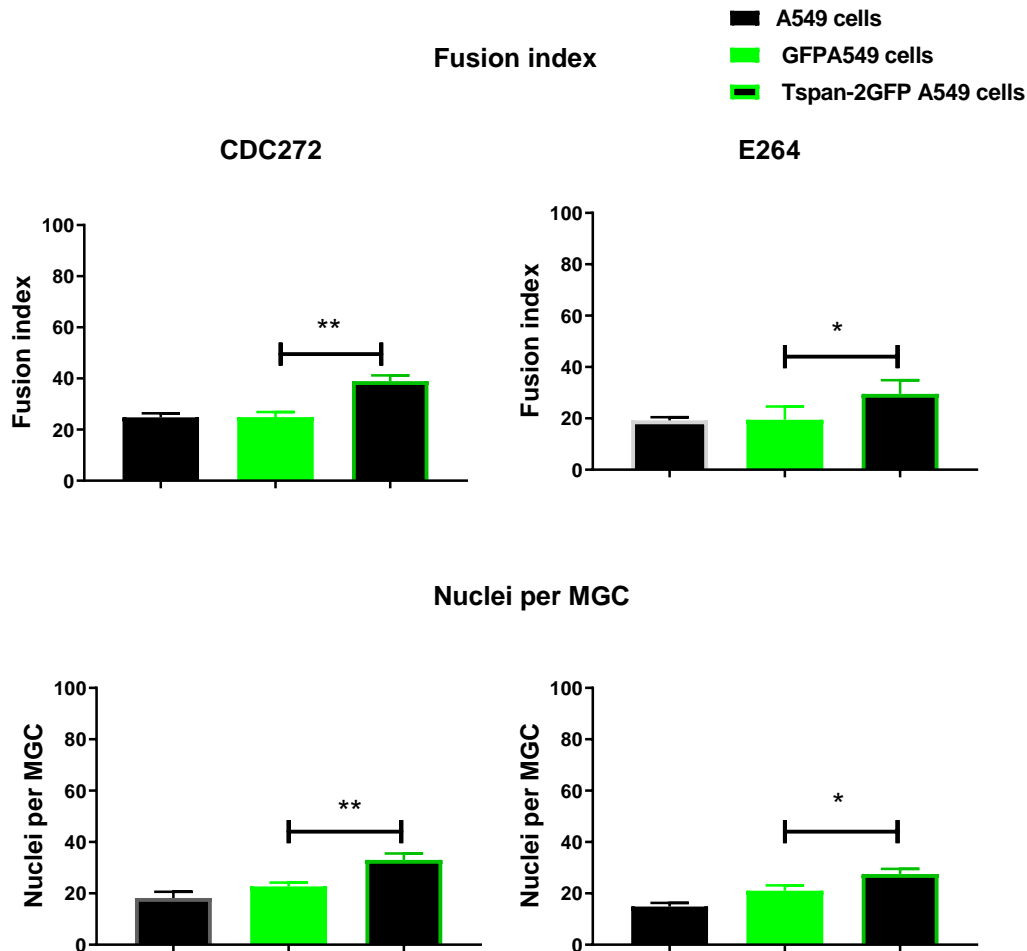


**Figure 5.13 Over-expression of Tspan-2 promotes MGC formation induced by both *B. thailandensis* strains.**

GFP, Tspan-2GFP and WT A549 cells were infected as described in **section 2.2.8**. Bars show fusion index and the number of nuclei per MGC in A549 cells infected by both *B. thailandensis* strains, CDC272 and E264. Black bars show the WT A549 cells; black bars with green borders show the GFP A549 cells; green bars show the Tspan-2GFP A549 cells infected at MOI 5. The effects of different treatments were tested by one-way ANOVA, where \*  $p < 0.05$ ; \*\*  $p < 0.01$  significant. The fusion index is the means ( $\pm$  SEM) of 5 experiments performed in 4 technical replicates.

### 5.3.3 Role of Tspan-partner proteins ADAM10, CD98 and CD172 $\alpha$ in *B. thailandensis* infection and MGC formation in A549 cells

#### 5.3.3.1 Role of ADAM10, CD98 and CD172 $\alpha$ in *B. thailandensis* infection

This experiment was to investigate if there is a role for ADAM10, CD98 and CD172 $\alpha$  in *B. thailandensis* infection, using antibodies against these host surface proteins. Briefly, the cells were treated with antibodies or isotype controls for 1hr and washed 2x with HBSS to remove all nonspecific binding. They were then infected with *B. thailandensis* for 2hr. The infected cells were washed 2x and lysed using TritonX-100. The lysis mixture was serially diluted

and plated onto LB agar plates for CFU counting. The results show that anti-ADAM10, CD98 and CD172 $\alpha$  antibodies have no effect on total bacterial infection and/or internalisation when compared with isotype control antibodies treatment for both *B. thailandensis* strains, as shown in **Fig 5.14**.

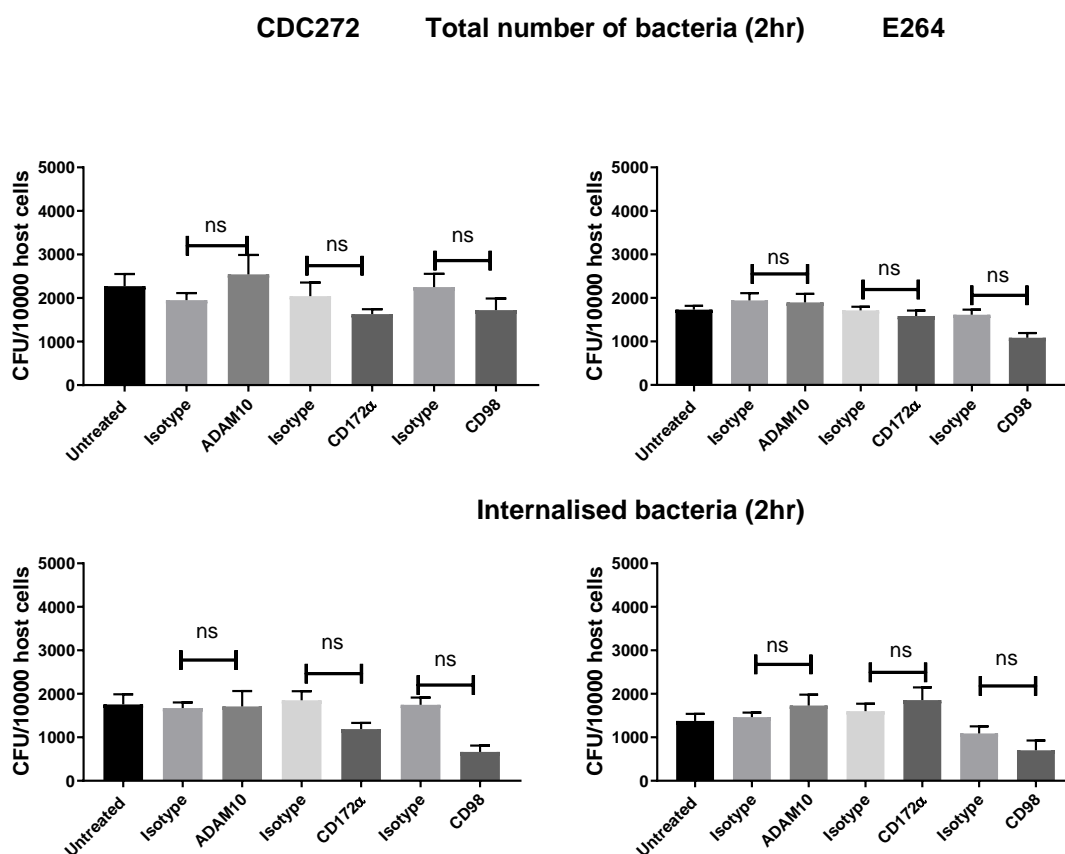


**Figure 5.14 Effect of anti-ADAM10, anti-CD98 and anti-CD172 $\alpha$  antibodies on *B. thailandensis* CDC272 and E264 infection of A549 cells.**

A549 cells were pre-treated with isotype control (JC1, IgG1 and IgG2) and anti-ADAM10, CD172 $\alpha$  and CD98 antibodies before infection. Bars show the total number of bacteria and/or internalised bacteria per 10000 cells for A549 cells infected by two bacterial strains, CDC272 and E264. The effects of different treatments were tested by one-way ANOVA, where ns=non-significant. The results are the means ( $\pm$  SEM) of 3 independent experiments each performed in 4 technical replicates.

### 5.3.3.2 Roles of ADAM10, CD98 and CD172 $\alpha$ in MGC formation

ADAM10, CD98 and CD172 $\alpha$  are known to be involved in the cell fusion process (Gautam and Acharya, 2014, Ohgimoto *et al.*, 1995, Verrier *et al.*, 2004). It was also observed that the level of these 3 Tspan-partner proteins consistently changed in response to fusogenic *B. thailandensis* strains, with no change for the non-fusogenic mutant at both gene and protein levels as described in **section 4.3.5** and **section 4.3.12**. The aim of this experiment was to investigate if antibodies against these proteins could affect MGC

formation after *B. thailandensis* infection. The cells were treated with anti-ADAM10, anti-CD98 and anti-CD172 $\alpha$  antibodies or isotype controls for 1hr and then washed. They were infected for 2hr and incubated with DMEM containing antibiotics for 16hr. The fusion index was quantified relative uninfected cells per field of view. MGCs were defined as cells containing 3 or more nuclei. Data shows that ADAM10 antibody enhanced MGC formation, and anti-CD172 $\alpha$  antibody reduced MGC formation significantly when compared with isotype treatment for one fusogenic bacterial strain CDC272 but not for E264. In contrast, the results show that there is no effect of antibody against CD98 or ADAM10 for either strain (**Fig 5.15**).

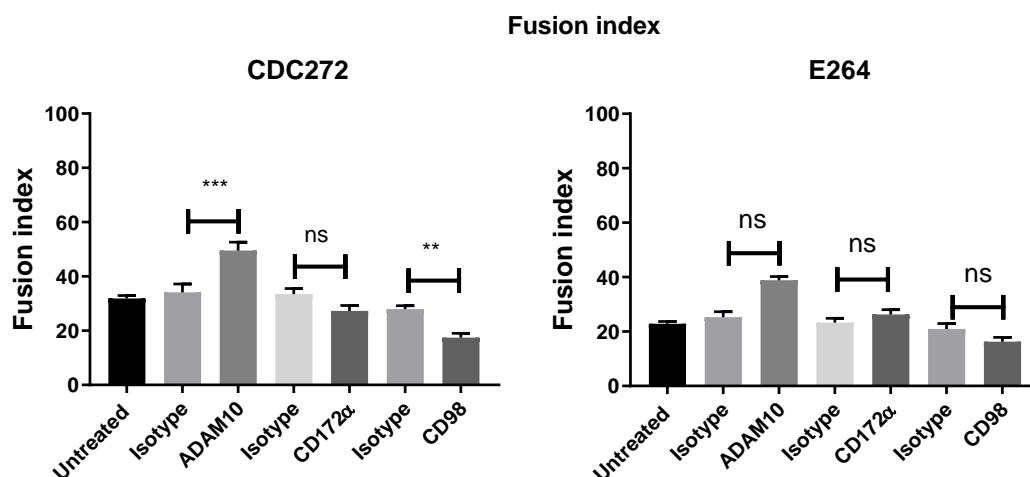


**Figure 5.15 Anti-ADAM10, anti-CD98 and anti-CD172 $\alpha$  antibodies reduce or enhance MGC formation induced by both *B. thailandensis* strains.**

A549 cells were pre-treated with isotype or anti-ADAM10, CD98 and CD172 $\alpha$  antibodies before *B. thailandensis* infection, as described in **section 2.2.7**. Bars show the fusion index for A549 cells infected by both fusogenic strains. The effects of different treatments were tested by one-way ANOVA, where \*\*  $p < 0.01$ ; \*\*\*  $p < 0.001$  significant; ns= non-significant. The fusion index are the means ( $\pm$  SEM) of 3 independent experiments each performed in 4 technical replicates.

## 5.4 Discussion

In this chapter, we investigated the roles of 4 Tspans (CD9, CD81, Tspan-2, and Tspan-13) and 3 Tspan-partner proteins (CD98, ADAM10 and CD172 $\alpha$ ). These were identified in chapter 4 as proteins that may have a role in either infection or/and MGC formation.

### 5.4.1 CD9 may be a negative regulator of MGC formation

The first aim of this study was to detect if CD9 plays a role in *B. thailandensis* infection. In **section 5.3.1.1**, the results showed that there is no effect of anti-

CD9 antibody on the bacteria infection and internalisation for both bacterial strains in A549 cells (**Fig 5.1**). In **section 5.3.1.4**, the results also showed that over-expression of CD9 in J774.2 cells also has no effect on total bacterial infection after 2hr and internalised bacteria after 18hr. These results are in agreement with other data from our group. For example, Elgawidi found that anti-CD9 antibody has no effect on *B. thailandensis* infection of J774.2 and RAW264 mouse macrophages (Elgawidi, 2016). In contrast, anti-CD9 antibody could decrease *Salmonella* infection of J774.2 cells and U937 human macrophages (Hassuna *et al.*, 2017). Furthermore, CD9 reduced the infection of *N. meningitides* (Green *et al.*, 2011). Our team also observed that anti-CD9 antibody significantly reduced the infection of *P. aeruginosa* of U937 and HaCaT cell lines (Alrahipi, 2017).

The second aim of this study was to determine if CD9 plays a role in MGC formation induced by fusogenic strains of *B. thailandensis*. In **section 5.3.1.2**, data clearly showed that anti-CD9 antibody treatment enhances the MGC formation compared with isotype control (**Fig 5.2**). In addition, over-expression of CD9GFP in J774.2 cells reduced MGC formation when compared with GFP and WT controls (**Fig 5.4**). These results are in agreement with findings of Takeda *et al.* who showed that anti-CD9 antibody enhances MGC formation (Takeda *et al.*, 2003). Parthasarathy *et al.* have also demonstrated that anti-CD9 antibody promotes MGC formation (Parthasarathy *et al.*, 2009).

#### 5.4.2 CD9-derived peptides and CD9EC2 reduce *B. thailandensis* infection and may inhibit MGC formation

This work aimed to demonstrate if recombinant GST-CD9EC2 or a peptide derived from CD9EC2 could reduce the MGC formation and/or *B. thailandensis* infection of A549 cells. In **section 5.3.1.5**, we showed that pre-treatment with peptide could decrease the total number of bacteria and/or internalised bacteria after 2 and 18hr in A549 cells. It has also been shown that these peptides can affect MGC formation (**Figs 5.5, 5.6 and 5.7**). However, we attempted to differentiate between treating cells before and after infection. The results showed that there is no effect on MGC formation if the

cells treated after infection. This suggests that the primary effect of these reagents is the inhibition of infection, rather than a direct effect on fusion.

We compared these results with other findings. For example, a reduction is found in MGC formation using GST-CD9EC2, but there was no effect of a shorter human CD9EC2-derived peptide on MGC formation and bacterial infection of J774.2 mouse macrophages (Elgawidi, 2016). It has been observed that GST-CD9EC2 could reduce MGC formation stimulated by Con-A (Parthasarathy *et al.*, 2009). The effect of these peptides was seen with other bacteria such as *P. aeruginosa* by a previous PhD student from University of Sheffield (Alrahimi, 2017). In her work, it has been observed that peptide 8005 could reduce *P. aeruginosa* adhesion. Ventress *et al.* observed that the adhesion of *S. aureus* could be reduced using a range of shorter peptides derived from GST-CD9EC2 (Ventress *et al.*, 2016).

#### 5.4.3 Tspan-2 and Tspan-13 are positive regulators of MGC formation and *B. thailandensis* infection

Tspan-2 was investigated using anti-Tspan-2 antibody treatment and over-expression of Tspan-2GFPA549 cells. Anti-Tspan-2 antibody reduced both MGC formation and total bacterial infection significantly compared with isotype antibody control. However, there were no differences between treated and non-treated infected cells in terms of bacterial internalisation. Tspan-2 over-expression significantly promoted MGC formation and the total bacterial infection. Tspan-2 has been implicated in both bacterial infection and MGC formation. We attempted to differentiate between the two possibilities by treating cells both before and after infection. The results showed significantly reduced MGC formation.

Tspan-2 has a similar sequence to CD81 and CD9 (Yaseen *et al.*, 2017), both known to affect MGC formation in a range of systems (Takeda *et al.*, 2003, Elgawidi, 2016, Hulme *et al.*, 2014, Parthasarathy *et al.*, 2009). It has been shown that Tspan-2 over-expression increases the size and number of cellular protrusions in host cells (Grossmann *et al.*, 2015). It has also been shown that these cellular protrusions are implicated in MGC formation by myoblasts induced by *B. thailandensis* E264 (French *et al.*, 2011). In addition,

Tspan-2 is known to play a proapoptotic role in B-cells by induction of JNK pathway (Hwang *et al.*, 2016).

Following treatment with an anti-Tspan-13 antibody before and after infection, the internalised bacteria or total bacterial infection reduced significantly, and the fusion index was decreased by more than 15% compared with control. We also attempted to differentiate between the two possibilities by treating cells before or after infection. The results showed significantly reduced MGC formation in both cases (**Fig 5.14** and **Fig 5.15**). There are no previous studies on the role of Tspan-13 in bacterial infection. However, Tspan-13 has a negative role in osteoclast formation. For example, Iwai *et al.* have shown that Tspan-13 has negative effects on osteoclast formation stimulated by RANKL (Iwai *et al.*, 2007).

#### 5.4.4 ADAM10, CD98 and CD172 $\alpha$ have little effect on bacterial infection but CD172 $\alpha$ may have a role in MGC formation in response to *B. thailandensis* infection

Here, we investigated the potential role of these Tspan-partners on MGC formation and bacterial infection by pre-treating A549 cells with antibodies against ADAM10, CD98 and CD172 $\alpha$ . As **Fig 5.14** shows, all antibodies had no effect on bacterial infection. In contrast, it has been reported that anti-ADAM10 antibody reduced the total bacterial infection of *P. aeruginosa* infecting lung cells (Antonelli *et al.*, 2017). ADAM10 also has a positive role in *S. aureus* infection (Von *et al.*, 2016). ADAM10 is also known as the receptor of  $\alpha$  toxin of *S. aureus* (Otto, 2014, DuMont and Torres, 2014). Li *et al.* have shown that CD172 $\alpha$ KO increased the *Salmonella* infection of the spleen in mice (Li *et al.*, 2012). That would suggest CD172 $\alpha$  has a negative role in *Salmonella* infection. Baral and Utaisincharoen reported that CD172 $\alpha$  has a negative role on TLR signalling and it is a negative regulator of iNOS expression in *B. pseudomallei*-infected macrophages, which has an important role in *B. pseudomallei* killing (Baral and Utaisincharoen, 2012). However, there is no study to show the role of CD98 in other bacterial infection.

In **section 5.3.3**, the antibody against ADAM10 had a large effect on fusion induced by *B. thailandensis*. The potential role of ADAM10 in MGC formation

is unknown. It was shown that ADAM10 can be regulated by TspanC8, which are important in many cell functions, in particular, cell fusion (Matthews *et al.*, 2017). Tspan-5 is a member of the TspanC8 family and is implicated in cell fusion of osteoclasts (Iwai *et al.*, 2007).

Here, it was shown that anti-CD172 $\alpha$  antibody has no effect on MGC formation in A549 cells induced by *B. thailandensis* (**Fig 5.15**). This result was different from previous findings. For example, Suparak *et al.* showed that anti-CD172 $\alpha$  could partially suppress MGC formation induced by *B. pseudomallei* (Suparak *et al.*, 2011). Furthermore, several studies have also reported that CD47 and CD172 $\alpha$  can regulate macrophages fusion induced by LPS. CD172 $\alpha$  is implicated in the cell fusion of macrophages (Yagi *et al.*, 2005, Han *et al.*, 2000, Suparak *et al.*, 2011). It is possible that there is a different role for CD172 $\alpha$  in different cells and different inducers.

The anti-CD98 antibody also appears to promote the MGC formation induced by *B. thailandensis* (**Fig 5.15**). This result was in agreement with Suparak *et al.* who found that anti-CD98 could suppress MGC formation after infection with *B. pseudomallei* (Suparak *et al.*, 2011). Interestingly, CD98 could modulate integrin  $\beta$ 1, which is regulated by CD9 and CD81 (Cai *et al.*, 2005). It is known that CD9 and CD81 are involved in the MGC formation (Takeda *et al.*, 2003, Takeda *et al.*, 2008).

## Chapter 6 Effect of manipulating the gene expression of 3 Tspans and ADAM10 on *B. thailandensis* infection and MGC formation

### 6.1 Introduction

Many studies examined the effects of knockout of Tspan genes to investigate their roles in cell function. For example, CD9 has an essential role in fertilisation, as CD9 knockout mouse females have defects in sperm-egg fusion (Kaji *et al.*, 2000). CD81 deletion from mice could affect the regulation of cell proliferation (Geisert Jr *et al.*, 2002). The deletion of CD81 also could reduce fertility in female mice, and the double knockout of CD9/CD81 leads to complete female infertility (Rubinstein *et al.*, 2006). However, the lack of CD9 from bone marrow cells enhances MGC formation compared to those of WT (Takeda *et al.*, 2003). CD9 and CD81 are involved in the formation of myofibrils. Furthermore, Takeda *et al.* (2003) have observed that double knockout of CD9/CD81 causes spontaneous cell fusion and increased osteoclastogenesis. Interestingly, our research team have previously observed that CD9 and CD82 knockout enhance MGC formation in mouse bone marrow-derived macrophages infected with *B. thailandensis* (Elgawidi, 2016).

Tspan-2 is a member of the Tspans family that has high sequence identity with CD9 and CD81, which have roles in cell fusion (Hemler, 2008, Yaseen *et al.*, 2017). Tspan-13 is also implicated in many cell functions, for example, in the progress of cell fusion, and metastasis of breast cancer (Iwai *et al.*, 2007, Arencibia *et al.*, 2009). CD9 is a cell membrane coordinator protein and it can interact with other Tspans and other partner molecules (Hemler, 2003, Hemler, 2008). ADAM10 is a partner protein for several Tspans which has many cell functions, including the proteolytic release of many cell-surface proteins (Seipold and Saftig, 2016). ADAM10 also can be regulated by Tspan-15 (Haining *et al.*, 2012, Jouannet *et al.*, 2016).

Potential roles for Tspan-2, Tspan-13, CD81, CD9 and ADAM10 proteins in MGC formation and *B. thailandensis* infection were identified in **chapter 4** and

**chapter 5.** To examine their roles in these processes, gene expression was disrupted. We tested 3 Tspans and ADAM10, however, we did not test CD81 because it has a similar negative effect on MGC formation to CD9 and the sequence of CD81 is very similar to CD9. Furthermore, as Tspan-15 has a large effect on ADAM10 expression (Haining *et al.*, 2012, Jouannet *et al.*, 2016), we also investigated Tspan-15 knockout (KO) in A549 cells whether it could affect the MGC formation and infection by *B. thailandensis*. ADAM10KO and Tspan-15KO A549 cells were provided by Dr Mike Tomlinson, University of Birmingham (UK) (Szyroka, 2019). CD9KO A549 cells were provided by Dr David Blake, Fort Lewis College (USA) (Blake *et al.*, 2018). Tspan-15 is a member of the TspanC8 subfamily (Tspan-5, Tspan-10, Tspan-14, Tspan-15, Tspan-17 and Tspan-33). Interestingly, Haining *et al.* have described that ADAM10 expression reduced by around 50% in Tspan-15KO A549 cells when compared with WT A549 cells (Haining *et al.*, 2012, Jouannet *et al.*, 2016).

## 6.2 Aims

The aims of this chapter are to investigate the roles in bacterial infection and MGC formation of: a) Tspan-2, Tspan-13, CD9 and ADAM10 using knockdown (KD), and b) CD9, Tspan-15 and ADAM10 using KO. The KD cells lines were made using siRNA transfection of A549 cells, and KO cell lines were obtained from collaborators as detailed in **chapter 2 (section 2.4.1.3)**.

## 6.3 Results

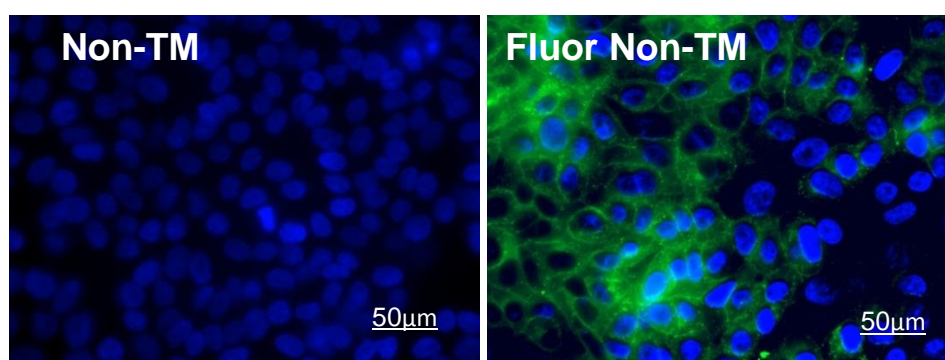
### 6.3.1 Transfection of A549 cells with Smart Pool siRNA

#### 6.3.1.1 Delivery efficiency of Smart Pool siRNA

Firstly, we needed to demonstrate that the Smart Pool siRNA transfection reagents could penetrate A549 cells. The efficiency of penetration was tested by both fluorescence microscopy and flow cytometry. To do this, 6mm coverslips were placed in 24 well plates and seeded with  $1 \times 10^5$  cells/ml, and the fluorescently labelled non-targeting control reagent was added to the cells according to the manufacturer's instructions. Secondly, to identify the optimum concentration, 25 or 100nM of Smart Pool siRNA or fluorescently labelled non-targeting reagents was added to 700 $\mu$ l serum free-DMEM, and

incubated for 24hr. Fluorescence microscopy was used to estimate the percentage of transfection by counting cells expressing the fluorescent control reagent. For flow cytometry, cells were grown and transfected in 24 well plates and washed 2x. Untreated and treated cells were analysed using flow cytometry as described in **section 2.2.10**. The results using 100nM of fluorescently labelled non-targeting siRNA showed that siRNA reagents KD penetrated more than 99% of A549 cells by flow cytometry, and fluorescence microscopy confirmed this (**Fig 6.1**). It seems that these reagents were efficient to be used in the next experiments.

A:



B:

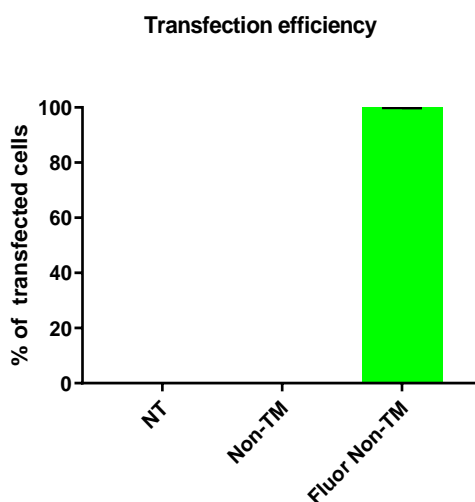


**Figure 6.1 Determination of *in vitro* transfection efficiency by fluorescence microscopy and flow cytometry.**

**A:** A549 cells were pre-treated with control siRNA examination reagent for 24hr, and uptake maintained by fluorescence microscopy. **B:** A549 cells ratios transfected with control siRNA materials, and uptake maintained by flow cytometry. Abbreviation NT=non-transfected cells, Non-TM=cells treated with non-targeting control materials, and Fluor non-TM=cells treated with fluorescently labelled non-targeting control materials. The results are the mean for 2 independent experiments each performed in 2 technical replicates.

### 6.3.1.2 Expression of CD9, Tspan-13 and ADAM10 on A549 cells after treatment with siRNA KD reagents

The A549 cells were treated with 100nM Smart Pool siRNA reagents to demonstrate the percentage of target knockdown after treatment with siRNA reagent using real-time qPCR and flow cytometry. The results show that when A549 cells were treated with appropriate siRNA materials, CD9 expression at total mRNA and protein levels was reduced by more than 70% compared with control non-targeting reagents. Data also shows that Tspan-13 also reduced more than 80% compared with the cells treated with non-targeting KD reagents. In addition, ADAM10 expression reduced more than 75% at the mRNA level, but only by 50% at the protein level on the cell surface expression (**Fig 6.2**).

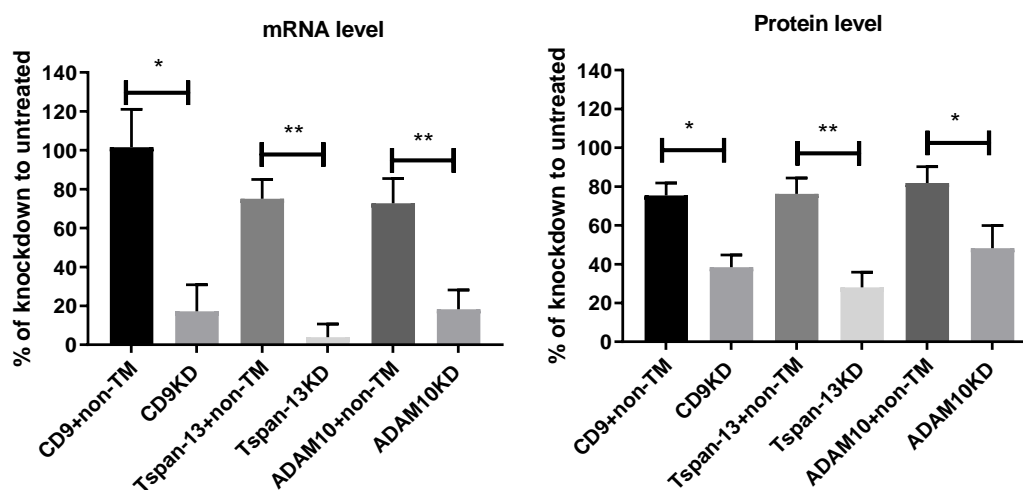


**Figure 6.2 CD9, Tspan-13 and ADAM10KD at mRNA and protein levels in A549 cells after 48hr treatment with Smart Pool siRNA and non-targeting KD materials.**

A549 were pre-treated with siRNA and then prepared to measure the mRNA and protein levels as described in **section 2.2.8.1** and **section 2.2.9**. The effects of different treatments were tested by unpaired t-test, where \*  $p < 0.05$ ; \*\*  $p < 0.01$  significant. Non-TM=cells treated with non-targeting control materials. The results are the means ( $\pm$  SEM) of 3 independent experiments each performed in 2 technical replicates.

### 6.3.1.3 Expression of Tspan-2 on A549 wild type cells and Tspan-2KD cells by real-time qPCR and flow cytometry

This work was performed jointly with a previous PhD student from University of Sheffield, Ibrahim Yaseen (Yaseen, 2017). Briefly, cells were grown overnight to reach 70-90% confluency prior to transfection. For one well of a 6-well plate, separate solutions of 10 $\mu$ l of 100nM siRNA in 190 $\mu$ l DMEM-

serum free and 5µl DharmaFECT reagent in 195µl DMEM-serum free were mixed and incubated for 5min at room temperature. The mixture was added in a dropwise fashion. After 24hr transfection, growth media were changed with fresh media. Cells were inspected for the gene KD after a further 48hr using qPCR or flow cytometry. The results show that there is a 40% reduction of Tspan-2 expression at the mRNA and protein levels compared with A549 cells treated with non-targeting KD reagents (**Fig 6.3**).

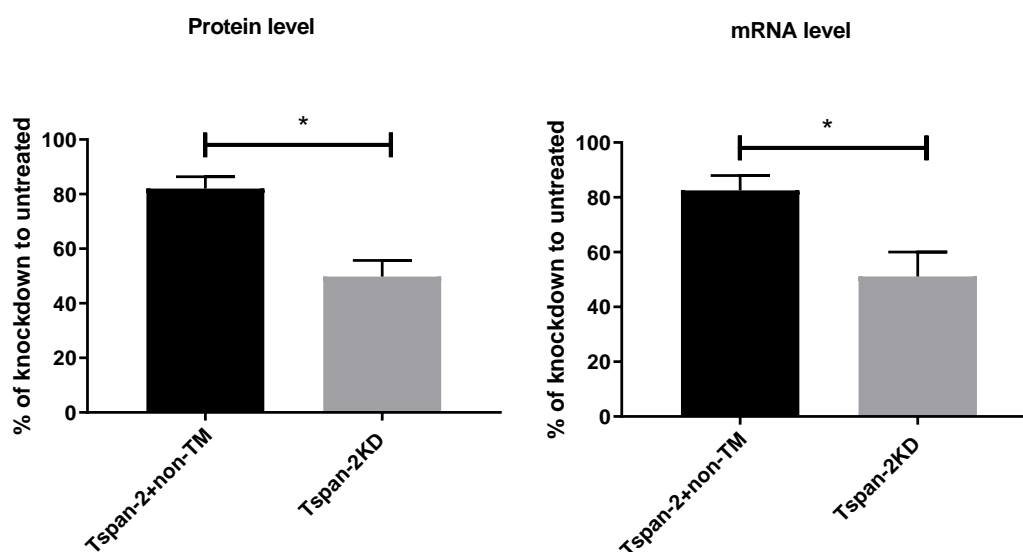


**Figure 6.3 Effect of Tspan-2KD at mRNA and protein levels in A549 cells after 72hr treatment with siRNA or non-targeting materials.**

A549 cells were transfected with DharmaFECT reagent and then were treated with 100nM siRNA or non-targeting materials, and then were prepared to measure the mRNA and protein levels as described in **section 2.2.9** and **section 2.2.10**. The effects of different treatments were tested by unpaired t-test, where \*  $p < 0.05$  significant. Non-TM=cells treated with non-targeting control materials. The results are the means ( $\pm$  SEM) of 3 independent experiments each performed in 2 technical replicates.

### 6.3.2 Effect of KD in *B. thailandensis* infection and MGC formation

#### 6.3.2.1 Effect of CD9KD on *B. thailandensis* infection and internalisation

CD9KD Smart Pool siRNA-treated A549 cells were used 48hr post-transfection. CD9KD and cells treated with non-targeting siRNA were infected for 2hr with *B. thailandensis* CDC272 and E264. Cells were washed 2x with HBSS and lysed to count the total number of bacteria by the addition of 100µl of 1% TritonX-100 for 15min. To count only internalised bacteria, the cells were incubated with DMEM containing antibiotics, washed and lysed using TritonX-100. The lysis mixture was serially diluted before 10µl of each dilution was plated onto LB agar plates for CFU counts. CFU was counted after 36hr

of incubation. The findings show that there is no significant difference between CD9KD cells or control cells treated with non-targeting reagents on the total bacterial infection or internalisation of both *B. thailandensis* strains, as shown in **Fig 6.4**.

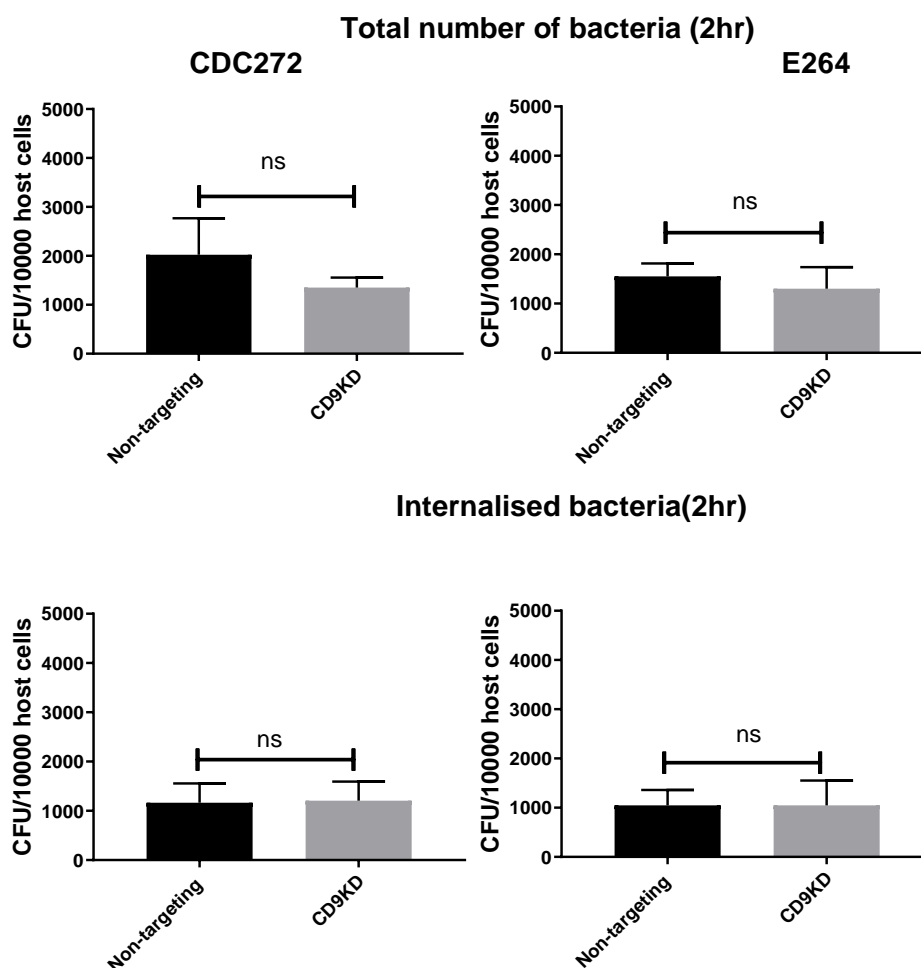


**Figure 6.4 Effect of CD9KD on *B. thailandensis* infection.**

A549 cells were pre-treated with KD reagents for CD9 before infection, as described in **section 2.2.8**. Bars show total number of bacteria and/or internalised bacteria per 10000 cells for A549 cells infected by both bacterial strains. The effects of different treatments were tested by unpaired t-test, where ns=non-significant. The results are the means ( $\pm$  SEM) of 3 independent experiments each performed in 4 technical replicates.

### 6.3.2.2 Effect of CD9KD reagents on MGC formation induced by *B. thailandensis*

The aim was to investigate if the CD9KD could also affect MGC formation induced by *B. thailandensis*. To do this, we treated the cells with Smart Pool siRNA reagent for 48hr. The control and KD A549 cells were infected by bacteria for 2hr and then washed and incubated with DMEM containing

amikacin and kanamycin antibiotics for 16hr. The fusion index was quantified relative to uninfected cells per field of view. MGCs were defined as cells containing 3 or more nuclei. Only *B. thailandensis* CDC272 strain, MGC formation and the number of nuclei per MGC were increased significantly in CD9KD A549 cells compared with A549 cells treated with non-targeting KD reagents, as shown in **Fig 6.5**.

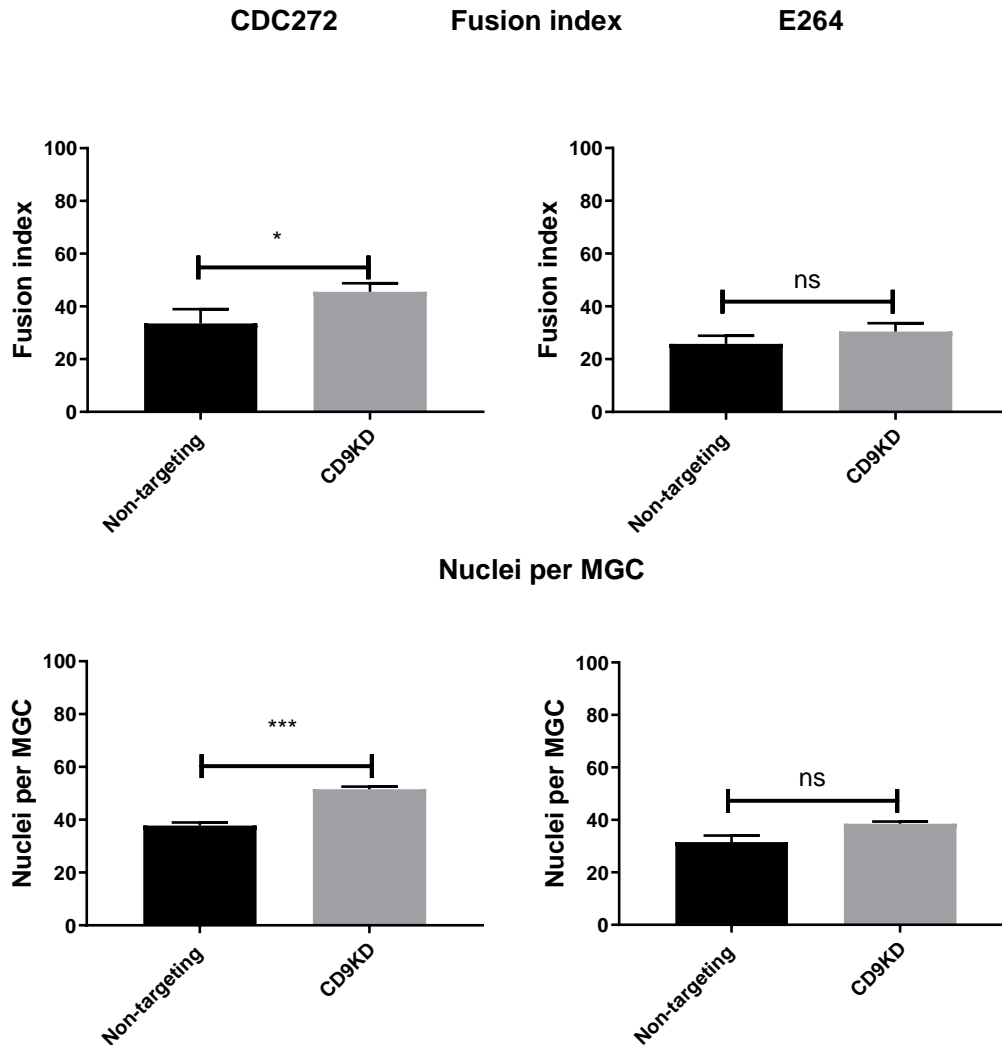


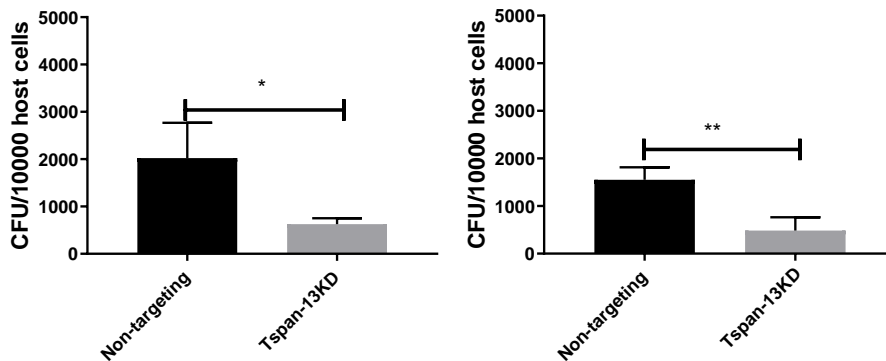
**Figure 6.5 Effect of CD9KD on MGC formation induced by both *B. thailandensis* strains.**

A549 cells were pre-treated CD9 siRNA KD reagents for 48hr and were infected *B. thailandensis* as described in **section 2.2.8**. Bars show the fusion index and the number of nuclei per MGC in A549 cells infected by both fusogenic strains. The effects of different treatments were tested by unpaired t-test, where \*  $p < 0.05$ ; \*\*\*  $p < 0.001$  significant, where ns=non-significant. The results are the means ( $\pm$  SEM) of 3 independent experiments each performed in 4 technical replicates.

### 6.3.2.3 Effect of Tspan-13KD on total *B. thailandensis* infection and internalisation

The effect of Tspan-13KD on *B. thailandensis* infection was investigated to support further data acquired using anti-Tspan-13 antibody. Briefly, we treated the cells with Smart Pool siRNA reagent for 48hr. Control and Tspan-13KD A549 cells were infected with *B. thailandensis* CDC272 and E264 for 2hr. To count total number of bacteria, the wells were lysed using 1% TritonX-100 for 15min. To count only internalised bacteria, the cells were incubated with DMEM containing antibiotics, washed and then lysed using TritonX-100. The lysis mixture was serially diluted and then plated onto LB agar plates. After 36hr of incubation at 37°C, CFU was determined. Data showed that the total number of bacteria per 10000 cells was decreased when compared with cells treated with non-targeting materials (**Fig 6.6**). Findings also showed that the internalisation of bacteria was decreased significantly when compared with cells treated with the non-targeting reagent.

### CDC272 Total number of bacteria (2hr) E264



### Internalised bacteria(2hr)

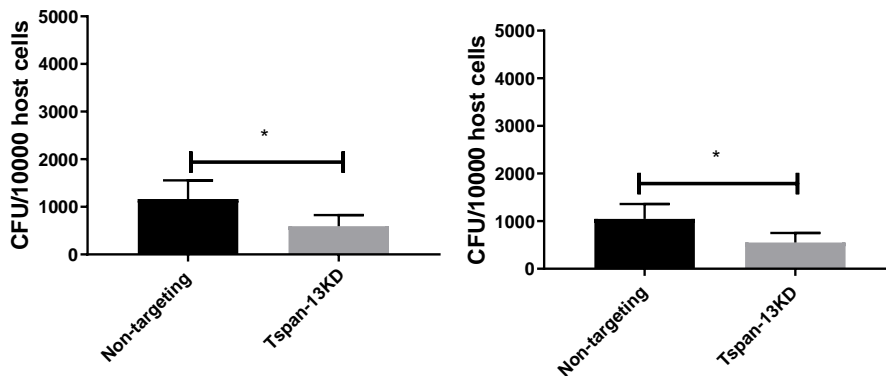


#### Figure 6.6 Effect of Tspan-13KD on *B. thailandensis* infection.

A549 cells were pre-treated with KD reagents for Tspan-13 before infection as described in **section 2.2.8**. Bars show the total number of bacteria and/or internalised bacteria per 10000 cells for both *B. thailandensis* strains, CDC272 and E264. The effects of different treatments were tested by unpaired t-test, where \*  $p < 0.05$ ; \*\*  $p < 0.01$  significant. The results are the means ( $\pm$  SEM) of 3 independent experiments each performed in 4 technical replicates.

#### 6.3.2.4 Effect of Tspan-13KD on MGC induced by *B. thailandensis*

The effect of Tspan-13KD on MGC formation was investigated to confirm our findings that acquired using anti-Tspan-13 antibody. Briefly, we treated the cells with Smart Pool siRNA for 48hr. Control and Tspan-13KD A549 cells were infected with *B. thailandensis* for 2hr and then washed and incubated with DMEM containing amikacin and kanamycin antibiotics for 16hr. The fusion index was quantified relative to uninfected cells per field of view. MGCs were defined as cells containing 3 or more nuclei. The fusion index and the number of nuclei per MGC were decreased significantly in infected Tspan-13KD cells relative to control cells (**Fig 6.7**).

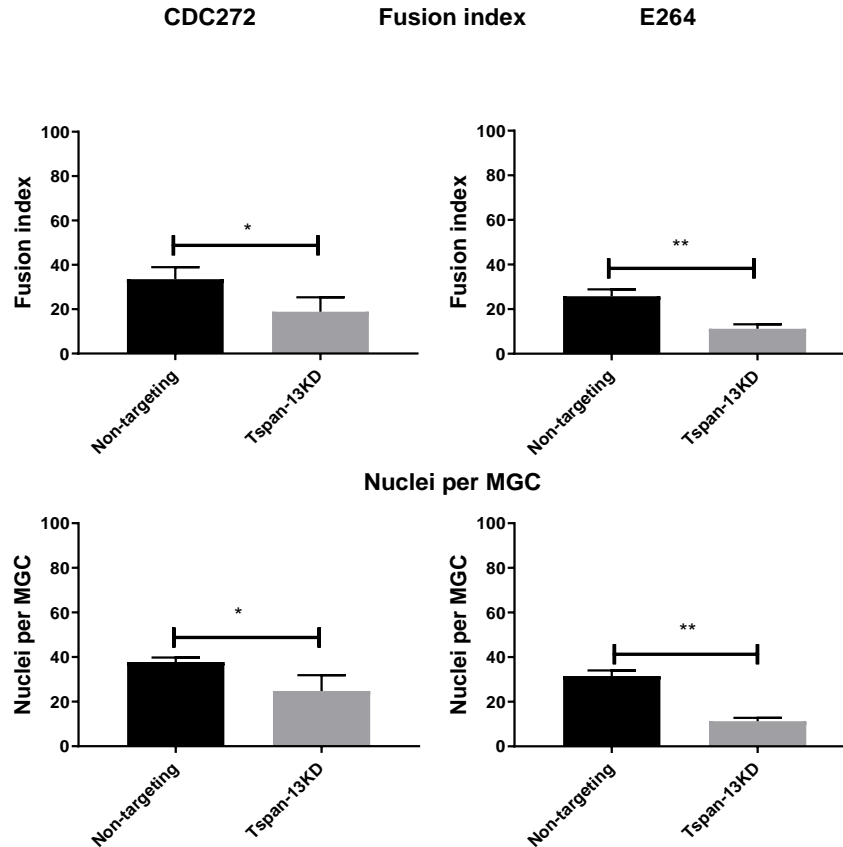


**Figure 6.7 Effect of Tspan-13KD on MGC formation induced by both *B. thailandensis* strains.**

A549 cells were pre-treated with Tspan-13 siRNA KD or non-targeting reagents for 48hr and were infected with *B. thailandensis*, as described in **section 2.2.8**. Bars show the fusion index and the nuclei per MGC in A549 cells infected by two strains. The effects of different treatments were tested by unpaired t-test, where \*  $p < 0.05$ ; \*\*  $p < 0.01$  significant. The results are the means ( $\pm$  SEM) of 3 independent experiments each performed in 4 technical replicates.

#### 6.3.2.5 Effect of Tspan-2KD on total *B. thailandensis* infection and MGC formation

Infection experiments were performed by myself, using Tspan-2KD A549 cells produced by another laboratory member (Yaseen, 2017). This work was performed only with one strain of *B. thailandensis*, (CDC272) because there was not enough KD material to screen two strains. Briefly, we treated the cells with DharmaFECT siRNA for 72hr. Control and Tspan-2KD A549 cells were infected with *B. thailandensis* CDC272 and E264 for 2hr. To count total number of bacteria, the wells were lysed using 1% TritonX-100 for 15min. To count only internalised bacteria, the cells were incubated with DMEM containing antibiotics, washed and then lysed using TritonX-100. The lysis mixture was serially diluted and then plated onto LB agar plates. After 36hr of

incubation at 37°C, CFU was determined. The total number of bacteria and internalised bacteria was reduced in the Tspan-2KD A549 cells when compared with cells treated with non-targeting reagents (**Fig 6.8A**).

To investigate the role of Tspan-2 in MGC formation, control and Tspan-2KD A549 cells were infected with *B. thailandensis* for 2hr and then washed and incubated with DMEM containing amikacin and kanamycin antibiotics for 16hr. The fusion index was quantified relative to uninfected cells per field of view. MGCs were defined as cells containing 3 or more nuclei. The fusion index and the number of nuclei per MGC were decreased significantly in infected Tspan-2KD cells relative to control cells (**Fig 6.8B**).

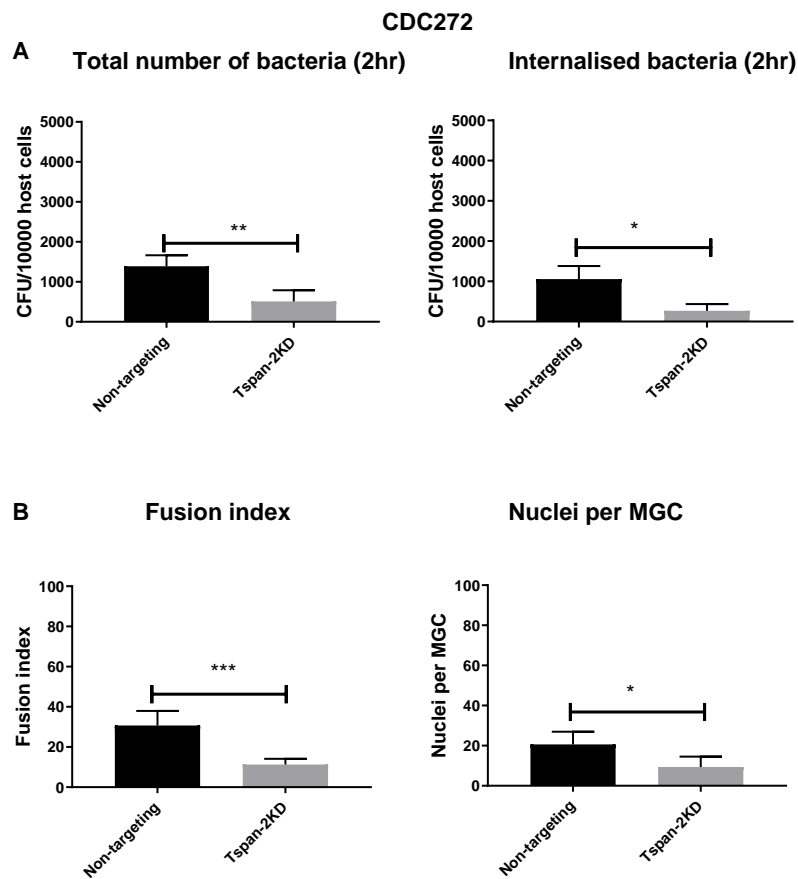


**Figure 6.8 Effect of Tspan-2KD on MGC formation and *B. thailandensis* infection.**

**A:** The upper panels show that A549 cells were pre-treated with KD reagents for Tspan-2 before infection as described in **section 2.2.8**. Bars show the total number of bacteria and/or internalised bacteria per 10000 cells for A549 cells infected by *B. thailandensis* CDC272. **B:** The lower panels show that A549 cells were pre-treated Tspan-2KD reagents for 72hr and infected *B. thailandensis* as described in **section 2.2.8**. Bars show the fusion index and the number of nuclei per MGC in A549 cells infected by *B. thailandensis* CDC272. The effects of different treatments were tested by unpaired t-test, where \*  $p < 0.05$ ; \*\*  $p < 0.01$ ; \*\*\*  $p < 0.001$  significant. The results are the means ( $\pm$  SEM) of 3 independent experiments each performed in 4 technical replicates.

### 6.3.2.6 Effect of ADAM10KD on total *B. thailandensis* infection and internalisation

To validate the results using anti-ADAM10 antibody, we studied the effect of ADAM10KD on *B. thailandensis* infection. Briefly, the cells were treated with ADAM10 targeting and non-targeting Smart Pool siRNA for 48hr. Control and ADAM10KD cells were infected for 2hr with *B. thailandensis* CDC272 and E264. To count the total number of bacteria, the cells were lysed by the addition of 1% TritonX-100 for 15min. To count only internalised bacteria, the cells were incubated with DMEM containing antibiotics, washed and lysed using TritonX-100. The lysis mixture was diluted and then was plated onto LB agar plates. CFU was counted after 36hr of incubation. The findings showed that ADAM10KD has no effect on the total number of bacteria and/or internalisation when compared with cells treated with non-targeting materials (Fig 6.9).

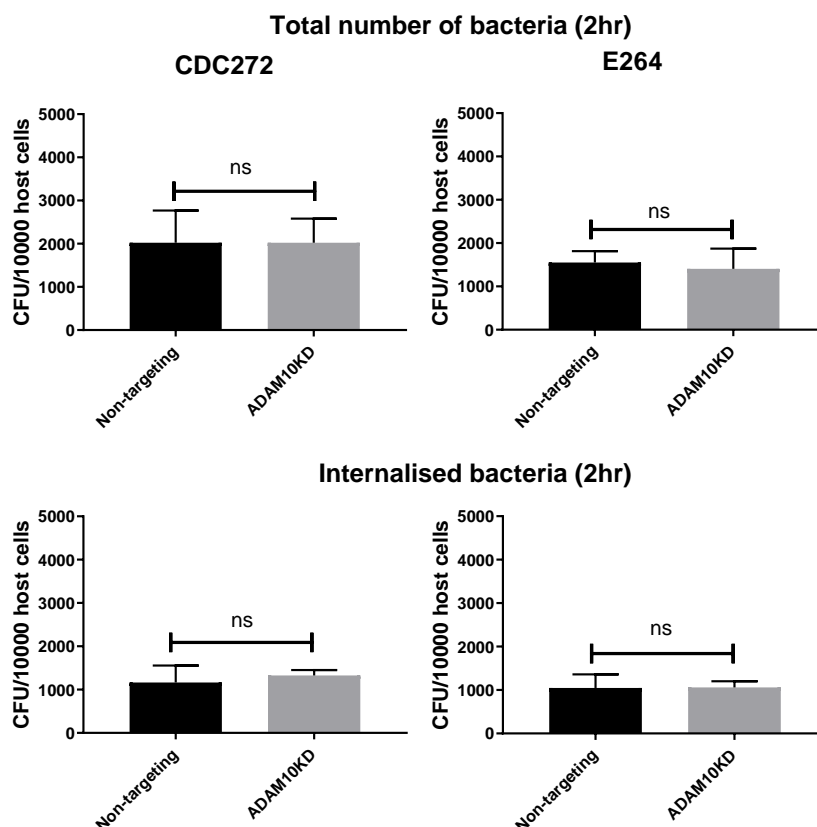


**Figure 6.9 Effect of ADAM10KD on *B. thailandensis* infection**

A549 cells were pre-treated with KD reagents for ADAM10 before infection as described in section 2.2.8. Bars show the total number of bacteria and/or internalised bacteria per 10000 cells for A549 cells infected by two *B. thailandensis*, CDC272 and E264. The effects of different treatments were tested by unpaired t-test, where ns: non-significant. The results are the means ( $\pm$  SEM) of 3 independent experiments each performed in 4 technical replicates.

### 6.3.2.7 Effect of ADAM10KD on MGC formation induced by *B. thailandensis*

To validate the results using anti-ADAM10 antibody, we studied the effect of ADAM10KD on MGC formation. Briefly, the cells were treated with ADAM10 targeting and non-targeting Smart Pool siRNA for 48hr. Control and ADAM10KD cells were infected with *B. thailandensis* for 2hr and then washed and incubated with DMEM containing amikacin and kanamycin antibiotics for 16hr. The fusion index was quantified relative to uninfected cells per field of view. MGCs were defined as cells containing 3 or more nuclei. The fusion index and nuclei per MGC were increased significantly in A549 cells with ADAM10KD reagents compared to cells treated with non-targeting reagents (Fig 6.10).

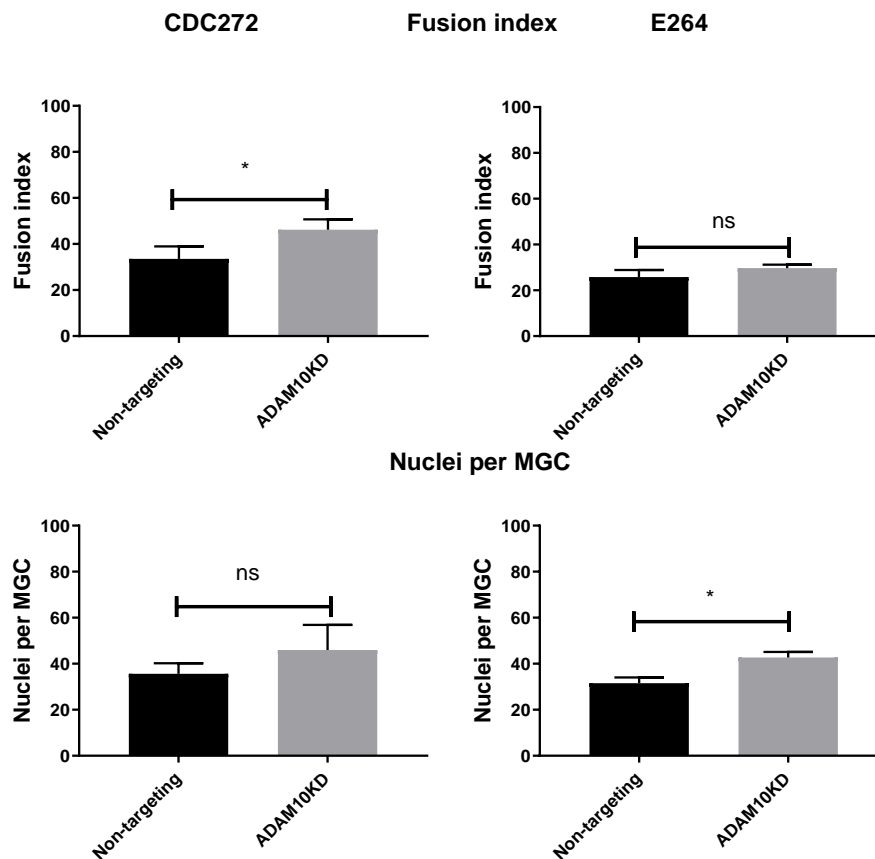


**Figure 6.10 Effect of ADAM10KD on MGC formation induced by both *B. thailandensis* strains.**

A549 cells were pre-treated with ADAM10 siRNA KD reagents for 48hr and were infected with *B. thailandensis* as described in section 2.2.8. Bars show the fusion index and the number of nuclei per MGC in A549 cells infected by two types of strains. The effects of different treatments were tested by unpaired t-test, where \*  $p < 0.05$  significant; ns is non-significant. The results are the means ( $\pm$  SEM) of 3 independent experiments each performed in 4 technical replicates.

### 6.3.3 CD9 expression in CD9KO A549 cells

The CD9KO A549 cells were produced by Dr. David J. Blake (Blake *et al.*, 2018) and the WT control cells obtained from the in-house cell bank. CD9KO and WT A549 cells were checked for CD9 expression using flow cytometry. Cells were harvested using non-enzymatic cell dissociation solution and stained with primary anti-CD9 antibody or isotype control for 45min, and then washed 2x with BBN. A FITC-labelled secondary antibody was used at the recommended concentration 1:250 for 45min. The negative controls here were cells treated with the binding buffer BBN or irrelevant antibody with the same isotype. The results show that ~82% of the WT A549 cells express CD9, but only ~2% of the CD9KO A549 cells express CD9, as shown in **Fig 6.11**.

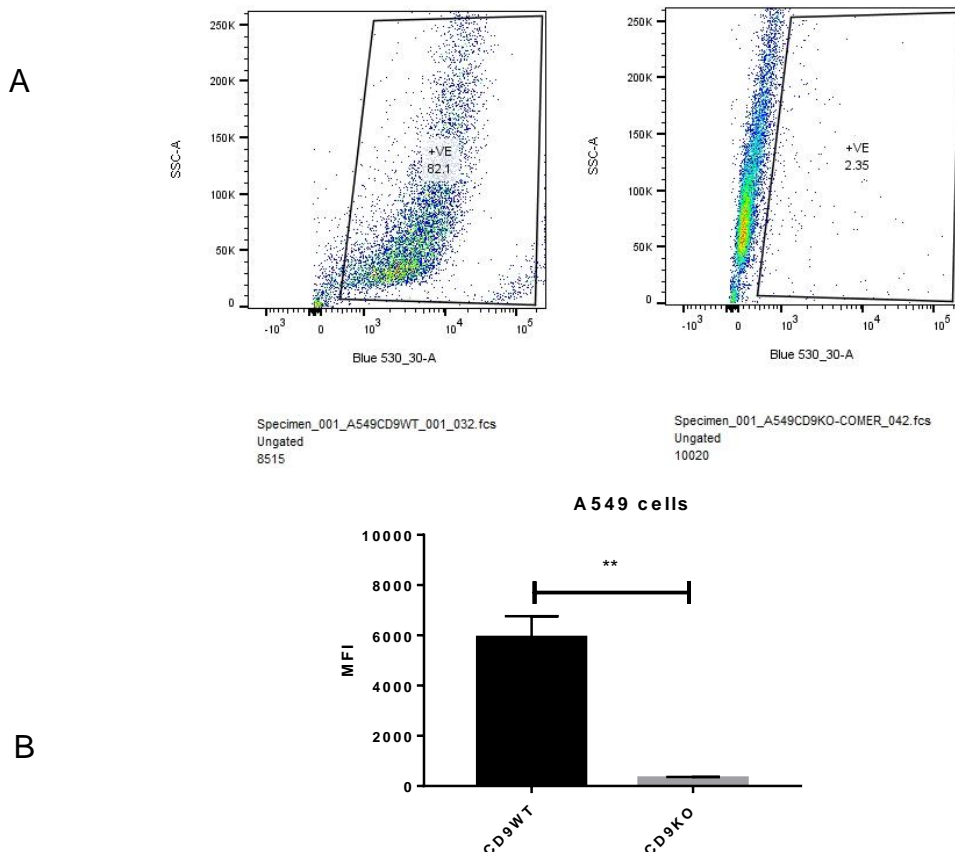


**Figure 6.11 Measurement of CD9 expression on WT and CD9KO A549 cells by flow cytometry.**

Cells were tested using anti-human CD9, isotype control (JC1) and secondary anti-mouse IgG-FITC. **A:** The upper panel shows the cell expressing CD9 on WT and KO A549 cells, respectively. **B:** The lower panel shows the median fluorescence intensity of CD9 on WT and CD9KO cells. The significance of differences between uninfected and infected cells was measured by t-test, where \*\*  $p < 0.01$  significant. The results are the means ( $\pm$  SEM) of 3 independent experiments each performed in 3 technical replicates.

### 6.3.3.1 Tspan-15 and ADAM10 expression in CD9KO A549 cells

CD9KO may affect the expression of other cell surface proteins. These experiments were performed to investigate the possible effect of CD9KO on the expression of Tspan-15 and ADAM10. However, mock-treated A549 cells from the Blake laboratory were not available for this study and WT A549 cells from University of Sheffield stocks were used instead. The levels of expression were measured using flow cytometric analysis, as described in **section 2.2.8**. The results show that the level of ADAM10 was slightly increased with CD9KO compared with WT A549, but not significantly. Tspan-15 expression was not changed on the surface of CD9KO cells compared to WT A549 cells, as shown in **Fig 6.12**. It seems that CD9KO has no effect on the cell surface expression of ADAM10 and Tspan-15 on A549 cells.

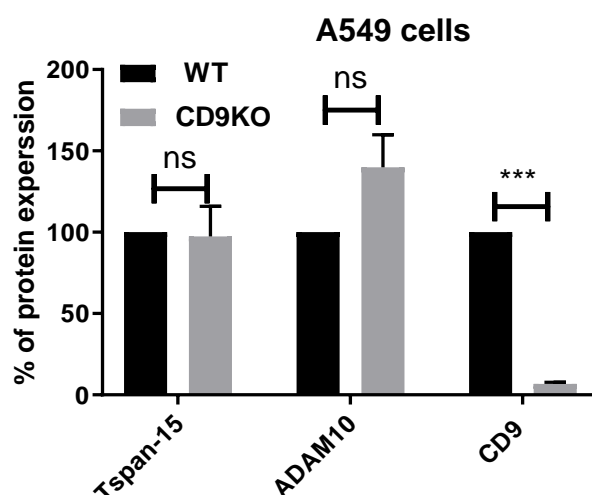


**Figure 6.12 Cell surface protein expression on WT and CD9KO A549 cells.**

Flow cytometry analysis was performed as described in **section 2.2.9**. The significance of differences between uninfected and infected cells was measured by t-test, where \*\*\*  $p < 0.001$  significant; ns=non-significant. The results are the means ( $\pm$  SEM) of 3 independent experiments each performed in 2 technical replicates.

### 6.3.3.2 Effect of CD9KO on total *B. thailandensis* infection and internalisation

The ability of *B. thailandensis* to infect CD9KO and WT A549 cell lines were investigated. The total bacterial infection for both strains of *B. thailandensis* was assessed in WT and CD9KO A549 cell lines after 2hr of infection. Briefly, both WT and CD9KO cells were infected for 2hr with *B. thailandensis* CDC272 and E264. Cells were washed 2x with HBSS and lysed to count the total number of bacteria by the addition of 100 $\mu$ l of 1% TritonX-100 for 15min. To count only internalised bacteria, the cells were incubated with DMEM

containing antibiotics, washed and lysed using TritonX-100. The lysis mixture was serially diluted before 10µl of each dilution was plated onto LB agar plates for CFU counts. It was observed that the infection after 2hr of *B. thailandensis* was very similar in both CD9KO and WT A549 cells for both strains of *B. thailandensis*, as demonstrated in **Fig 6.13**. These confirmed the KD results that CD9 has no role in the adhesion and uptake of *B. thailandensis*.

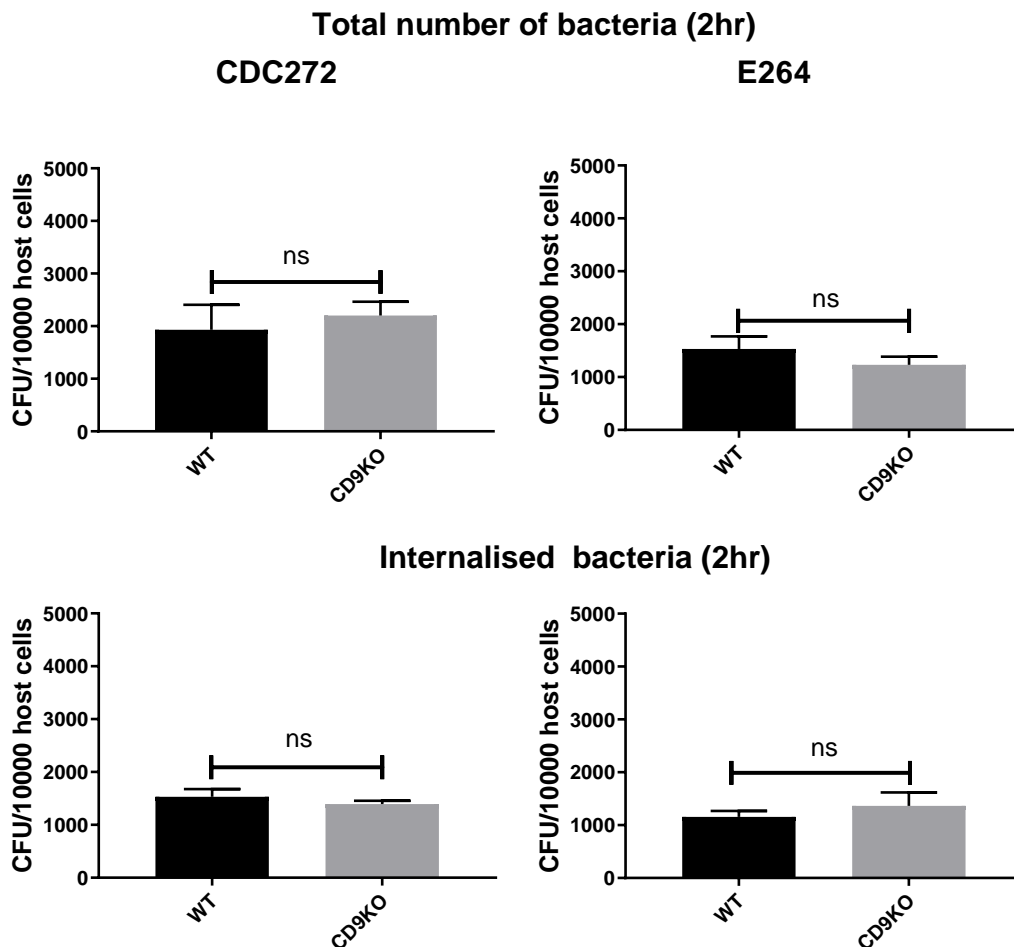


**Figure 6.13 Effect of CD9KO in A549 cells on *B. thailandensis* infection.**

A549 cells were infected by *B. thailandensis*, as described in **section 2.2.8**. Bars show the total number of bacteria and/or internalised bacteria per 10000 cells for A549 cells infected by two bacterial strains, CDC272 and E264. The effects of different treatments were tested by unpaired t-test, ns=non-significant. The results are the means ( $\pm$  SEM) of 3 independent experiments each performed in 4 technical replicates.

### 6.3.3.3 Effect of CD9KO on MGC formation induced by *B. thailandensis*

These investigations were to confirm our results with CD9KD on MGC formation induced by *B. thailandensis* infection. To do this, the WT and KO A549 cells were infected with bacteria for 2hr and then washed and incubated

with DMEM containing amikacin and kanamycin antibiotics for 16hr. The fusion index was quantified relative to uninfected cells per field of view. MGCs were defined as cells containing 3 or more nuclei. Fusion index was significantly increased in CD9KO A549 cells when compared with WT A549 cells infected by both *B. thailandensis* strains, but only CDC272-infected cells contained significantly higher numbers of nuclei per MGC, as shown in **Fig 6.14**.

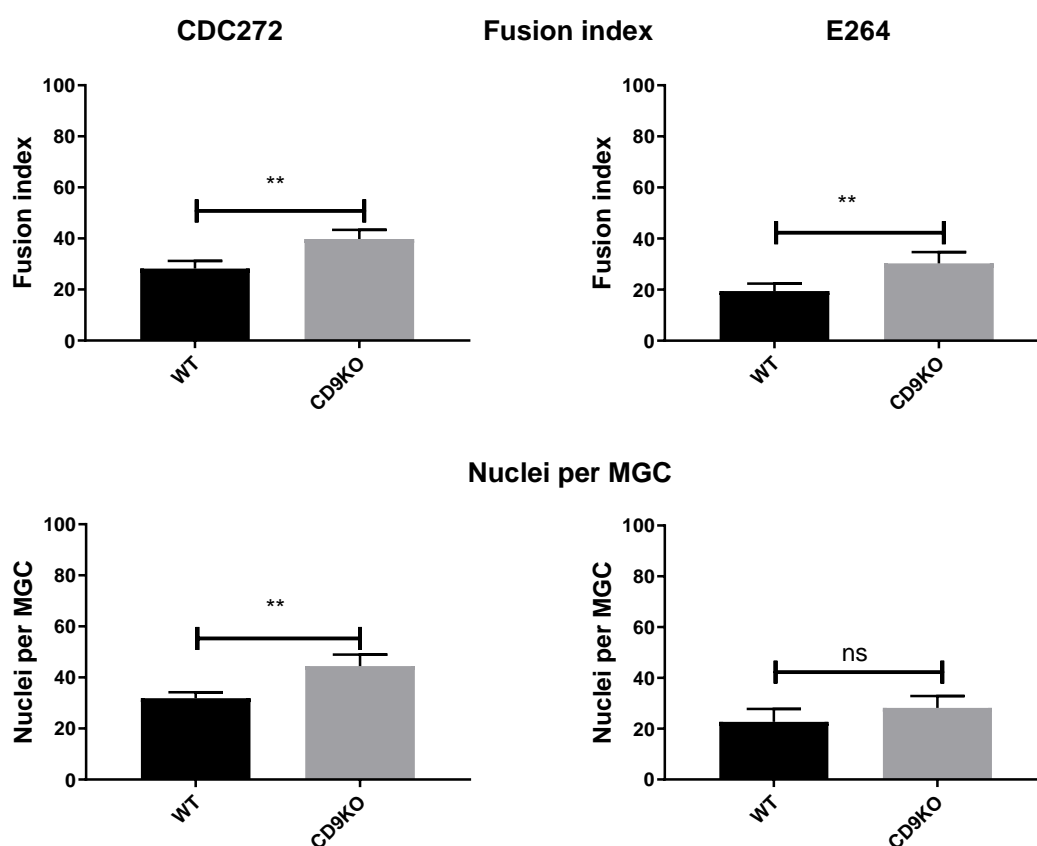


**Figure 6.14 Effect of CD9KO on MGC formation induced by both *B. thailandensis* strains.**

A549 cells were infected by *B. thailandensis*, as described in **section 2.2.8**. Bars show the fusion index and the number of nuclei per MGC in A549 cells infected by two strains. The effects of different treatments were tested by unpaired t-test, where \*\* p<0.01 significant; ns=non-significant. The results are the means ( $\pm$  SEM) of 3 independent experiments each performed in 4 technical replicates.

#### 6.3.4 ADAM10 expression in ADAM10KO and WT A549 cells

ADAM10KO and WT control A549 cells were obtained from Dr Mike Tomlinson (University of Birmingham) (Szyroka, 2019). ADAM10 expression was measured using flow cytometry to confirm that the cells do not express this protein. Briefly, cells were harvested using non-enzymatic cell

dissociation solution and stained with primary anti-ADAM10 antibody and isotype control for 45min, and then washed 2x with BBN. A FITC-labelled secondary antibody was used at the recommended concentration 1:250 for 45min. The negative controls here were cells treated with the binding buffer BBN or irrelevant antibody with the same isotype. The results show that the percentage of cells that express ADAM10 on WT A549 cells was ~96%, but only ~9% of ADAM10KO cells express this protein (**Fig 6.15**).

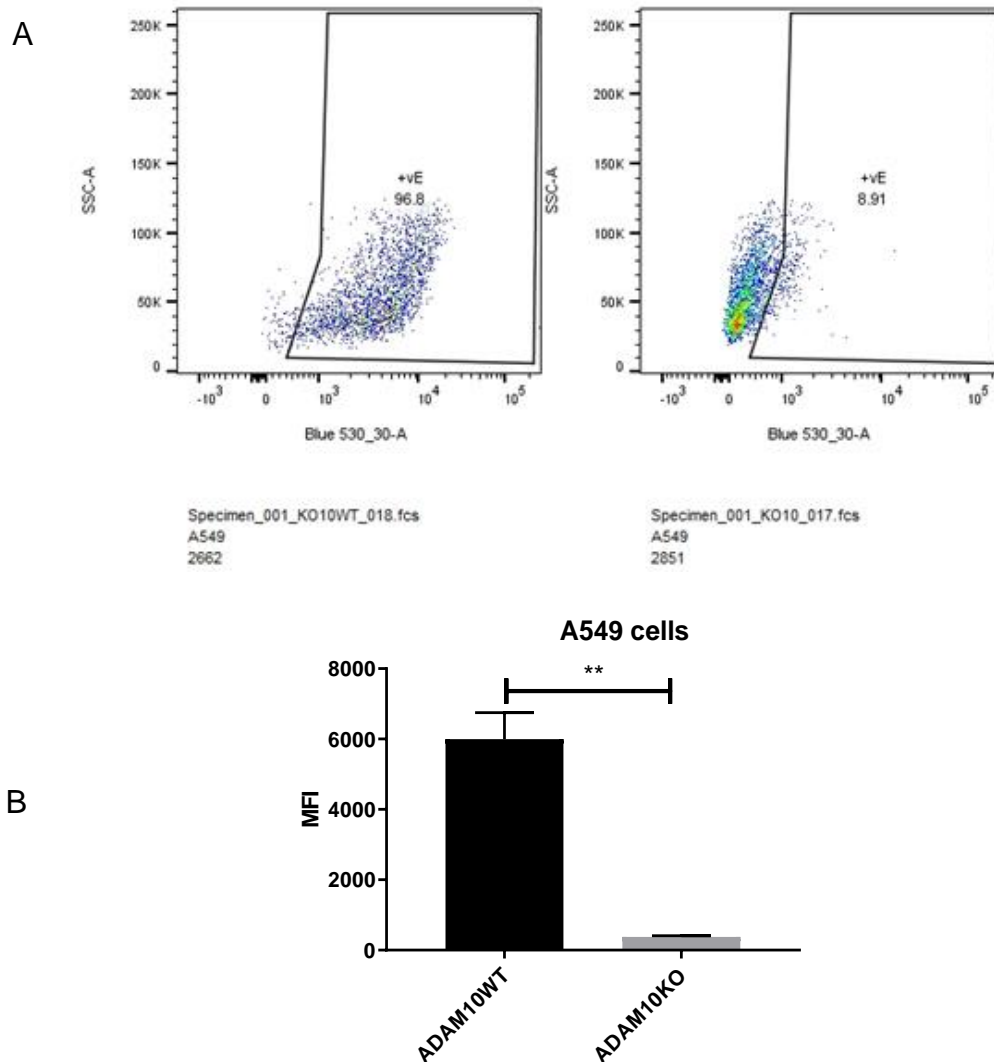


**Figure 6.15 ADAM10 expression on WT and ADAM10KO A549 cells by flow cytometry.**

Cells were tested using primary anti-human ADAM10, isotype control (JC1) and secondary anti-mouse IgG-FITC. **A**: The upper panel shows the fluorescence intensity of ADAM10 on WT and KO A549 cells, respectively. **B**: The lower panel shows the median fluorescence intensity of ADAM10 on WT and ADAM10KO cells. The significance of differences between uninfected and infected cells was measured by t-test, where \*\* p<0.01 significant. The results are the means ( $\pm$  SEM) of 3 independent experiments each performed in 2 technical replicates.

#### 6.3.4.1 CD9 and Tspan-15 expression in ADAM10KO and WT A549 cells

Flow cytometric analysis was used to measure the levels of protein expression on the cell surface as described in **section 2.2.9**. The findings show that CD9 and Tspan-15 were normally expressed on ADAM10KO A549 when compared to WT A549 cells. It is apparent that there are no effects of ADAM10KO on the expression of Tspan-15 and CD9 on A549 cells (**Fig 6.16**).

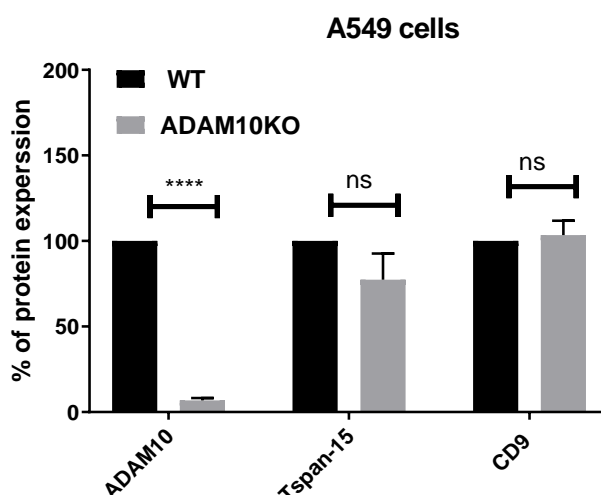


**Figure 6.16 Cell surface molecule expression on ADAM10KO and WT A549 cells.**

Flow cytometry analysis was performed as described in **section 2.2.9**. The significance of differences between uninfected and infected cells was measured by t-test, where \*\*\*\*  $p < 0.0001$  significant; ns=non-significant. The results are the means ( $\pm$  SEM) of 3 independent experiments each performed in 3 technical replicates.

#### 6.3.4.2 Effect of ADAM10KO on total *B. thailandensis* infection and internalisation

These investigations were to confirm our results with ADAM10KD on *B. thailandensis* infection, in particular for the total number of bacteria and internalised bacteria after 2hr of infection. In brief, both ADAM10KO and WT A549 cells were seeded in 96 well plates. Both ADAM10WT and ADAM10KO cells were infected for 2hr with *B. thailandensis* CDC272 and E264. A549 cells were washed 2x with HBSS and lysed to count the total number of bacteria by the addition of 100 $\mu$ l of 1% TritonX-100 for 15min. To count only internalised bacteria, the cells were incubated with DMEM containing antibiotics, washed and lysed using TritonX-100. The lysis mixture was serially diluted before 10 $\mu$ l of each dilution was plated onto LB agar plates for

CFU counts. The results show there is no effect of ADAM10KO on the total number of bacteria and internalised bacteria. *B. thailandensis* infection of ADAM10KO A549 cells was consistent with ADAM10KD A549 cells (**Fig 6.17**).

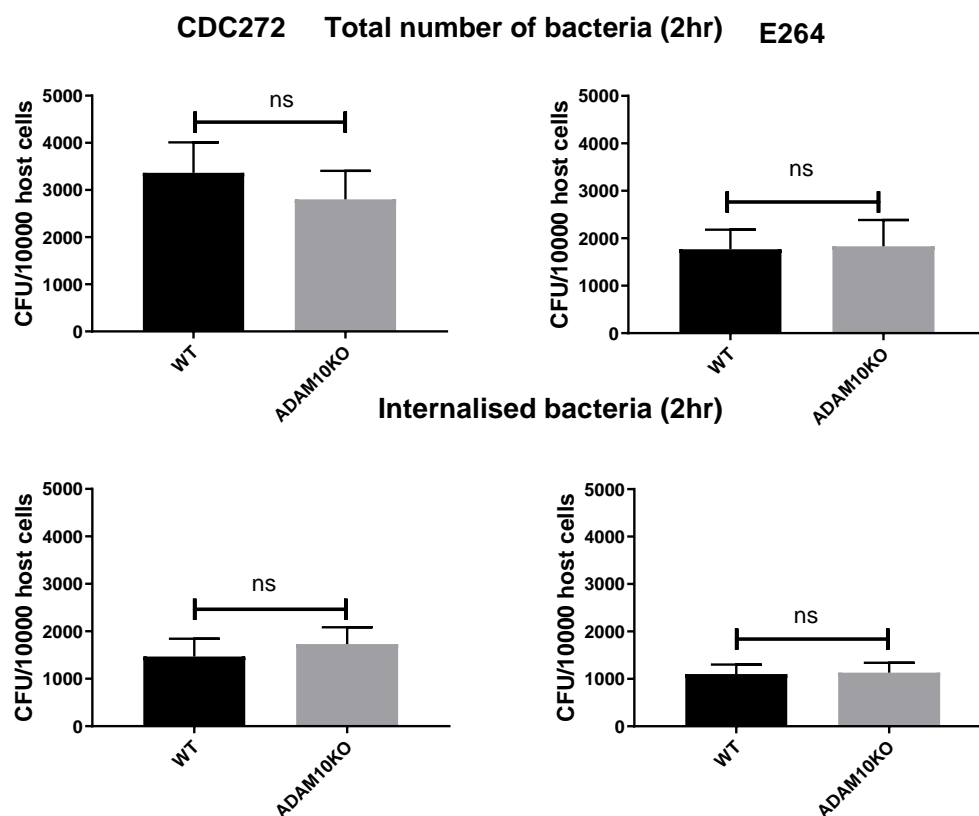


**Figure 6.17 Effect of ADAM10KO in A549 cells on total *B. thailandensis* infection.**

A549 cells were infected by *B. thailandensis*, as described in **section 2.2.8**. Bars show total number of bacteria and/or internalised bacteria per 10000 cells for A549 cells infected by two *B. thailandensis* strains, CDC272 and E264. The effects of different treatments were tested by unpaired t-test, ns=non-significant. The results are the means ( $\pm$  SEM) of 3 independent experiments each performed in 4 technical replicates.

#### 6.3.4.3 Effect of ADAM10KO on MGC induced by *B. thailandensis*

These experiments were performed to confirm our findings with ADAM10KD. To do this, the WT and KO A549 cells were infected by bacteria for 2hr and then washed and incubated with DMEM containing amikacin and kanamycin antibiotics for 16hr. The fusion index was quantified relative to uninfected cells per field of view. MGCs were defined as cells containing 3 or more nuclei. The data did not correlate with our findings with ADAM10KD A549 cells. ADAM10KO has no effect on fusion index compared with WT A549 cells

infected by both *B. thailandensis* strains, and has no effect on the number of nuclei per MGC (Fig 6.18).

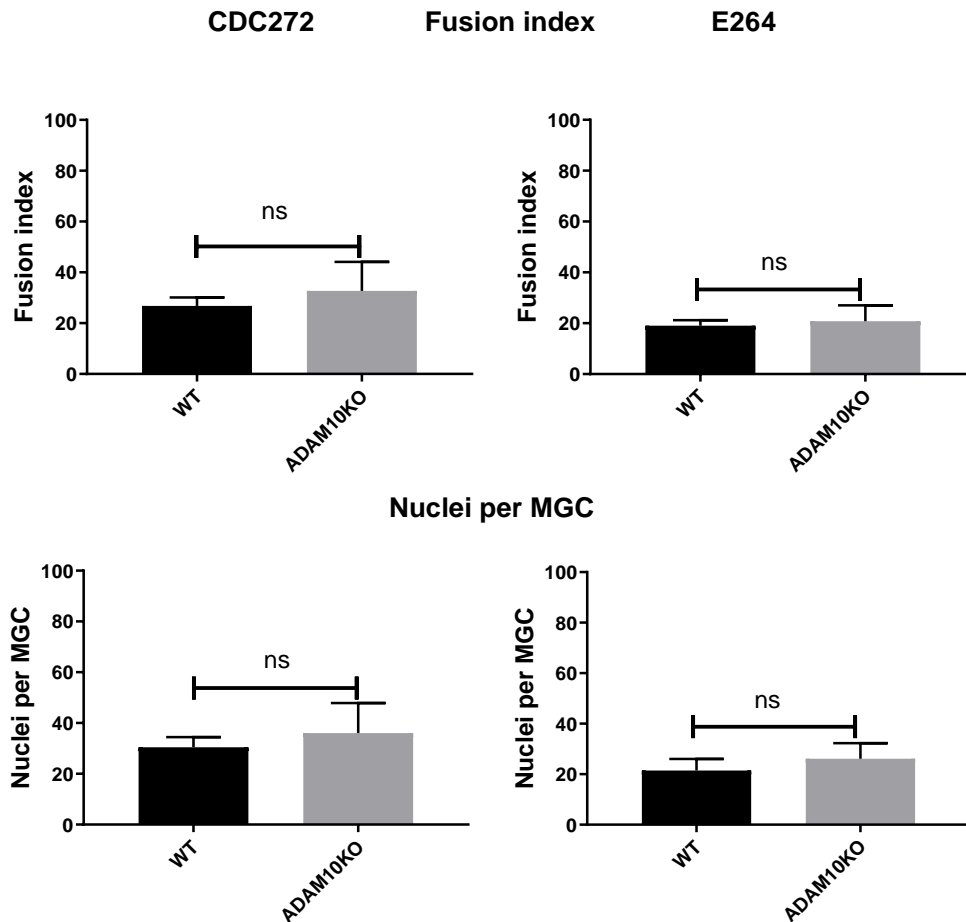


**Figure 6.18 Effect of ADAM10KO on MGC formation induced by both *B. thailandensis* strains.**

A549 cells were infected by *B. thailandensis*, as described in section 2.2.8. Bars show the fusion index and the number of nuclei per MGC in A549 cells infected by two types of *B. thailandensis* strains. The effects of different treatments were tested by unpaired t-test, where ns=non-significant. The results are the means ( $\pm$  SEM) of 7 independent experiments each performed in 4 technical replicates.

### 6.3.5 Tspan-15 expression in Tspan-15KO and WT A549 cells

Tspan-15KO and WT control A549 cells were obtained from Dr Mike Tomlinson (University of Birmingham) (Szyroka, 2019). Tspan-15KO and WT A549 cells were checked for Tspan-15 expression using flow cytometry. Cells were harvested using non-enzymatic cell dissociation solution and stained with primary anti-CD9 antibody and isotype control for 45min, and then washed 2x with BBN. A FITC-labelled secondary antibody was used at the recommended concentration 1:250 for 45min. The negative controls here were cells treated with the binding buffer BBN or irrelevant antibody with the

same isotype. The results show that the percentage of cells that express Tspan-15 on WT A549 cells was ~75%, but only ~6% of Tspan-15KO cells express this protein (**Fig 6.19**).

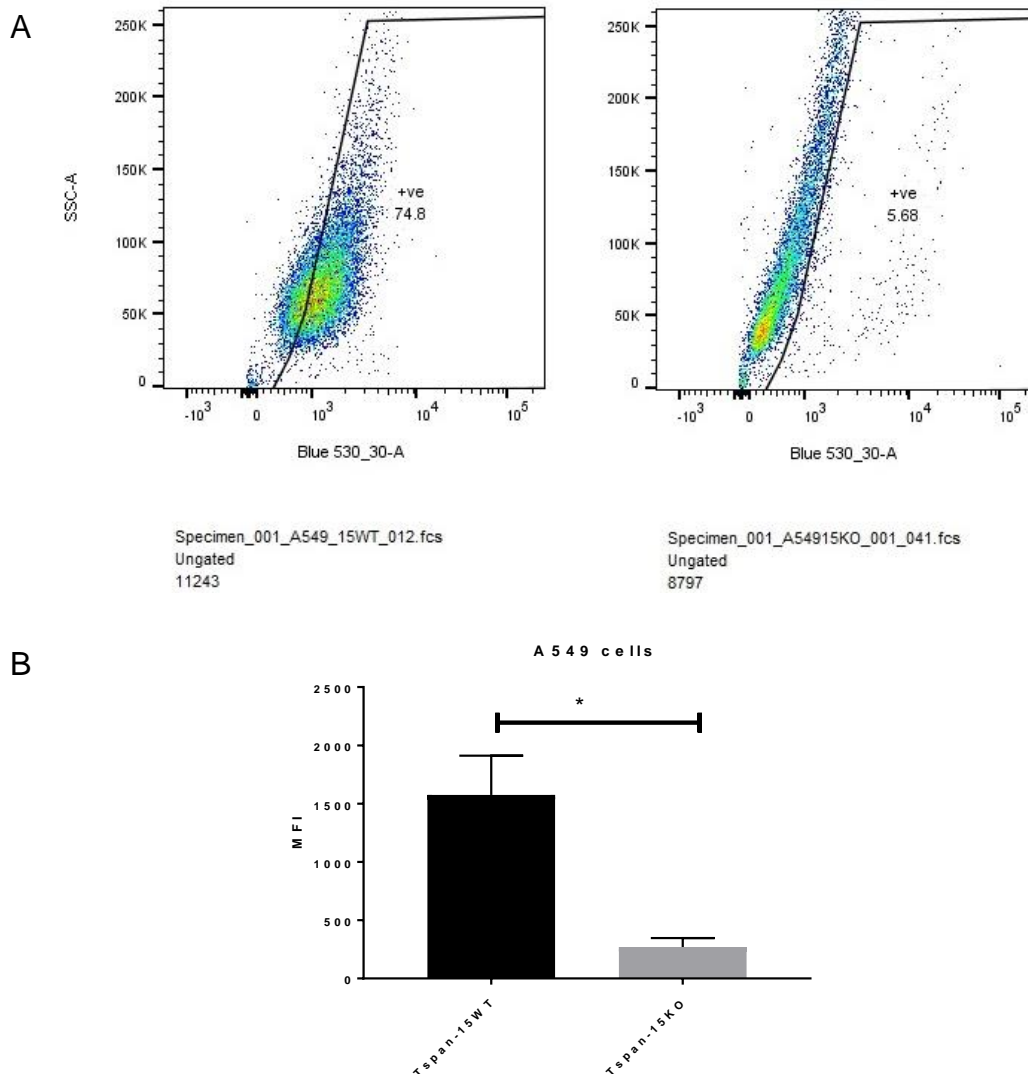


**Figure 6.19 Tspan-15 expression on WT and Tspan-15KO A549 cells by flow cytometry.**

Cells were tested using primary anti-human Tspan-15, isotype control (JC1) and secondary anti-mouse IgG-FITC. **A:** The upper panel shows the population expressing Tspan-15 on WT and KO A549 cells, respectively. **B:** The lower panel shows the median fluorescence intensity of Tspan-15 on WT and Tspan-15KO cells. The significance of differences between uninfected and infected cells was measured by t-test, where \*  $p < 0.05$  significant. The results are the means ( $\pm$  SEM) of 3 independent experiments each performed in 2 technical replicates.

### 6.3.5.1 CD9 and ADAM10 expression on Tspan-15KO and WT A549 cells

Tspan-15KO may affect the expression of other cell surface proteins. These experiments were performed to investigate the possible effect of Tspan-15KO on the expression of CD9 and ADAM10. The expression levels of CD9 and

ADAM10 were measured using flow cytometric analysis. The findings show that ADAM10 was reduced by more than 50% on the surface of KO A549 compared to WT, and the level of CD9 was also reduced significantly. It seems that Tspan-15KO can regulate ADAM10 and CD9 expression in A549 cells (**Fig 6.20**).

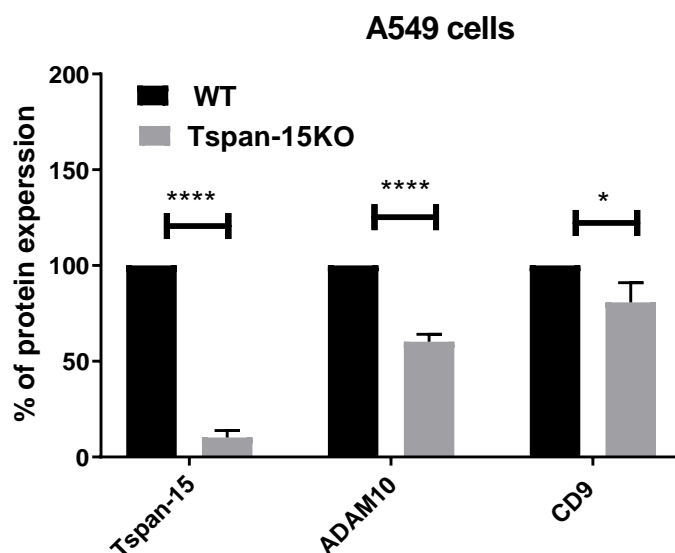


**Figure 6.20 Cell surface molecules expression on WT and Tspan-15KO A549 cells.**

Flow cytometry analysis was performed as described in **section 2.2.9**. The significance of differences between uninfected and infected cells was measured by t-test, where \*  $p < 0.05$ ; \*\*\*\*  $p < 0.0001$  significant. The results are the means ( $\pm$  SEM) of 3 independent experiments each performed in 3 technical replicates.

#### 6.3.5.2 Tspan15 expression after infection with *B. thailandensis*

This experiment was performed to investigate if Tspan-15 is changed in response to 18hr of *B. thailandensis* infection using flow cytometry. The results show that there is no change in the levels of Tspan-15 during the infection by *B. thailandensis* CDC272 and E264 or by *B. thailandensis* E264- $\Delta$ tssK, as described in **Fig 6.21**. These indicated that Tspan-15 is not changed in response to *B. thailandensis* infection.

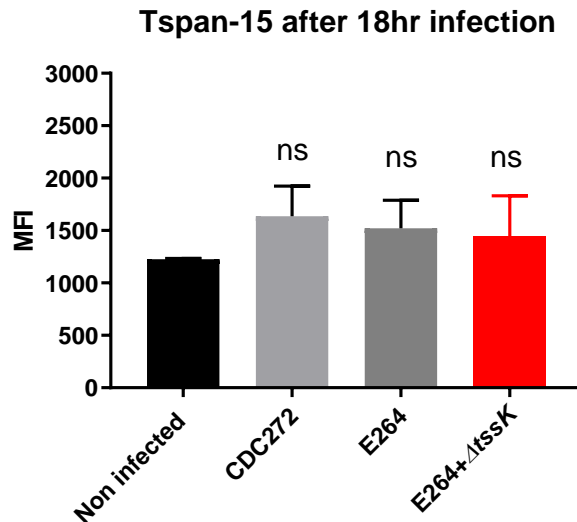


**Figure 6.21 Tspan-15 protein expression after infection on the surface of A549 cells.**

A549 cells were infected with either fusogenic *B. thailandensis* CDC272 or E264 or non-fusogenic mutant E264  $\Delta$ tssK. A549 cells left uninfected were used as controls. After 16hr of kanamycin and amikacin treatment, cells were stained with primary anti-Tspan-15 antibody for 45min, and then analysed by flow cytometry. The significance of differences between uninfected and infected cells was measured by one-way ANOVA, where ns=non-significant. The results are the means ( $\pm$  SEM) of 2 independent experiments each performed in 2 technical replicates.

#### 6.3.5.3 Role of Tspan-15 on *B. thailandensis* infection

The effect of Tspan-15KO and antibody on bacterial infection was investigated. In brief, the WT and Tspan-15KO A549 cells were seeded in 96 wells plates. 8 wells of WT A549 cells were treated with the anti-Tspan-15 antibody or isotype control for 1hr, and then the cells were washed. Both cell types were infected for 2hr with *B. thailandensis* CDC272 and E264. A549 cells were washed 2x with HBSS and lysed to count the total number of bacteria by the addition of 100 $\mu$ l of 1% TritonX-100 for 15min. To count only internalised bacteria, the cells were incubated with DMEM containing antibiotics, washed and lysed using TritonX-100. The lysis mixture was serially diluted before 10 $\mu$ l of each dilution was plated onto LB agar plates for CFU counts. It was observed that Tspan-15KO has a slight effect on *B. thailandensis* infection but was not significantly different when compared with WT A549 cells. Data also showed that anti-Tspan-15 antibody has no effect on total number of bacteria or internalised bacteria when compared with isotype control treatment (**Fig 6.22**).

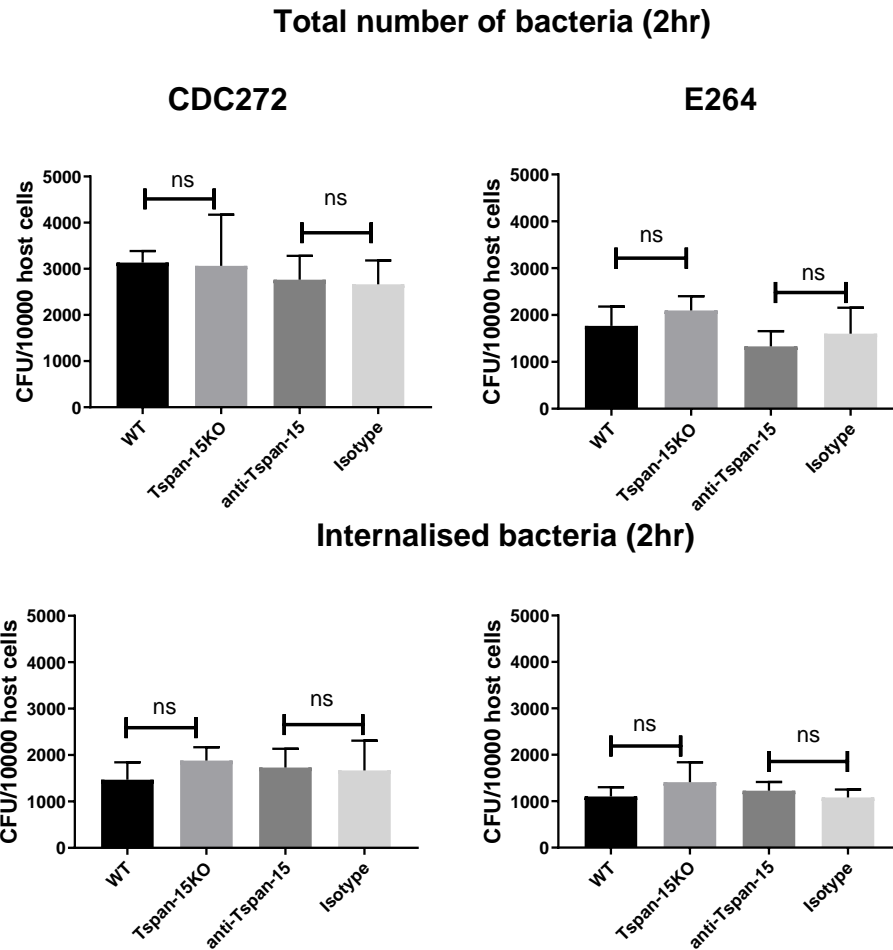


**Figure 6.22 Effect of Tspan-15KO and anti-Tspan-15 antibody on *B. thailandensis* infection in A549 cells.**

A549 cells were pre-treated with anti-Tspan-15 and JC1 for 1hr, and then WT, Tspan-15KO and A549 treated with antibody were infected for 2hr, as described in **section 2.2.8**. Bars show the total bacterial infection and/or internalised bacteria per 10000 cells for A549 cells infected by two bacterial strains, CDC272 and E264. The effects of different treatments were tested by unpaired t-test, where ns=non-significant. The results are the means ( $\pm$  SEM) of 3 independent experiments each performed in 4 technical replicates.

#### 6.3.5.4 Role of Tspan-15 on MGC formation induced by *B. thailandensis*

These experiments were performed to investigate the effect of anti-Tspan-15 antibody and Tspan-15KO on MGC formation and the number of nuclei per MGC. To do this, the WT and Tspan-15KO A549 cells were seeded in 96 wells plates. Some WT A549 cells were treated with the anti-Tspan-15 antibody for 1hr, and then the cells were washed. The WT and Tspan-15KO A549 cells were infected with bacteria for 2hr, and then washed and incubated with DMEM containing amikacin and kanamycin antibiotics for 16hr. The fusion index was quantified relative to uninfected cells per field of view.

MGCs were defined as cells containing 3 or more nuclei. MGC formation and nuclei per MGC were significantly increased with Tspan-15KO A549 cells when compared with WT A549 cells infected by both *B. thailandensis* strains (Fig 6.23). Data also showed that anti-Tspan-15 antibody has no effect on MGC formation in WT A549 cells when compared with isotype control for both *B. thailandensis* strains, and has no effect on the number of nuclei per MGC (Fig 6.23).

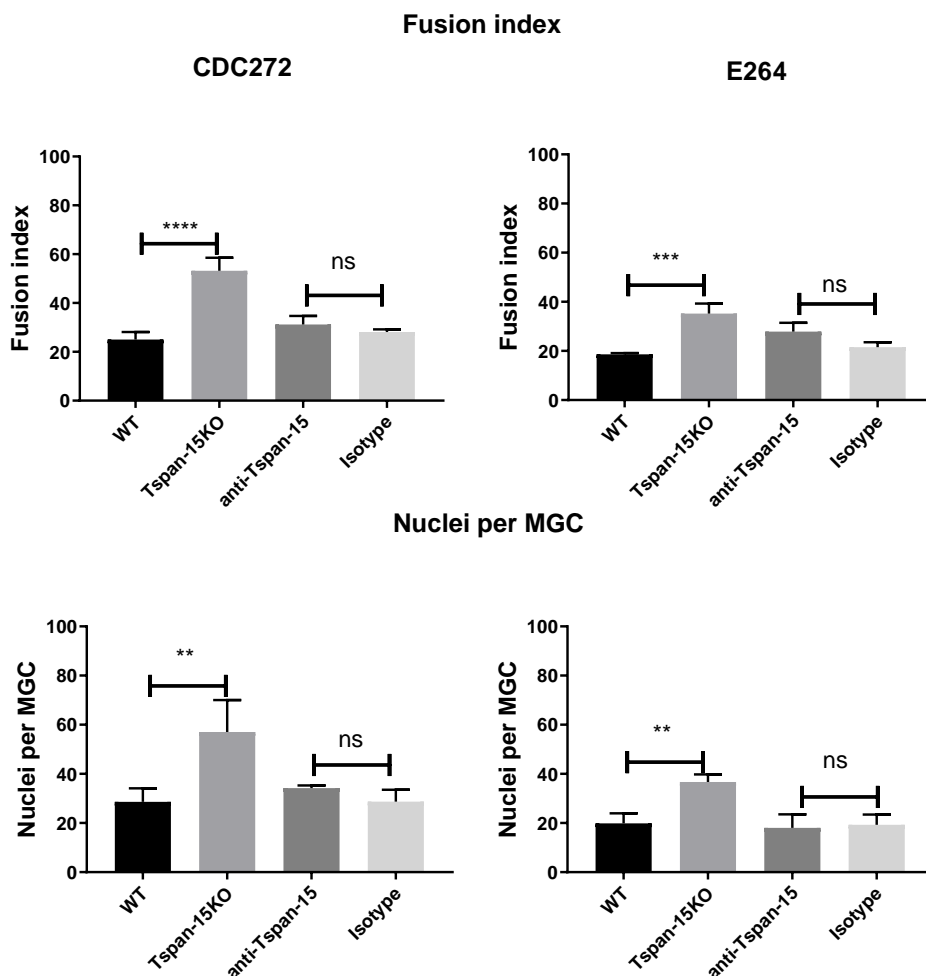


**Figure 6.23 Effect of Tspan-15KO and anti-Tspan-15 antibody on MGC formation induced by both *B. thailandensis* strains.**

A549 cells were infected by *B. thailandensis*, as described in section 2.2.8. Bars show the fusion index and the number of nuclei per MGC in A549 cells infected by two *B. thailandensis* strains. The significance of differences between uninfected and infected cells was measured by t-test where \*\* p < 0.01; \*\*\* p < 0.001; \*\*\*\* p < 0.0001 significant; ns = non-significant. The results are the means ( $\pm$  SEM) of 3 independent experiments each performed in 4 technical replicates.

## 6.4 Discussion

### 6.4.1 CD9 negatively regulates MGC formation in response to *B. thailandensis* infection

This section aimed to confirm that CD9 has no effect on the total number of bacteria or internalised bacteria, and has a negative role in MGC formation induced by *B. thailandensis*. Results showed that CD9KD and KO have no effect on infection with both strains of *B. thailandensis* (**Fig 6.3** and **Fig 6.13**). These findings are in agreement with other data from members in our laboratory: CD9KO in mouse macrophages had no effect on *B. thailandensis* infection (Elgawidi, 2016). In contrast, a previous PhD student from University of Sheffield has shown that CD9KO in mouse macrophages has an important effect on *Salmonella* infection (Ali, 2016). Furthermore, it has been observed that CD9 is involved in adhesion of several types of bacteria to human epithelial cell lines (Green *et al.*, 2011). It seems that CD9 may have no effect on *B. thailandensis* infection, but could contribute to other bacterial infections.

Both KD and KO of CD9 in A549 cells increased the fusion index compared with WT A549 and increased the number of nuclei per MGC induced by *B. thailandensis* CDC272, but not E264 (**Fig 6.4** and **Fig 6.14**). It seems that CD9 has a negative effect on MGC formation and the number of nuclei per MGC. Our data were supported by a member of our laboratory (Elgawidi, 2016) who also found that *B. thailandensis* increased MGC formation in the mouse CD9KO bone marrow-derived macrophages when compared to WT.

### 6.4.2 Tspan-2 and Tspan-13 play a role in MGC formation and *B. thailandensis* infection

The aim of this section was to investigate the effects of Tspan-2KD and Tspan-13KD on *B. thailandensis* infection. In **sections 6.3.2.3** and **section 6.3.2.5**, data showed that Tspan-2KD and Tspan-13KD could reduce *B. thailandensis* infection of A549 cells (**Fig 6.6** and **Fig 6.8**). In **section 5.5.4.2** and **section 5.5.4.4**, data indicated that anti-Tspan-13 and anti-Tspan-2 antibodies decreased the total bacterial infection of *B. thailandensis* and internalised bacteria after 2hr of infection. To the best of our knowledge, this

study is the first to observe that these two Tspans are implicated in *B. thailandensis* infection.

We observed that Tspan-2 also positively regulates MGC formation induced by *B. thailandensis* (**Fig 6.8**). Tspan-2 has a similar sequence to CD9 and CD81, which are involved in MGC formation (Yaseen *et al.*, 2017). It has been found that Tspan-2 could interact with CD44, which has a positive role in cell fusion (Sterling *et al.*, 1998). Tspan-2 is also a partner protein of MT1-MMP (Sterling *et al.*, 1998). This interaction could cause the cell membrane of neighbour macrophages to fuse (Weiguo *et al.*, 2006). In addition, Arndt *et al.* found that Tspan-2 could induce the formation of cellular protrusions in epithelial cells (Arndt *et al.*, 2015). These protrusions could be involved in cellular fusion (Sung and Weaver, 2011).

There are only a limited number of publications on Tspan-13 function. It is hard to clarify the specific role of Tspan-13 in MGC formation induced by *B. thailandensis* infection. However, Iwai *et al.* observed that Tspan-13 is involved in cell fusion in bone marrow induced by RANKL (Iwai *et al.*, 2007). Subsequently, the same scientific team also described that Tspan-13KD could induce osteoclastogenesis and MGC formation in RAW264 mouse macrophages (Iwai *et al.*, 2007). These findings might be inconsistent with our findings regarding the role of Tspan-13 in MGC formation. However, Iwai *et al.* used different stimulation factors and cell lines.

#### 6.4.3 Effect of ADAM10KD and KO on *B. thailandensis* infection and MGC formation in A549 cells

ADAM10 has several functions: the regulation of cell development, cell adhesion, cell fusion and bacterial infection (Dreymueller *et al.*, 2012, Matthews *et al.*, 2017). In this section, the aim was to investigate if ADAM10 has a role in *B. thailandensis* infection or MGC formation.

In **section 6.3.2.6** and **section 6.3.4.1**, data shows that ADAM10KD and KO have no effect on *B. thailandensis* infection. It seems that ADAM10 is not required for *B. thailandensis* infection but is required for other bacteria species. For example, it has been observed that ADAM10 is implicated in *S. aureus* and *P. aeruginosa* infection (Hassan and Nelson, 2002).

In **section 6.3.2.7** and **section 6.3.4.2**, findings show that ADAM10KD in A549 cells significantly increased MGC formation, while ADAM10KO had no effect on MGC formation and number of nuclei. These results might be explained by the minor role of ADAM10 with no direct impact on MGC formation. It has been observed that ADAM10 interacts with Tspan-5, known to be involved in MGC formation (Reyat *et al.*, 2017). Furthermore, ADAM10KO might cause a reduction or enhancement of the expression of other Tspans, which are involved in MGC formation. Other proteins might compensate for ADAM10 when it is absent from the cells for many passages (KO) but this might not occur when the protein is only temporarily downregulated (KD).

#### 6.4.4 Tspan-15KO enhances MGC formation

Tspan-15 is a member of an evolutionarily conserved sub-family of Tspans, the TspanC8 which includes Tspan-5, Tspan-10, Tspan-14, Tspan-15, Tspan-17, and Tspan-33. ADAM10 can interact with the TspanC8 sub-family and can be regulated in particular by Tspan-15. Tspan-15 can regulate many Tspans and Tspan-partner proteins (Haining *et al.*, 2012, Jouannet *et al.*, 2016).

Here, we investigated the roles of Tspan-15 in infection with *B. thailandensis* and the resulting MGC formation in lung epithelial cells. Here, I have shown that the protein level of Tspan-15 did not change after infection with either the fusogenic or the non-fusogenic strain E264- $\Delta$ tssK (**Fig 6.21**). We also observed that anti-Tspan-15 antibody has no effect on *B. thailandensis* infection and MGC formation (**Figs 6.22 and 6.23**). In **section 6.3.5.1**, data shows that Tspan-15KO can reduce the surface expression of ADAM10 and CD9 (**Fig 6.20**). Interestingly, we found that Tspan-15KO increased MGC formation, and had a slight effect on *B. thailandensis* infection. These findings could suggest that Tspan-15 has no direct role in MGC formation or *B. thailandensis* infection. However, other effects of Tspan-15KO, such as a negative effect on cell surface expression of other proteins or activation of some proinflammatory responses, could affect MGC formation and *B. thailandensis* infection. These findings are supported by Jouannet *et al.* who have shown the negative effect of Tspan-15KO on ADAM10 cell surface expression (Jouannet *et al.*, 2016). For example, Weiss found that ADAM10

mediated shedding of some cell surface proteins, which could be promoted by Tspan-15 (Weiss, 2018). They also found Tspan-15 could activate nuclear factor- $\kappa$ B (NF- $\kappa$ B). It is known that NF- $\kappa$ B is important in proinflammatory responses to *B. thailandensis* infection (Wiersinga, 2017). However, these results could give us an interesting question for future experiments.

## Chapter 7 General discussion

### 7.1 Summary

Melioidosis is a serious infectious disease caused by *B. pseudomallei*. This bacterium is closely related to *B. thailandensis* (Christoph *et al.*, 2009). They provoke the same immune responses and have the same mechanism of infection (Chen *et al.*, 2006, Reginsson *et al.*, 2012, Lertpatanasuwan *et al.*, 1999, Brett *et al.*, 1997). Recently, it was observed that *B. thailandensis* E555 is a very good surrogate for *B. pseudomallei* because it has similar responses to the intracellular environment during the infection of the J774.1 mouse macrophage cell line (Kovacs-Simon *et al.*, 2019). MGC formation is a histopathological feature of melioidosis (Wong *et al.*, 1995, Hsu, 2012). MGC formation appears to aid bacterial spreading to other cells while minimizing exposure to the host immune system (Wong *et al.*, 1995). However, the specific role of MGC formation in bacterial pathogenesis is still not fully understood.

As explained in **chapter 1**, Tspan molecules are a superfamily of membrane proteins that coordinate several membrane-associated functions such as trafficking, adhesion and bacterial infection (Monk and Partridge, 2012). Tspans have also been implicated in many cell fusion processes, including myoblast fusion (Charrin *et al.*, 2013, Hemler, 2001), virus-induced cell fusion (Fukudome *et al.*, 1992, Gordón-Alonso *et al.*, 2006, Menelaos *et al.*, 2014), sperm-egg fusion (Le Naour *et al.*, 2000, Rubinstein *et al.*, 2006, Jankovičová *et al.*, 2015), and macrophage and monocyte fusion during MGC formation (Takeda *et al.*, 2003, Ishii *et al.*, 2006, Parthasarathy *et al.*, 2009, Hulme *et al.*, 2014). Another role of Tspans is in bacterial infection. For example, Hassuna *et al.* have demonstrated the role of CD9 and CD81 in *Salmonella* infection (Hassuna *et al.*, 2017). Ventress *et al.* have demonstrated that CD9 has a role in *S. aureus* infection in keratinocyte cells (Ventress *et al.*, 2016). Green *et al.* have also described a role for CD9, CD151 and CD63 in the infection of human epithelial cells by several types of bacteria, including *Neisseria* sp, *E. coli* and *Streptococcus pneumoniae* (Green *et al.*, 2011). Our research team have observed that the CD9KO can affect the early stages of

bacterial infection (30min to 60min) by *B. thailandensis* (Elgawidi, 2016). However, antibodies that bind Tspans have no effect on *B. thailandensis* infection in RAW264 and J774.2 cells after 2hr of infection.

**In chapter 3**, it was shown that a fusogenic strain of *B. thailandensis* could induce not only a mouse macrophage cell line but also A549 cells to form MGC. These results were in agreement with other researchers who have shown that *B. thailandensis* can induce different cell lines to form MGC (Boddey *et al.*, 2007, Schwarz *et al.*, 2014, Chiang *et al.*, 2015, Michevaviteva *et al.*, 2017). GFP and mCherry tags on MGC formation have no effect on MGC when expressed in *B. thailandensis*. A previous PhD student from University of Sheffield has shown that a mutant (E264- $\Delta$ tssK) of *B. thailandensis* cannot promote infected cells to form MGC in RAW264 cells (Hall, 2016). Here, it was also found that a mutant of E264- $\Delta$ tssK, cannot induce MGC in either A549 or J774.2 cells despite causing a similar bacterial infection to the WT bacteria. It seems that mutant E264- $\Delta$ tssK is a suitable choice as a way of discriminating between changes in host cells caused by infection and changes that lead to MGC formation.

**In chapter 4**, it was hypothesised that Tspans and Tspan-partner proteins would have altered expression levels in response to *B. thailandensis* infection in J774.2 and A549 cells. It was also hypothesized that the expression of some innate immunity and cell signalling genes would also alter in response to bacterial infection. I found that most Tspans and Tspan-partners are highly expressed at the mRNA level in J774.2 and A549 cells. These findings are similar to many published studies. For example, Iwai and co-workers detected the expression of all 12 Tspan genes studied in the mouse macrophage cell line RAW264 (Iwai *et al.*, 2007). Haining and colleagues also tested A549 cells and found all of the TspanC8 subfamily were expressed (Haining *et al.*, 2012). Mélanie *et al.* has also detected CD151 expression in A549 cells (Mélanie *et al.*, 2010). The next step was to investigate changes in all Tspans at the mRNA level in response to infection by both *B. thailandensis* strains in both cell lines. To select which Tspans are involved in MGC formation and not simply in *B. thailandensis* infection, both cell lines were infected by fusogenic WT and non-fusogenic *B. thailandensis* E264- $\Delta$ tssK. After 18 hours of

infection it was observed that mRNA levels of Tspan-2 and Tspan-13 increased significantly with WT fusogenic strains but not with E264- $\Delta$ tssK, while Tspan-5, CD81, CD9 decreased significantly only with WT.

The changes to 4 candidate Tspans in MGC formation were further examined at the protein level using flow cytometry to detect protein expression (antibodies to Tspan-5 are not currently available). Data showed that expression of Tspan-2 and Tspan-13 increased in response to fusogenic *B. thailandensis* strains compared with E264- $\Delta$ tssK, while CD9 and CD81 were not changed at protein level after 18hr infection compared with the non-fusogenic strain. Theoretically, the size of fused cells could be too large to flow through the cytometer nozzles, and so these cells would be absent from the analysis. An alternative method for quantifying protein expression in cells could involve the use of western blotting. Another explanation is that the wrong time points were chosen. Ideally, more experiments would be performed to investigate other earlier or later time-points. Only cell surface protein levels were investigated and so we could use permeabilisation to detect intracellular proteins in flow cytometry, or western blot to detect total protein expression.

Tspan-partner proteins expression were also examined using the same criteria. Our findings showed that only 3 Tspan-partners changed mRNA levels following WT *B. thailandensis* infection with WT but not with the mutant. CD172 $\alpha$  and ADAM10 decreased, and CD98 increased in expression. Studies have reported that several Tspan-partner proteins are involved in MGC formation and bacterial infection including CD98, CD44 and DC-STAMP (Ozge *et al.*, 2009, Yagi *et al.*, 2005, Martinez *et al.*, 2009, Weiguo *et al.*, 2006). These studies were in agreement with our findings, suggesting no role of CD44 or DC-STAMP and a positive role of CD98 in MGC formation. Our data are also supported by Paola *et al* who have shown that CD98 expression is increased by activating integrin during fusion of the human placental trophoblast cell line BeWo (Paola *et al.*, 2007). Furthermore, our data is in agreement with Verrier *et al* who observed that ADAM10 is involved in cell fusion in the MG63 osteosarcoma cell line (Verrier *et al.*, 2004). Interestingly, our results were not supported by Acharya and co-workers who found that

CD172 $\alpha$  expression at the mRNA level increased during fusion of malignant cells (Gautam and Acharya, 2014).

In **chapter 5**, it was shown that binding of antibodies to cell surface CD9 and ADAM10 can enhance MGC formation, whereas antibodies against Tspan-2 and Tspan-13 can inhibit MGC formation. CD98 antibodies also reduced formation of MGC. Many studies are in agreement with these findings, for example, Suparak and co-researchers have shown that using anti-CD98 antibody can affect cell fusion in U937 human macrophages (Suparak *et al.*, 2011), while a previous PhD student from University of Sheffield has shown that anti-CD9 and anti-CD81 antibodies enhance MGC formation induced by *B. thailandensis* in J774.2 mouse macrophages (Elgawidi, 2016). Furthermore, 8005 peptide from CD9EC2 was tested. The results showed that peptide 8005 reduces *B. thailandensis* infection of A549 cells. This peptide has the same effect on other bacterial infections, such as *S. aureus* and *P. aeruginosa* (unpublished data Rahaf Issa) (Alrahimi, 2017). Anti-Tspan-2 and Tspan-13 antibody treatment before and after infection can inhibit MGC formation, as well as reduce the total bacterial infection. To the best of our knowledge, there are no previous studies that agree or disagree with these findings.

As shown in **chapter 4**, there were no significant differences in protein levels of ADAM10, CD172 $\alpha$  and CD98 following *B. thailandensis* infection of A549 cells, relative to uninfected cells. However, antibodies against ADAM10 and CD98 molecules were shown to affect MGC formation. The progression or suppression of MGC formation may not be dependent on simply the expression levels of these surface molecules. To the best of our knowledge, this is the first investigation to notice that host surface molecules play a role in MGC formation induced by *B. thailandensis* in A549 cells. It is possible that Tspans and Tspan-partner proteins could facilitate the attachment of cells to each other, bringing their membrane into close contact, during infection with *B. thailandensis*. It also seems that *B. thailandensis* could favour MGC formation by modulating the protein expression and/or activity of such molecules.

In **chapter 6**, KD of Tspan-2 and Tspan-13 confirmed the positive role of these Tspans in MGC formation. The KD and KO of CD9 and ADAM10 confirmed their negative roles in MGC formation induced by *B. thailandensis*. In addition, Tspan-15KO A549 cells have been used in this study. The findings showed that the KO of Tspan-15 in A549 cells increased MGC formation induced by *B. thailandensis*, which could be due to changes in CD9 and ADAM10.

Tspan-2 is a partner to CD9 and CD81 (Terada *et al.*, 2002, Yaseen *et al.*, 2017), which are both involved in MGC formation, and is also a partner to CD44 (Otsubo *et al.*, 2014). CD44 is important in intracellular replication of *L. monocytogenes* in bone marrow-derived macrophages (Eriksson *et al.*, 2003). This close association of Tspan-2 with CD9 may have promoted *B. thailandensis* uptake, perhaps by a cooperative role of Tspan-2 with CD44, which is up-regulated upon infection (Eriksson *et al.*, 2003).

We observed that Tspan-13 has a role in both infection and MGC formation. There are only limited publications that describe the role of Tspan-13 in MGC formation, so it is hard to explain the specific positive role of Tspan-13 in MGC formation. However, Iwai *et al.* have described a negative role of Tspan-13 in osteoclastogenesis induced by RANKL pathway in RAW264. In contrast, a study has described Tspan-13 as being involved positively in apoptosis in hTERT from human osteosarcoma cells (Jaiswal *et al.*, 2018).

Similar to the results presented here, CD9KO has previously been shown to enhance MGC formation (Takeda *et al.*, 2003). Similarly, one of our lab members found that CD9KO caused enhancement of MGC formation in mouse bone marrow-derived macrophages infected with *B. thailandensis* (Elgawidi, 2016). However, Miyado *et al.* made different findings. They found CD9KO in mice eggs prevented fusion with sperm (Miyado *et al.*, 2000). Thus, CD9 might be involved in several different processes with different functions.

It is known that ADAM10 is a partner to several Tspans, including CD9 and CD81 (Haining *et al.*, 2012). ADAM10KO appeared not to significantly enhance fusion, whereas ADAM10KD and antibody treatment appeared to cause enhancement of MGC formation induced by *B. thailandensis*. In

addition, as we found in **chapter 6**, Tspan-15KO causes an enhancement of MGC formation and reduces ADAM10 expression at the cell surface by 50%. That could explain the minor role of ADAM10 in MGC formation induced by *B. thailandensis*. However, these enhancements need further experiments. Moreover, a study has shown the interaction of ADAM10 with Tspan-5, which is involved in cell fusion (Iwai *et al.*, 2007, Reyat *et al.*, 2017). It was supposed that ADAM10 might play a minor role in MGC formation. No study has yet described a role for ADAM10 in *B. thailandensis* infection, but there is evidence of involvement in other bacterial infections. For example, ADAM10 acts as a receptor for *S. aureus* and *P. aeruginosa* (Hassan and Nelson, 2002, Ichiro *et al.*, 2011, Wang *et al.*, 2012).

## 7.2 Limitations

There are several limitations to this study, partly due to limited funding and time. Not all anti-Tspan antibodies are commercially available, and Tspan-5 could not be investigated fully. The other point is that only surface protein expression was examined instead of total cellular protein expression, which is a problem because some Tspans act intracellularly (e.g. CD63, CD9 and CD81) (Monk and Partridge, 2012). Moreover, the cells that underwent KO/KD approaches had not been investigated in regard to other functional activity such as migration, adhesion, trafficking and cell proliferation which could help to explain another role of Tspan molecules in MGC formation. The KO/KD approach was carried out for selected Tspans/Tspan-partners not for all candidates because of limited time and funding. No *in vivo* studies were included, that would be useful to fully understand the role of these proteins in MGC formation in response to bacterial infection using antibodies and peptides. However, it might be addressed in future work. Finally, the main pathogen of melioidosis, which is *B. pseudomallei*, could not be used in this study, because it is classified as hazard group 3 and we have no permission to use this pathogen in our lab.

## 7.3 Conclusions

It can be concluded from this work that:

- CD9 and CD81 are negative regulators of MGC formation
- 8005 peptide from EC2 of CD9 can significantly reduce *B. thailandensis* infection.
- Tspan-5 may also act as a negative regulator of fusion
- Tspan-2 and Tspan-13 are required for total bacterial infection and may also act as positive regulators of MGC formation
- Tspan partner proteins ADAM10 and CD98 may act as regulators of fusion.

## 7.4 Future work

Ultimately, it is highly recommended to investigate the role of selected Tspans and Tspan-partners *in vivo*, to test whether they have some responses to *B. thailandensis* infection, and the main causative agent of melioidosis, *B. pseudomallei*. It is also recommended to investigate these selected Tspans with other bacterial and fungal infections. Furthermore, we highly recommended testing peptide 8005 on *B. pseudomallei* infections of different types of cell lines and *in vivo*. In addition, we can synthesise other peptides from other selected Tspans or its partners and examine them with *B. thailandensis* or other bacterial infections. Finally, we can advise the use of peptides or antibodies against these selected Tspans and partner as treatments to avoid the *B. pseudomallei* infection in its endemic area. However, it needs more experimental investigations for further validation and to confirm our suggestions.

## References

- ADLER, B. 2011. Strategies for intracellular survival of *Burkholderia pseudomallei*. *Frontiers in Microbiology*, 2, 170.
- ADLER, N. R. L., STEVENS, M. P., DEAN, R. E., SAINT, R. J., PANKHANIA, D., PRIOR, J. L., ATKINS, T. P., KESSLER, B., NITHICHANON, A. & LERTMEMONGKOLCHAI, G. 2015. Systematic mutagenesis of genes encoding predicted autotransported proteins of *Burkholderia pseudomallei* identifies factors mediating virulence in mice, net intracellular replication and a novel protein conferring serum resistance. *PLoS One*, 10, e0121271.
- ALI, F. 2016. Investigating the role of tetraspanin proteins in *Salmonella* infection, University of Sheffield. Department of Molecular biology and Biotechnology. Ph.D., University of Sheffield
- ALRAHIMI, S. J. 2017. The Role of Tetraspanins and their Peptide Fragments in *Pseudomonas aeruginosa* Adherence to Human Cells. University of Sheffield, Department of Infection, Immunity & Cardiovascular Disease. Ph.D., University of Sheffield.
- AMY, D., ERIK-JAN, K., BROWN, A. N., PHILIPP, P. & CAPLAN, M. J. 2003. The tetraspanin CD63 enhances the internalization of the H,K-ATPase beta-subunit. *National Academy of Sciences of the United States of America* 100, 15560-15565.
- ANDERSON, J. M. 2000. Multinucleated giant cells. *Current Opinion in Hematology*, 7, 40-47.
- ANDREU, Z. & YÁÑEZ-MÓ, M. 2014. Tetraspanins in extracellular vesicle formation and function. *Frontiers in Immunology*, 5, 442.
- ANTONELLI, A., DI MAGGIO, S., REJMAN, J., SANVITO, F., ROSSI, A., CATUCCI, A., GORZANELLI, A., BRAGONZI, A., BIANCHI, M. E. & RAUCCI, A. 2017. The shedding-derived soluble receptor for advanced glycation endproducts sustains inflammation during acute *Pseudomonas aeruginosa* lung infection. *Biochimica et Biophysica Acta (BBA)-General Subjects*, 1861, 354-364.
- ANTUNES, A. L. S., TRENTIN, D. S., BONFANTI, J. W., PINTO, C. C. F., PEREZ, L. R. R., MACEDO, A. J. & BARTH, A. L. 2010. Application of a feasible method for determination of biofilm antimicrobial susceptibility in staphylococci. *Apmis*, 118, 873-877.
- ARENCIBIA, J. M., MARTÍN, S., PÉREZ-RODRÍGUEZ, F. J. & BONNIN, A. 2009. Gene expression profiling reveals overexpression of TSPAN13 in prostate cancer. *International Journal of Oncology*, 34, 457-463.
- ARNDT, G., NOUHAD, B., PETRA, B., ANNA, H., FRANZISKA, W., LUISE, A. & ULRICH, S. J. M. S. B. 2015. Phospho-tyrosine dependent protein-protein interaction network. *Molecular Systems Biology* 11, 794.
- ASHDOWN, L. 1979. An improved screening technique for isolation of *Pseudomonas pseudomallei* from clinical specimens. *Pathology*, 11, 293-297.
- ATKINS, T., PRIOR, R., MACK, K., RUSSELL, P., NELSON, M., PRIOR, J., ELLIS, J., OYSTON, P. C., DOUGAN, G. & TITBALL, R. W. 2002. Characterisation of an acapsular mutant of *Burkholderia pseudomallei* identified by signature tagged mutagenesis. *Journal of Medical Microbiology*, 51, 539-553.
- AUBIN, J. E. & BONNELYE, E. 2000. Osteoprotegerin and its ligand: a new paradigm for regulation of osteoclastogenesis and bone resorption. *Osteoporosis International*, 11, 905-913.
- BAEK, J. M., KIM, J.-Y., JUNG, Y., MOON, S.-H., CHOI, M. K., KIM, S. H., LEE, M. S., KIM, I. & OH, J. 2015. Mollugin from *Rubea cordifolia* suppresses receptor activator of nuclear factor- $\kappa$ B ligand-induced osteoclastogenesis and bone resorbing activity in vitro and prevents lipopolysaccharide-induced bone loss in vivo. *Phytomedicine*, 22, 27-35.

- BALEATO, R. M., GUTHRIE, P. L., GUBLER, M.-C., ASHMAN, L. K. & ROSELLI, S. 2008. Deletion of CD151 results in a strain-dependent glomerular disease due to severe alterations of the glomerular basement membrane. *The American journal of pathology*, 173, 927-937.
- BARAL, P. & UTAISINCHAROEN, P. 2012. Involvement of signal regulatory protein  $\alpha$ , a negative regulator of Toll-like receptor signaling, in impairing the MyD88-independent pathway and intracellular killing of *Burkholderia pseudomallei* -infected mouse macrophages. *Infection and immunity*, 80, 4223-4231.
- BARNES, J. L. & KETHEESAN, N. 2007. Development of protective immunity in a murine model of melioidosis is influenced by the source of *Burkholderia pseudomallei* antigens. *Immunology and Cell Biology*, 85, 551-557.
- BARREIRO, O., YÁÑEZ-MÓ, M., SALA-VALDÉS, M., GUTIÉRREZ-LÓPEZ, M. D., OVALLE, S., HIGGINBOTTOM, A., MONK, P. N., CABAÑAS, C. & SÁNCHEZ-MADRID, F. 2005. Endothelial tetraspanin microdomains regulate leukocyte firm adhesion during extravasation. *Blood*, 105, 2852-2861.
- BARRETT, A. R., KANG, Y., INAMASU, K. S., SON, M. S., VUKOVICH, J. M. & HOANG, T. T. 2008. Genetic tools for allelic replacement in *Burkholderia* species. *Applied and Environmental Microbiology*, 74, 4498-4508.
- BEARE, A., STOCKINGER, H., ZOLA, H. & NICHOLSON, I. 2008. Monoclonal antibodies to human cell surface antigens. *Current Protocols in Immunology*, 80, A. 4A. 1-A. 4A. 73.
- BEATTY, W. L. 2006. Trafficking from CD63-positive late endocytic multivesicular bodies is essential for intracellular development of *Chlamydia trachomatis*. *Journal of Cell Science*, 119, 350-359.
- BEATTY, W. L., J INFECTION & IMMUNITY 2008. Late endocytic multivesicular bodies intersect the chlamydial inclusion in the absence of CD63. 76, 2872-2881.
- BENANTI, E. L., NGUYEN, C. M. & WELCH, M. D. 2015. Virulent *Burkholderia* species mimic host actin polymerases to drive actin-based motility. *Cell*, 161, 348-360.
- BERDITCHEVSKI, F. 2001. Complexes of tetraspanins with integrins: more than meets the eye. *Journal of Cell Science*, 114, 4143-4151.
- BLAKE, D. J., MARTISZUS, J. D., LONE, T. H. & FENSTER, S. D. 2018. Ablation of the CD9 receptor in human lung cancer cells using CRISPR/Cas alters migration to chemoattractants including IL-16. *Cytokine*, 111, 567-570.
- BIERNE, H., HAMON, M. & COSSART, P. 2012. Epigenetics and bacterial infections. *Cold Spring Harbor perspectives in medicine*, 2, a010272.
- BINGLE, L. E., BAILEY, C. M. & PALLEN, M. J. 2008. Type VI secretion: a beginner's guide. *Current Opinion in Microbiology*, 11, 3-8.
- BISHOP, B. L., DUNCAN, M. J., JEONGMIN, S., GUOJIE, L., DAVID, Z. & ABRAHAM, S. N. 2007. Cyclic AMP-regulated exocytosis of *Escherichia coli* from infected bladder epithelial cells. *Nature Medicine*, 13, 625-630.
- BO, X., GE, Z., SHIU-YUNG, C., ELLEN, S., XIANG-PENG, K., XUE-RU, W., TUNG-TIEN, S. & COSTELLO, C. E. 2006. Distinct glycan structures of uroplakins Ia and Ib: structural basis for the selective binding of FimH adhesin to uroplakin Ia. *Journal of Biological Chemistry*, 281, 14644-53.
- BODDEY, J. A., DAY, C. J., FLEGG, C. P., ULRICH, R. L., STEPHENS, S. R., BEACHAM, I. R., MORRISON, N. A. & PEAK, I. R. 2007. The bacterial gene *lfpA* influences the potent induction of calcitonin receptor and osteoclast-related genes in *Burkholderia pseudomallei* -induced TRAP-positive multinucleated giant cells. *Cellular microbiology*, 9, 514-531.
- BORISOVA, M., YONG, S., BUNTRU, A., WÖRNER, S., ZIEGLER, W. H. & HAUCK, C. R. 2013. Integrin-mediated internalization of *Staphylococcus aureus* does not require vinculin. *Cell Biology*, 14, 2-2.

- BOUCHEIX, C. & RUBINSTEIN, E. 2001. Tetraspanins. *Cellular and Molecular Life Sciences CMLS*, 58, 1189-1205.
- BOUKERB, A. M., MARTI, R. & COURNOYER, B. 2015. Genome Sequences of Three Strains of the *Pseudomonas aeruginosa* PA7 Clade. *Genome Announc*, 3.
- BOYLE, W. J., SIMONET, W. S. & LACEY, D. L. 2003. Osteoclast differentiation and activation. *Nature Medicine*, 423, 337.
- BREITBACH, K., ROTTNER, K., KLOCKE, S., ROHDE, M., JENZORA, A., WEHLAND, J. & STEINMETZ, I. 2003. Actin-based motility of *Burkholderia pseudomallei* involves the Arp 2/3 complex, but not N-WASP and Ena/VASP proteins. *Cellular microbiology*, 5, 385-393.
- BRENNAN, C. W., VERHAAK, R. G., MCKENNA, A., CAMPOS, B., NOUSHMEHR, H., SALAMA, S. R., ZHENG, S., CHAKRAVARTY, D., SANBORN, J. Z. & BERMAN, S. H. 2013. The somatic genomic landscape of glioblastoma. *Cell*, 155, 462-477.
- BRETT, P., DESHAZER, D. & WOODS, D. 1997. Characterization of *Burkholderia pseudomallei* and *Burkholderia pseudomallei* -like strains. *Epidemiology & Infection*, 118, 137-148.
- BRETT, P. J., DESHAZER, D. & WOODS, D. E. 1998. *Burkholderia thailandensis* sp. nov., a *Burkholderia pseudomallei* -like species. *International Journal of Systematic Bacteriology*, 48, 317-320.
- BRETT, P. J. & WOODS, D. E. 2000. Pathogenesis of and immunity to melioidosis. *Acta Trop*, 74, 201-10.
- BROWN, M. 2011. Inception of the metastatic phenotype by macrophage-cancer cell fusion. Ph.D., Utrecht university.
- BROWN, N. F., BODDEY, J. A., FLEGG, C. P. & BEACHAM, I. R. 2002. Adherence of *Burkholderia pseudomallei* cells to cultured human epithelial cell lines is regulated by growth temperature. *Infection and Immunity*, 70, 974-980.
- BURTICK, M. N., BRETT, P. J., HARDING, S. V., NGUGI, S. A., RIBOT, W. J., CHANTRATITA, N., SCORPIO, A., MILNE, T. S., DEAN, R. E. & FRITZ, D. L. 2011. The cluster 1 type VI secretion system is a major virulence determinant in *Burkholderia pseudomallei*. *Infection and Immunity*, 79, 1512-1525.
- BURTICK, M. N., BRETT, P. J., NAIR, V., WARAWA, J. M., WOODS, D. E. & GHERARDINI, F. C. 2008. *Burkholderia pseudomallei* type III secretion system mutants exhibit delayed vacuolar escape phenotypes in RAW 264.7 murine macrophages. *Infection and Immunity*, 76, 2991-3000.
- BURTICK, M. N., BRETT, P. J. & WOODS, D. E. 2002. Molecular and physical characterization of *Burkholderia mallei* O antigens. *Journal of Bacteriology*, 184, 849-852.
- BURTICK, M. N., DESHAZER, D., NAIR, V., GHERARDINI, F. C. & BRETT, P. J. 2010. *Burkholderia mallei* cluster 1 type VI secretion mutants exhibit growth and actin polymerization defects in RAW 264.7 murine macrophages. *Infection and immunity*, 78, 88-99.
- CAI, S., BULUS, N., FONSECA-SIESSER, P. M., CHEN, D., HANKS, S. K., POZZI, A. & ZENT, R. 2005. CD98 modulates integrin  $\beta$ 1 function in polarized epithelial cells. *Journal of Cell Science*, 118, 889-899.
- CAMPBELL, I. D. & GINSBERG, M. H. 2004. The talin-tail interaction places integrin activation on FERM ground. *Trends in Biochemical Sciences*, 29, 429-435.
- CANTOR, J. M. & GINSBERG, M. H. 2012. CD98 at the crossroads of adaptive immunity and cancer. *Journal of Cell Science*, 125, 1373-1382.
- CEBALLOS-OLVERA, I., SAHOO, M., MILLER, M. A., DEL BARRIO, L. & RE, F. 2011. Inflammasome-dependent pyroptosis and IL-18 protect against *Burkholderia pseudomallei* lung infection while IL-1 $\beta$  is deleterious. *PLoS Pathogens*, 7, e1002452.

- CHAIMOWITZ, N. S., DAE-JOONG, K., DEAN, L. M. & CONRAD, D. H. 2012. ADAM10 regulates transcription factor expression required for plasma cell function. *Plos One*, 7, e42694.
- CHAKRABORTY, A. K., PAWELEK, J., IKEDA, Y., MIYOSHI, E., KOLESNIKOVA, N., FUNASAKA, Y., ICHIHASHI, M. & TANIGUCHI, N. 2001. Fusion hybrids with macrophage and melanoma cells up-regulate N-acetylglucosaminyltransferase V, beta1-6 branching, and metastasis. *Cell Growth & Differentiation: the Molecular Biology Journal of the American Association for Cancer Research*, 12, 623-630.
- CHAN, K. G., CHEN, J. W., TEE, K. K., CHANG, C. Y., YIN, W. F. & CHAN, X. Y. 2015. Whole-Genome Analysis of Quorum-Sensing *Burkholderia* sp. Strain A9. *Genome Announc*, 3.
- CHANCHAMROEN, S., KEWCHAROENWONG, C., SUSANENGRAT, W., ATO, M. & LERTMEMONGKOLCHAI, G. 2009. Human polymorphonuclear neutrophil responses to *Burkholderia pseudomallei* in healthy and diabetic subjects. *Infection and Immunity*, 77, 456-463.
- CHARLES, J. F. & ALIPRANTIS, A. O. J. T. I. 2014. Osteoclasts: more than 'bone eaters'. *Molecular Medicine*, 20, 449-459.
- CHAROENSAP, J., UTAISINCHAROEN, P., ENGERING, A. & SIRISINHA, S. 2009. Differential intracellular fate of *Burkholderia pseudomallei* 844 and *Burkholderia thailandensis* UE5 in human monocyte-derived dendritic cells and macrophages. *BMC Immunology*, 10, 20.
- CHARRIN, S., JOUANNET, S., BOUCHEIX, C. & RUBINSTEIN, E. 2014. Tetraspanins at a glance. *Journal of Cell Science*, 127, 3641-3648.
- CHARRIN, S., LATIL, M., SOAVE, S., POLESSKAYA, A., CHRÉTIEN, F., BOUCHEIX, C. & RUBINSTEIN, E. 2013. Normal muscle regeneration requires tight control of muscle cell fusion by tetraspanins CD9 and CD81. *Nature Communications*, 4, 1674.
- CHARRIN, S., MANIÉ, S., OUALID, M., BILLARD, M., BOUCHEIX, C. & RUBINSTEIN, E. 2002. Differential stability of tetraspanin/tetraspanin interactions: role of palmitoylation. *FEBS Letters*, 516, 139-144.
- CHARRIN, S., LATIL, M., SOAVE, S., POLESSKAYA, A., CHRETIEN, F., BOUCHEIX, C. & RUBINSTEIN, E. 2013. Normal muscle regeneration requires tight control of muscle cell fusion by tetraspanins CD9 and CD81. *Nature Communications*, 4, 1674.
- CHEN, Y., HSIAO, Y., LIN, H., LIU, Y. & CHEN, Y. 2006. Tropical and travel-associated diseases. *J Trop Med Hyg*, 74, 345-347.
- CHEN, Y., WONG, J., SUN, G. W., LIU, Y., TAN, G. Y. G. & GAN, Y. H. 2011. Regulation of Type VI Secretion System during *Burkholderia pseudomallei* Infection. *Infection and Immunity*, 79, 3064-73.
- CHIANG, C.-Y., ULRICH, R. L., ULRICH, M. P., EATON, B., OJEDA, J. F., LANE, D. J., KOTA, K. P., KENNY, T. A., LADNER, J. T. & DICKSON, S. P. 2015. Characterization of the murine macrophage response to infection with virulent and avirulent *Burkholderia* species. *BMC microbiology*, 15, 259.
- CHIU, Y. H. & RITCHLIN, C. T. 2016. DC-STAMP: A key regulator in osteoclast differentiation. *Journal of Cellular Physiology*, 231, 2402-2407.
- CHRISTOPH, W., GÜNTER, D., PHILIPPE, R., JULIA, R. & DETLEV, S. 2009. *Burkholderia pseudomallei* misidentified by automated system. *Emerging Infectious Diseases*, 15, 1799-1801.
- CHUA, K., CHAN, Y. & GAN, Y. 2003. Flagella are virulence determinants of *Burkholderia pseudomallei*. *Infection and immunity*, 71, 1622-1629.
- CIANFANELLI, F. R., MONLEZUN, L. & COULTHURST, S. J. 2016. Aim, load, fire: the type VI secretion system, a bacterial nanoweapon. *Trends in Microbiology*, 24, 51-62.

- COBURN, B., SEKIROV, I. & FINLAY, B. B. 2007. Type III secretion systems and disease. *Clinical Microbiology Reviews*, 20, 535-549.
- COMOLLI, J. C., WAITE, L. L., MOSTOV, K. E. & ENGEL, J. N. 1999. Pili binding to asialo-GM1 on epithelial cells can mediate cytotoxicity or bacterial internalization by *Pseudomonas aeruginosa*. *Infection and Immunity*, 67, 3207-14.
- COSTA, T. R., FELISBERTO-RODRIGUES, C., MEIR, A., PREVOST, M. S., REDZEJ, A., TROKTER, M. & WAKSMAN, G. 2015. Secretion systems in Gram-negative bacteria: structural and mechanistic insights. *Nature Reviews Microbiology*, 13, 343-359.
- COTTER, S. E., SURANA, N. K. & GEME, J. W. S. 2005. Trimeric autotransporters: a distinct subfamily of autotransporter proteins. *Trends in Microbiology*, 13, 199-205.
- COULTHURST, S. 2019. The Type VI secretion system: a versatile bacterial weapon. 165, 503-515.
- CRIGHTON, D., WILKINSON, S. & RYAN, K. M. 2007. DRAM links autophagy to p53 and programmed cell death. *Autophagy*, 3, 72-74.
- CURRIE, B. J. 2003. Melioidosis: an important cause of pneumonia in residents of and travellers returned from endemic regions. *European Respiratory Journal*, 22, 542-550.
- CURRIE, B. J., DANCE, D. A. & CHENG, A. C. 2008. The global distribution of *Burkholderia pseudomallei* and melioidosis: an update. *Transactions of the Royal Society of Tropical Medicine and Hygiene*, 102, S1-S4.
- D'ELIA, R., SAINT, R., NEWSTEAD, S., CLARK, G. & ATKINS, H. 2017. Mitogen-activated protein kinases (MAPKs) are modulated during in vitro and in vivo infection with the intracellular bacterium *Burkholderia pseudomallei*. *European Journal of Clinical Microbiology & Infectious Diseases*, 36, 2147-2154.
- DANCE, D. 2014. Treatment and prophylaxis of melioidosis. *International Journal of Antimicrobial Agents*, 43, 310-318.
- DANCE, D. A. 2000. Melioidosis as an emerging global problem. *Acta Trop*, 74, 115-9.
- DAUTIN, N. & BERNSTEIN, H. D. 2007. Protein secretion in gram-negative bacteria via the autotransporter pathway\*. *Annu. Rev. Microbiol.*, 61, 89-112.
- DAVID, J., BELL, R. E. & CLARK, G. C. 2015. Mechanisms of Disease: Host-Pathogen Interactions between *Burkholderia* Species and Lung Epithelial Cells. *Frontiers in cellular and infection microbiology*, 5.
- DE CHASTELLIER, C. & BERCHE, P. 1994. Fate of *Listeria monocytogenes* in murine macrophages: evidence for simultaneous killing and survival of intracellular bacteria. *Infection and Immunity*, 62, 543-553.
- DE KIEVIT, T. R. & IGLEWSKI, B. H. 2000. Bacterial quorum sensing in pathogenic relationships. *Infection and immunity*, 68, 4839-4849.
- DEFIFE, K. M., JENNEY, C. R., MCNALLY, A. K., COLTON, E. & ANDERSON, J. M. 1997. Interleukin-13 induces human monocyte/macrophage fusion and macrophage mannose receptor expression. *The Journal of Immunology*, 158, 3385-3390.
- DELAGUILLAUMIE, A., LAGAUDRIERE-GESBERT, C., POPOFF, M. R. & CONJEAUD, H. 2002. Rho GTPases link cytoskeletal rearrangements and activation processes induced via the tetraspanin CD82 in T lymphocytes. *Journal of Cell Science*, 115, 433-43.
- DENG, Y. & WU, X. 2000. Peg3/Pw1 promotes p53-mediated apoptosis by inducing Bax translocation from cytosol to mitochondria. *Proceedings of the National Academy of Sciences*, 97, 12050-12055.
- DESALLE, R., MARES, R. & GARCIA-ESPAÑA, A. 2010. Evolution of cysteine patterns in the large extracellular loop of tetraspanins from animals, fungi,

- plants and single-celled eukaryotes. *Molecular Phylogenetics and Evolution*, 56, 486-491.
- DESHAZER, D., BRETT, P. J., BURTNICK, M. N. & WOODS, D. E. 1999. Molecular characterization of genetic loci required for secretion of exoproducts in *Burkholderia pseudomallei*. *Journal of Bacteriology*, 181, 4661-4664.
- DESHAZER, D., BRETT, P. J., CARLYON, R. & WOODS, D. E. 1997. Mutagenesis of *Burkholderia pseudomallei* with Tn5-OT182: isolation of motility mutants and molecular characterization of the flagellin structural gene. *Journal of Bacteriology*, 179, 2116-2125.
- DIRK-STEFFEN, S., PAMELA, K., MARTINA, S. L. & MARGOT, Z. L. J. 2004. CD44 variant isoforms associate with tetraspanins and EpCAM. *Exp Cell Res. Experimental Cell Research*, 297, 329-347.
- DOMINGUEZ-BELLO, M. G., COSTELLO, E. K., CONTRERAS, M., MAGRIS, M., HIDALGO, G., FIERER, N. & KNIGHT, R. 2010. Delivery mode shapes the acquisition and structure of the initial microbiota across multiple body habitats in newborns. *Proceedings of the National Academy of Sciences*, 107, 11971-11975.
- DREYMUELLER, D., PRUESSMEYER, J., GROTH, E. & LUDWIG, A. J. 2012. The role of ADAM-mediated shedding in vascular biology. *European Journal of Cell Biology*, 91, 472-485.
- DRUAR, C., YU, F., BARNES, J. L., OKINAKA, R. T., CHANTRATITA, N., BEG, S., STRATILO, C. W., OLIVE, A. J., SOLTES, G. & RUSSELL, M. L. 2008. Evaluating *Burkholderia pseudomallei* Bip proteins as vaccines and Bip antibodies as detection agents. *FEMS Immunology & Medical Microbiology*, 52, 78-87.
- DUELLI, D. & LAZEBNIK, Y. 2003. Cell fusion: a hidden enemy? *Journal of Cancer Cell*, 3, 445-448.
- DUMONT, A. L. & TORRES, V. J. 2014. Cell targeting by the *Staphylococcus aureus* pore-forming toxins: it's not just about lipids. *Trends in microbiology*, 22, 21-27.
- EDWARDS, T. E., PHAN, I., ABENDROTH, J., DIETERICH, S. H., MASOUDI, A., GUO, W., HEWITT, S. N., KELLEY, A., LEIBLY, D., BRITTNACHER, M. J., STAKER, B. L., MILLER, S. I., VAN VOORHIS, W. C., MYLER, P. J. & STEWART, L. J. 2010. Structure of a *Burkholderia pseudomallei* Trimeric Autotransporter Adhesin Head. *PLoS One*, 5.
- EKCHARIYAWAT, P., PUDLA, S., LIMPOSUWAN, K., ARJCHAROEN, S., SIRISINHA, S. & UTAISINCHAROEN, P. 2005. *Burkholderia pseudomallei* - induced expression of suppressor of cytokine signaling 3 and cytokine-inducible src homology 2-containing protein in mouse macrophages: a possible mechanism for suppression of the response to gamma interferon stimulation. *Infection and Immunity*, 73, 7332-9.
- EKCHARIYAWAT, P., PUDLA, S., LIMPOSUWAN, K., ARJCHAROEN, S., SIRISINHA, S. & UTAISINCHAROEN, P. 2007. Expression of suppressor of cytokine signaling 3 (SOCS3) and cytokine-inducible Src homology 2-containing protein (CIS) induced in *Burkholderia pseudomallei* —infected mouse macrophages requires bacterial internalization. *Microbial Pathogenesis*, 42, 104-110.
- EKPO, P., RUNGPANICH, U., PONGSUNK, S., NAIGOWIT, P. & PETKANACHANAPONG, V. 2007. Use of protein-specific monoclonal antibody-based latex agglutination for rapid diagnosis of *Burkholderia pseudomallei* infection in patients with community-acquired septicemia. *Clin. Vaccine Immunol.*, 14, 811-812.
- ELENA, M., FABRIZIO, G., DANIELA, M., STEFANO, R., ANDREAS, J., ROBERTA, E., BARBARA, B., FLAMINIO, C., CARLO, S. & ALESSANDRO, P. 2007.

- Synapse-associated protein-97 mediates alpha-secretase ADAM10 trafficking and promotes its activity. *Journal of Neuroscience*, 27, 1682-1691.
- ELGAWIDI, A. 2016. The role of tetraspanins in multinucleated giant cell formation induced by *Burkholderia thailandensis*. University of Sheffield. Department of Molecular Biology and Biotechnology. Ph.D., University of Sheffield.
- ELLERMAN, D. A., HA, C., PRIMAKOFF, P., MYLES, D. G. & DVEKSLER, G. S. 2003. Direct binding of the ligand PSG17 to CD9 requires a CD9 site essential for sperm-egg fusion. *Molecular Biology of the Cell*, 14, 5098-5103.
- EMMANUEL, D., FRANCK, C., JEAN-FRANÇOIS, O., JULIEN, M., CLAUDE, B., PHILIPPE, M., FRANÇOIS, S. & ERIC, R. J. 2012. TspanC8 tetraspanins regulate ADAM10/Kuzbanian trafficking and promote Notch activation in flies and mammals. *Journal of Cell Biology*, 199, 481.
- ERIC, R., AHMED, Z., MICHEL, P., EDYTA, W., JEAN-PHILIPPE, W., SHOSHANA, L., FRANÇOIS, L. N. & CLAUDE, B. J. 2006. Reduced fertility of female mice lacking CD81. *Developmental Biology*, 290, 351-358.
- ERIKSSON, E., DONS, L., ROTHFUCHS, A. G., HELDIN, P., WIGZELL, H. & ROTTENBERG, M. E. J. 2003. CD44-regulated intracellular proliferation of *Listeria monocytogenes*. *Infection and Immunity*, 71, 4102-4111.
- EISSA, N., HUSSEIN, H., WANG, H., RABBI, M. F., BERNSTEIN, C. N. & GHIA, J.-E. J. P. O. 2016. Stability of reference genes for messenger RNA quantification by real-time PCR in mouse dextran sodium sulfate experimental colitis. 11, e0156289.
- ESSEX-LOPRESTI, A. E., BODDEY, J. A., THOMAS, R., SMITH, M. P., HARTLEY, M. G., ATKINS, T., BROWN, N. F., TSANG, C. H., PEAK, I. R. & HILL, J. 2005. A type IV pilin, PilA, contributes to adherence of *Burkholderia pseudomallei* and virulence in vivo. *Infection and Immunity*, 73, 1260-1264.
- ESTRADA-DE LOS SANTOS, P., ROJAS-ROJAS, F. U., TAPIA-GARCÍA, E. Y., VÁSQUEZ-MURRIETA, M. S. & HIRSCH, A. M. 2016. To split or not to split: an opinion on dividing the genus *Burkholderia*. *Annals of Microbiology*, 66, 1303-1314.
- FAIS, S., BURGIO, V. L., SILVESTRI, M., CAPOBIANCHI, M. R., PACCHIAROTTI, A. & PALLONE, F. 1994. Multinucleated giant cells generation induced by interferon-gamma. Changes in the expression and distribution of the intercellular adhesion molecule-1 during macrophages fusion and multinucleated giant cell formation. *Laboratory Investigation; a Journal of Technical Methods and Pathology*, 71, 737-744.
- FERTITTA, L., MONSEL, G., DELAROCHE, M., FOURNIOLS, E., BROSSIER, F. & CAUMES, E. 2018. Cutaneous melioidosis: Two cases of chronic primary forms. *Journal of the European Academy of Dermatology and Venereology*, 32, e270-e272.
- FINK, S. L. & COOKSON, B. T. 2005. Apoptosis, pyroptosis, and necrosis: mechanistic description of dead and dying eukaryotic cells. *Infection and Immunity*, 73, 1907-1916.
- FRANCO, M., D'HAESELEER, P. M., BRANDA, S. S., LIOU, M. J., HAIDER, Y., SEGELKE, B. W. & EL-ETR, S. H. 2018. Proteomic profiling of *Burkholderia thailandensis* during host infection using bio-orthogonal noncanonical amino acid tagging (BONCAT). *Frontiers in Cellular and Infection Microbiology*, 8.
- FREDERIKSEN, R. F. & LEISNER, J. J. 2015. Effects of *Listeria monocytogenes* EGD-e and *Salmonella enterica* ser. Typhimurium LT2 chitinases on intracellular survival in *Dictyostelium discoideum* and mammalian cell lines. *FEMS Microbiology Letters*, 362, fmv067.
- FRENCH, C. T., TOESCA, I. J., WU, T.-H., TESLAA, T., BEATY, S. M., WONG, W., LIU, M., SCHRÖDER, I., CHIOU, P.-Y. & TEITELL, M. A. 2011. Dissection of the *Burkholderia* intracellular life cycle using a photothermal nanoblade. *Proceedings of the National Academy of Sciences*, 108, 12095-12100.

- FU, H.-L., SHAO, L., WANG, Q., JIA, T., LI, M. & YANG, D.-P. 2013. A systematic review of p53 as a biomarker of survival in patients with osteosarcoma. *Tumor Biology*, 34, 3817-3821.
- FUKUDOME, K., FURUSE, M., IMAI, T., NISHIMURA, M., TAKAGI, S., HINUMA, Y. & YOSHIE, O. 1992. Identification of membrane antigen C33 recognized by monoclonal antibodies inhibitory to human T-cell leukemia virus type 1 (HTLV-1)-induced syncytium formation: altered glycosylation of C33 antigen in HTLV-1-positive T cells. *Journal of Virology*, 66, 1394-1401.
- GALSON, D. L. & ROODMAN, G. D. 2011. Origins of Osteoclasts. *Osteoimmunology*. Elsevier.
- GALYOV, E. E., BRETT, P. J. & DESHAZER, D. 2010. Molecular insights into *Burkholderia pseudomallei* and *Burkholderia mallei* pathogenesis. *Annual Review of Microbiology*, 64, 495-517.
- GARCIA-ESPAÑA, A., CHUNG, P.-J., SARKAR, I. N., STINER, E., SUN, T.-T. & DESALLE, R. 2008. Appearance of new tetraspanin genes during vertebrate evolution. *Genomics*, 91, 326-334.
- GARCIA-ESPAÑA, A., CHUNG, P.-J., ZHAO, X., LEE, A., PELLICER, A., YU, J., SUN, T.-T. & DESALLE, R. 2006. Origin of the tetraspanin uroplakins and their co-evolution with associated proteins: implications for uroplakin structure and function. *Molecular Phylogenetics and Evolution*, 41, 355-367.
- GARDNER, S., GROSS, S. M., DAVID, L. L., KLIMEK, J. E. & ROTWEIN, P. 2015. Separating myoblast differentiation from muscle cell fusion using IGF-I and the p38 MAP kinase inhibitor SB202190. *American Journal of Physiology-Cell Physiology*.
- GARNER, J. M., HERR, M. J., HODGES, K. B. & JENNINGS, L. K. 2016. The utility of tetraspanin CD9 as a biomarker for metastatic clear cell renal cell carcinoma. *Biochemical/Biophysical Research Communications*, 471, 21-25.
- GASSER, A. & MÖST, J. J. 1999. Generation of multinucleated giant cells in vitro by culture of human monocytes with Mycobacterium bovis BCG in combination with cytokine-containing supernatants. *Infection and Immunity*, 67, 395-402.
- GAUSTER, M., MANINGER, S., SIWETZ, M., DEUTSCH, A., EL-HELIEBI, A., KOLB-LENZ, D., HIDEN, U., DESOYE, G., HERSE, F. & PROKESCH, A. 2018. Downregulation of p53 drives autophagy during human trophoblast differentiation. *Cellular and molecular life sciences*, 75, 1839-1855.
- GAUTAM, P. & ACHARYA, A. 2014. Suppressed Expression of Homotypic Multinucleation, Extracellular Domains of CD 172 $\alpha$  (SIRP- $\alpha$ ) and CD 47 (IAP) Receptors in TAM s UpRegulated by Hsp70–Peptide Complex in Dalton's Lymphoma. *Scandinavian Journal of Immunology*, 80, 22-35.
- GEISERT JR, E. E., WILLIAMS, R. W., GEISERT, G. R., FAN, L., ASBURY, A. M., MAECKER, H. T., DENG, J. & LEVY, S. 2002. Increased brain size and glial cell number in CD81-null mice. *Journal of Comparative Neurology*, 453, 22-32.
- GIBNEY, K. B., MACGREGOR, L., LEDER, K., TORRESI, J., MARSHALL, C., EBELING, P. R. & BIGGS, B.-A. 2008. Vitamin D Deficiency Is Associated with Tuberculosis and Latent Tuberculosis Infection in Immigrants from Sub-Saharan Africa. *Clinical Infectious Diseases*, 46, 443-446.
- GILMORE, G., BARNES, J., KETHEESAN, N. & NORTON, R. 2007. Use of antigens derived from *Burkholderia pseudomallei*, *B. thailandensis*, and *B. cepacia* in the indirect hemagglutination assay for melioidosis. *Clinical and Vaccine Immunology*, 14, 1529-1531.
- GLASS, M. B., GEE, J. E., STEIGERWALT, A. G., CAVUOTI, D., BARTON, T., HARDY, R. D., GODOY, D., SPRATT, B. G., CLARK, T. A. & WILKINS, P. P. 2006. Pneumonia and Septicemia Caused by *Burkholderia thailandensis* in the United States. *Journal of Clinical Microbiology*, 44, 4601-4604.

- GONZALES, P. E., SOLOMON, A., MILLER, A. B., LEESNITZER, M. A., SAGI, I. & MILLA, M. E. 2004. Inhibition of the Tumor Necrosis Factor- $\alpha$ -converting Enzyme by Its Pro Domain. 279, 31638-31645.
- GONZÁLEZ-CORTÉS, C., REYES-RUVALCABA, D., DIEZ-TASCÓN, C. & RIVERO-LEZCANO, O. M. 2009. Apoptosis and oxidative burst in neutrophils infected with *Mycobacterium* spp. *Immunology Letters*, 126, 16-21.
- GORDÓN-ALONSO, M., YAÑEZ-MÓ, M., BARREIRO, O., ÁLVAREZ, S., MUÑOZ-FERNÁNDEZ, M. Á., VALENZUELA-FERNÁNDEZ, A. & SÁNCHEZ-MADRID, F. 2006. Tetraspanins CD9 and CD81 Modulate HIV-1-Induced Membrane Fusion. *The Journal of Immunology*, 177, 5129-5137.
- GORI, A. H., AHMED, K., MARTINEZ, G., MASAKI, H., WATANABE, K. & NAGATAKE, T. 1999. Mediation of attachment of *Burkholderia pseudomallei* to human pharyngeal epithelial cells by the asialoganglioside GM1-GM2 receptor complex. *The American Journal of Tropical Medicine and Hygiene*, 61, 473-5.
- GRAY, M. L. & KILLINGER, A. 1966. *Listeria monocytogenes* and listeric infections. *Bacteriological Reviews*, 30, 309.
- GREEN, L. R., MONK, P. N., PARTRIDGE, L. J., MORRIS, P., GORRINGE, A. R. & READ, R. C. 2011. Cooperative Role for Tetraspanins in Adhesin-Mediated Attachment of Bacterial Species to Human Epithelial Cells. 79, 2241-2249.
- GROOT, A. J., ROGER, H., SANAZ, Y., HODIN, C. M., KARINA, R., PAUL, S., JAN, T. & MARC, V. 2014. Regulated proteolysis of NOTCH2 and NOTCH3 receptors by ADAM10 and presenilins. *Molecular Cellular Biology*, 34, 2822.
- GROSSMANN, A., BENLASFER, N., BIRTH, P., HEGELE, A., WACHSMUTH, F., APELT, L. & STELZL, U. 2015. Phospho-tyrosine dependent protein-protein interaction network. *Molecular systems biology*, 11, 794.
- HA, C. T. 2004. Pregnancy Specific Glycoprotein 17 Binds to the Extracellular Loop 2 of its Receptor, CD9, and Induces the Secretion of IL-10, IL-6, PGE2 and TGF $\beta$ 1 in Murine Macrophages. *Uniformed Services University of the Health Sciences Bethesda*. UNIFORMED SERVICES UNIV OF THE HEALTH SCIENCES BETHESDA.
- HAASE, R., KIRSCHNING, C. J., SING, A., SCHRÖTTNER, P., FUKASE, K., KUSUMOTO, S., WAGNER, H., HEESEMANN, J. & RUCKDESCHL, K. 2003. A dominant role of Toll-like receptor 4 in the signaling of apoptosis in bacteria-faced macrophages. *The Journal of Immunology*, 171, 4294-4303.
- HAINING, E. J., JING, Y., BAILEY, R. L., KABIR, K., RICHARD, C., SCHICKWANN, T., WATSON, S. P., JON, F., PALOMA, G. & TOMLINSON, M. G. 2012. The TspanC8 subgroup of tetraspanins interacts with A disintegrin and metalloprotease 10 (ADAM10) and regulates its maturation and cell surface expression. *Journal of Biological Chemistry*, 287, 39753-39765.
- HALL, J. 2016. Investigating the role of the type VI secretion system-associated genes of *Burkholderia thailandensis*. University of Sheffield, Department of Infection, Immunity & Cardiovascular Disease. Ph.D., University of Sheffield
- HAN, X., STERLING, H., CHEN, Y., SAGINARIO, C., BROWN, E. J., FRAZIER, W. A., LINDBERG, F. P. & VIGNERY, A. 2000. CD47, a ligand for the macrophage fusion receptor, participates in macrophage multinucleation. *Journal of Biological Chemistry*, 275, 37984-37992.
- HARAGA, A., WEST, T. E., BRITTNACHER, M. J., SKERRETT, S. J. & MILLER, S. I. 2008. *Burkholderia thailandensis* as a model system for the study of the virulence-associated type III secretion system of *Burkholderia pseudomallei*. *Infection and Immunity*, 76, 5402-5411.
- HASSAN, A. S. & NELSON, C. C. 2002. Benign eyelid tumors and skin diseases. *International Ophthalmology Clinics*, 42, 135-149.
- HASSAN, N. F., KAMANI, N., MESZAROS, M. M. & DOUGLAS, S. D. 1989. Induction of multinucleated giant cell formation from human blood-derived

- monocytes by phorbol myristate acetate in in vitro culture. *The Journal of Immunology*, 143, 2179-2184.
- HASSUNA, N. 2010. *The role of tetraspanins in the uptake of intracellular pathogens*. Ph.D., The University of Sheffield.
- HASSUNA, N. A., MONK, P. N., ALI, F., READ, R. C. & PARTRIDGE, L. J. 2017. A role for the tetraspanin proteins in Salmonella infection of human macrophages. *Journal of Infection*, 75, 115.
- HÄUßLER, S., ROHDE, M. & STEINMETZ, I. 1999. Highly resistant *Burkholderia pseudomallei* small colony variants isolated in vitro and in experimental melioidosis. *Medical microbiology and immunology*, 188, 91-97.
- HELMING, L. & GORDON, S. 2009. Molecular mediators of macrophage fusion. *Trends in Cell Biology*, 19, 514-522.
- HEMARAJATA, P., BAGHDADI, J. D., HOFFMAN, R. & HUMPHRIES, R. M. 2016. *Burkholderia pseudomallei*: Challenges for the Clinical Microbiology Laboratory. *Journal of Clinical Microbiology*, 54, 2866-2873.
- HEMLER, M. E. 2001. Specific tetraspanin functions. *The Journal of Cell Biology*, 155, 1103-1108.
- HEMLER, M. E. 2003. Tetraspanin proteins mediate cellular penetration, invasion, and fusion events and define a novel type of membrane microdomain. *Annual review of cell and developmental biology*, 19, 397-422.
- HEMLER, M. E. 2005. Tetraspanin functions and associated microdomains. *Nature Reviews Molecular Cell Biology*, 6, 801-811.
- HEMLER, M. E. 2008. Targeting of tetraspanin proteins—potential benefits and strategies. *Nature Reviews Drug Discovery*, 7, 747.
- HENGGE-ARONIS, R. 2002. Signal transduction and regulatory mechanisms involved in control of the  $\sigma$ S (RpoS) subunit of RNA polymerase. *Microbiology and Molecular Biology Reviews*, 66, 373-395.
- HERNÁNDEZ-GIL, I., GRACIA, M. A. A., PINGARRÓN, M. & JEREZ, L. 2006. Physiological bases of bone regeneration II. The remodeling process. *Med Oral Patol Oral Cir Bucal*, 11, E151-215.
- HERR, M. J., MABRY, S. E., JAMESON, J. F. & JENNINGS, L. K. 2013. Pro-MMP-9 upregulation in HT1080 cells expressing CD9 is regulated by epidermal growth factor receptor. *Biochemical Biophysical Research Communications*, 442, 99-104.
- HIGUCHI, S., TABATA, N., TAJIMA, M., ITO, M., TSURUDOME, M., SUDO, A., UCHIDA, A. & ITO, Y. 1998. Induction of human osteoclast-like cells by treatment of blood monocytes with anti-fusion regulatory protein-1/CD98 monoclonal antibodies. *Journal of Bone and Mineral Research*, 13, 44-49.
- HOBOLT-PEDERSEN, A.-S., DELAISSÉ, J.-M. & SØE, K. 2014. Osteoclast Fusion is Based on Heterogeneity Between Fusion Partners. *Calcified Tissue International*, 95, 73-82.
- HONG, I. K., JIN, Y. J., BYUN, H. J., JEOUNG, D. I., KIM, Y. M. & LEE, H. 2006. Homophilic interactions of Tetraspanin CD151 up-regulate motility and matrix metalloproteinase-9 expression of human melanoma cells through adhesion-dependent c-Jun activation signaling pathways. *Journal of Biological Chemistry*, 281, 24279-92.
- HOR, JYH L., WHITNEY, PAUL G., ZAID, A., BROOKS, ANDREW G., HEATH, WILLIAM R. & MUELLER, SCOTT N. 2015. Spatiotemporally Distinct Interactions with Dendritic Cell Subsets Facilitates CD4+ and CD8+ T Cell Activation to Localized Viral Infection. *Immunity*, 43, 554-565.
- HORTON, R. E., GRANT, G. D., MATTHEWS, B., BATZLOFF, M., OWEN, S. J., KYAN, S., FLEGG, C. P., CLARK, A. M., ULETT, G. C., MORRISON, N., PEAK, I. R. & BEACHAM, I. R. 2013. Quorum Sensing Negatively Regulates Multinucleate Cell Formation during Intracellular Growth of *Burkholderia pseudomallei* in Macrophage-Like Cells. *PLoS One*, 8

- HSU, Y.-H. 2012. Melioidosis. *Tzu Chi Medical Journal*, 4, 212.
- HUANG, S., YUAN, S., DONG, M., SU, J., YU, C., SHEN, Y., XIE, X., YU, Y., YU, X. & CHEN, S. 2005. The phylogenetic analysis of tetraspanins projects the evolution of cell–cell interactions from unicellular to multicellular organisms. *Genomics*, 86, 674-684.
- HUANG, W., FEBBRAIO, M. & SILVERSTEIN, R. L. 2011. CD9 tetraspanin interacts with CD36 on the surface of macrophages: a possible regulatory influence on uptake of oxidized low density lipoprotein. *Plos One*, 6, e29092.
- HULME, R. S., HIGGINBOTTOM, A., PALMER, J., PARTRIDGE, L. J. & MONK, P. N. 2014. Distinct regions of the large extracellular domain of tetraspanin CD9 are involved in the control of human multinucleated giant cell formation. *PloS one*, 9, e116289.
- HUMPTON, T. J. & VOUSDEN, K. H. 2016. Regulation of cellular metabolism and hypoxia by p53. *Cold Spring Harbor perspectives in medicine*, 6, a026146.
- HUOVILA, A. P., ALMEIDA, E. A. & WHITE, J. M. J. C. O. I. C. B. 1996. ADAMs and cell fusion. 8, 692-699.
- HWANG, I.-H., PARK, J., KIM, J. M., KIM, S. I., CHOI, J.-S., LEE, K.-B., YUN, S. H., LEE, M.-G., PARK, S. J. & JANG, I.-S. 2016. Tetraspanin-2 promotes glucotoxic apoptosis by regulating the JNK/ $\beta$ -catenin signaling pathway in human pancreatic  $\beta$  cells. *The FASEB Journal*, 30, 3107-3116.
- ICHIRO, I., NAKO, I., WILKE, G. A., POWERS, M. E., FRANK, K. M., YANG, W. & JULIANE, B. W. 2011. A *Staphylococcus aureus* pore-forming toxin subverts the activity of ADAM10 to cause lethal infection in mice. *Nature Medicine*, 17, 1310.
- ISHII, M., IWAI, K., KOIKE, M., OHSHIMA, S., KUDO-TANAKA, E., ISHII, T., MIMA, T., KATADA, Y., MIYATAKE, K. & UCHIYAMA, Y. 2006. RANKL-induced expression of tetraspanin CD9 in lipid raft membrane microdomain is essential for cell fusion during osteoclastogenesis. *Journal of Bone Mineral Research*, 21, 965-976.
- IWAI, K., ISHII, M., OHSHIMA, S., MIYATAKE, K. & SAEKI, Y. 2007. Expression and Function of Transmembrane-4 Superfamily (Tetraspanin) Proteins in Osteoclasts: Reciprocal Roles of Tspan-5 and NET-6 during Osteoclastogenesis. *Allergy International*, 56, 457-463.
- IWAMOTO, R., HIGASHIYAMA, S., MITAMURA, T., TANIGUCHI, N., KLAGSBRUN, M. & MEKADA, E. 1994. Heparin-binding EGF-like growth factor, which acts as the diphtheria toxin receptor, forms a complex with membrane protein DRAP27/CD9, which up-regulates functional receptors and diphtheria toxin sensitivity. *The EMBO Journal*, 13, 2322-2330.
- JACKSON, J. G., PANT, V., LI, Q., CHANG, L. L., QUINTÁS-CARDAMA, A., GARZA, D., TAVANA, O., YANG, P., MANSHOURI, T. & LI, Y. 2012. p53-mediated senescence impairs the apoptotic response to chemotherapy and clinical outcome in breast cancer. *Cancer Cell*, 21, 793-806.
- JAISWAL, R. K., KUMAR, P., KUMAR, M. & YADAVA, P. K. 2018. hTERT promotes tumor progression by enhancing TSPAN13 expression in osteosarcoma cells. *Molecular Carcinogenesis*, 57, 1038-1054.
- JANKOVIČOVÁ, J., SIMON, M., ANTALÍKOVÁ, J., CUPPEROVÁ, P. & MICHÁLKOVÁ, K. J. 2015. Role of tetraspanin CD9 molecule in fertilization of mammals. *Physiological Research*, 64.
- JEGANATHAN, S., FIORINO, C., NAIK, U., SONG SUN, H. & HARRISON, R. E. 2014. Modulation of osteoclastogenesis with macrophage M1-and M2-inducing stimuli. *PloS One*, 9, e104498.
- JILANI, M. S. A., ROBAYET, J. A. M., MOHIUDDIN, M., HASAN, M. R., AHSAN, C. R. & HAQ, J. A. 2016. *Burkholderia pseudomallei* : its detection in soil and seroprevalence in Bangladesh. *PLoS Neglected Tropical Diseases*, 10, e0004301.

- JIRAVIRIYAKUL, A. 2010. Strategies for generating antibodies for the studies of tetraspanin proteins characterisation of tetraspanin Tspan-11. University of Sheffield Department of Molecular Biology and Biotechnology. Ph.D., University of Sheffield.
- JONES, D., GLIMCHER, L. H. & ALIPRANTIS, A. O. 2011. Osteoimmunology at the nexus of arthritis, osteoporosis, cancer, and infection. *The Journal of Clinical Investigation*, 121, 2534-2542.
- JOUANNET, S., SAINT-POL, J., FERNANDEZ, L., NGUYEN, V., CHARRIN, S., BOUCHEIX, C., BROU, C., MILHIET, P. E. & RUBINSTEIN, E. 2016. TspanC8 tetraspanins differentially regulate the cleavage of ADAM10 substrates, Notch activation and ADAM10 membrane compartmentalization. *Cellular Molecular Life Sciences*, 73, 1895-1915.
- JUAN, C., JIAN, L. & DUBOSE, T. D. 2005. CD63 interacts with the carboxy terminus of the colonic H<sup>+</sup>-K<sup>+</sup>-ATPase to decrease plasma membrane localization and 86Rb<sup>+</sup> uptake. *American Journal of Physiology Cell Physiology*, 288, C1279.
- KAJI, K., ODA, S., SHIKANO, T., OHNUKI, T., UEMATSU, Y., SAKAGAMI, J., TADA, N., MIYAZAKI, S. & KUDO, A. 2000. The gamete fusion process is defective in eggs of Cd9-deficient mice. *Nature Genetics*, 24, 279-282.
- KANG, W. T., VELLASAMY, K. M. & VADIVELU, J. 2016. Eukaryotic pathways targeted by the type III secretion system effector protein, BipC, involved in the intracellular lifecycle of *Burkholderia pseudomallei*. *Scientific Reports*, 6, 33528.
- KASHEF, J., DIANA, T., OELGESCHLÄGER, M. & NAZARENKO, I. 2013. Expression of the tetraspanin family members Tspan3, Tspan4, Tspan5 and Tspan7 during *Xenopus laevis* embryonic development. *Gene Expression Patterns*, 13, 1-11.
- KATANGWE, T., PURCELL, J., BAR-ZEEV, N., DENIS, B., MONTGOMERY, J., ALAERTS, M., HEYDERMAN, R. S., DANCE, D. A., KENNEDY, N. & FEASEY, N. 2013. Human melioidosis, Malawi, 2011. *Emerging Infectious Diseases*, 19, 981.
- KAZAROV, A. R., YANG, X., STIPP, C. S., SEHGAL, B. & HEMLER, M. E. 2002. An extracellular site on tetraspanin CD151 determines  $\alpha 3$  and  $\alpha 6$  integrin-dependent cellular morphology. *The Journal of Cell Biology*, 158, 1299-1309.
- KELLER, L. & SURETTE, M. G. 2006. Communication in bacteria: an ecological and evolutionary perspective. *Nature Reviews Microbiology*, 4, 249.
- KESPICHAYAWATTANA, W., INTACHOTE, P., UTAISINCHAROEN, P. & SIRISINHA, S. 2004. Virulent *Burkholderia pseudomallei* is more efficient than avirulent *Burkholderia thailandensis* in invasion of and adherence to cultured human epithelial cells. *Microbial Pathogenesis*, 36, 287-292.
- KESPICHAYAWATTANA, W., RATTANACHETKUL, S., WANUN, T., UTAISINCHAROEN, P. & SIRISINHA, S. 2000. *Burkholderia pseudomallei* induces cell fusion and actin-associated membrane protrusion: a possible mechanism for cell-to-cell spreading. *Infection and Immunity*, 68, 5377-5384.
- KHAKHUM, N., BHARAJ, P., MYERS, J. N., TAPIA, D., KILGORE, P. B., ROSS, B. N., WALKER, D. H., ENDSLEY, J. J. & TORRES, A. G. 2019. *Burkholderia pseudomallei*  $\Delta$ tonB  $\Delta$ hcp1 Live Attenuated Vaccine Strain Elicits Full Protective Immunity against Aerosolized Melioidosis Infection. *mSphere*, 4, e00570-18.
- KOSKINEN, C., PERSSON, E., BALDOCK, P., STENBERG, Å., BOSTRÖM, I., MATOZAKI, T., OLDENBORG, P.-A. & LUNDBERG, P. 2013. Lack of CD47 impairs bone cell differentiation and results in an osteopenic phenotype in vivo due to impaired signal regulatory protein  $\alpha$  (SIRP $\alpha$ ) signaling. *Journal of Biological Chemistry*, 288, 29333-29344.
- KOVACS-SIMON, A., HEMSLEY, C. M., SCOTT, A. E., PRIOR, J. L. & TITBALL, R. W. 2019. *Burkholderia thailandensis* strain E555 is a surrogate for the

- investigation of *Burkholderia pseudomallei* replication and survival in macrophages. *BMC Microbiology*, 19, 97.
- KOVALENKO, O. V., YANG, X. H. & HEMLER, M. E. 2007. A novel cysteine cross-linking method reveals a direct association between claudin-1 and tetraspanin CD9. *Molecular & Cellular Proteomics*, 6, 1855-1867.
- KRACHLER, A. M., WOOLERY, A. R. & ORTH, K. 2011. Manipulation of kinase signaling by bacterial pathogens. *J Cell Biol*, 195, 1083-92.
- KRAUS, G. 1991. *Mapping of autoantibody epitopes of the novel tetraspanin 7 autoantigen relevant in type 1 diabetes*. University of Zagreb.
- LAKKARAJU, A. & RODRIGUEZ-BOULAN, E. 2008. Itinerant exosomes: emerging roles in cell and tissue polarity. *Trends in Cell Biology*, 18, 199-209.
- LAMKANFI, M. & DIXIT, V. M. 2010. Manipulation of host cell death pathways during microbial infections. *Cell Host & Microbe*, 8, 44-54.
- LAMOTHE, J. & VALVANO, M. A. 2008. *Burkholderia cenocepacia*-induced delay of acidification and phagolysosomal fusion in cystic fibrosis transmembrane conductance regulator (CFTR)-defective macrophages. *Microbiology*, 154, 3825-3834.
- LASARRE, B. & FEDERLE, M. J. 2013. Exploiting quorum sensing to confuse bacterial pathogens. *Microbiology and Molecular Biology Reviews*, 77, 73-111.
- LAUSTED, C., DAHL, T., WARREN, C., KING, K., SMITH, K., JOHNSON, M., SALEEM, R., AITCHISON, J., HOOD, L. & LASKY, S. R. 2004. POSaM: a fast, flexible, open-source, inkjet oligonucleotide synthesizer and microarrayer. *Genome Biology*, 5, R58.
- LAZAR ADLER, N. R., GOVAN, B., CULLINANE, M., HARPER, M., ADLER, B. & BOYCE, J. D. 2009. The molecular and cellular basis of pathogenesis in melioidosis: how does *Burkholderia pseudomallei* cause disease? *FEMS Microbiol Rev*, 33, 1079-99.
- LE NAOUR, F., RUBINSTEIN, E., JASMIN, C., PRENANT, M. & BOUCHEIX, C. 2000. Severely Reduced Female Fertility in CD9-Deficient Mice. *Science*, 287, 319-321.
- LENGWEHASATIT, I., NUCHTAS, A., TUNGPRADABKUL, S., SIRISINHA, S. & UTAISINCHAROEN, P. 2008. Involvement of *B. pseudomallei* RpoS in apoptotic cell death in mouse macrophages. *Microbial Pathogenesis*, 44, 238-245.
- LENNINGS, J., WEST, T. E. & SCHWARZ, S. 2019. The *Burkholderia* type VI secretion system 5: composition, regulation and role in virulence. *Frontiers in Microbiology*, 9.
- LERTPATANASUWAN, N., SERMSRI, K., PETKASEAM, A., TRAKULSOMBOON, S. & SUPUTTAMONGKOL, T. Y. 1999. Arabinose-Positive *Burkholderia pseudomallei* Infection in Humans: Case Report. *Clinical Infectious Diseases*, 28, 2.
- LEUNG, K. T., CHAN, K. Y. Y., NG, P. C., LAU, T. K., CHIU, W. M., TSANG, K. S., LI, C. K., KONG, C. K. L. & LI, K. 2011. The tetraspanin CD9 regulates migration, adhesion, and homing of human cord blood CD34+ hematopoietic stem and progenitor cells. *Blood*, 117, 1840-1850.
- LEVINE, A. J. 2009. The common mechanisms of transformation by the small DNA tumor viruses: The inactivation of tumor suppressor gene products: p53. *Virology*, 384, 285-293.
- LEVY, S. & SHOHAM, T. 2005. Protein-protein interactions in the tetraspanin web. *Physiology*, 20, 218-224.
- LI, L.-X., ATIF, S. M., SCHMIEL, S. E., LEE, S.-J. & MCSORLEY, S. J. 2012. Increased susceptibility to *Salmonella* infection in signal regulatory protein  $\alpha$ -deficient mice. *The Journal of Immunology*, 189, 2537-2544.

- LI, L., BO, H., WEI, M., LIU, DONGMING, Z., COX, J. V. & XIN, A., ZHANG 2007. Tetraspanin CD151 promotes cell migration by regulating integrin trafficking. *Journal of Biological Chemistry*, 282, 31631.
- LIMMATHUROTSAKUL, D., GOLDING, N., DANCE, D. A., MESSINA, J. P., PIGOTT, D. M., MOYES, C. L., ROLIM, D. B., BERTHERAT, E., DAY, N. P., PEACOCK, S. J. & HAY, S. I. 2016. Predicted global distribution of *Burkholderia pseudomallei* and burden of melioidosis. *Nat Microbiol*, 1.
- LIMMATHUROTSAKUL, D. & PEACOCK, S. J. 2011. Melioidosis: a clinical overview. *British Medical Bulletin*, 99, 125-139.
- LIMMATHUROTSAKUL, D., WONGRATANACHEEWIN, S., TEERAWATTANASOOK, N., WONGSUVAN, G., CHAISUKSANT, S., CHETCHOTISAKD, P., CHAOWAGUL, W., DAY, N. P. & PEACOCK, S. J. 2010. Increasing incidence of human melioidosis in Northeast Thailand. *The American journal of tropical medicine and hygiene*, 82, 1113-1117.
- LONGHURST, C. M., WHITE, M. M., WILKINSON, D. A. & JENNINGS, L. K. 1999. A CD9, alphaIIb beta3, integrin-associated protein, and GPIb/V/IX complex on the surface of human platelets is influenced by alphaIIb beta3 conformational states. *European Journal of Biochemistry*, 263, 104.
- LUMJIAKTASE, P., DIGGLE, S. P., LOPRASERT, S., TUNGPRADABKUL, S., DAYKIN, M., CAMARA, M., WILLIAMS, P. & KUNAKORN, M. 2006. Quorum sensing regulates dpsA and the oxidative stress response in *Burkholderia pseudomallei*. *Microbiology*, 152, 3651-3659.
- MA, L., ZHANG, G. & DOYLE, M. P. 2011. Green fluorescent protein labeling of *Listeria*, *Salmonella*, and *Escherichia coli* O157: H7 for safety-related studies. *PLoS One*, 6, e18083.
- MACLAUCHLAN, S., SKOKOS, E. A., MEZMARICH, N., ZHU, D. H., RAOOF, S., SHIPLEY, J. M., SENIOR, R. M., BORNSTEIN, P. & KYRIAKIDES, T. R. 2009. Macrophage fusion, giant cell formation, and the foreign body response require matrix metalloproteinase 9. *Journal of Leukocyte Biology*, 85, 617-626.
- MAECKER, H. T., TODD, S. C. & LEVY, S. 1997. The tetraspanin superfamily: molecular facilitators. *The FASEB Journal*, 11, 428-442.
- MARLOVITS, T. C. & STEBBINS, C. E. 2010. Type III secretion systems shape up as they ship out. *Current Opinion in Microbiology*, 13, 47-52.
- MARTINEZ, F. O., HELMING, L. & GORDON, S. 2009. Alternative activation of macrophages: an immunologic functional perspective. *Annual Review of Immunology*, 27, 451-483.
- MASCIOPINTO, F., CAMPAGNOLI, S., ABRIGNANI, S., UEMATSU, Y. & PILERI, P. 2001. The small extracellular loop of CD81 is necessary for optimal surface expression of the large loop, a putative HCV receptor. *Virus Research*, 80, 1-10.
- MATHUR, A., HAYWARD, J. A. & MAN, S. M. 2018. Molecular mechanisms of inflammasome signaling. *Journal of Leukocyte Biology*, 103, 233-257.
- MATTHEWS, A. L., NOY, P. J., REYAT, J. S. & TOMLINSON, M. G. 2017. Regulation of A disintegrin and metalloproteinase (ADAM) family sheddases ADAM10 and ADAM17: The emerging role of tetraspanins and rhomboids. *Platelets*, 28, 333-341.
- MCNALLY, A. K. & ANDERSON, J. M. 2002.  $\beta$ 1 and  $\beta$ 2 integrins mediate adhesion during macrophage fusion and multinucleated foreign body giant cell formation. *The American Journal of Pathology*, 160, 621-630.
- MCNALLY, A. K. & ANDERSON, J. M. 2005. Multinucleated giant cell formation exhibits features of phagocytosis with participation of the endoplasmic reticulum. *Experimental and Molecular Pathology*, 79, 126-135.

- MCNALLY, A. K., DEFIFE, K. M. & ANDERSON, J. M. 1996. Interleukin-4-induced macrophage fusion is prevented by inhibitors of mannose receptor activity. *The American Journal of Pathology*, 149, 975.
- MCNALLY, A. K., MACEWAN, S. R., ANDERSON, J. M. J. J. O. B. M. R. P. A. A. O. J. O. T. S. F. B., THE JAPANESE SOCIETY FOR BIOMATERIALS., BIOMATERIALS, T. A. S. F. & BIOMATERIALS, T. K. S. F. 2007.  $\alpha$  subunit partners to  $\beta$ 1 and  $\beta$ 2 integrins during IL-4-induced foreign body giant cell formation. *Journal of Biomedical Materials Research*, 82, 568-574.
- MÉLANIE, F., CLAUDIA, M., SIMONA, C., ENRICO, T., ANDREA, B., LORENA, C., LIVIO, T., COMOGLIO, P. M. & LUCA, T. J. 2010. The tetraspanin CD151 is required for Met-dependent signaling and tumor cell growth. *Journal of Biological Chemistry*, 285, 38756-64.
- MENELAOS, S., MARIE, L., ROY, N. H. & MARKUS, T. 2014. Evidence showing that tetraspanins inhibit HIV-1-induced cell-cell fusion at a post-hemifusion stage. *Viruses*, 6, 1078-1090.
- MIAO, E. A., LEAF, I. A., TREUTING, P. M., MAO, D. P., DORS, M., SARKAR, A., WARREN, S. E., WEWERS, M. D. & ADEREM, A. 2010. Caspase-1-induced pyroptosis is an innate immune effector mechanism against intracellular bacteria. *Nature Immunology*, 11, 1136.
- MICHEVA-VITEVA, S. N., SHOU, Y., GANGULY, K., WU, T. H. & HONG-GELLER, E. 2017. PKC- $\eta$ -MARCKS Signaling Promotes Intracellular Survival of Unopsonized *Burkholderia thailandensis*. *Frontiers in cellular and infection microbiology*, 7, 231.
- MILDE, R., RITTER, J., TENNENT, G. A., LOESCH, A., MARTINEZ, F. O., GORDON, S., PEPYS, M. B., VERSCHOOR, A. & HELMING, L. 2015. Multinucleated giant cells are specialized for complement-mediated phagocytosis and large target destruction. *Cell reports*, 13, 1937-1948.
- MIRKINA, I., HADZIJUSUFOVIC, E., KREPLER, C., MIKULA, M., MECHTCHERIAKOVA, D., STROMMER, S., STELLA, A., JENSEN-JAROLIM, E., HÖLLER, C. & WACHECK, V. 2014. Phenotyping of human melanoma cells reveals a unique composition of receptor targets and a subpopulation co-expressing ErbB4, EPO-R and NGF-R. *PLoS One*, 9, e84417.
- MIRZAYANS, R., ANDRAIS, B. & MURRAY, D. 2018. Roles of polyploid/multinucleated giant cancer cells in metastasis and disease relapse following anticancer treatment. *Cancers*, 10, 118.
- MITAMURA, T., IWAMOTO, R., UMATA, T., YOMO, T., URABE, I., TSUNEOKA, M. & MEKADA, E. 1992. The 27-kD diphtheria toxin receptor-associated protein (DRAP27) from vero cells is the monkey homologue of human CD9 antigen: expression of DRAP27 elevates the number of diphtheria toxin receptors on toxin-sensitive cells. *Journal of Cell Biology*, 118, 1389.
- MIYADO, K., YAMADA, G., YAMADA, S., HASUWA, H., NAKAMURA, Y., RYU, F., SUZUKI, K., KOSAI, K., INOUE, K. & OGURA, A. 2000. Requirement of CD9 on the egg plasma membrane for fertilization. *Science*, 287, 321-324.
- MÓNICA, S. V., ANGELES, U., STÉPHANIE, C., ERIC, R., HEMLER, M. E., FRANCISCO, S. M. & MARÍA, Y. E. M. 2006. EWI-2 and EWI-F link the tetraspanin web to the actin cytoskeleton through their direct association with ezrin-radixin-moesin proteins. *Journal of Biological Chemistry*, 281, 19665-75.
- MONK, P. & J PARTRIDGE, L. 2012. Tetraspanins-gateways for infection. *Infectious Disorders-Drug Targets (Formerly Current Drug Targets-Infectious Disorders)*, 12, 4-17.
- MORAES, T. F., SPRETER, T. & STRYNADKA, N. C. 2008. Piecing together the type III injectisome of bacterial pathogens. *Current Opinion in Structural Biology*, 18, 258-266.

- MORTENSEN, K., LICHTENBERG, J., THOMSEN, P. & LARSSON, L. 2004. Spontaneous fusion between cancer cells and endothelial cells. *Cellular Molecular Life Sciences CMLS*, 61, 2125-2131.
- MÖST, J., NEUMAYER, H. P. & DIERICH, M. P. 1990. Cytokine-induced generation of multinucleated giant cells in vitro requires interferon- $\gamma$  and expression of LFA-1. *European Journal of Immunology*, 20, 1661-1667.
- MÖST, J., SPÖTL, L., MAYR, G., GASSER, A., SARTI, A. & DIERICH, M. P. 1997. Formation of multinucleated giant cells in vitro is dependent on the stage of monocyte to macrophage maturation. *Blood*, 89, 662-671.
- MYNOTT, T. L., CROSSETT, B. & PRATHALINGAM, S. R. 2002. Proteolytic Inhibition of Salmonella enterica Serovar Typhimurium-Induced Activation of the Mitogen-Activated Protein Kinases ERK and JNK in Cultured Human Intestinal Cells. *Infection and Immunity*, 70, 86-95.
- N MONK, P. & J PARTRIDGE, L. 2012. Tetraspanins-gateways for infection. *Infectious Disorders-Drug Targets (Formerly Current Drug Targets-Infectious Disorders)*, 12, 4-17.
- NAMBA, K., NISHIO, M., MORI, K., MIYAMOTO, N., TSURUDOME, M., ITO, M., KAWANO, M., UCHIDA, A. & ITO, Y. 2001. Involvement of ADAM9 in multinucleated giant cell formation of blood monocytes. *Cellular Immunology*, 213, 104-113.
- NGAUY, V., LEMESHEV, Y., SADKOWSKI, L. & CRAWFORD, G. 2005. Cutaneous melioidosis in a man who was taken as a prisoner of war by the Japanese during World War II. *Journal of Clinical Microbiology*, 43, 970-972.
- NICKERSON, C. A. & CURTISS, R. 1997. Role of sigma factor RpoS in initial stages of Salmonella typhimurium infection. *Infection and Immunity*, 65, 1814-1823.
- NIKAIDO, H. 2003. Molecular basis of bacterial outer membrane permeability revisited. *Microbiology and Molecular Biology Reviews*, 67, 593-656.
- NOBUO, T., KAREN, B., MIKE, K., SHONA, M., BROPHY, P. J., CLAUDE, B., CARL, B., GRAHAME, K. & TRAPP, B. D. 2002. The tetraspanin protein, CD9, is expressed by progenitor cells committed to oligodendrogenesis and is linked to beta1 integrin, CD81, and Tspan-2. *Glia*, 40, 350.
- NYDEGGER, S., KHURANA, S., KREMENTSOV, D. N., FOTI, M. & THALI, M. 2006. Mapping of tetraspanin-enriched microdomains that can function as gateways for HIV-1. *The Journal of Cell Biology*, 173, 795-807.
- OHGIMOTO, S., TABATA, N., SUGA, S., NISHIO, M., OHTA, H., TSURUDOME, M., KOMADA, H., KAWANO, M., WATANABE, N. & ITO, Y. 1995. Molecular characterization of fusion regulatory protein-1 (FRP-1) that induces multinucleated giant cell formation of monocytes and HIV gp160-mediated cell fusion. FRP-1 and 4F2/CD98 are identical molecules. *The Journal of Immunology*, 155, 3585-3592.
- OKAMOTO, H., MIZUNO, K. & HORIO, T. 2003. Langhans-type and foreign-body-type multinucleated giant cells in cutaneous lesions of sarcoidosis. *Acta Dermato-Venereologica*, 83, 171-174.
- OREN, R., TAKAHASHI, S., DOSS, C., LEVY, R. & LEVY, S. 1990. TAPA-1, the target of an antiproliferative antibody, defines a new family of transmembrane proteins. *Molecular and cellular biology*, 10, 4007-4015.
- OTSUBO, C., OTOMO, R., MIYAZAKI, M., MATSUSHIMA-HIBIYA, Y., KOHNO, T., IWAKAWA, R., TAKESHITA, F., OKAYAMA, H., ICHIKAWA, H. & SAYA, H. 2014. TSPAN2 is involved in cell invasion and motility during lung cancer progression. *Cell reports*, 7, 527-538.
- OTTO, M. 2014. *Staphylococcus aureus* toxins. *Current opinion in microbiology*, 17, 32-37.
- OZGE, U. K., BECKER, S. N., HONGJU, D., WEI, Z., PRIOR, J. L., DAVID, P. W., FRAZIER, W. A. & WEILBAECHER, K. N. 2009. CD47 regulates bone mass and tumor metastasis to bone. *Cancer Research*, 69, 3196.

- OZYILMAZ, E., AKAN, O. A., GULHAN, M., AHMED, K. & NAGATAKE, T. 2005. Major bacteria of community-acquired respiratory tract infections in Turkey. *Japanese journal of infectious diseases*, 58, 50-52.
- PALACZ-WROBEL, M., BORKOWSKA, P., PAUL-SAMOJEDNY, M., KOWALCZYK, M., FILA-DANILOW, A., SUCHANEK-RAIF, R., KOWALSKI, J. J. B. & PHARMACOTHERAPY 2017. Effect of apigenin, kaempferol and resveratrol on the gene expression and protein secretion of tumor necrosis factor alpha (TNF- $\alpha$ ) and interleukin-10 (IL-10) in RAW-264.7 macrophages. 93, 1205-1212.
- PAOLA, D., CHRISTIAN, H. C., REDMAN, C. W. G., SARGENT, I. L. & BOYD, C. A. R. 2007. Differential effect of cross-linking the CD98 heavy chain on fusion and amino acid transport in the human placental trophoblast (BeWo) cell line. *Biochimica et Biophysica Acta (BBA)-Biomembranes*, 1768, 401-410.
- PAPPENHEIMER, A. M., JR. 1977. Diphtheria toxin. *Annual Review of Biochemistry*, 46, 69-94.
- PARRISH, N. M., DICK, J. D. & BISHAI, W. R. 1998. Mechanisms of latency in *Mycobacterium tuberculosis*. *Trends in Microbiology*, 6, 107-112.
- PARTHASARATHY, V., MARTIN, F., HIGGINBOTTOM, A., MURRAY, H., MOSELEY, G. W., READ, R. C., MAL, G., HULME, R., MONK, P. N. & PARTRIDGE, L. J. 2009. Distinct roles for tetraspanins CD9, CD63 and CD81 in the formation of multinucleated giant cells. *Immunology*, 127, 237-248.
- PATIL, R. H., BABU, R., KUMAR, M. N., KUMAR, K. K., HEGDE, S. M., RAMESH, G. T., SHARMA, S. C. J. M. & BIOCHEMISTRY, C. 2015. Apigenin inhibits PMA-induced expression of pro-inflammatory cytokines and AP-1 factors in A549 cells. 403, 95-106.
- PEELING, R. W. & BRUNHAM, R. C. 1996. Chlamydiae as pathogens: new species and new issues. *Emerging Infectious Diseases*, 2, 307.
- PEGORARO, G., EATON, B. P., ULRICH, R. L., LANE, D. J., OJEDA, J. F., BAVARI, S., DESHAZER, D. & PANCHAL, R. G. 2014. A high-content imaging assay for the quantification of the *Burkholderia pseudomallei* induced multinucleated giant cell (MNGC) phenotype in murine macrophages. *BMC microbiology*, 14, 98.
- PERRY, M. B., MACLEAN, L. L., SCHOLLAARDT, T., BRYAN, L. E. & HO, M. 1995. Structural characterization of the lipopolysaccharide O antigens of *Burkholderia pseudomallei*. *Infection and Immunity*, 63, 3348-3352.
- PETER, S. 2009. Sperm-egg adhesion and fusion in mammals. *Expert Reviews in Molecular Medicine*.
- PHUONG, D. M., TRUNG, T. T., BREITBACH, K., TUAN, N. Q., NÜBEL, U., FLUNKER, G., KHANG, D. D., QUANG, N. X. & STEINMETZ, I. 2008. Clinical and microbiological features of melioidosis in northern Vietnam. *Transactions of the Royal Society of Tropical Medicine and Hygiene*, 102, S30-S36.
- PILS, S., SCHMITTER, T., NESKE, F. & HAUCK, C. R. 2006. Quantification of bacterial invasion into adherent cells by flow cytometry. *Journal of Microbiological Methods*, 65, 301-310.
- PIZARRO-CERDÁ, J., PAYRASTRE, B., WANG, Y. J., VEIGA, E., YIN, H. L. & COSSART, P. 2010. Type II phosphatidylinositol 4-kinases promote *Listeria monocytogenes* entry into target cells. *Cellular Microbiology*, 9, 2381-2390.
- POLYAK, K., XIA, Y., ZWEIER, J. L., KINZLER, K. W. & VOGELSTEIN, B. 1997. A model for p53-induced apoptosis. *Nature*, 389, 300-305.
- POSTLETHWAITE, A. E., JACKSON, B. K., BEACHEY, E. H. & KANG, A. H. 1982. Formation of multinucleated giant cells from human monocyte precursors. Mediation by a soluble protein from antigen- and mitogen-stimulated lymphocytes. *The Journal of Experimental Medicine*, 155, 168-178.

- POTISAP, C., KHAN, M. A. W., BOONMEE, A., RODRIGUES, J. L. M., WONGRATANACHEEWIN, S. & SERMSWAN, R. W. 2018. *Burkholderia pseudomallei* -absent soil bacterial community results in secondary metabolites that kill this pathogen. 8, 136.
- PROX, J., WILLENBROCK, M., WEBER, S., LEHMANN, T., SCHMIDT-ARRAS, D., SCHWANBECK, R., SAFTIG, P. & SCHWAKE, M. 2012. Tetraspanin15 regulates cellular trafficking and activity of the ectodomain sheddase ADAM10. *Cellular Molecular Life Sciences*, 69, 2919-2932.
- PUAH, S. M. 2014. *Molecular characterization of putative virulence determinants and identification of specific immunogenic polypeptides for the serological diagnosis of Burkholderia pseudomallei infections/Puah Suat Moi*. University of Malaya.
- PUISSEUR, M.-P., LAY, G., GILLERON, M., BOTELLA, L., NIGOU, J., MARRAKCHI, H., MARI, B., DUTEYRAT, J.-L., GUERARDEL, Y. & KREMER, L. 2007. Mycobacterial lipomannan induces granuloma macrophage fusion via a TLR2-dependent, ADAM9-and  $\beta$ 1 integrin-mediated pathway. *The Journal of Immunology*, 178, 3161-3169.
- PUMIRAT, P., CUCCUI, J., STABLER, R. A., STEVENS, J. M., MUANGSOMBUT, V., SINGSUKSAWAT, E., STEVENS, M. P., WREN, B. W. & KORBSRISATE, S. 2010. Global transcriptional profiling of *Burkholderia pseudomallei* under salt stress reveals differential effects on the Bsa type III secretion system. *BMC microbiology*, 10, 171.
- RACHKOVSKY, M., SODI, S., CHAKRABORTY, A., AVISSAR, Y., BOLOGNIA, J., MCNIFF, J. M., PLATT, J., BERMUDEZ, D. & PAWELEK, J. 1998. Melanomax macrophage hybrids with enhanced metastatic potential. *Clinical Experimental Metastasis*, 16, 299-312.
- RAY, K., MARTEYN, B., SANSONETTI, P. J. & TANG, C. M. 2009. Life on the inside: the intracellular lifestyle of cytosolic bacteria. *Nature Reviews Microbiology*, 7, 333-340.
- REBOUD, E., BOUILLOT, S., PATOT, S., BÉGANTON, B., ATTRÉE, I. & HUBER, P. J. P. P. 2017. *Pseudomonas aeruginosa* ExlA and *Serratia marcescens* ShlA trigger cadherin cleavage by promoting calcium influx and ADAM10 activation. 13, e1006579.
- RECKSEIDLER-ZENTENO, S. L., DEVINNEY, R. & WOODS, D. E. 2005. The capsular polysaccharide of *Burkholderia pseudomallei* contributes to survival in serum by reducing complement factor C3b deposition. *Infection and Immunity*, 73, 1106-1115.
- REGINSSON, G. W., SHELKE, S. A., ROUILLON, C., WHITE, M. F., SIGURDSSON, S. T. & SCHIEMANN, O. 2012. Protein-induced changes in DNA structure and dynamics observed with noncovalent site-directed spin labeling and PELDOR. *Nucleic Acids Research*, 41, e11-e11.
- REISSIG, A., COPETTI, R., MATHIS, G., MEMPEL, C., SCHULER, A., ZECHNER, P., ALIBERTI, S., NEUMANN, R., KROEGEL, C. & HOYER, H. 2012. Lung Ultrasound in the Diagnosis and Follow-up of Community-Acquired Pneumonia: A Prospective, Multicenter, Diagnostic Accuracy Study. *Chest*, 142, 965-972.
- REYAT, J. S., CHIMEN, M., NOY, P. J., SZYROKA, J., RAINGER, G. E. & TOMLINSON, M. G. 2017. ADAM10-Interacting Tetraspanins Tspan5 and Tspan17 Regulate VE-Cadherin Expression and Promote T Lymphocyte Transmigration. *Journal of Immunology*, 199, ji1600713.
- RHEE, I., DAVIDSON, D., SOUZA, C. M., VACHER, J. & VEILLETTE, A. 2013. Macrophage fusion is controlled by the cytoplasmic protein tyrosine phosphatase PTP-PEST/PTPN12. *Molecular and Cellular Biology*, 33, 2458-2469.

- ROSKAMS, J. & MELLICK, A. S. 2002. *Lab ref: a handbook of recipes, reagents, and other reference tools for use at the bench*, CSHL Press.
- RUBINSTEIN, E., ZIYYAT, A., PRENANT, M., WROBEL, E., WOLF, J.-P., LEVY, S., LE NAOUR, F. & BOUCHEIX, C. 2006. Reduced fertility of female mice lacking CD81. *Developmental biology*, 290, 351-358.
- RUBINSTEIN, E., ZIYYAT, A., WOLF, J. P., NAOUR, F. L. & BOUCHEIX, C. 2006. The molecular players of sperm-egg fusion in mammals. *Seminars in Cell Developmental Biology*, 17, 254-263.
- SAGINARIO, C., STERLING, H., BECKERS, C., KOBAYASHI, R., SOLIMENA, M., ULLU, E. & VIGNERY, A. 1998. MFR, a putative receptor mediating the fusion of macrophages. *Molecular and Cellular Biology*, 18, 6213-6223.
- SALA-VALDÉS, M., AILANE, N., GRECO, C., RUBINSTEIN, E. & BOUCHEIX, C. 2012. Targeting tetraspanins in cancer. *Expert Opinion on Therapeutic Targets*, 16, 985-997.
- SAMBROOK, J. & RUSSELL, D. W. 2006. The Hanahan method for preparation and transformation of competent *E. coli*: high-efficiency transformation. *Cold Spring Harbor Protocols*, 2006, pdb. prot3942.
- SANDOR, M., WEINSTOCK, J. V. & WYNN, T. A. 2003. Granulomas in schistosome and mycobacterial infections: a model of local immune responses. *Trends in immunology*, 24, 44-52.
- SAUNDERS, B. M. & BRITTON, W. J. 2007. Life and death in the granuloma: immunopathology of tuberculosis. *Immunology and cell biology*, 85, 103-111.
- SHELL, M. A., ULRICH, R. L., RIBOT, W. J., BRUEGGEMANN, E. E., HINES, H. B., CHEN, D., LIPSCOMB, L., KIM, H. S., MRÁZEK, J. & NIERMAN, W. C. 2007. Type VI secretion is a major virulence determinant in *Burkholderia mallei*. *Molecular Microbiology*, 64, 1466-1485.
- SCHWARZ, S., SINGH, P., ROBERTSON, J. D., LEROUX, M., SKERRETT, S. J., GOODLETT, D. R., WEST, T. E. & MOUGOUS, J. D. 2014. VgrG-5 is a *Burkholderia* type VI secretion system-exported protein required for multinucleated giant cell formation and virulence. *Infection and Immunity*, 82, 1445-1452.
- SCHWARZ, S., WEST, T. E., BOYER, F., CHIANG, W.-C., CARL, M. A., HOOD, R. D., ROHMER, L., TOLKER-NIELSEN, T., SKERRETT, S. J. & MOUGOUS, J. D. 2010. *Burkholderia* type VI secretion systems have distinct roles in eukaryotic and bacterial cell interactions. *PLoS Pathogens*, 6, e1001068.
- SCHWEIZER, H. P., LIMMATHUROTSAKUL, D. & PEACOCK, S. J. 2014. New insights from the 7th World Melioidosis Congress 2013. *Emerg Infect Dis*, 20.
- SEALS, D. F. & COURTNEIDGE, S. A. 2003. The ADAMs family of metalloproteases: multidomain proteins with multiple functions. *Genes & Development*, 17, 7-30.
- SEEHAFER, J. G., TANG, S. C., SLUPSKY, J. R. & SHAW, A. R. 1988. The functional glycoprotein CD9 is variably acylated: localization of the variably acylated region to a membrane-associated peptide containing the binding site for the agonistic monoclonal antibody 50H. 19. *Biochimica et Biophysica Acta (BBA)-Protein Structure and Molecular Enzymology*, 957, 399-410.
- SEGOVIA-SILVESTRE, T., KOLDING, I., JENSEN, V., KARSDAL, M. & HENRIKSEN, K. 2009. Osteopetrosis associated transmembrane protein 1 is a chloride channel 7 functional subunit that increases its ability to acidify intracellular compartments. *Bone*, S243.
- SEIGNEURET, M., DELAGUILLAUMIE, A., LAGAUDRIÈRE-GESBERT, C. & CONJEAUD, H. 2001. Structure of the Tetraspanin Main Extracellular Domain A PARTIALLY CONSERVED FOLD WITH A STRUCTURALLY VARIABLE DOMAIN INSERTION. *Journal of Biological Chemistry*, 276, 40055-40064.

- SEIPOLD, L. & SAFTIG, P. 2016. The Emerging Role of Tetraspanins in the Proteolytic Processing of the Amyloid Precursor Protein. *Frontiers in Molecular Neuroscience*, 9.
- SHALOM, G., SHAW, J. G. & THOMAS, M. S. 2007. In vivo expression technology identifies a type VI secretion system locus in *Burkholderia pseudomallei* that is induced upon invasion of macrophages. *Microbiology*, 153, 2689-2699.
- SHAMS, A. M., ROSE, L. J., HODGES, L. & ARDUINO, M. J. 2007. Survival of *Burkholderia pseudomallei* on Environmental Surfaces. *Appl Environ Microbiol*, 73, 8001-4.
- SHILAGARDI, K., LI, S., LUO, F., MARIKAR, F., DUAN, R., JIN, P., KIM, J. H., MURNEN, K. & CHEN, E. H. 2013. Actin-propelled invasive membrane protrusions promote fusogenic protein engagement during cell-cell fusion. *Science*, 340, 359-363.
- SHUSTER, M. I., HAN, L., LE BEAU, M. M., DAVIS, E., SAWICKI, M., LESE, C. M., PARK, N. H., COLICELLI, J. & GOLLIN, S. M. 2000. A consistent pattern of RIN1 rearrangements in oral squamous cell carcinoma cell lines supports a breakage-fusion-bridge cycle model for 11q13 amplification. *Genes, Chromosomes and Cancer*, 28, 153-163.
- SILVA, E. B. & DOW, S. 2013. Development of *Burkholderia mallei* and *pseudomallei* vaccines. *Frontiers in Cellular and Infection Microbiology*, 3, 10.
- SIMONET, W., LACEY, D., DUNSTAN, C., KELLEY, M., CHANG, M.-S., LÜTHY, R., NGUYEN, H., WOODEN, S., BENNETT, L. & BOONE, T. 1997. Osteoprotegerin: a novel secreted protein involved in the regulation of bone density. *Cell*, 89, 309-319.
- SITTHIDET, C., KORBSRISATE, S., LAYTON, A. N., FIELD, T. R., STEVENS, M. P. & STEVENS, J. M. 2011. Identification of motifs of *Burkholderia pseudomallei* BimA required for intracellular motility, actin binding, and actin polymerization. *Journal of bacteriology*, 193, 1901-1910.
- SMITH, M., ANGUS, B., WUTHIEKANUN, V. & WHITE, N. 1997. Arabinose assimilation defines a nonvirulent biotype of *Burkholderia pseudomallei*. *Infection and immunity*, 65, 4319-4321.
- SMITH, D. B. & JOHNSON, K. S. 1988. Single-step purification of polypeptides expressed in *Escherichia coli* as fusions with glutathione S-transferase. *Gene*, 67, 31-40.
- SONG, I., KIM, J. H., KIM, K., JIN, H. M., YOUN, B. U. & KIM, N. 2009. Regulatory mechanism of NFATc1 in RANKL-induced osteoclast activation. *FEBS Letters*, 583, 2435-2440.
- SONG, Y., XIE, C., ONG, Y.-M., GAN, Y.-H. & CHUA, K.-L. 2005. The BpsIR quorum-sensing system of *Burkholderia pseudomallei*. *Journal of Bacteriology*, 187, 785-790.
- STERLING, H., SAGINARIO, C. & VIGNERY, A. 1998. CD44 occupancy prevents macrophage multinucleation. *Journal of Cell Biology*, 143, 837-847.
- STEVENS, M. P. & GALYOV, E. E. 2004. Exploitation of host cells by *Burkholderia pseudomallei*. *International Journal of Medical Microbiology*, 293, 549-555.
- STEVENS, M. P., HAQUE, A., ATKINS, T., HILL, J., WOOD, M. W., EASTON, A., NELSON, M., UNDERWOOD-FOWLER, C., TITBALL, R. W. & BANCROFT, G. J. 2004. Attenuated virulence and protective efficacy of a *Burkholderia pseudomallei* bsa type III secretion mutant in murine models of melioidosis. *Microbiology*, 150, 2669-2676.
- STEVENS, M. P., STEVENS, J. M., JENG, R. L., TAYLOR, L. A., WOOD, M. W., HAWES, P., MONAGHAN, P., WELCH, M. D. & GALYOV, E. E. 2005. Identification of a bacterial factor required for actin-based motility of *Burkholderia pseudomallei*. *Molecular Microbiology*, 56, 40-53.
- STEVENS, M. P., WOOD, M. W., TAYLOR, L. A., MONAGHAN, P., HAWES, P., JONES, P. W., WALLIS, T. S. & GALYOV, E. E. 2002. An Inv/Mxi-Spa-like

- type III protein secretion system in *Burkholderia pseudomallei* modulates intracellular behaviour of the pathogen. *Molecular Microbiology*, 46, 649-659.
- STIPP, C. & KOLESNIKOVA, T., ME 2001. EWI-2 is a major CD9 and CD81 partner and member of a novel Ig protein subfamily. *Journal of Biological Chemistry*, 276, 40545-40554.
- STIPP, C. S. 2010. Laminin-binding integrins and their tetraspanin partners as potential antimetastatic targets. *Expert Reviews in Molecular Medicine*, 12.
- STIPP, C. S., KOLESNIKOVA, T. V. & HEMLER, M. E. 2003. Functional domains in tetraspanin proteins. *Trends in Biochemical Sciences*, 28, 106-112.
- SUBRAMONI, S. & VENTURI, V. 2009. LuxR-family 'solos': bachelor sensors/regulators of signalling molecules. *Microbiology*, 155, 1377-1385.
- SUBSIN, B., THOMAS, M. S., KATZENMEIER, G., SHAW, J. G., TUNGPRADABKUL, S. & KUNAKORN, M. 2003. Role of the stationary growth phase sigma factor RpoS of *Burkholderia pseudomallei* in response to physiological stress conditions. *Journal of Bacteriology*, 185, 7008-7014.
- SUNG, B. H. & WEAVER, A. M. 2011. Regulation of lysosomal secretion by cortactin drives fibronectin deposition and cell motility. *Bioarchitecture*, 1, 4.
- SUPARAK, S., KESPICHAYAWATTANA, W., HAQUE, A., EASTON, A., DAMNIN, S., LERTMEMONGKOLCHAI, G., BANCROFT, G. J. & KORBSRISATE, S. 2005. Multinucleated giant cell formation and apoptosis in infected host cells is mediated by *Burkholderia pseudomallei* type III secretion protein BipB. *Journal of Bacteriology*, 187, 6556-6560.
- SUPARAK, S., MUANGSOMBUT, V., RIYAPA, D., STEVENS, J. M., STEVENS, M. P., LERTMEMONGKOLCHAI, G. & KORBSRISATE, S. 2011. *Burkholderia pseudomallei* -induced cell fusion in U937 macrophages can be inhibited by monoclonal antibodies against host cell surface molecules. *Microbes and Infection*, 13, 1006-1011.
- SUZUKI, M., TACHIBANA, I., TAKEDA, Y., HE, P., MINAMI, S., IWASAKI, T., KIDA, H., GOYA, S., KIJIMA, T. & YOSHIDA, M. 2009. Tetraspanin CD9 negatively regulates lipopolysaccharide-induced macrophage activation and lung inflammation. *The Journal of Immunology*, 182, 6485-6493.
- SZYROKA, J. 2019. Regulation of the 'molecular scissor'ADAM10 by tetraspanin Tspan15. University of Birmingham.
- TAKAHASHI, Y., BIGLER, D., ITO, Y. & WHITE, J. M. 2001. Sequence-specific interaction between the disintegrin domain of mouse ADAM 3 and murine eggs: role of  $\beta$ 1 integrin-associated proteins CD9, CD81, and CD98. *Molecular Biology of the Cell*, 12, 809-820.
- TAKASHIMA, T., OHNISHI, K., TSUYUGUCHI, I. & KISHIMOTO, S. 1993. Differential regulation of formation of multinucleated giant cells from concanavalin A-stimulated human blood monocytes by IFN-gamma and IL-4. *The Journal of Immunology*, 150, 3002-3010.
- TAKEDA, Y., HE, P., TACHIBANA, I., ZHOU, B., MIYADO, K., KANEKO, H., SUZUKI, M., MINAMI, S., IWASAKI, T. & GOYA, S. 2008. Double deficiency of tetraspanins CD9 and CD81 alters cell motility and protease production of macrophages and causes chronic obstructive pulmonary disease-like phenotype in mice. *Journal of Biological Chemistry*, 283, 26089-26097.
- TAKEDA, Y., TACHIBANA, I., MIYADO, K., KOBAYASHI, M., MIYAZAKI, T., FUNAKOSHI, T., KIMURA, H., YAMANE, H., SAITO, Y. & GOTO, H. 2003. Tetraspanins CD9 and CD81 function to prevent the fusion of mononuclear phagocytes. *The Journal of Cell Biology*, 161, 945-956.
- TAKITO, J., NAKAMURA, M., YODA, M., TOHMONDA, T., UCHIKAWA, S., HORIUCHI, K., TOYAMA, Y. & CHIBA, K. 2012. The transient appearance of zipper-like actin superstructures during the fusion of osteoclasts. *Journal of Cell Science*, 125, 662-672.

- TAKITO, J., OTSUKA, H., YANAGISAWA, N., ARAI, H., SHIGA, M., INOUE, M., NONAKA, N. & NAKAMURA, M. 2015. Regulation of osteoclast multinucleation by the actin cytoskeleton signaling network. *Journal of Cellular Physiology*, 230, 395-405.
- TARRANT, J. M., ROBB, L., VAN SPRIEL, A. B. & WRIGHT, M. D. 2003. Tetraspanins: molecular organisers of the leukocyte surface. *Trends in Immunology*, 24, 610-617.
- TEITELBAUM, J. E., JOHNSON, C. & CYR, J. S. 2006. The use of D-ribose in chronic fatigue syndrome and fibromyalgia: a pilot study. *Journal of Alternative Complementary Medicine*, 12, 857-862.
- TEITELBAUM, S. L. 2005. Osteoclasts; culprits in inflammatory osteolysis. *Arthritis Research & Therapy*, 8, 201.
- TERADA, N., BARACSKAY, K., KINTER, M., MELROSE, S., BROPHY, P. J., BOUCHEIX, C., BJARTMAR, C., KIDD, G. & TRAPP, B. D. 2002. The tetraspanin protein, CD9, is expressed by progenitor cells committed to oligodendrogenesis and is linked to  $\beta 1$  integrin, CD81, and Tspan- 2. *Glia*, 40, 350-359.
- THAM, T. N., GOUIN, E., RUBINSTEIN, E., BOUCHEIX, C., COSSART, P. & PIZARRO-CERDA, J. 2010. Tetraspanin CD81 is required for *Listeria monocytogenes* invasion. *Infection and Immunity*, 78, 204-209.
- THIBAUT, F., VALADE, E. & VIDAL, D. 2004. Identification and discrimination of *Burkholderia pseudomallei*, *B. mallei*, and *B. thailandensis* by real-time PCR targeting type III secretion system genes. *Journal of Clinical Microbiology*, 42, 5871-5874.
- TODRES, E., NARDI, J. & ROBERTSON, H. 2000. The tetraspanin superfamily in insects. *Insect Molecular Biology*, 9, 581-590.
- TOESCA, I. J., FRENCH, C. T. & MILLER, J. F. 2014. The Type VI secretion system spike protein VgrG5 mediates membrane fusion during intercellular spread by pseudomallei group *Burkholderia* species. *Infection and Immunity*, 82, 1436-1444.
- TSIPI, S., RANJANI, R., CLAUDE, B., ERIC, R., POE, J. C., TEDDER, T. F. & SHOSHANA, L. 2003. The tetraspanin CD81 regulates the expression of CD19 during B cell development in a postendoplasmic reticulum compartment. *Journal of Immunology*, 171, 4062-72.
- TU, L., SUN, T. T. & KREIBICH, G. 2002. Specific heterodimer formation is a prerequisite for uroplakins to exit from the endoplasmic reticulum. *Molecular Biology of the Cell*, 13, 4221.
- UTAISINCHAROEN, P., ANUNTAGOOL, N., LIMPOSUWAN, K., CHAISURIYA, P. & SIRISINHA, S. 2003. Involvement of beta interferon in enhancing inducible nitric oxide synthase production and antimicrobial activity of *Burkholderia pseudomallei*-infected macrophages. *Infection and Immunity*, 71, 3053-3057.
- UTAISINCHAROEN, P., ARJCHAROEN, S., LIMPOSUWAN, K., TUNGPRADABKUL, S. & SIRISINHA, S. 2006. *Burkholderia pseudomallei* RpoS regulates multinucleated giant cell formation and inducible nitric oxide synthase expression in mouse macrophage cell line (RAW 264.7). *Microb Pathog*, 40, 184-9.
- UTAISINCHAROEN, P., TANGTHAWORNCHAIKUL, N., KESPICHAYAWATTANA, W., CHAISURIYA, P. & SIRISINHA, S. 2001. *Burkholderia pseudomallei* interferes with inducible nitric oxide synthase (iNOS) production: a possible mechanism of evading macrophage killing. *Microbiology and Immunology*, 45, 307-313.
- VALDIVIA, R. H. 1998. Flow cytometry and bacterial pathogenesis. *Current Opinion in Microbiology*, 1, 359-363.
- VAN SPRIEL, A. B. & FIGDOR, C. G. 2010. The role of tetraspanins in the pathogenesis of infectious diseases. *Microbes and Infection*, 12, 106-112.

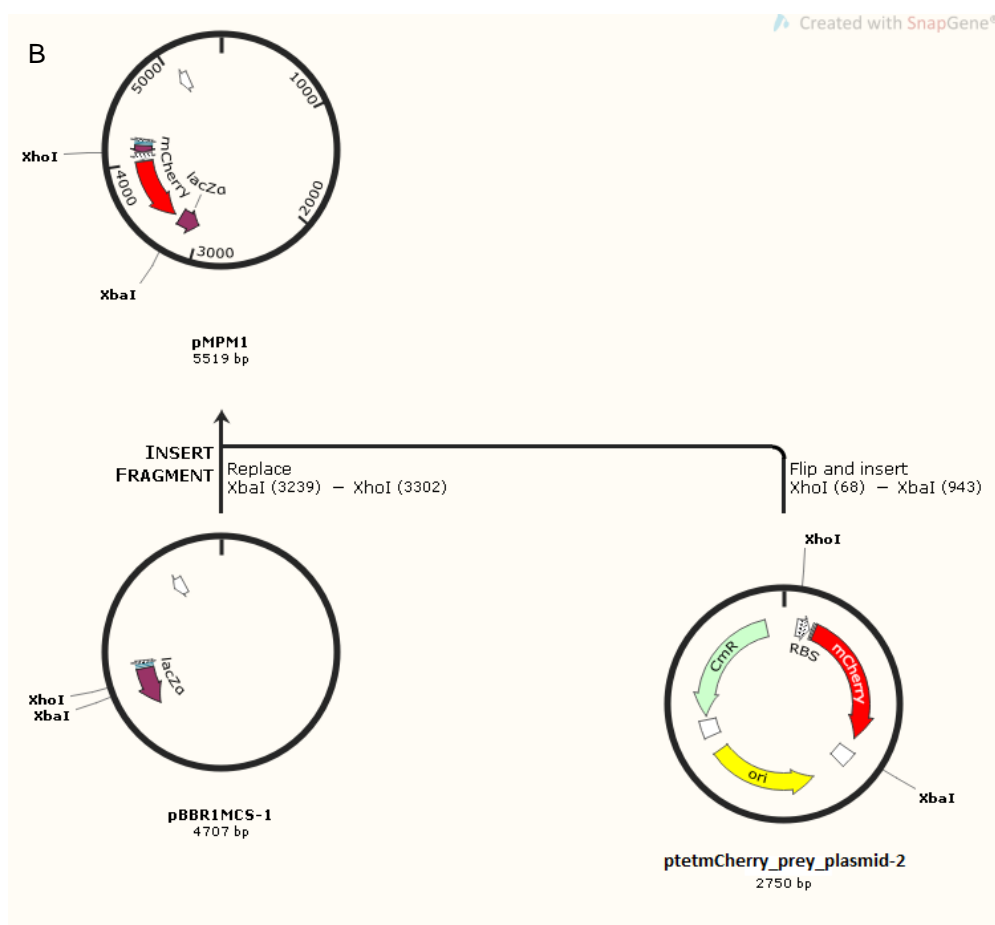
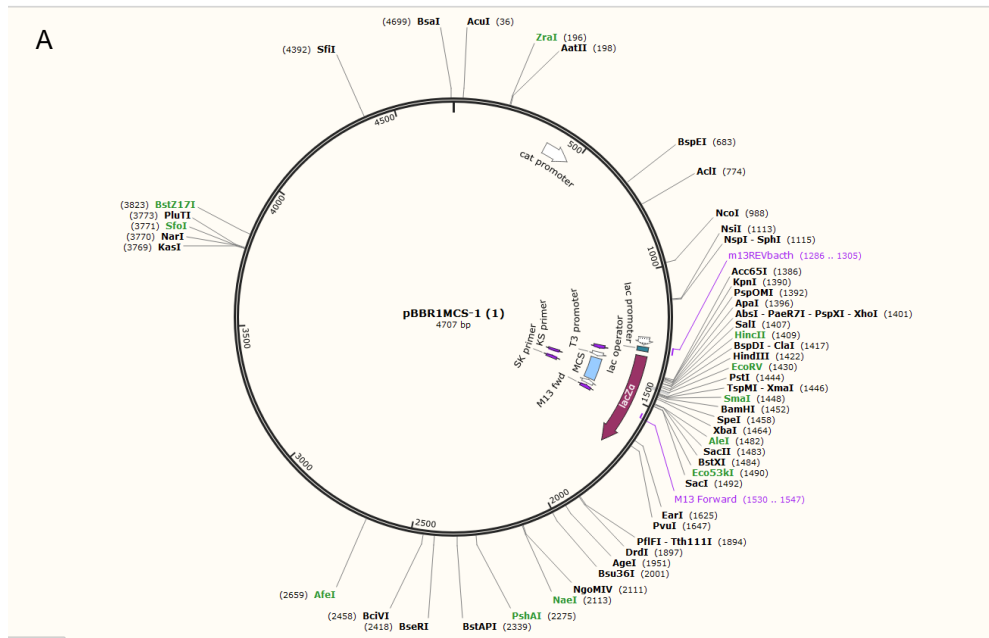
- VANDER BROEK, C. W. & STEVENS, J. M. 2017. Type III Secretion in the Melioidosis Pathogen *Burkholderia pseudomallei*. *Front Cell Infect Microbiol*, 7, 255.
- VANICHA, V. & KANYAWIM, K. 2006. Sulforhodamine B colorimetric assay for cytotoxicity screening. *Nature Protocols*, 1, 1112-1116.
- VENTRESS, J. K., PARTRIDGE, L. J., READ, R. C., COZENS, D., MACNEIL, S. & MONK, P. N. 2016. Peptides from Tetraspanin CD9 Are Potent Inhibitors of *Staphylococcus aureus* Adherence to Keratinocytes. *Plos One*, 11, e0160387.
- VERRIER, S., HOGAN, A., MCKIE, N. & HORTON, M. 2004. ADAM gene expression and regulation during human osteoclast formation. *Bone*, 35, 34-46.
- VIGNERY, A. 2005. Macrophage fusion: the making of osteoclasts and giant cells. *Journal of Experimental Medicine*, 202, 337-340.
- VIGNERY, A. 2008. Macrophage Fusion. *Cell Fusion*. Springer.
- VON, H. G., RIVAS, A. J., NEUKIRCH, C., KLEIN, S., HAMM, C., QIN, Q., MEYENBURG, M., FÜSER, S., SAFTIG, P. & HELLMANN, N. 2016. Dissecting the role of ADAM10 as a mediator of *S. aureus*  $\alpha$ -toxin action. *Biochemical Journal*, 473, 1929.
- WALI, J., MASTERS, S. & THOMAS, H. 2013. Linking metabolic abnormalities to apoptotic pathways in beta cells in type 2 diabetes. *Cells*, 2, 266-283.
- WAND, M. E., MÜLLER, C. M., TITBALL, R. W. & MICHELL, S. L. 2011. Macrophage and *Galleria mellonella* infection models reflect the virulence of naturally occurring isolates of *B. pseudomallei*, *B. thailandensis* and *B. oklahomensis*. *BMC microbiology*, 11, 11.
- WANG, K., KANG, L., ANAND, A., LAZAROVITS, G. & MYSORE, K. S. 2007. Monitoring in planta bacterial infection at both cellular and whole-plant levels using the green fluorescent protein variant GFPuv. *New Phytologist*, 174, 212-223.
- WANG, R., SUN, X., WANG, C. Y., HU, P., CHU, C.-Y., LIU, S., ZHAU, H. E. & CHUNG, L. W. 2012. Spontaneous cancer-stromal cell fusion as a mechanism of prostate cancer androgen-independent progression. *PLoS One*, 7, e42653.
- WANG, X. X. & PFENNINGER, K. H. 2006. Functional analysis of SIRPalpha in the growth cone. *Journal of Cell Science*, 119, 172.
- WEIGUO, C., JUAN ZHANG, K., QING, Z., HUA-ZHU, K., CÉCILE, C. & AGNÈS, V. 2006. The intracellular domain of CD44 promotes the fusion of macrophages. *Blood*, 107, 796.
- WEISS, A. R. 2018. *The Role of the Tissue Inhibitor of Metalloproteinase Family in the Bone Marrow Niche*. University of Toronto (Canada).
- WEST, T. E., FREVERT, C. W., LIGGITT, H. D. & SKERRETT, S. J. 2008. Inhalation of *Burkholderia thailandensis* results in lethal necrotizing pneumonia in mice: a surrogate model for pneumonic melioidosis. *Transactions of the Royal Society of Tropical Medicine and Hygiene*, 102, S119-S126.
- WEST, T. E., MYERS, N. D., LIGGITT, H. D. & SKERRETT, S. J. 2012. Murine pulmonary infection and inflammation induced by inhalation of *Burkholderia pseudomallei*. *International Journal of Experimental Pathology*, 93, 421-428.
- WHITELEY, L., HAUG, M., KLEIN, K., WILLMANN, M., BOHN, E., CHIANTIA, S. & SCHWARZ, S. 2017. Cholesterol and host cell surface proteins contribute to cell-cell fusion induced by the *Burkholderia* type VI secretion system 5. *PloS one*, 12, e0185715.
- WHITELEY, L., MEFFERT, T., HAUG, M., WEIDENMAIER, C., HOPF, V., BITSCHAR, K., SCHITTEK, B., KOHLER, C., STEINMETZ, I. & WEST, T. E. 2017. Entry, intracellular survival, and multinucleated-giant-cell-forming activity of *Burkholderia pseudomallei* in human primary phagocytic and nonphagocytic cells. *Infection and immunity*, 85, e00468-17.

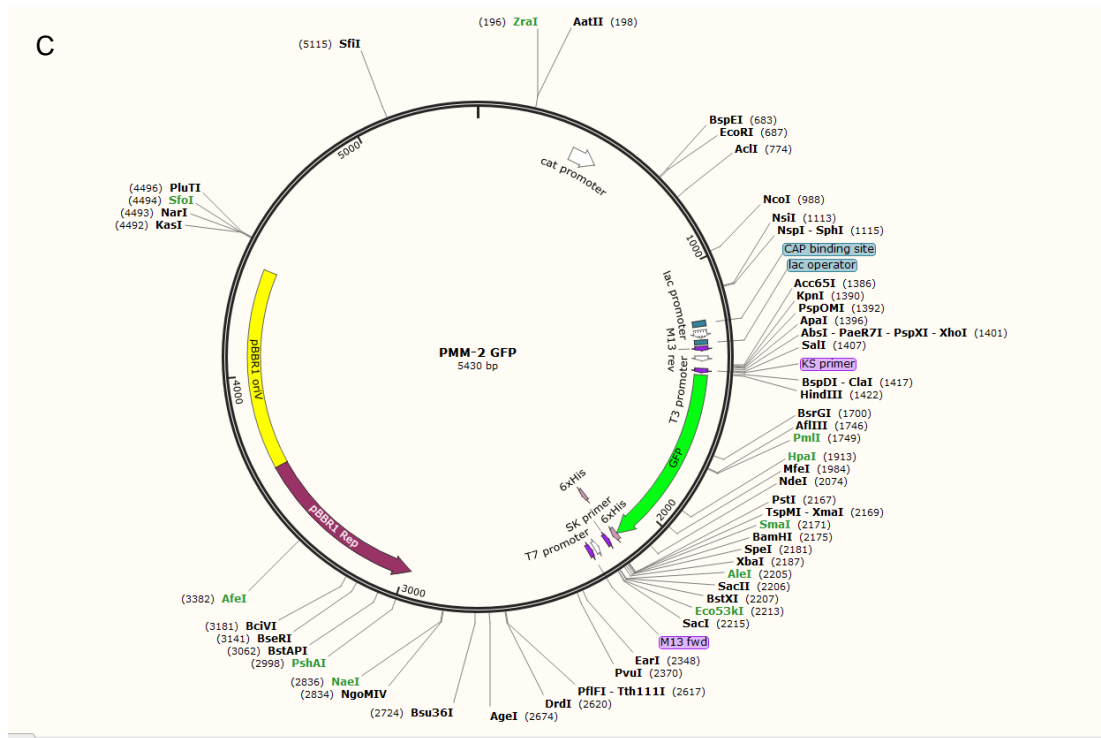
- WHITFIELD, C. & TRENT, M. S. 2014. Biosynthesis and export of bacterial lipopolysaccharides. *Annual Review of Biochemistry*, 83, 99-128.
- WHITMORE, A. 1913. An account of a glanders-like disease occurring in Rangoon. *Epidemiology & Infection*, 13, 1-34.
- WHITMORE, A. & KRISHNASWAMI, C. 1912. A hitherto undescribed infective disease in Rangoon. *The Indian Medical Gazette*, 47, 262.
- WIERSINGA, W. J., CURRIE, B. J. & PEACOCK, S. J. 2012. Melioidosis. *New England Journal of Medicine*, 367, 1035-1044.
- WIERSINGA, W. J., DE VOS, A. F., DE BEER, R., WIELAND, C. W., ROELOFS, J. J., WOODS, D. E. & VAN DER POLL, T. 2008. Inflammation patterns induced by different *Burkholderia* species in mice. *Cellular Microbiology*, 10, 81-87.
- WIERSINGA, W. J., VAN DER POLL, T., WHITE, N. J., DAY, N. P. & PEACOCK, S. J. 2006. Melioidosis: insights into the pathogenicity of *Burkholderia pseudomallei*. *Nature Reviews Microbiology*, 4, 272.
- WIKRAIPHAT, C., CHAROENSAP, J., UTAISINCHAROEN, P., WONGRATANACHEEWIN, S., TAWEECHAI SUPAPONG, S., WOODS, D. E., BOLSCHER, J. G. & SIRISINHA, S. 2009. Comparative in vivo and in vitro analyses of putative virulence factors of *Burkholderia pseudomallei* using lipopolysaccharide, capsule and flagellin mutants. *FEMS Immunology & Medical Microbiology*, 56, 253-259.
- WILSON, J. R. & CORLETT, N. 2005. *Evaluation of human work*, CRC press.
- WONG, K., PUTHUCHEARY, S. & VADIVELU, J. 1995. The histopathology of human melioidosis. *Histopathology*, 26, 51-55.
- WONGPROMPITAK, P., SIRISINHA, S. & CHAIYAROJ, S. C. 2009. Differential gene expression profiles of lung epithelial cells exposed to *Burkholderia pseudomallei* and *Burkholderia thailandensis* during the initial phase of infection. *Asian Pacific journal of allergy and immunology*, 27, 59.
- WU, X. R., SUN, T. T. & MEDINA, J. J. 1996. In vitro binding of type 1-fimbriated *Escherichia coli* to uroplakins Ia and Ib: relation to urinary tract infections. *Proceedings of the National Academy of Sciences of the United States of America*, 93, 9630-9635.
- XIN, A., ZHANG, LANE, W. S., STEPHANIE, C., ERIC, R. & LEI, L. 2003. EWI2/PGRL associates with the metastasis suppressor KAI1/CD82 and inhibits the migration of prostate cancer cells. *Cancer Research*, 63, 2665.
- YAGI, M., MIYAMOTO, T., SAWATANI, Y., IWAMOTO, K., HOSOGANE, N., FUJITA, N., MORITA, K., NINOMIYA, K., SUZUKI, T. & MIYAMOTO, K. 2005. DC-STAMP is essential for cell-cell fusion in osteoclasts and foreign body giant cells. *Journal of Experimental Medicine*, 202, 345-351.
- YÁÑEZ-MÓ, M., TEJEDOR, R., ROUSSELLE, P. & SÁNCHEZ-MADRID, F. 2001. Tetraspanins in intercellular adhesion of polarized epithelial cells: spatial and functional relationship to integrins and cadherins. *Journal of Cell Science*, 114, 577-587.
- YANG, X., CLAAS, C., KRAEFT, S.-K., CHEN, L. B., WANG, Z., KREIDBERG, J. A. & HEMLER, M. E. 2002. Palmitoylation of tetraspanin proteins: modulation of CD151 lateral interactions, subcellular distribution, and integrin-dependent cell morphology. *Molecular Biology of the Cell*, 13, 767-781.
- YANG, X., KOVALENKO, O. V., TANG, W., CLAAS, C., STIPP, C. S. & HEMLER, M. E. 2004. Palmitoylation supports assembly and function of integrin-tetraspanin complexes. *The Journal of Cell Biology*, 167, 1231-1240.
- YASEEN, I. H., MONK, P. N. & PARTRIDGE, L. J. 2017. Tspan2: a tetraspanin protein involved in oligodendrogenesis and cancer metastasis. *Biochemical Society Transactions*, 45, 465-475.
- YASHIRO-OHTANI, Y., ZHOU, X. Y., TOYO-OKA, K., TAI, X. G., PARK, C. S., HAMAOKA, T., ABE, R., MIYAKE, K. & FUJIWARA, H. 2000. Non-CD28 costimulatory molecules present in T cell rafts induce T cell costimulation by

- enhancing the association of TCR with rafts. *Journal of Immunology*, 164, 1251-1259.
- YAUCH, R. L. & HEMLER, M. E. 2000. Specific interactions among transmembrane 4 superfamily (TM4SF) proteins and phosphoinositide 4-kinase. *Biochemical Journal*, 351, 629-637.
- YOON, S.-B., LEE, Y.-J., PARK, S. K., KIM, H.-C., BAE, H., KIM, H. M., KO, S.-G., CHOI, H. Y., OH, M. S. & PARK, W. 2009. Anti-inflammatory effects of *Scutellaria baicalensis* water extract on LPS-activated RAW 264.7 macrophages. *Journal of Ethnopharmacology*, 125, 286-290.
- YOSHIKI, K. & BOYD, C. A. R. 2004. RNA interference-induced reduction in CD98 expression suppresses cell fusion during syncytialization of human placental BeWo cells. *Febs Letters*, 577, 473-477.
- YOUNT, J. S., ZHANG, M. M. & HANG, H. C. 2013. Emerging roles for protein S-palmitoylation in immunity from chemical proteomics. *Current Opinion in Chemical Biology*, 17, 27-33.
- YU, Y., KIM, H. S., CHUA, H. H., LIN, C. H., SIM, S. H., LIN, D., DERR, A., ENGELS, R., DESHAZER, D. & BIRREN, B. 2006. Genomic patterns of pathogen evolution revealed by comparison of *Burkholderia pseudomallei*, the causative agent of melioidosis, to avirulent *Burkholderia thailandensis*. *BMC Microbiology*, 6, 46.
- ZELM, M. C., VAN, JULIE, S., BRIGITTE, A., FRANÇOISE, M., LILIANE, S., FRANÇOISE, J., ALINA, F., CHIUNG-CHI, K., SHOSHANA, L. & DONGEN, J. J. M., VAN 2010. CD81 gene defect in humans disrupts CD19 complex formation and leads to antibody deficiency. *Journal of Clinical Investigation*, 120, 1265.
- ZHANG, X. A., BONTRAGER, A. L. & HEMLER, M. E. 2001. Transmembrane-4 superfamily proteins associate with activated protein kinase C (PKC) and link PKC to specific  $\beta$ 1 integrins. *Journal of Biological Chemistry*, 276, 25005-25013.
- ZHANG, Z., REENSTRA, W., WEINER, D. J., LOUBOUTIN, J.-P. & WILSON, J. M. 2007. The p38 Mitogen-Activated Protein Kinase Signaling Pathway Is Coupled to Toll-Like Receptor 5 To Mediate Gene Regulation in Response to *Pseudomonas aeruginosa* Infection in Human Airway Epithelial Cells. *Infection and Immunity*, 75, 5985-5992.
- ZHOU, B., LIU, L., REDDIVARI, M. & ZHANG, X. A. 2004. The palmitoylation of metastasis suppressor KAI1/CD82 is important for its motility-and invasiveness-inhibitory activity. *Cancer Research*, 64, 7455-7463.
- ZHOU, G., MO, W. J., SEBBEL, P., MIN, G., NEUBERT, T. A., GLOCKSHUBER, R., WU, X. R., SUN, T. T. & KONG, X. P. 2001. Uroplakin Ia is the urothelial receptor for uropathogenic *Escherichia coli*: evidence from in vitro FimH binding. *Journal of Cell Science*, 114, 4095-4103.
- ZHOU, J., FUJIWARA, T., YE, S., LI, X. & ZHAO, H. 2014. Downregulation of Notch Modulators, Tetraspanin 5 and 10, Inhibits Osteoclastogenesis in Vitro. *Calcified Tissue International*, 95, 209-217.
- ZIYYAT, A., RUBINSTEIN, E., MONIER-GAVELLE, F., BARRAUD, V., KULSKI, O., PRENANT, M., BOUCHEIX, C., BOMSEL, M. & WOLF, J. P. 2006. CD9 controls the formation of clusters that contain tetraspanins and the integrin alpha 6 beta 1, which are involved in human and mouse gamete fusion. *Journal of Cell Science*, 119, 416-424.
- ZUETER, A., YEAN, C. Y., ABUMARZOUQ, M., RAHMAN, Z. A., DERIS, Z. Z. & HARUN, A. 2016. The epidemiology and clinical spectrum of melioidosis in a teaching hospital in a North-Eastern state of Malaysia: a fifteen-year review. *BMC Infect Dis*, 16, 333.

ZUIDSCHERWOUDE, M., GÖTTFERT, F., DUNLOCK, V. M. E., FIGDOR, C. G., VAN DEN BOGAART, G. & VAN SPRIEL, A. B. 2015. The tetraspanin web revisited by super-resolution microscopy. *Scientific Reports*, 5, 12201.

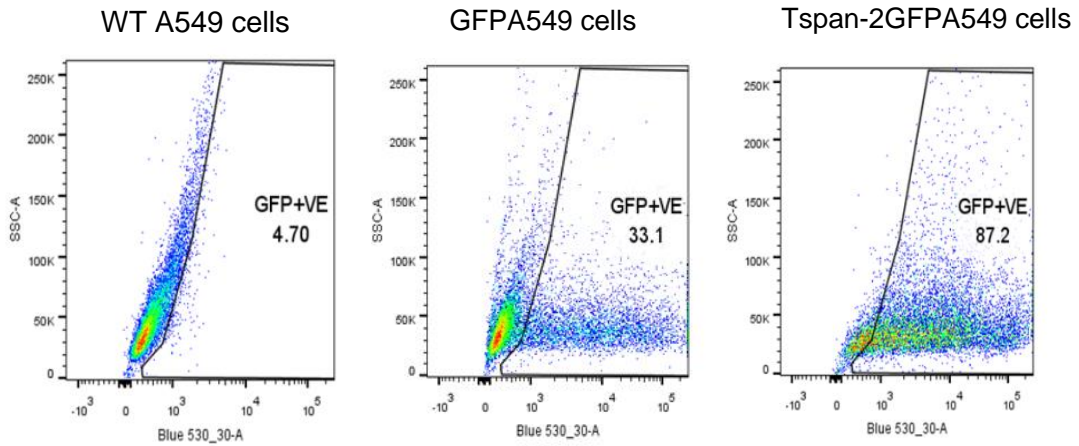
## Appendix





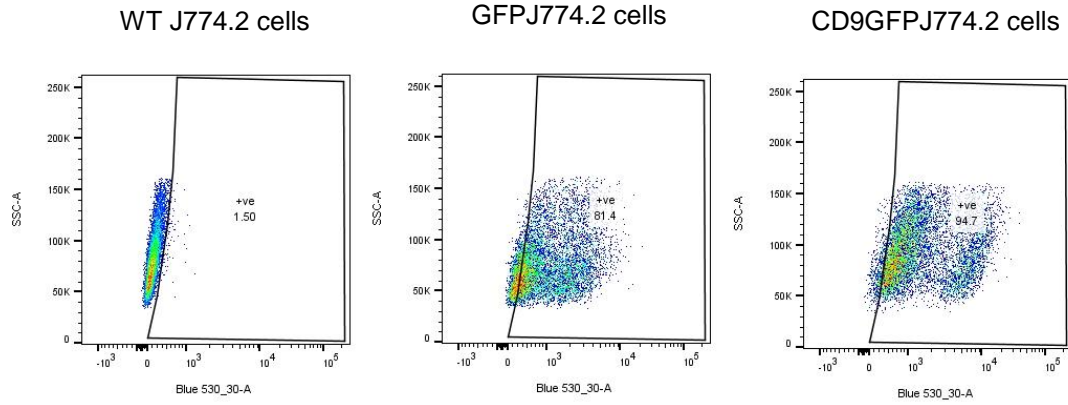
**Appendix Figure 1 Maps of pBBR-MCS1, pBBR-MCS1-GFP and pBBR-MCS1-mCherry plasmids.**

**A:** Parental pBBR-MCS-1 plasmid. **B:** pBBR-MCS-1 mCherry plasmid constructed by transferring the smaller fragment generated from the digestion of p<sub>tet</sub>mCherry-prey with HindIII and XhoI into pBBR-MCS-1, digested with the same enzymes. **C:** pBBR-MCS-1-GFP plasmid constructed by transferring the smaller fragment generated from the digestion of pSHAFT-GFP -prey with HindIII and PstI into pBBR-MCS-1 digested with the same enzymes.



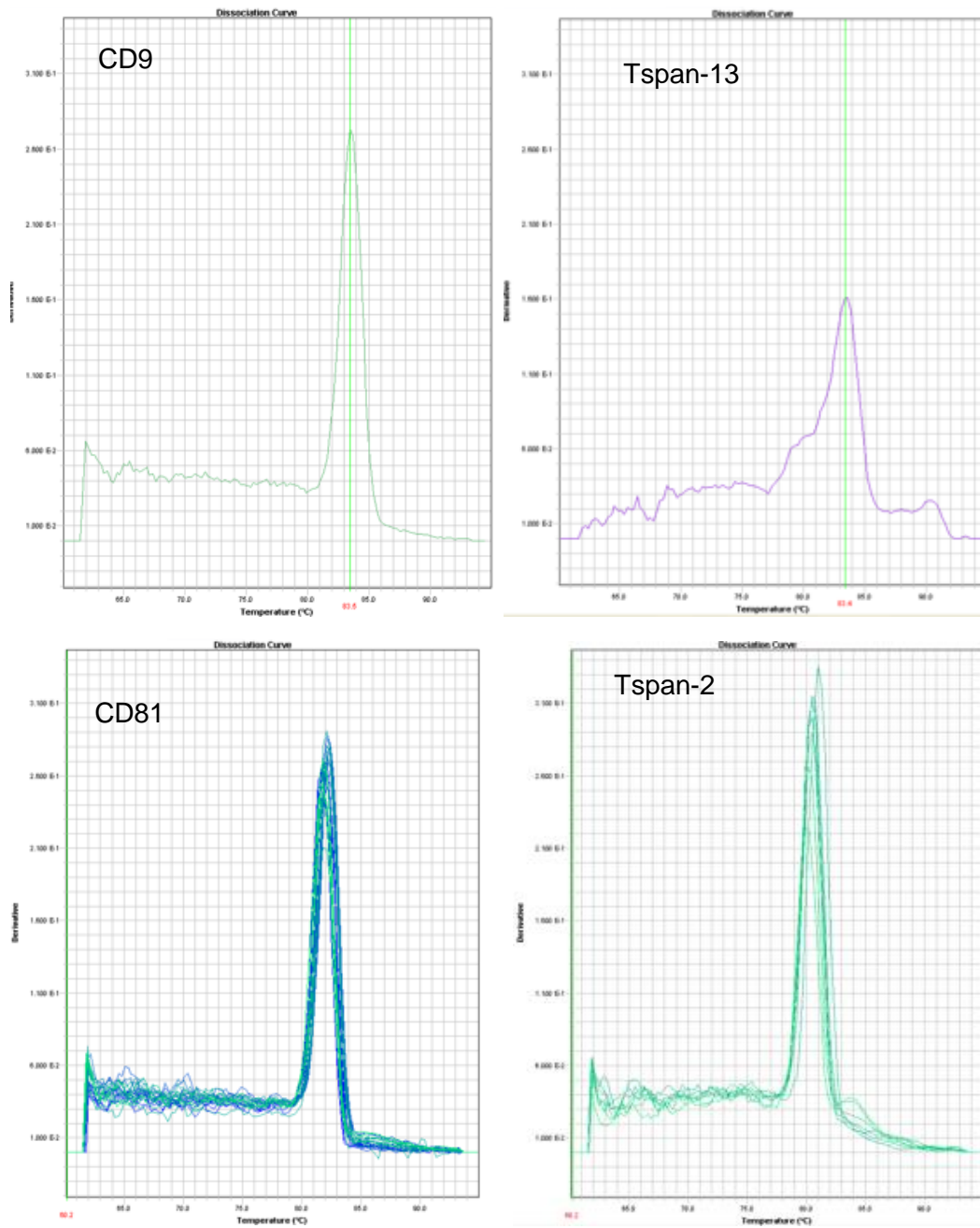
**Appendix Figure 2 Flow cytometry of transfected GFP and Tspan-2GFP A549 cells.**

Dot plots from FACS analysis of the transfected and sorted cells compared with the untransfected A549 control; the percentage GFP+ve population is shown on diagram. SSC-A denotes side-angle-scatter, Blue 530-30-A for the relative intensity of GFP (detector supplied with 530/30 filter type).



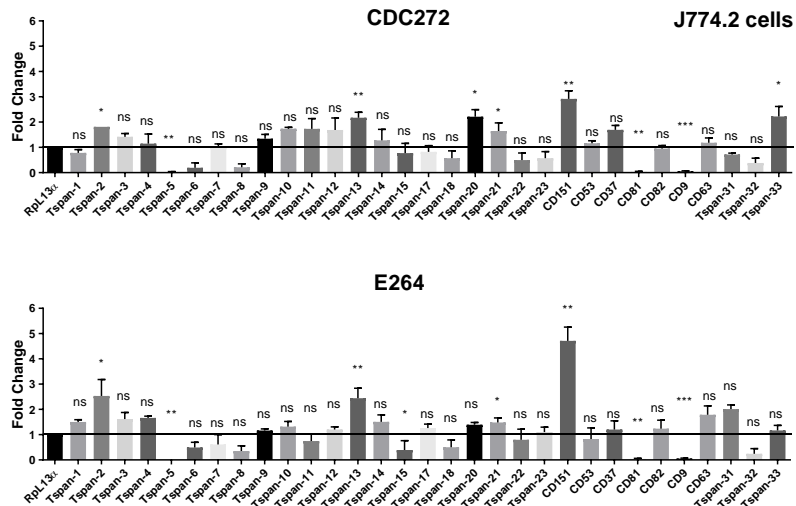
**Appendix Figure 3 Flow cytometry of transfected GFP and CD9GFPJ774.2 cells.**

Dot plots from FACS analysis of the transfected and sorted cells compared with the untransfected J774.2 control; the percentage GFP+ve population is shown on diagram. SSC-A denotes side-angle-scatter, Blue 530-30-A for the relative intensity of GFP (detector supplied with 530/30 filter type).



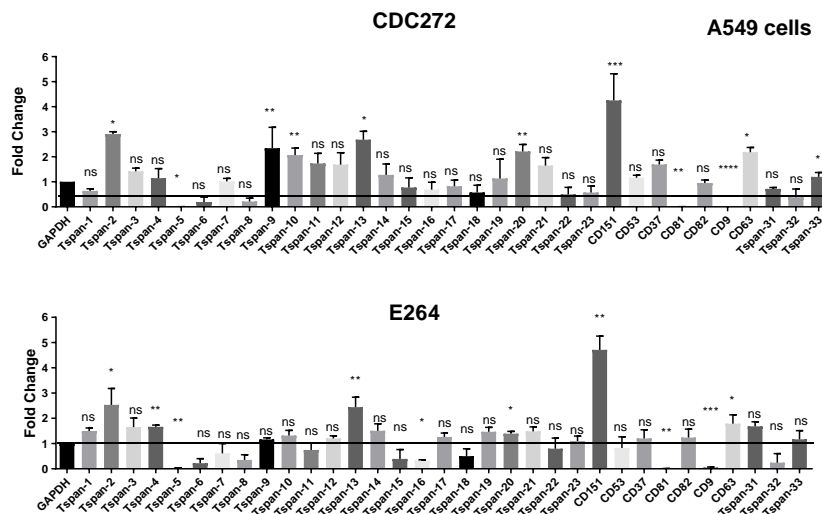
**Appendix Figure 4 Validation of qPCR primer specificity.**

A single peak on the melting curve analysis indicates a single PCR product. These optimization are representative for all qPCR experiments.



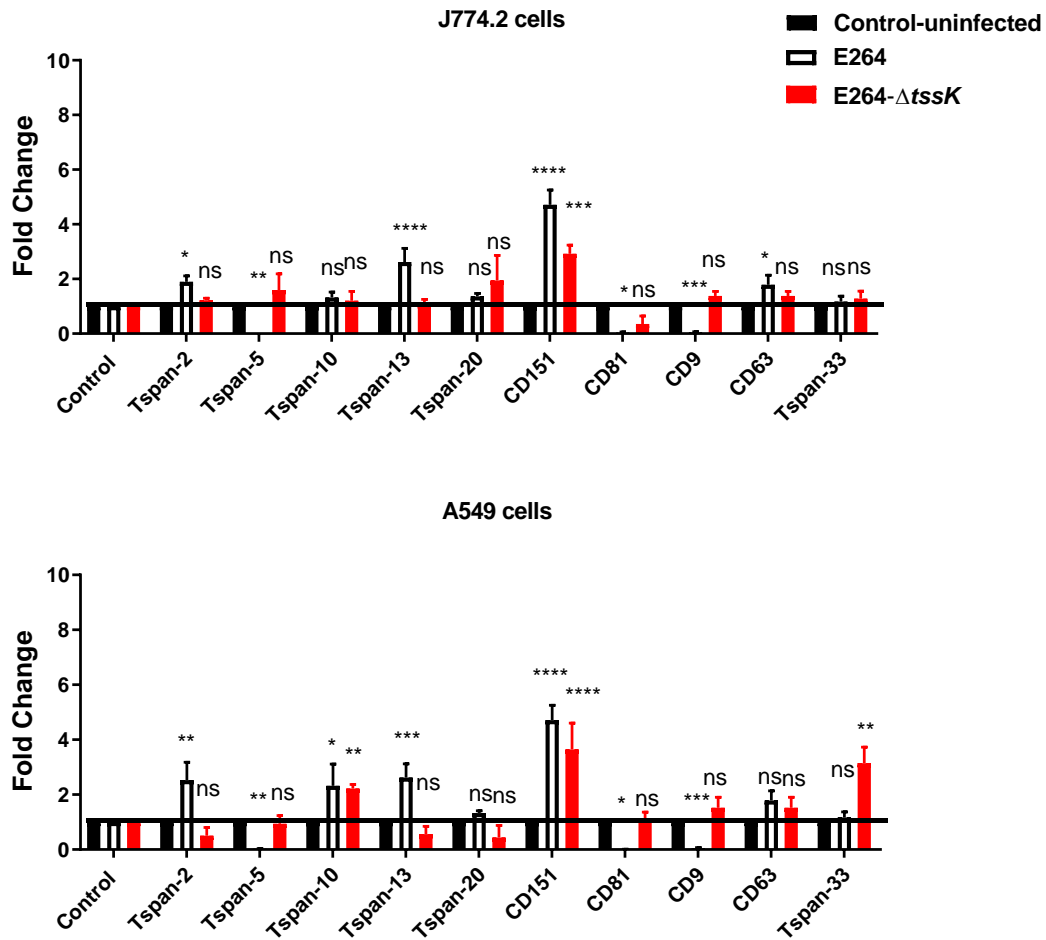
**Appendix Figure 5A Changes in Tspan genes expression in response to both *B. thailandensis* fusogenic and non- fusogenic strains.**

Tspan genes expression were measured by qPCR after 18hr infection with *B. thailandensis* CDC272 and E264. Expression of Tspan was calculated using the  $2^{-\Delta\Delta C_t}$  method relative to the results to the house keeping genes Rpl13 $\alpha$ . 8 Tspan showed changes in both host cell types. The significance of differences was tested by one-way ANOVA, where \* p<0.05; \*\* p<0.01; \*\*\* p<0.001 significant; ns=non-significant. The results are the means ( $\pm$  SEM) of 3 independent experiments each performed in 2 technical replicates.



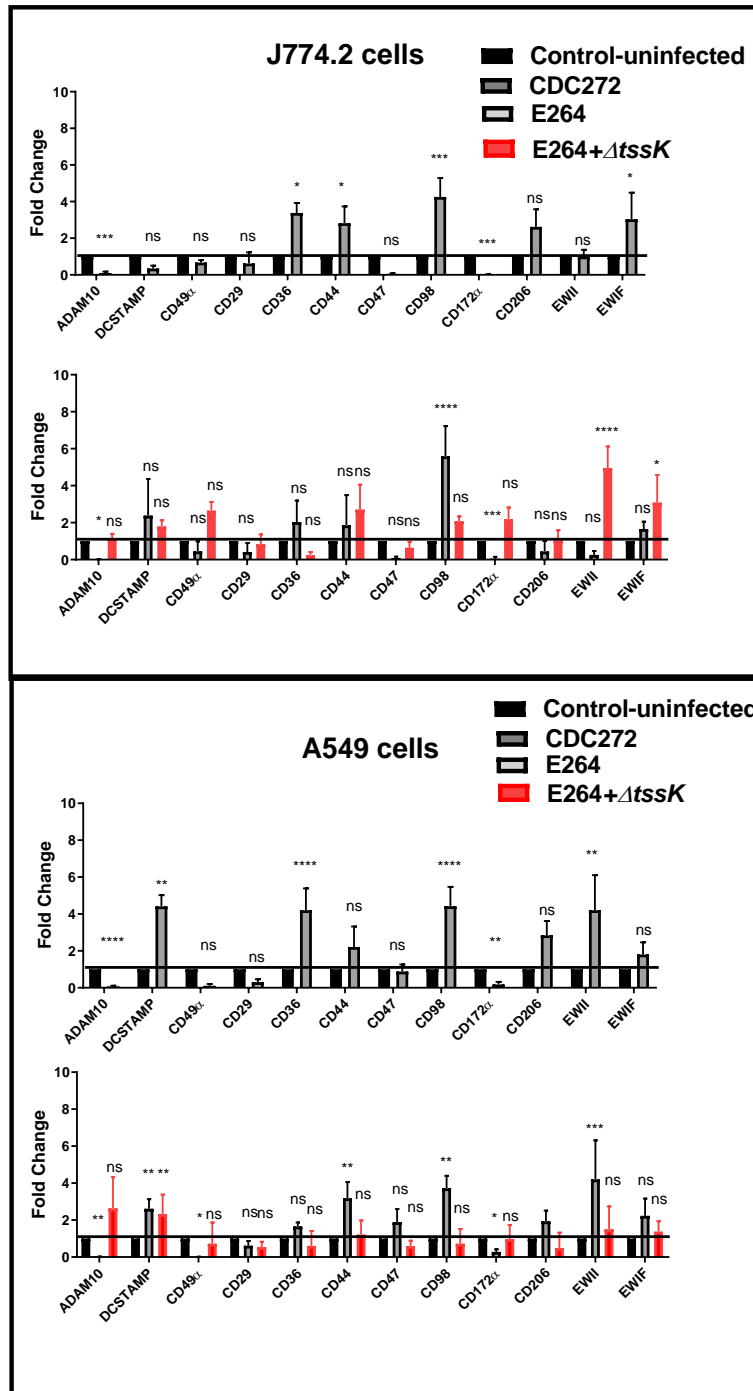
**Appendix Figure 5B Changes in Tspan genes expression in response to both *B. thailandensis* fusogenic and non- fusogenic strains.**

Tspan genes expression were measured by qPCR after 18hr infection with *B. thailandensis* CDC272 and E264. Expression of Tspan was calculated using the  $2^{-\Delta\Delta C_t}$  method relative to the results to the house keeping genes GAPDH. 10 Tspan showed changes in both host cell types. The significance of differences was tested by one-way ANOVA, where \* p<0.05; \*\* p<0.01; \*\*\* p<0.001 significant; ns=non-significant. The results are the means ( $\pm$  SEM) of 3 independent experiments each performed in 2 technical replicates.



**Appendix Figure 5C Changes in Tspan genes expression in response to both *B. thailandensis* fusogenic and non- fusogenic strains.**

Tspan genes expression were measured by qPCR after 18hr infection with *B. thailandensis* CDC272 or E264 and non-fusogenic mutant (E264- $\Delta tssK$ ). Expression of Tspan was calculated using the  $2^{-\Delta\Delta C_t}$  method relative to the results to the house keeping genes Rpl13a and GAPDH. 5 Tspan showed consistent changes in both host cell types, and no change with non-fusogenic mutant (E264- $\Delta tssK$ ). The significance of differences was tested by one-way ANOVA, where \*  $p < 0.05$ ; \*\*  $p < 0.01$ ; \*\*\*  $p < 0.001$  significant; ns=non-significant. The results are the means ( $\pm$  SEM) of 3 independent experiments each performed in 2 technical replicates.



**Appendix Figure 6 Changes in Tspan-partner genes expression in response to both *B. thailandensis* fusogenic and non-fusogenic strains.**

Tspan-partner genes expression were measured by qPCR after 18hr infection with *B. thailandensis* CDC272 or E264 and non-fusogenic mutant (E264- $\Delta tssK$ ). Expression of Tspan partners was calculated using the  $2^{-\Delta\Delta C_t}$  method relative to the housekeeping gene  $\beta$ -actin. 3 Tspans showed consistent changes in both host cell types, and no change with non-fusogenic mutant (E264- $\Delta tssK$ ). The significance of differences was tested by one-way ANOVA, where \*  $p < 0.05$ ; \*\*  $p < 0.01$ ; \*\*\*  $p < 0.001$  significant; ns=non-significant. The results are the means ( $\pm$  SEM) of 3 independent experiments each performed in 2 technical replicates.

Genes	NRT (No- reverse transcriptase)		NRNA (No-RNA sample)	
	<b>GAPDH</b>	39.931763	35.14805	Undetermined
<b>Tspan-1</b>	28.99355	29.73428	Undetermined	35.46973
<b>Tspan-2</b>	32.01488	31.457602	Undetermined	34.31121
<b>Tspan-3</b>	33.28066	35.41695	36.942593	34.817585
<b>Tspan-4</b>	27.331385	27.61647	Undetermined	Undetermined
<b>Tspan-5</b>	Undetermined	Undetermined	Undetermined	Undetermined
<b>Tspan-6</b>	Undetermined	Undetermined	Undetermined	Undetermined
<b>Tspan-7</b>	25.130657	28.451052	Undetermined	Undetermined
<b>Tspan-8</b>	34.979122	Undetermined	36.744892	38.351868
<b>Tspan-9</b>	31.989952	31.60617	35.661633	34.85089
<b>Tspan-10</b>	30.511805	30.511805	34.821	36.603764
<b>Tspan-11</b>	29.11388	28.41412	Undetermined	Undetermined
<b>Tspan-12</b>	31.194061	31.194061	39.931763	39.931763
<b>Tspan-13</b>	Undetermined	34.31121	33.13016	34.456974
<b>Tspan-14</b>	Undetermined	28.910097	34.415993	37.634903
<b>Tspan-15</b>	33.479237	Undetermined	38.000103	39.757984
<b>Tspan-16</b>	29.215239	28.62408	30.595415	30.595415
<b>Tspan-17</b>	33.788227	33.788227	34.462414	35.136116
<b>Tspan-18</b>	34.896137	33.360744	35.109177	35.109177
<b>Tspan-19</b>	Undetermined	Undetermined	Undetermined	Undetermined
<b>Tspan-20</b>	32.667362	Undetermined	32.377937	33.257576
<b>Tspan-21</b>	Undetermined	Undetermined	34.837246	39.627895
<b>Tspan-22</b>	Undetermined	Undetermined	Undetermined	Undetermined
<b>Tspan-23</b>	Undetermined	Undetermined	Undetermined	Undetermined
<b>CD151</b>	Undetermined	Undetermined	Undetermined	Undetermined
<b>CD53</b>	Undetermined	Undetermined	Undetermined	Undetermined
<b>CD37</b>	Undetermined	34.190094	Undetermined	34.11498
<b>CD81</b>	Undetermined	Undetermined	Undetermined	36.527473
<b>CD82</b>	Undetermined	Undetermined	Undetermined	Undetermined
<b>CD9</b>	37.008453	Undetermined	36.35095	37.497417
<b>CD63</b>	33.03921	37.261692	34.586628	33.99199
<b>Tspan-31</b>	32.29289	32.29289	34.21766	33.61503
<b>Tspan-32</b>	29.951612	29.951612	30.593681	30.593681
<b>Tspan-33</b>	34.121746	33.715054	34.817585	34.817585

**Appendix Table 1 Representative data from a single qPCR experiment.**

Two negative controls were used to validate the data of real time-qPCR which were no RNA sample (NRNA) and no reverse transcriptase enzyme to RNA sample (NRT) in the first step of cDNA synthesis. The data shows the raw  $C_t$  values of a representative single experiment; 2 technical replicates. Undetermined means no SYBR fluorescent signal.